INFLUENCE OF OVERLOOKED CHLORINATING AGENTS ON THE KINETICS OF ORGANIC COMPOUND HALOGENATION

by

Stephanie S. Lau

A dissertation submitted to Johns Hopkins University in conformity with the requirements for the degree of Doctor of Philosophy

Baltimore, Maryland
October 2017

Abstract

Free available chlorine (FAC) is the most commonly used chemical disinfectant for drinking water treatment. While FAC protects humans from waterborne pathogens, it can react with a wide variety of organic compounds to produce disinfection byproducts (DBPs) that are known or anticipated to be toxic. Determining the kinetics of organic compound chlorination could improve our understanding of the health risks associated with DBPs. Most researchers assume HOCl to be the predominant active chlorinating agent in FAC, but a few studies have shown that Cl_2 and Cl_2O, which are minor constituents of FAC under typical drinking water treatment conditions, can play important roles in the chlorination of moderately-reactive organic compounds. Are those compounds anomalies? Or is the influence of Cl_2 and Cl_2O on chlorination kinetics more prevalent than is presently recognized? We aim to address these questions by examining the kinetics of phenol and alkene chlorination.

To investigate the importance of Cl_2, Cl_2O, and HOCl for six (chloro)phenols and three ionones, we conducted kinetic experiments in which solution pH, chloride concentration, and chlorine dose were systematically varied. For all the (chloro)phenols and ionones examined, addition of chloride at millimolar levels enhanced chlorination rates at pH < 7. As $[Cl_2]$ is proportional to $[Cl^-]$ and $[H^+]$, our results are consistent with Cl_2 serving as a chlorinating agent. For some of the less reactive (chloro)phenols and ionones, Cl_2O is also important at high chlorine doses. The second-order rate constants we computed for different chlorinating agents indicate that Cl_2 and Cl_2O are intrinsically more reactive than is HOCl. Furthermore, in accordance with the reactivity-selectivity principle, selectivity for Cl_2 and Cl_2O increases as the reactivity of an organic compound

decreases. Therefore, despite the low concentrations of Cl_2 and Cl_2O in drinking water treatment settings, the potential roles of these chlorine species in organic compound chlorination should not be underestimated.

Another focus of our work is the development of a novel method for quenching and quantifying free chlorine and free bromine. Many traditional quenchers for free halogens (e.g., sodium sulfite, sodium thiosulfate, and ascorbic acid) are reducing agents that can interact with redox-labile analytes. We propose to use 1,3,5-trimethoxybenzene (TMB) for quenching free halogens instead. TMB rapidly reacts with excess free chlorine and free bromine to form monohalogenated products. We found that TMB did not interact with redox-labile DBPs that otherwise degraded in the presence of traditional quenchers. Moreover, TMB was as effective as sodium thiosulfate when used as a quencher in kinetic experiments involving the chlorination of 2,4-dichlorophenol and bromination of anisole. By quantifying TMB and its halogenated products in the quenched samples, we were also able to determine the concentrations of free halogens that were present at the time of quenching. Findings from our work show that TMB can serve as an effective quencher in aqueous halogenation experiments that involve redox-labile analytes and/or that require selective quantification of residual free halogens.

Advisor: A. Lynn Roberts

Readers: John D. Sivey, Alan T. Stone

Acknowledgements

First and foremost, I want to thank my advisor, Lynn Roberts, for her guidance and support throughout my PhD. She has motivated me to do the best work that I can do, and I am grateful for everything she has taught me about conducting research, interpreting results, and communicating my findings.

I also want to thank the other members of my dissertation committee. Alan Stone has been generous with his time and knowledge, and I appreciate how he encourages me to think more broadly about the implications of my research. John Sivey has been a knowledgeable and helpful collaborator, and his PhD research was a source of inspiration for much of my own work.

The (former and current) faculty and staff of DoGEE / EHE have all contributed positively to my PhD experience. In particular, I have learned a lot about environmental engineering from Ed Bouwer, Bill Ball, and Kai Loon Chen. Furthermore, I am grateful for the assistance of Huan Luong and Keith Ritchie in keeping the lab instruments happy.

Former students of this department have also been very helpful. I want to thank Jin Yang and Philip Flanders for showing me how to run various lab instruments when I first started doing research, Li Tang and Qian Zhang for sharing their DQE and GBO experiences, Katie Onesios Barry and Jess Lawson for their advice on grad school in general, and Hongtai Huang and Saamrat Kasina for their friendship.

I could not have asked for better colleagues in the Roberts Lab. Sonali Abraham has helped me collect some of the data presented in this dissertation. I had a great time sharing a lab with Rebecca Phillips, Ben Prince, and Ed Park during the first couple of years of my PhD. Mike Rose has been a fantastic labmate in the past few years, and I will

sorely miss the thought-provoking conversations we had while performing routine lab tasks.

I have met many wonderful people who made my time in Baltimore enjoyable. Experiences that are especially memorable include going to salsa dancing with Lulu, making cheesecakes with Carmen and Karen, learning ballroom dancing from MT and Saranthip, and marching for science with Grace. Other friends, particularly Rachel, Xiao, Daisuke, Kate, Sarah, Sid, Raymond, and Alex, also helped me relax and have fun outside the lab.

Finally, I want to thank my family for being my biggest cheerleaders throughout my PhD. My parents and aunt Fong have always believed in me. They brought peace and calm whenever I felt overwhelmed. I would not have been able to make it through this long journey without their unconditional love and support.

Table of Contents

List of Tables

List of Figures and Schemes

1. Introduction

1. 1. Chlorination in Drinking Water Treatment

Chlorine was first used as a disinfectant for drinking water treatment in the early 1900s.[1] After more than a century, chlorination remains standard practice in most drinking water treatment plants in the United States (**Figure 1-1**) and other parts of the world. Chlorine is usually applied in two stages during drinking water treatment; it is added during primary disinfection to inactivate microorganisms in the water, and it is also applied to maintain a disinfectant residual in the distribution system.[1] Chlorine is inexpensive compared with alternative disinfectants (e.g., chloramines, chlorine dioxide, ozone, and UV) and is effective in inactivating many planktonic bacteria.[2]

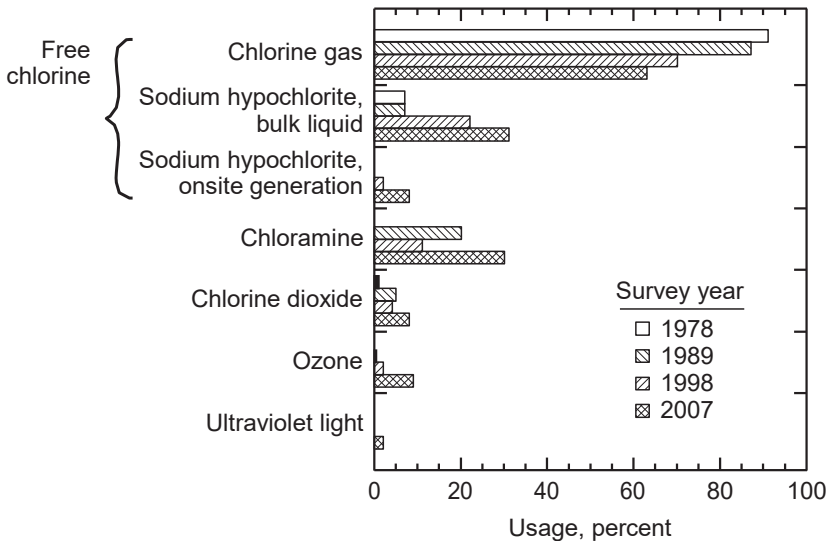

Figure 1-1. Disinfectant use in municipal drinking water treatment in the United States (reproduced from ref. 1).

The chlorine that is used in drinking water treatment can come in several different forms. The most common sources of chlorine employed by water utilities in the U.S. are chlorine gas ($Cl_{2\,(g)}$) and sodium hypochlorite (NaOCl) solutions; solid calcium hypochlorite ($Ca(OCl)_{2\,(s)}$) is also used in some small systems.[1] When chlorine gas is bubbled into water, it dissolves rapidly to form a concentrated solution of hypochlorous acid (HOCl) and hypochlorite (OCl^-):[3]

$$Cl_{2\,(g)} \rightleftharpoons Cl_{2\,(aq)} \tag{1-1}$$

$$Cl_{2\,(aq)} + H_2O \rightleftharpoons HOCl + Cl^- + H^+ \tag{1-2}$$

$$HOCl \rightleftharpoons OCl^- + H^+ \tag{1-3}$$

Both sodium hypochlorite and calcium hypochlorite release OCl^- when dissolved in water. The major difference between using chlorine gas and hypochlorite solutions is that a base may be added to neutralize the pH of the water in the former case, whereas an acid may be needed to offset the basicity of the reagents in the latter case.[4] Regardless of the source of chlorine used, HOCl (pK_a = 7.54 at 25 °C, ref. 5) and OCl^- contribute appreciably to the total free chlorine concentration at the range of pH values typically encountered in drinking water treatment.

Free chlorine, also known as free available chlorine (FAC), refers to the sum of the species with a chlorine atom in the 0 [a] or +1 oxidation state that are not combined with ammonia or organic nitrogen.[3] In the context of drinking water treatment, FAC is usually defined as the sum of HOCl and OCl^- because these are the most abundant Cl(+1)

[a] Although each chlorine atom in Cl_2 formally has an oxidation state of zero, chemically it reacts as if one chlorine were present in the +1 oxidation state and the other in the –1 oxidation state.

species. As HOCl is a more potent disinfectant than is OCl^-, primary disinfection should ideally occur at pH 7 or lower.[1]

1. 2. Chlorine and Disinfection Byproducts (DBPs)

An unintended consequence of drinking water disinfection is the formation of disinfection byproducts (DBPs) upon reactions of the disinfectant with organic constituents (and, for some disinfectants, halides) in the water. Chronic exposure to DBPs has been associated with increased risks for bladder and colorectal cancers, early-term miscarriages, and low birth weight.[6] Bladder cancer, in particular, correlates most strongly with exposure to drinking water DBPs.[7] Even though more than 700 DBPs have been identified,[8] their toxicities and the mechanisms by which they are formed (and sometimes transformed) remain poorly understood.

DBPs that are associated with chlorination first gained widespread attention in the 1970s, when chloroform and other trihalomethanes (THMs) were identified and quantified in chlorinated waters.[9-10] Since then, many more chlorination DBPs have been identified, including haloacetic acids (HAAs), haloacetonitriles, halonitromethanes, and haloacetaldehydes.[11] Nonetheless, at least 40% of the total organic halogen (TOX) formed from chlorination consists of unknown DBPs (**Figure 1-2**). THMs and HAAs, which together account for approximately 50% of the TOX from chlorination, are regulated by the U.S. Environmental Protection Agency (EPA).[12] In order to comply with DBP regulations, U.S. utilities have increasingly switched to other disinfection methods in recent years. For instance, chloramination was used for primary disinfection and/or

maintenance of disinfectant residual in 30% of the water utilities surveyed by the American Water Works Association in 2007 (**Figure 1-1**).

Switching disinfectants, however, is not a panacea for the DBP dilemma. Chloramines can also produce THMs and HAAs, albeit at concentrations that are lower than those produced from chlorination.[13] More worrying is the fact that chloramination can lead to the formation of unregulated DBPs (e.g., nitrogenous DBPs) that are known or anticipated to be more toxic than are the regulated ones,[6] not to mention that there is a strong association between switching to chloramines and leaching of Pb^{2+} from the distribution system and premise plumbing.[14] Ozonation produces bromate (BrO_3^-), which is a suspected carcinogen[15] and is regulated by the U.S. EPA. Using chlorine dioxide leads to the formation of chlorate (ClO_3^-) and chlorite (ClO_2^-), the latter of which is regulated.[12] Because the health implications of these alternative disinfectants have not been fully assessed, chlorination is likely to remain widely used in drinking water treatment for the foreseeable future.

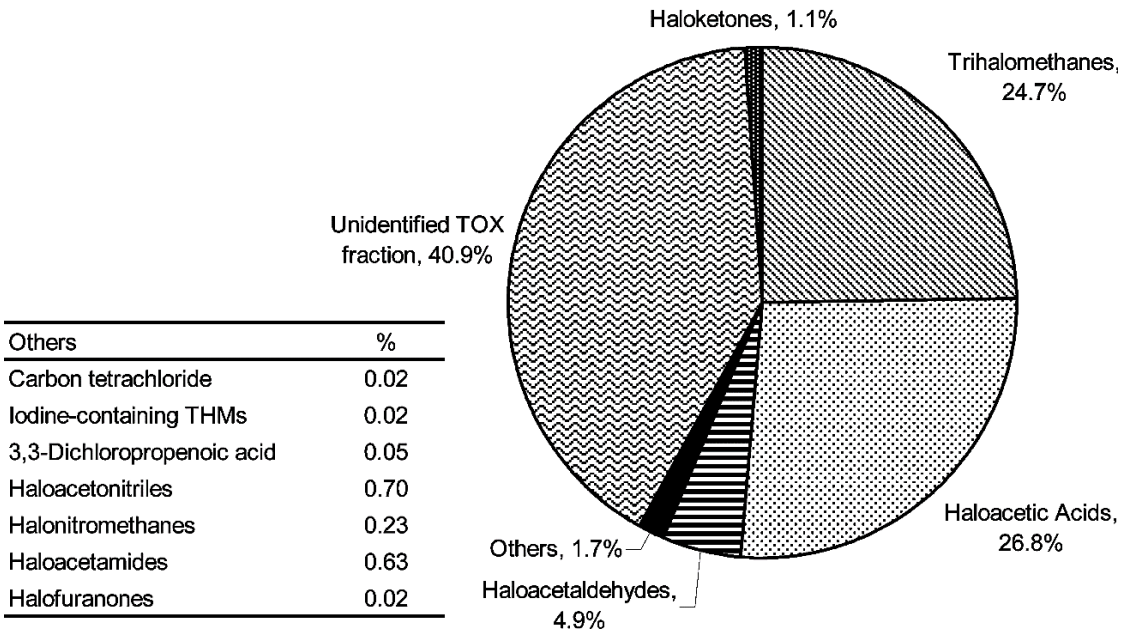

Others	%
Carbon tetrachloride	0.02
Iodine-containing THMs	0.02
3,3-Dichloropropenoic acid	0.05
Haloacetonitriles	0.70
Halonitromethanes	0.23
Haloacetamides	0.63
Halofuranones	0.02

Figure 1-2. Percent distribution of various disinfection byproducts (DBPs) in total organic halogen (TOX) formed from the chlorination of natural organic matter (reproduced from ref. 11).

1. 3. Kinetics of Chlorination Reactions

In order to devise effective strategies for minimizing the health risks associated with chlorination DBPs, we need to develop a thorough understanding of the reactions of FAC with DBP precursors. FAC can interact with organic compounds through oxidation, substitution, and addition reactions.[16] Chlorination kinetics of various compounds have been investigated, and many rate constants are available in the literature.[2]

Chlorination reactions are thought to be second-order overall (first-order in [FAC] and first-order in [organic compound]). HOCl is a much more reactive chlorinating agent than is OCl^- for many organic compounds.[2] While other chlorine species (e.g., Cl_2 and

Cl_2O) may be present in FAC, their concentrations are orders of magnitude lower than those of HOCl and OCl^- at pH 6–8 (**Figure 1-3**). Thus, HOCl is often assumed to be the predominant chlorinating agent in FAC under typical drinking water treatment conditions.

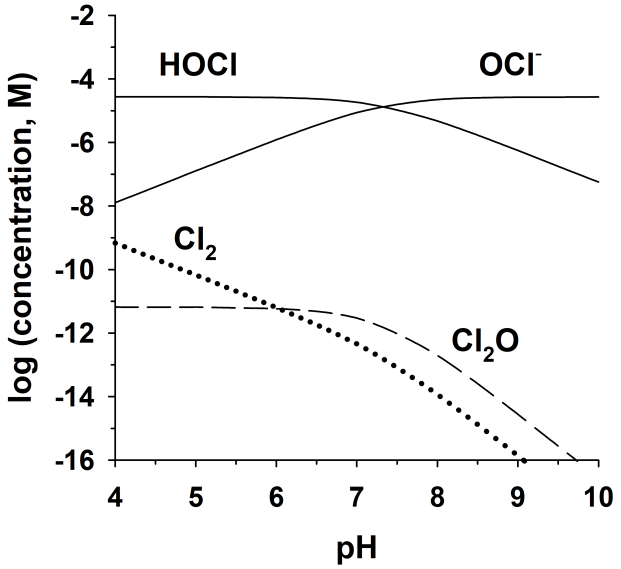

Figure 1-3. Speciation of free available chlorine (FAC) at 25 °C under conditions typical of drinking water treatment: [FAC] = 28 μM (2 mg/L as Cl_2, ref. 1), [Cl^-] = 0.23 mM (8 mg/L, mean chloride concentration in North American rivers, ref. 17).

Hypochlorous acidium ion (H_2OCl^+) has been proposed to be a reactive species that can account for the increase in chlorination rates observed for some organic compounds at pH < 6. H_2OCl^+ is the conjugate acid of HOCl and has an estimated pK_a of -3 to -4.[18] Given the low pK_a of H_2OCl^+, the concentration of this proposed chlorinating agent will be orders of magnitude lower than that of HOCl at pH > 0. Nonetheless, H_2OCl^+ is hypothesized to be more electrophilic than is HOCl, partly because H_2OCl^+

has a positive charge and partly because H_2O (from H_2OCl^+) is a better leaving group than is OH^- (from HOCl).

It has been suggested that H_2OCl^+ can be an important chlorinating agent for compounds such as anisole,[19] resorcinol,[20] phenol,[21] β-estradiol,[22] bisphenol A,[23] and 3-methylanisole.[24] The main supporting evidence for H_2OCl^+ is that the experimental rate constants for the chlorination of these compounds appear to depend on $[H^+]$ at low pH. For example, a model of the form of equation 1-4 has been proposed to describe the apparent second-order rate constant (k_{app}) for phenol:[21]

$$k_{app} = k_{H^+,\,ArOH}\,[H^+]\,f_{HOCl}\,f_{ArOH} + k_{HOCl,\,ArOH}\,f_{HOCl}\,f_{ArOH} + k_{HOCl,\,ArO^-}\,f_{HOCl}\,f_{ArO^-} \quad (1\text{-}4)$$

where f_{HOCl} represents the fraction of $[HOCl]_T$ in the HOCl form; f_{ArOH} and f_{ArO^-} represent the fractions of total phenol ($[phenol]_T$) in the acid (ArOH) and conjugate base (ArO^-) forms, respectively. The specific-acid catalysis term in equation 1-4 is interpreted as a pre-equilibrium step that leads to the formation of H_2OCl^+.

Despite the number of previous researchers who hypothesized a role for H_2OCl^+ as a chlorinating agent, this chlorine species has never been detected using established spectrometric methods.[18] The elusive nature of H_2OCl^+ led some researchers to question whether the high reactivities of certain organic compounds at low pH could be due to reactions with Cl_2 instead. Cl_2 is anticipated to be more electrophilic than is HOCl because Cl^- (from Cl_2) is a better leaving group than is OH^- (from HOCl). The formation of Cl_2 in FAC solutions is favored at low pH and in the presence of chloride (equation 1-5). Even though the concentration of Cl_2 is low under typical drinking water treatment

conditions (**Figure 1-3**), Cl_2 could potentially influence the kinetics of organic compound chlorination due to its high intrinsic reactivity.[25-28]

$$HOCl + Cl^- + H^+ \rightleftharpoons Cl_2 + H_2O \qquad \log K_{Cl_2} = 2.72 \qquad (1\text{-}5)$$

(ref. 29, 25 °C, corrected to 0 M ionic strength using the Davies equation)

Chloride has traditionally been viewed as unreactive in chlorination reactions. Equation 1-5, however, illustrates that chloride can act as a catalyst for chlorination reactions via the formation of Cl_2. In laboratory studies, the amount of chloride present in reaction solutions is rarely reported or controlled. A common source of chloride is the hydrochloric acid (HCl) used for pH adjustments, and one study has shown that the chlorination rate of triclosan at pH < 6 was enhanced when HCl, rather than sulfuric acid (H_2SO_4), was used to adjust solution pH.[30] Even in the absence of other reagents, commercial NaOCl solutions usually contain equimolar concentrations of Cl^- and OCl^- since they are manufactured by bubbling gaseous Cl_2 into water and then adding two moles of NaOH for every mole of Cl_2 (equation 1-6).[3] NaOCl also degrades over time to produce Cl^-, O_2, and ClO_3^-.[3] As a result, depending on the concentrations of FAC used, there may be an appreciable amount of chloride in reaction solutions. Without measuring chloride concentrations in their reactors, previous researchers may have overlooked the contribution of Cl_2 in their experiments.

$$Cl_{2\,(aq)} + 2\,NaOH \rightleftharpoons NaOCl + NaCl + H_2O \qquad (1\text{-}6)$$

Appreciable amounts of chloride may also be present in the water to be chlorinated during drinking water treatment. While chloride concentrations in most surface waters are well below the U.S. EPA-designated secondary maximum contaminant level (SMCL) of 250 mg/L, they have increased steadily in many rivers and streams in the northeastern U.S. over the past 20-40 years.[31-32] The rise in chloride levels is strongly associated with urbanization, and the maximum chloride concentrations recorded at certain monitoring stations in urban areas exceed 250 mg/L.[32] In addition, water utilities are required to perform enhanced coagulation on surface waters with total organic carbon (TOC) concentrations ≥ 2.0 mg/L before chemical disinfection;[33] the ferric chloride ($FeCl_3$) that may be used as a coagulant can represent an important source of chloride. Furthermore, seawater desalination is gaining traction in some parts of the world. As desalination does not remove all the chloride present in the feed water, chloride concentrations in desalinated waters are likely to be higher than those in freshwaters. Seawater intrusion due to sea-level rise may lead to an increase in chloride levels in potable groundwaters as well. When chlorinating real waters that contain elevated chloride concentrations, the influence of Cl_2 on the kinetics of organic compound chlorination and DBP (trans)formation can become significant.

Another chlorinating agent in FAC that has received little attention in the aqueous chlorination literature is Cl_2O, although the high reactivity of Cl_2O for alkenes and aromatic compounds in organic solvents has been documented in the chemistry literature.[34] Cl_2O formation is favored when high chlorine doses are used (equation 1-7). As laboratory experiments often employ chlorine doses that are much higher than those typically encountered in drinking water treatment, the potential influence of Cl_2O on

chlorination kinetics in laboratory settings should not be dismissed without experimental evidence.

$$2\,\mathrm{HOCl} \;\rightleftharpoons\; \mathrm{Cl_2O} + \mathrm{H_2O} \qquad (1\text{-}7)$$

$\log K_{\mathrm{Cl_2O}} = -2.06$ (ref. 35, corrected to 25 °C according to ref. 26)

Because $[Cl_2O]$ is proportional to $[HOCl]^2$, rates of reactions in which Cl_2O is the most important chlorinating agent will be second-order—not first-order—in [HOCl]. Yet, when computing second-order rate constants, the pseudo-first-order rate constant (k_{obs}) obtained from experiments are often divided by $[FAC]_o$ in an attempt to normalize variations in the initial chlorine dose. The resulting values are known as apparent rate constants (k_{app}), and the inherent assumption is that the reactions are first-order in [FAC]. Sometimes k_{obs} values are divided by [HOCl] when computing second-order rate constants (k_{HOCl}) under the assumption that HOCl is the only chlorinating agent. When the rates of chlorination reactions deviate from first-order dependence on [HOCl] due to the influence of Cl_2O, or if Cl_2 contributes appreciably to observed reaction rates, the values of k_{HOCl} reported in the literature will likely overestimate the actual reactivity of HOCl.

Despite the low concentrations of Cl_2 and Cl_2O under typical drinking water treatment conditions, these overlooked chlorinating agents have been shown to influence the reaction kinetics of *p*-xylene,[25] dimethenamid,[26] 3-methylanisole,[27] 1,3-dimethoxybenzene,[27] antipyrine,[36] and aminopyrine.[37] The high intrinsic reactivities of Cl_2 and Cl_2O can, in some cases, compensate for their low concentrations. Whether Cl_2

and Cl_2O are important for organic compounds other than the ones listed above is the question that motivated the research described in Chapters 2 and 4.

1. 4. Quenching Agents for Free Chlorine and Free Bromine

Researchers engaged in DBP research sometimes struggle to find appropriate quenchers for their experiments. Most of the commonly used quenchers for free chlorine, including sodium sulfite (Na_2SO_3), sodium thiosulfate ($Na_2S_2O_3$), and ascorbic acid, are reducing agents that rapidly transform free chlorine into chloride. When free bromine is present, these quenchers will reduce it to bromide. Problems arise when these quenchers encounter analytes that can undergo redox reactions. Redox-labile analytes can be transformed by the quenchers, leading to inaccuracies in the quantification of these analytes. Instances of analyte transformation in the presence of various quenchers (e.g., sodium sulfite, sodium arsenite, sodium borohydride, and ascorbic acid) have been reported in the literature, with sodium sulfite having the greatest propensity for reducing redox-labile organic compounds.[38] Even ascorbic acid, which is considered milder than the sulfur-based quenchers, can cause the dechlorination of some *N*-chloro compounds (i.e., organic chloramines).[39-40]

Ammonium chloride (NH_4Cl) is sometimes used to quench free chlorine in the presence of redox-labile analytes. Unlike the sulfur-based quenchers and ascorbic acid, ammonium chloride reacts with free chlorine to form monochloramine, which is less reactive than is free chlorine for most organic compounds.[3] Ammonium chloride is, however, only suitable for compounds that do not undergo chloramination. When free

bromine is present, ammonium chloride would also be unsuitable because bromamines are more reactive than are chloramines.[41]

An alternative approach to quenching free chlorine and free bromine would be to use an organic compound that rapidly undergoes halogenation upon reactions with free halogens. This type of quencher essentially competes with the analytes of interest for residual chlorine and/or bromine. 2,6-Dichlorophenol has been used as a quencher for free chlorine and free bromine in a previous study,[42] although the effectiveness of this quenching procedure has not been rigorously tested. Moreover, issues with 2,6-dichlorophenol precipitating during some of the reaction time courses were reported.

Another organic compound that may be used as a free halogen quencher is 1,3,5-trimethoxybenzene (TMB). The reaction of TMB with free chlorine at pH < 8 is rapid,[27] and TMB forms a stable monochlorinated product when present in excess of free chlorine. Similarly, TMB forms a stable monobrominated product when present in excess of free bromine.[43] By quantifying the halogenation products of TMB, the concentrations of free halogens that were present at the time of quenching can be determined. In fact, TMB has been used as a probe to quantify the free bromine produced by human eosinophils.[43] The feasibility of using TMB as a quencher for free chlorine and free bromine in halogenation kinetic experiments (in the context of DBP research) is examined in Chapter 3.

1. 5. Thesis Organization

The results from three projects are presented and discussed in this dissertation. In Chapter 2, the influence of Cl_2, Cl_2O, and HOCl on the chlorination kinetics of phenol

and five chlorophenols is investigated. Chapter 3 focuses on the development of a novel quenching method for free chlorine and free bromine using 1,3,5-trimethoxybenzene. In Chapter 4, the roles of Cl_2, Cl_2O, and HOCl in the chlorination of three structurally-related alkenes are examined. Major findings from these studies, as well as broader implications and future research needs, are summarized in Chapter 5.

In addition to the five chapters, there are three appendices that contain supporting information for the three projects. Appendix A (associated with Chapter 2) contains procedures for chloride purification and FAC measurements, details of data modeling, and experimental rate constants for the six (chloro)phenols. Appendix B (associated with Chapter 3) contains a list of the reagents used and details of various analytical methods. Appendix C (associated with Chapter 4) contains the synthesis procedures for hypothesized intermediates/products of β-ionone chlorination, mass spectra of these intermediates/products, details of data modeling, and experimental rate constants for the three ionones.

1. 6. References

1. Crittenden, J. C.; Trussell, R. R.; Hand, D. W.; Howe, K. J.; Tchobanoglous, G. *MWH's Water Treatment: Principles and Design*, 3rd ed.; John Wiley & Sons: Hoboken, New Jersey, 2012.

2. Deborde, M.; von Gunten, U. Reactions of chlorine with inorganic and organic compounds during water treatment – Kinetics and mechanisms: A critical review. *Water Res.* **2008,** *42*, 13-51.

3. Black & Veatch Corporation. *White's Handbook of Chlorination and Alternative Disinfectants*, 5th ed.; John Wiley & Sons: Hoboken, New Jersey, 2010.

4. Benjamin, M. M.; Lawler, D. F. *Water Quality Engineering*. John Wiley & Sons: Hoboken, New Jersey, 2013.

5. Morris, J. C. The acid ionization constant of HOCl from 5 to 35°. *J. Phys. Chem.* **1966,** *70*, 3798-3805.

6. Richardson, S. D.; Plewa, M. J.; Wagner, E. D.; Schoeny, R.; DeMarini, D. M. Occurrence, genotoxicity, and carcinogenicity of regulated and emerging disinfection by-products in drinking water: A review and roadmap for research. *Mutat. Res.* **2007,** *636*, 178-242.

7. Richardson, S. D.; Kimura, S. Y. Water analysis: Emerging contaminants and current issues. *Anal. Chem.* **2016,** *88*, 546-582.

8. Plewa, M. J.; Richardson, S. D. Disinfection by-products in drinking water, recycled water and wastewater: Formation, detection, toxicity and health effects: Preface. *J. Environ. Sci.* **2017,** *58*, 1.

9. Bellar, T. A.; Lichtenberg, J. J. Determining volatile organics at microgram-per-litre levels by gas chromatography. *J. Am. Water Works Assoc.* **1974,** *66*, 739-744.

10. Rook, J. J. Formation of haloforms during the chlorination of natural water. *Water Treatment Exam.* **1974,** *23*, 234–243.

11. Pressman, J. G.; Richardson, S. D.; Speth, T. F.; Miltner, R. J.; Narotsky, M. G.; Hunter, E. S., III; Rice, G. E.; Teuschler, L. K.; McDonald, A.; Parvez, S.; Krasner, S. W.; Weinberg, H. S.; McKague, A. B.; Parrett, C. J.; Bodin, N.; Chinn, R.; Lee, C.-F. T.; Simmons, J. E. Concentration, chlorination, and chemical analysis of drinking water for disinfection byproduct mixtures health effects research: U.S. EPA's Four Lab Study. *Environ. Sci. Technol.* **2010,** *44*, 7184-7192.

12. U.S. Environmental Protection Agency (EPA). *Comprehensive Disinfectants and Disinfection Byproducts Rules (Stage 1 and Stage 2): Quick Reference Guide*, Washington, D.C., 2010.

13. Hua, G.; Reckhow, D. A. Comparison of disinfection byproduct formation from chlorine and alternative disinfectants. *Water Res.* **2007,** *41*, 1667-1678.

14. Renner, R. Plumbing the depths of D.C.'s drinking water crisis. *Environ. Sci. Technol.* **2004,** *38*, 224A-227A.

15. Kurokawa, Y.; Maekawa, A.; Takahashi, M.; Hayashi, Y. Toxicity and carcinogenicity of potassium bromate: A new renal carcinogen. *Environ. Health Perspect.* **1990,** *87*, 309-335.

16. Larson, R. A.; Weber, E. J. *Reaction Mechanisms in Environmental Organic Chemistry*. CRC Press: Boca Raton, Florida, 1994.

17. Wetzel, R. G. *Limnology: Lake and River Ecosystems*, 3rd ed.; Academic Press: San Diego, 2001.

18. Arotsky, J.; Symons, M. C. R. Halogen cations. *Q. Rev. Chem. Soc.* **1962,** *16*, 282-297.

19. Swain, C. G.; Crist, D. R. Mechanisms of chlorination by hypochlorous acid. The last of chlorinium ion, Cl^+. *J. Am. Chem. Soc.* **1972,** *94*, 3195-3200.

20. Rebenne, L. M.; Gonzalez, A. C.; Olson, T. M. Aqueous chlorination kinetics and mechanism of substituted dihydroxybenzenes. *Environ. Sci. Technol.* **1996,** *30*, 2235-2242.

21. Gallard, H.; Von Gunten, U. Chlorination of phenols: Kinetics and formation of chloroform. *Environ. Sci. Technol.* **2002,** *36*, 884-890.

22. Deborde, M.; Rabouan, S.; Gallard, H.; Legube, B. Aqueous chlorination kinetics of some endocrine disruptors. *Environ. Sci. Technol.* **2004,** *38*, 5577-5583.

23. Gallard, H.; Leclercq, A.; Croué, J.-P. Chlorination of bisphenol A: kinetics and by-products formation. *Chemosphere* **2004,** *56*, 465-473.

24. Pinkston, K. E.; Sedlak, D. L. Transformation of aromatic ether- and amine-containing pharmaceuticals during chlorine disinfection. *Environ. Sci. Technol.* **2004,** *38*, 4019-4025.

25. Voudrias, E. A.; Reinhard, M. A kinetic model for the halogenation of *p*-xylene in aqueous HOCl solutions containing Cl^- and Br^-. *Environ. Sci. Technol.* **1988,** *22*, 1056-1062.

26. Sivey, J. D.; McCullough, C. E.; Roberts, A. L. Chlorine monoxide (Cl_2O) and molecular chlorine (Cl_2) as active chlorinating agents in reaction of dimethenamid with aqueous free chlorine. *Environ. Sci. Technol.* **2010,** *44*, 3357-3362.

27. Sivey, J. D.; Roberts, A. L. Assessing the reactivity of free chlorine constituents Cl_2, Cl_2O, and HOCl toward aromatic ethers. *Environ. Sci. Technol.* **2012,** *46*, 2141-2147.

28. Lau, S. S.; Abraham, S. M.; Roberts, A. L. Chlorination revisited: Does Cl^- serve as a catalyst in the chlorination of phenols? *Environ. Sci. Technol.* **2016,** *50*, 13291-13298.

29. Wang, T. X.; Margerum, D. W. Kinetics of reversible chlorine hydrolysis: Temperature dependence and general-acid/base-assisted mechanisms. *Inorg. Chem.* **1994,** *33*, 1050-1055.

30. Rule, K. L.; Ebbett, V. R.; Vikesland, P. J. Formation of chloroform and chlorinated organics by free-chlorine-mediated oxidation of triclosan. *Environ. Sci. Technol.* **2005,** *39*, 3176-3185.

31. Kaushal, S. S.; Groffman, P. M.; Likens, G. E.; Belt, K. T.; Stack, W. P.; Kelly, V. R.; Band, L. E.; Fisher, G. T. Increased salinization of fresh water in the northeastern United States. *Proc. Natl. Acad. Sci. USA* **2005,** *102*, 13517-13520.

32. Mullaney, J. R.; Lorenz, D. L.; Arntson, A. D. Chloride in groundwater and surface water in areas underlain by the glacial aquifer system, northern United States. *U.S. Geological Survey Scientific Investigations Report (2009–5086).* 2009.

33. U.S. Environmental Protection Agency (EPA). *Enhanced Coagulation and Enhanced Precipitative Softening Guidance Manual*, Washington, D.C., 1999

34. Renard, J. J.; Bolker, H. I. The chemistry of chlorine monoxide (dichlorine monoxide). *Chem. Rev.* **1976,** *76*, 487-508.

35. Roth, W. A. Note on thermo-chemistry of chlorine monoxide. *Z. Phys. Chem. Abt. A* **1942,** *191*, 248-250.

36. Cai, M.-Q.; Feng, L.; Jiang, J.; Qi, F.; Zhang, L.-Q. Reaction kinetics and transformation of antipyrine chlorination with free chlorine. *Water Res.* **2013,** *47*, 2830-2842.

37. Cai, M.-Q.; Feng, L.; Zhang, L.-Q. Transformation of aminopyrine in the presence of free available chlorine: Kinetics, products, and reaction pathways. *Chemosphere* **2017,** *171*, 625-634.

38. Kristiana, I.; Lethorn, A.; Joll, C.; Heitz, A. To add or not to add: The use of quenching agents for the analysis of disinfection by-products in water samples. *Water Res.* **2014,** *59*, 90-98.

39. Wood, T. P.; Basson, A. E.; Duvenage, C.; Rohwer, E. R. The chlorination behaviour and environmental fate of the antiretroviral drug nevirapine in South African surface water. *Water Res.* **2016,** *104*, 349-360.

40. Yu, Y.; Reckhow, D. A. Formation and occurrence of *N*-chloro-2,2-dichloroacetamide, a previously overlooked nitrogenous disinfection byproduct in chlorinated drinking waters. *Environ. Sci. Technol.* **2017,** *51*, 1488-1497.

41. Duirk, S. E.; Valentine, R. L. Bromide oxidation and formation of dihaloacetic acids in chloraminated water. *Environ. Sci. Technol.* **2007,** *41*, 7047-7053.

42. Shah, A. D.; Liu, Z.-Q.; Salhi, E.; Hofer, T.; Werschkun, B.; von Gunten, U. Formation of disinfection by-products during ballast water treatment with ozone, chlorine, and peracetic acid: influence of water quality parameters. *Environ. Sci.: Water Res. Technol.* **2015,** *1*, 465-480.

43. Mayeno, A. N.; Curran, A. J.; Roberts, R. L.; Foote, C. S. Eosinophils preferentially use bromide to generate halogenating agents. *J. Biol. Chem.* **1989,** *264*, 5660-5668.

2. Chlorination revisited: Does Cl^- serve as a catalyst in the chlorination of phenols? *

2. 1. Abstract

The aqueous chlorination of (chloro)phenols are some of the best-studied reactions in the environmental literature. Previous researchers have attributed these reactions to two chlorine species: HOCl (at circum-neutral and high pH) and H_2OCl^+ (at low pH). In this study, we seek to examine the roles that two largely overlooked chlorine species, Cl_2 and Cl_2O, may play in the chlorination of (chloro)phenols. Solution pH, chloride concentration, and chlorine dose were systematically varied in order to assess the importance of different chlorine species as chlorinating agents. Our findings indicate that chlorination rates at pH < 6 increase substantially when chloride is present, attributed to the formation of Cl_2. At pH 6.0 and a chlorine dose representative of drinking water treatment, Cl_2O is predicted to have at best a minor impact on chlorination reactions, whereas Cl_2 may contribute more than 80% to the overall chlorination rate depending on the (chloro)phenol identity and chloride concentration. While it is not possible to preclude H_2OCl^+ as a chlorinating agent, we were able to model our low-pH data by considering Cl_2 only. Even traces of chloride can generate sufficient Cl_2 to influence chlorination kinetics, highlighting the role of chloride as a catalyst in chlorination reactions.

* Reproduced in part with permission from: Lau, S. S.; Abraham, S. M.; Roberts, A. L. Chlorination revisited: Does Cl^- serve as a catalyst in the chlorination of phenols? *Environ. Sci. Technol.* **2016**, *50*, 13291-13298. Copyright 2016, American Chemical Society. S.S.L. collected approximately 75% of the experimental data and did all of the writing.

2. 2. Introduction

Aqueous chlorine, also known as free available chlorine (FAC), is one of the most widely used disinfectants in drinking water and wastewater treatment processes worldwide. While FAC is critical for protecting consumers from waterborne illnesses, it can react with synthetic compounds and natural organic matter (NOM) to generate disinfection byproducts (DBPs), some of which are known or anticipated to be hazardous to human health.[1] The most abundant chlorine species in solutions of FAC are HOCl and OCl^-, with the latter being much less important than the former in electrophilic aromatic substitutions.[2] Thus, HOCl (pK_a = 7.54 at 25 °C, ref. 3) is usually assumed to be the sole chlorinating agent at circum-neutral and high pH.

At acidic pH, other chlorinating agents may be present in FAC solutions. The chlorination rates of some organic compounds appear to depend on $[H^+]$ at low pH,[4-12] a phenomenon that has been attributed to reactions with H_2OCl^+, the conjugate acid of HOCl with an estimated pK_a of -3 to -4 (**Figure 2-1**).[13] Due to its positive charge, H_2OCl^+ has been postulated to be a more reactive electrophile than is HOCl;[14] however, no one has managed to detect H_2OCl^+ using established spectrometric methods. The elusive nature of H_2OCl^+ has led researchers to question whether the high reactivities of some compounds at low pH could be due to reactions with $Cl_{2\,(aq)}$ instead. The formation of Cl_2 in FAC solutions is favored at low pH and in the presence of chloride:

$$HOCl + Cl^- + H^+ \rightleftharpoons Cl_{2\,(aq)} + H_2O \qquad (2\text{-}1)$$

where $\log K_{Cl_2} = 2.72$ (ref. 15, 25 °C, corrected to 0 M ionic strength using the Davies equation).

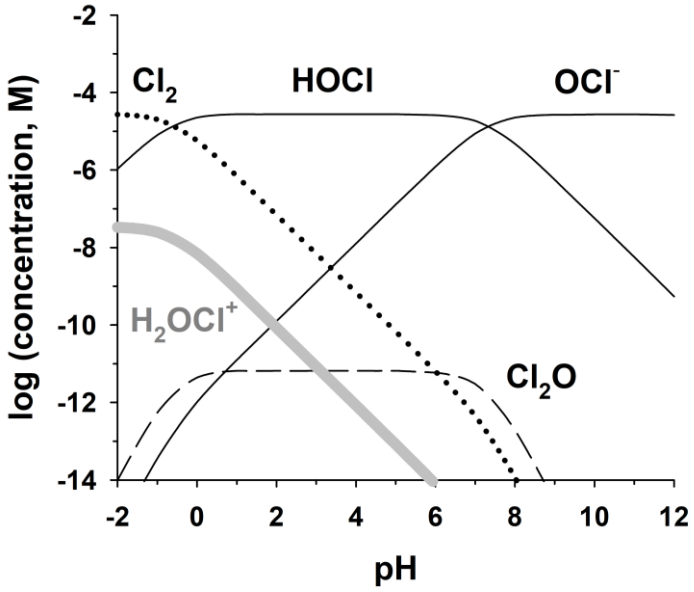

Figure 2-1. Speciation of free available chlorine (FAC) at 25 °C under typical drinking water chlorination conditions: $[FAC]_o$ = 28 μM (2.0 mg/L as Cl_2) and $[Cl^-]$ = 0.30 mM (~10 mg/L). The pK_a of H_2OCl^+ is estimated to be between -3 and -4;[13] a pK_a of -3.5 was assumed in calculating $[H_2OCl^+]$ for this figure.

One study used Raman spectroscopy to pinpoint Cl_2 (rather than H_2OCl^+) as the active low-pH chlorine species involved in the oxidation of several secondary alcohols.[16] The importance of Cl_2 in chlorination reactions has also been shown for several pharmaceuticals,[17-21] an herbicide,[22] and aromatic ethers.[23] Nevertheless, studies from as recent as 2015 and 2016 continue to dismiss Cl_2 without experimental evidence.[24-26] Furthermore, with few exceptions, previous researchers who reported second-order rate constants for Cl_2 did not systematically vary $[Cl^-]$ in their experiments, potentially yielding estimates with large uncertainties.

To explore whether Cl_2 has broader significance as a chlorinating agent, we chose to re-examine the reaction kinetics of phenol and its chlorinated derivatives with aqueous chlorine. Phenol is often invoked as a model for phenolic moieties in NOM,[27] and

(chloro)phenols are widespread micropollutants in the environment.[28] Phenol is chlorinated successively via electrophilic aromatic substitution to form 2-chlorophenol (2-CP), 4-chlorophenol (4-CP), 2,4-dichlorophenol (2,4-DCP), 2,6-dichlorophenol (2,6-DCP), and 2,4,6-trichlorophenol (TCP).[29] Subsequent reactions of TCP with FAC lead to the formation of non-aromatic compounds, with the end products being chloroform[6, 30] and trichloroacetic acid.[31]

The reaction kinetics of all six of these (chloro)phenols in the presence of FAC were first studied by Lee and Morris.[32] At pH < 6, the reaction rates of some (chloro)phenols increased with decreasing pH. Noting the presence of 1 mM Cl^- in their reactors, Lee and Morris hypothesized that reactions with Cl_2 could explain the observed reaction kinetics at low pH. Gallard and von Gunten,[6] however, argued that 1 mM of Cl^- was too low to generate sufficient Cl_2 to influence reaction kinetics. They attributed the high reactivities of some (chloro)phenols at pH < 6 to reactions with H_2OCl^+ and proposed a model of the form of equation 2-2 to describe the apparent second-order rate constant (k_{app}) for phenol in the presence of FAC:

$$k_{app} = k_{H^+, ArOH}[H^+] f_{HOCl} f_{ArOH} + k_{HOCl, ArOH} f_{HOCl} f_{ArOH} + k_{HOCl, ArO^-} f_{HOCl} f_{ArO^-} \quad (2\text{-}2)$$

where f_{HOCl} represents the fraction of $[HOCl]_T$ in the HOCl form; f_{ArOH} and f_{ArO^-} represent the fractions of total phenol ($[phenol]_T$) in the conjugate acid (ArOH) and phenolate (ArO^-) forms, respectively. Neither group of researchers conducted additional experiments that would either support or refute the ability of Cl_2 to act as a chlorinating agent for (chloro)phenols.

Aside from Cl_2, $Cl_2O_{(aq)}$ is another overlooked chlorine species in aqueous chlorine that has emerged as an important chlorinating agent for some organic compounds.[10, 19-23, 33] Cl_2O exists in equilibrium with HOCl, and its formation is favored at high [FAC]:

$$2\,HOCl \rightleftharpoons Cl_2O + H_2O \quad (2\text{-}3)$$

where $\log K_{Cl_2O} = -2.06$ (ref. 34, corrected to 25 °C according to ref. 22). To our knowledge, the influence of Cl_2O on the reaction kinetics of all six (chloro)phenols has not been previously investigated.

In this study, we systematically varied the solution pH, [Cl^-], and [FAC] in order to examine the influence of Cl_2, Cl_2O, and HOCl on the reaction kinetics of six (chloro)phenols. Second-order rate constants for Cl_2, Cl_2O, and HOCl were computed by comparing the experimental rate coefficients to the predicted speciations of different chlorinating agents. An enhancement in chlorination rates in the presence of chloride would implicate Cl_2 as a chlorinating agent. One mole of chloride is consumed for each mole of Cl_2 formed (equation 2-1); moreover, one mole of Cl^- is regenerated for every mole of Cl_2 that reacts with (chloro)phenol (equation 2-4). Thus, to the extent that Cl_2 represents a potent chlorinating agent, chloride ion could prove of underappreciated significance as a chlorination catalyst.

$$ArOH + Cl_2 \rightarrow Cl\text{–}ArOH + H^+ + Cl^- \quad (2\text{-}4)$$

2. 3. Materials and Methods

All aqueous solutions were prepared using reverse osmosis water that had been distilled in a Barnstead Mega-Pure system (Thermo Scientific) and further purified in a Milli-Q system (EMD Millipore). Commercial sodium hypochlorite (NaOCl) solutions (laboratory grade, 5.65–6%) from Fisher Scientific served as the source of FAC and were standardized iodometrically every week according to Standard Methods 4500-Cl B.[35] To minimize chlorine demand, all glassware was soaked in a concentrated FAC solution (≥ 0.5 M) for at least 8 hours and thoroughly rinsed with Milli-Q water before use.

2-Chlorophenol (≥ 98%), 2,6-dichlorophenol (99%), and 2,4-dichlorophenol (99%) were purchased from Acros Organics. Phenol (≥ 99%), sodium nitrate (≥ 99.0%), and potassium iodide (≥ 99.0%) were purchased from Sigma-Aldrich. 4-Chlorophenol (≥ 99%) and 2,4,6-trichlorophenol (98%) were purchased from Aldrich. Glacial acetic acid (certified ACS), methanol (Optima® LC/MS), sodium hydroxide (certified ACS), and sodium chloride (certified ACS) were obtained from Fisher Scientific. Sodium thiosulfate pentahydrate (99.5–101.0%) was purchased from Alfa Aesar. Sodium bicarbonate, sodium dihydrogen phosphate, and disodium hydrogen phosphate (all ACS grade) were obtained from J. T. Baker. Nitric acid was acquired from EMD. With the exception of sodium chloride (see Appendix A), all reagents were used without further purification.

Kinetic Experiments. All experiments were carried out in batch reactors (40-mL amber glass vials with PTFE-lined caps). Once all the reagents had been added, the reactors were kept inside a stainless-steel constant-temperature water bath for the entire duration of the experiments. Each reactor contained 30 mL of reaction solution; we found that the presence of headspace in reactors did not affect reaction kinetics, implying that the

chlorine and (chloro)phenol species do not partition appreciably into the headspace. The ionic strength (0.1 M) was set by adding sodium nitrate ($NaNO_3$). Solution pH was controlled by adding 10 mM of acetate (pH 3–6), phosphate (pH 6–8), or carbonate (pH > 8) buffer. No pH buffer was used in experiments at pH < 3. The pH was adjusted using small volumes of HNO_3 or NaOH. Measurements revealed that the pH changed by less than 0.05 pH unit over the course of each experiment.

Reaction kinetics in the presence of FAC were determined for each (chloro)phenol separately. Stock solutions of (chloro)phenols were made by dissolving the neat compounds in methanol, and spiking solutions of (chloro)phenols were made by diluting the methanolic stocks with water. The initial concentration of each (chloro)phenol was 2 μM in most experiments, and the final methanol content in the reactor was less than 0.05% (v/v). Working solutions of FAC were prepared fresh daily by diluting the commercial NaOCl stock solution with water. Kinetic experiments were carried out under pseudo-first-order conditions in which [FAC] ≈ $[FAC]_o$ ≈ constant. Values of $[FAC]_o$ in the majority of experiments were as follows: 125 μM for phenol, 2-CP, 2,4-DCP, and 2,6-DCP; 160 μM for 4-CP; 185 μM for TCP. To verify that [FAC] decreased by <10% over the course of the experiments, [FAC] in selected reactors was monitored through the reaction of FAC with KI, yielding I_3^-, which was measured by UV-visible spectrophotometry (see the following section for details).

Each kinetic experiment began with placing the reactors containing $NaNO_3$ and pH buffer (if added) in a water bath set at 25 ± 0.1 °C. After the reaction solution reached thermal equilibration, 1 mL of the FAC working solution was added to each reactor. The reactors were shaken and returned to the water bath. After allowing 8 minutes for

chlorine species to equilibrate, reactions were initiated by spiking each reactor with 0.30 mL of the methanolic (chloro)phenol solution using a microliter glass syringe. The reactors were mixed by shaking vigorously for 5 seconds and then returned to the water bath. Samples (2 mL) were collected periodically from the reactors using glass syringes and were transferred to autosampler vials containing a molar excess of sodium thiosulfate ($[S_2O_3^{2-}]_o$ / $[FAC]_o \geq 1.5$) to quench the reaction. Efforts were made to follow the degradation of the parent compound for three half-lives.

The effect of varying $[Cl^-]$ on reaction kinetics was investigated by adding 1–5 mM of sodium chloride (NaCl) to the reactor. $[NaNO_3]$ was adjusted to maintain constant ionic strength (i.e., $[NaCl] + [NaNO_3] = 0.1$ M). Previous researchers detected trace bromide (Br^-) in commercial sources of NaCl.[22] The NaCl used in this study was recrystallized in our laboratory to reduce the Br^- contamination. The recrystallization procedure is described in Appendix A.

Reaction orders in [HOCl] were assessed by varying $[FAC]_o$ at selected pH values while maintaining all other reaction conditions constant. The ranges of $[FAC]_o$ used varied with the (chloro)phenol: 125–640 μM for phenol; 125–520 μM for 2-CP; 80–805 μM for 4-CP; 80–600 μM for 2,4-DCP; 43–520 μM for 2,6-DCP; 185–825 μM for TCP. Reaction orders in [4-CP] and [2,4-DCP] were determined by the method of initial rates (ref. 36). The concentrations of $NaNO_3$ and pH buffers were also varied in separate experiments.

Monitoring [FAC]. For each (chloro)phenol, [FAC] was monitored as a function of time at selected pH values to ensure that pseudo-first-order conditions ($[FAC] \approx [FAC]_o \approx$ constant) were maintained throughout the experiments. [FAC] was determined using a

UV-visible spectrophotometric method adapted from ref. 37. Briefly, 2 mL of reaction solution was added to a glass vial containing 0.5 mL of 0.17 M potassium iodide (KI) solution. The FAC in the reaction solution stoichiometrically oxidizes I^- to triiodide (I_3^-). The absorbance of I_3^- was monitored at 351 nm (ϵ = 26200 L mol^{-1} cm^{-1}) using a Shimadzu UV-1800 UV-visible spectrophotometer with a 1-cm path length. The concentration of I_3^- (and hence [FAC]) was calculated using the Beer-Lambert law.

Control experiments conducted in the presence of each pH buffer employed (but in the absence of (chloro)phenols) revealed < 5% loss of [FAC] over 1.5 hours, a time in excess of the duration of most of our experiments (data not shown). Therefore, FAC was not consumed at appreciable rates through reactions with our pH buffers.

Analysis of (Chloro)phenols. The degradation of the parent compound and the formation of chlorophenol product(s) were monitored using high-performance liquid chromatography (HPLC). The HPLC system consisted of a Waters 1525 binary pump, an XBridge Shield RP 18 column with 5-µm particles (4.6 × 150 mm), and a Waters 2996 photodiode array detector. The mobile phase consisted of (A) acetic acid (0.24% v/v, pH 3) and (B) methanol (Optima LC/MS, Fisher Scientific). The gradient elution program used was as follows: 0–8 min, 70% B; 8–10 min, 80% B. For TCP, only the degradation of the parent compound was monitored.

Data Modeling. Pseudo-first-order rate coefficients (k_{obs}) for the degradation of (chloro)phenols were determined from linear regressions of the experimental $\ln[(\text{chloro})\text{phenol}]_T$ versus time data. Second-order rate constants for Cl_2, Cl_2O, and HOCl were computed using nonlinear least-squares regressions in *SigmaPlot 12.5* (Systat Software). A detailed description of the data fitting procedure is in Appendix A.

2. 4. Results and Discussion

Chlorination experiments were carried out under pseudo-first-order conditions in which [FAC] ≈ $[FAC]_o$ ≈ constant (≫ $[(chloro)phenol]_o$) to elucidate the influence of various chlorine species on the reaction kinetics of six (chloro)phenols. Pseudo-first-order rate coefficients (k_{obs}) for the degradation of each (chloro)phenol were obtained from linear regressions of the $ln[(chloro)phenol]_T$ versus time data (example data for phenol are shown in Appendix A, **Figure A-3**). The overall rate for the degradation of each (chloro)phenol (represented by $[ArOH]_T$) can be described as

$$-\frac{d[ArOH]_T}{dt} = k_{obs}\,[ArOH]_T \quad (2\text{-}5)$$

where $[ArOH]_T = [ArOH] + [ArO^-]$.

Effects of Varying pH and [Cl⁻]. The log k_{obs} versus pH data collected at different $[Cl^-]_{added}$ for phenol are shown in **Figure 2-2a**. At pH > 9, k_{obs} decreases with increasing pH. At pH < 9 and without added chloride, k_{obs} decreases with decreasing pH until pH 4.7, at which point k_{obs} increases with decreasing pH. Adding 1 and 5 mM Cl^- while maintaining constant ionic strength led to a pronounced increase in k_{obs} at pH < 6. The enhancement in phenol reaction rates with increasing $[Cl^-]_{added}$ at low pH can be attributed to reactions with Cl_2—rather than H_2OCl^+—since $[Cl_2]$ depends on both $[Cl^-]$ and $[H^+]$ (equation 1-1). Chloride addition had no appreciable effect on reaction rates at pH > 6, indicating that the influence of Cl_2 on reaction rates at neutral to high pH is negligible.

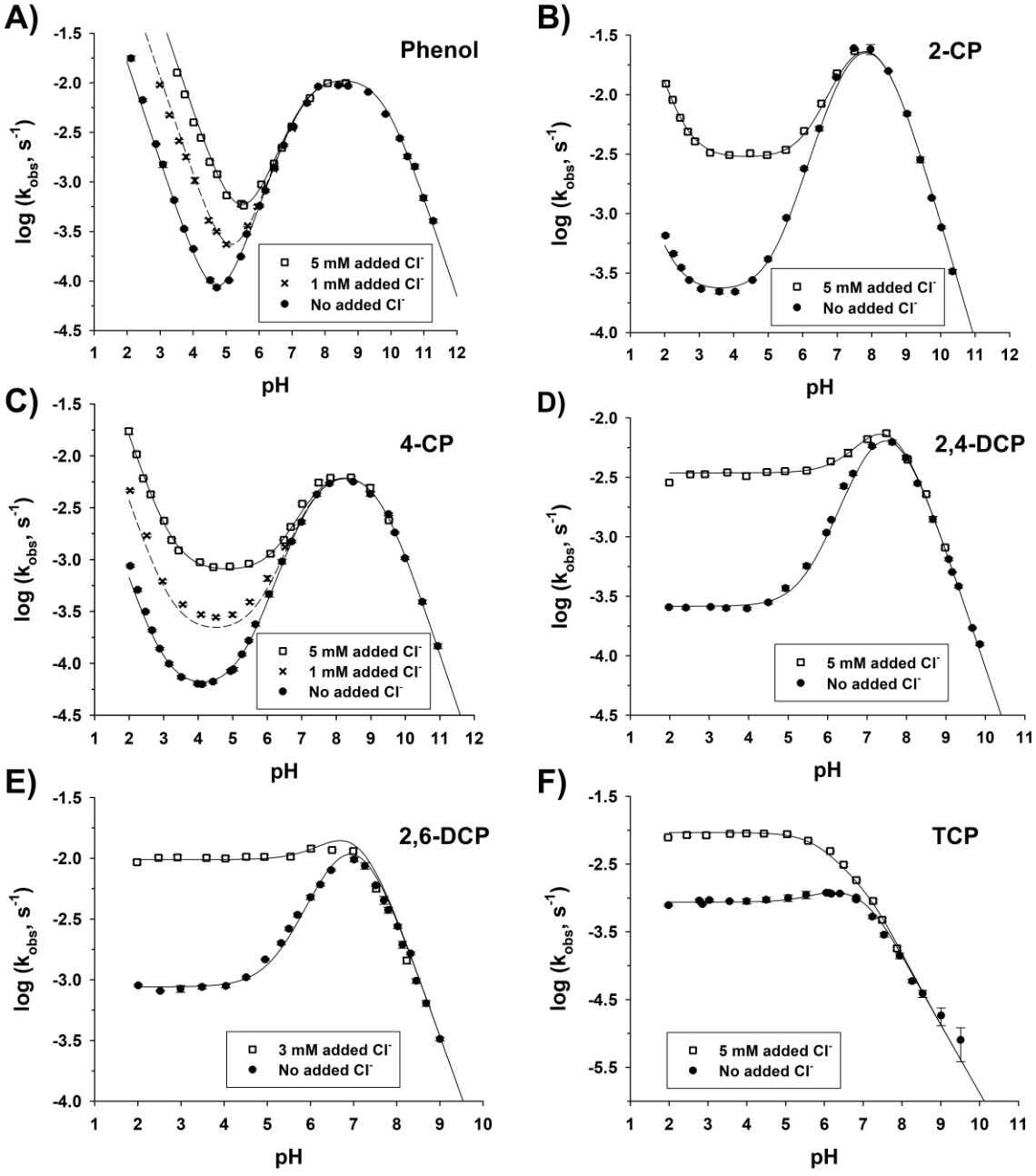

Figure 2-2. Pseudo-first-order rate coefficients (k_{obs}) as function of pH for **(A)** phenol, **(B)** 2-CP, **(C)** 4-CP, **(D)** 2,4-DCP, **(E)** 2,6-DCP, and **(D)** TCP. Reaction conditions: $[(\text{chloro})\text{phenol}]_o$ = 2 μM; $[NaCl]_o$ = 1 or 5 mM (if added); [pH buffer] = 10 mM; ionic strength = 0.1 M; T = 25 °C. $[FAC]_o$ = 125 μM for phenol, 2-CP, 2,4-DCP, and 2,6-DCP; $[FAC]_o$ = 160 μM for 4-CP; $[FAC]_o$ = 185 μM for TCP. Error bars indicate 95% confidence intervals (smaller than symbols if not shown). Solid lines are fits to a model of the form of equation 2-6 (phenol, 2-CP, and 4-CP), equation 2-7 (2,4-DCP), or equation 2-8 (2,6-DCP and TCP). The dashed lines in **(A)** and **(B)** represent the model prediction of k_{obs} based on equation 2-6.

The log k_{obs} versus pH data for the five chlorophenols are also shown in **Figure 2-2**. The variations in k_{obs} with pH for 2-CP and 4-CP (**Figures 2-2b** and **2-2c**, respectively) are similar to those for phenol, but those for 2,4-DCP, 2,6-DCP, and TCP are markedly different. For the dichlorophenols, k_{obs} reaches a maximum at pH 7–8 and plateaus at low pH (**Figures 2-2d** and **2-2e**). The log k_{obs} versus pH data for TCP show two distinct regions; k_{obs} decreases with increasing pH at pH > 6.5, while revealing little dependence on pH at pH < 6.5 (**Figure 2-2f**). Despite differences in the shapes of the log k_{obs} versus pH data, adding 1–5 mM Cl^- leads to a significant increase in k_{obs} for all (chloro)phenols at pH < 6 to 7.

The emphasis on "added" Cl^- is necessary because our ion chromatographic measurements confirm the presence of Cl^- in reactors to which no NaCl was added (**Figure 2-3**; see discussion in Appendix A). For example, we found that a reactor with $[FAC]_o$ = 0.125 mM contained 0.17 mM Cl^-, with the Cl^- coming primarily from the commercial NaOCl stock solutions. The concentration of chloride contributed by our FAC solutions was taken into account in modeling the experimental data.

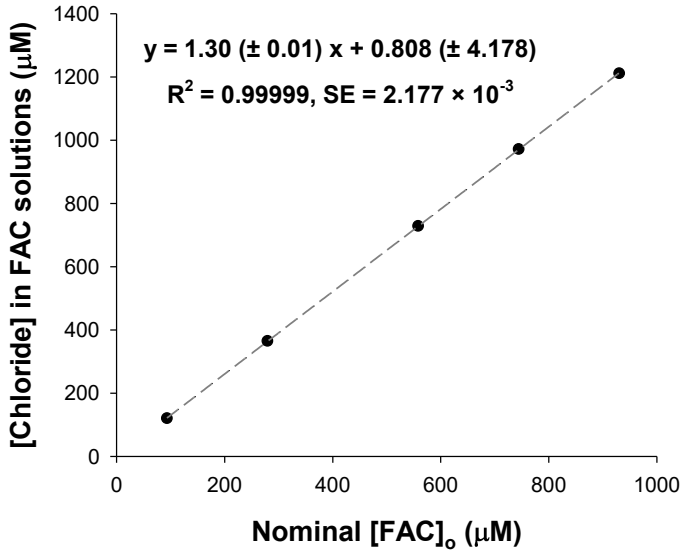

Figure 2-3. Concentration of chloride contributed by the NaOCl stock solution as a function of nominal $[FAC]_o$. The FAC solutions were made by diluting a commercial NaOCl stock with Milli-Q water. No other reagents were added to the FAC solutions. Uncertainties indicate 95% confidence intervals.

Effects of Varying [FAC] and [(Chloro)phenol]. For each (chloro)phenol, kinetic experiments with varying $[FAC]_o$ were conducted at selected pH values in order to assess the reaction order (n) in [HOCl]. The plots of log k_{obs} versus log $[HOCl]_o$ and their corresponding slopes (i.e., n) for phenol are shown in **Figure 2-4a**. In the absence of added Cl^-, n reaches a maximum value (1.71 ± 0.05) at pH 4.7 and approaches 1 as the pH increases. When Cl^- is added at pH 4.7 while maintaining constant ionic strength, the value of n decreases with increasing $[Cl^-]_{added}$. The log k_{obs} versus log $[HOCl]_o$ data for the other chlorophenols (**Figures 2-4b** to **2-4f**) show trends that are similar to the one for phenol; the value of n in the absence of added Cl^- is close to 2 at low pH and approaches 1 as the pH increases.

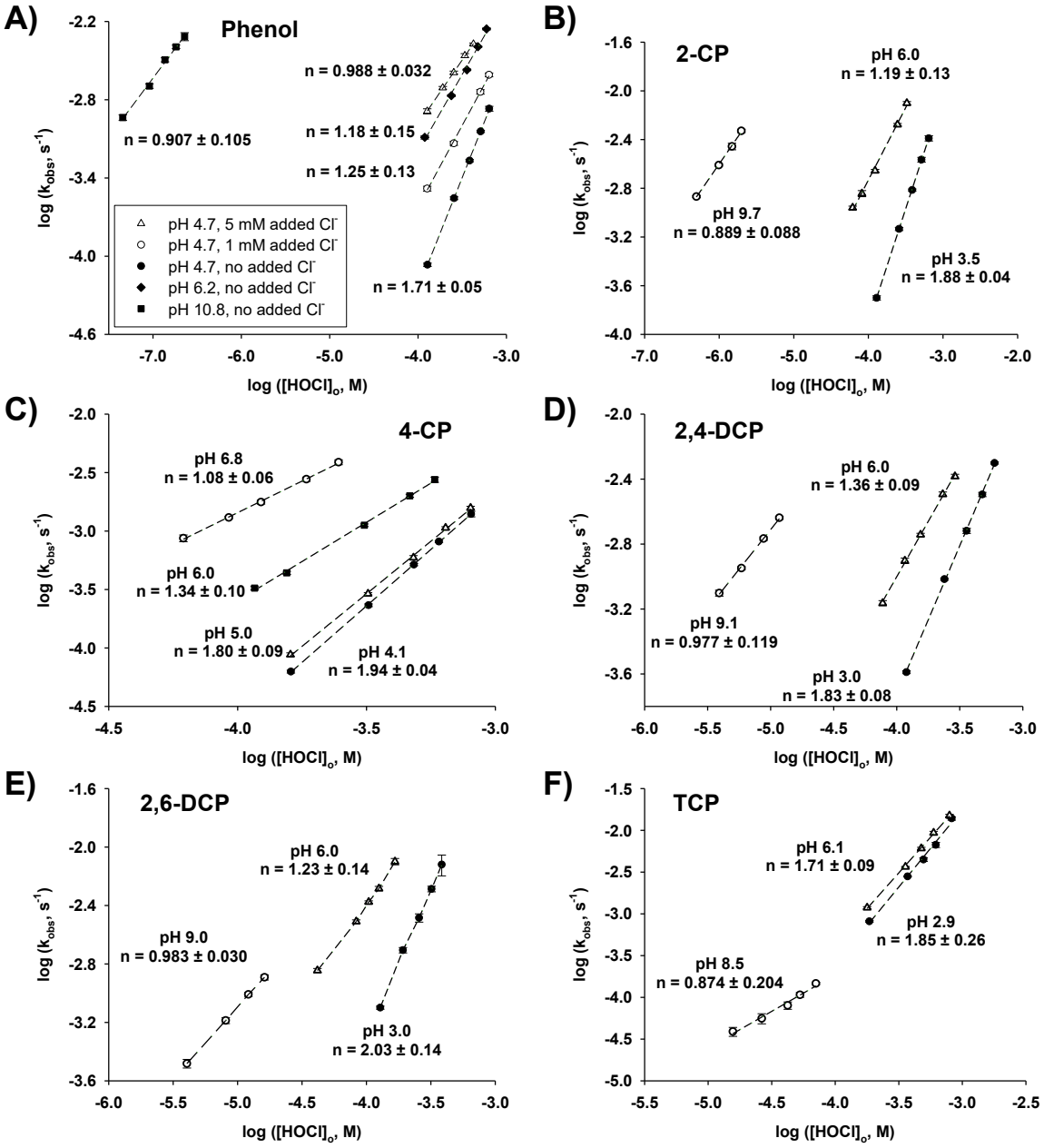

Figure 2-4. Plots of log k_{obs} versus log $[HOCl]_o$ at different pH values for **(A)** phenol, **(B)** 2-CP, **(C)** 4-CP, **(D)** 2,4-DCP, **(E)** 2,6-DCP, and **(F)** TCP. Reaction conditions: $[chlorophenol]_o$ = 2 μM; [pH buffer] = 10 mM; ionic strength = 0.1 M; T = 25 °C; $[FAC]_o$ = 125–640 μM for phenol, 125–520 μM for 2-CP, 80–805 μM for 4-CP, 80–600 μM for 2,4-DCP, 43–520 μM for 2,6-DCP, 185–825 μM for TCP. No NaCl was added unless otherwise indicated. Uncertainties in the slopes (*n*) denote 95% confidence intervals.

The second-order dependence of k_{obs} on [HOCl] could be interpreted as evidence that either Cl_2O or Cl_2 is the predominant chlorinating agent at low pH. Since $[Cl_2O]$ is proportional to $[HOCl]^2$ (equation 2-3), a reaction that depends only on Cl_2O would have an *n* of 2. On the other hand, as the concentration of chloride impurity in our FAC solutions was close to that of HOCl at pH < 6.5, the near second-order dependence is also consistent with Cl_2 as a reactive species. The dependence of k_{obs} on $[Cl_2]$ could masquerade as a second-order dependence on [HOCl] when $[Cl^-] \approx [HOCl]$ because $[Cl_2] = K_{Cl_2}[HOCl][Cl^-][H^+]$. Indeed, the apparent second-order dependence on [HOCl] in the chlorination of fluoranthene and naphthalene has been attributed to reactions with Cl_2.[38] An influence of Cl_2 could, therefore, cause *n* to be greater than 1 at low pH if [HOCl] and $[Cl^-]$ are approximately equal (see Appendix A for a more detailed discussion). The importance of Cl_2 diminishes with increasing pH, leading *n* to approach 1 at higher pH. When NaCl is added to the reactor, the reaction solution is no longer equimolar in $[Cl^-]$ and [HOCl], so the reaction becomes first-order in [HOCl].

The good adherence to exponential decay of the parent compound under pseudo-first order conditions in which $[FAC] \approx [FAC]_o \gg [(chloro)phenol]_o$ is consistent with the reactions under investigation being first-order in [(chloro)phenol] (sample data for phenol are shown in Appendix A, **Figure A-3**). We also used the method of initial rates[36] for selected chlorophenols to determine the reaction order in $[(chloro)phenol]_o$. Plots of log (initial rate) versus log $[(chloro)phenol]_o$ for 4-CP and 2,4-DCP result in straight lines with slopes close to 1 (**Figure 2-5**), thus confirming that the reactions are first-order in $[(chloro)phenol]_o$.

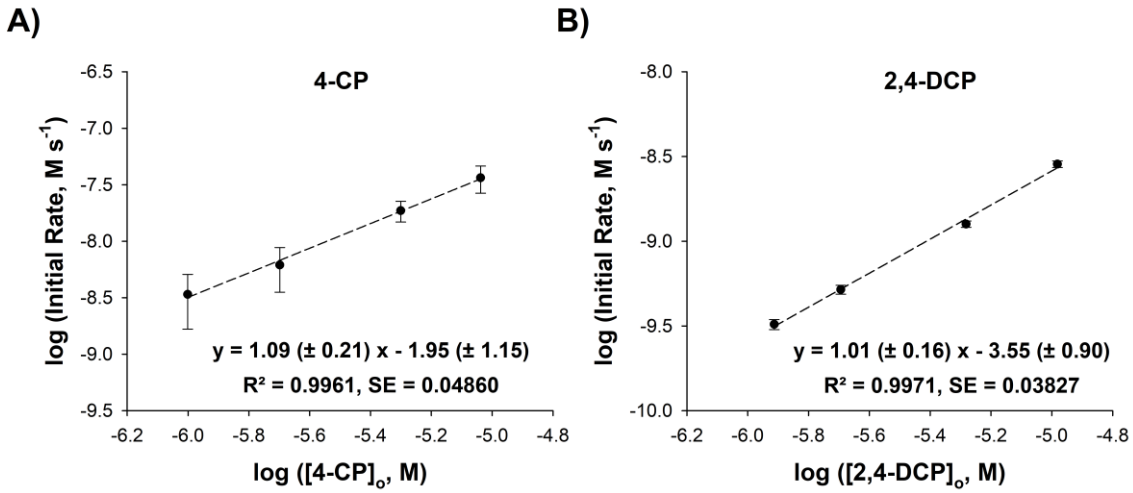

Figure 2-5. Initial chlorination rates as a function of initial (chloro)phenol concentrations for **(A)** 4-CP and **(B)** 2,4-DCP. Reaction conditions: [acetate buffer] = 10 mM, ionic strength = 0.1 M, T = 25 °C. For 4-CP, pH = 5.0, $[FAC]_o$ = 330 μM, $[4\text{-CP}]_o$ = 1–10 μM. For 2,4-DCP, pH = 4.1, $[FAC]_o$ = 120 μM, $[2,4\text{-DCP}]_o$ = 1–9 μM. Error bars indicate 95% confidence intervals.

Effects of Other Reactor Constituents. Control experiments in which the methanol concentration in the reactor was varied showed that methanol has no appreciable effect on chlorination kinetics at concentrations < 0.1% v/v (data not shown). Varying the ionic strength (i.e., [$NaNO_3$]) similarly did not affect chlorination rates. Varying the concentrations of pH buffers generally had no appreciable effect on chlorination kinetics (data not shown). The only exception is the catalysis of TCP reactions by acetate buffer at pH > 2.8 (**Figure 2-6**). This acetate buffer catalysis effect has been attributed to the formation of acetyl hypochlorite ($CH_3C(O)OCl$) from the reaction of HOCl with acetic acid.[39-43] We extrapolated the values of k_{obs} to $[acetate]_{tot} = 0$ at each pH value. The extrapolated k_{obs} values are the ones shown in **Figure 2-2f** and the ones used in data modeling.

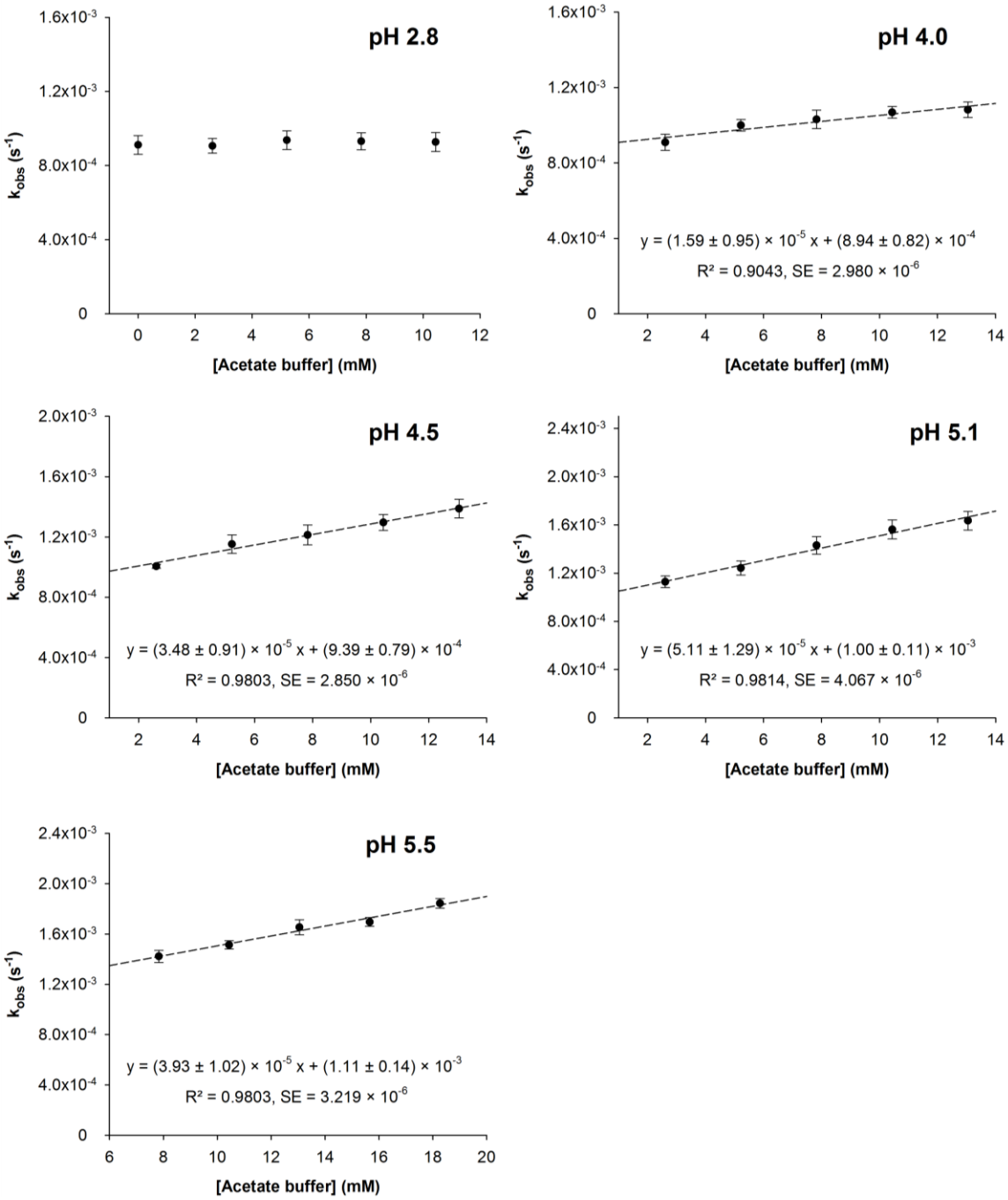

Figure 2-6. Chlorination rate constants (k_{obs}) as a function of acetate buffer concentration for TCP at different pH values. Reaction conditions: $[\mathrm{FAC}]_o$ = 185 μM, $[\mathrm{TCP}]_o$ = 2 μM, ionic strength = 0.1 M, T = 25 °C. Error bars and uncertainties indicate 95% confidence intervals.

Data Modeling. Second-order rate constants for the reactions of (chloro)phenols with Cl_2, Cl_2O, and HOCl were computed by nonlinear least-squares regressions using *SigmaPlot 12.5*, and the second-order rate constants were estimated from iterative data fittings. Terms that did not improve the model fit were not included in the final model (see Appendix A for details). For phenol, 2-CP, and 4-CP, the final model is

$$k_{obs} = k_{HOCl,\,ArO^-}[HOCl]\,f_{ArO^-} + k_{Cl_2O,\,ArOH}[Cl_2O]\,f_{ArOH} + k_{Cl_2,\,ArOH}[Cl_2]\,f_{ArOH} + k_{Cl_2,\,ArO^-}[Cl_2]\,f_{ArO^-} \quad (2\text{-}6)$$

where f_{ArOH} and f_{ArO^-} represent the fractions of [(chloro)phenol]$_T$ in the conjugate acid (ArOH) and phenolate (ArO^-) forms, respectively. As **Figure 2-2a** shows, equation 2-6 gives a good fit to the log k_{obs} versus pH data for phenol at $[Cl^-]_{added}$ = 0 and 5 mM, and it is able to predict the log k_{obs} versus pH data at $[Cl^-]_{added}$ = 1 mM. The model is also able to fit the 2-CP and 4-CP data well at all values of $[Cl^-]_{added}$ (**Figures 2-2b** and **2-2c**, respectively).

Despite the similarity in the shapes of the log k_{obs} versus pH data for 2,4-DCP (**Figure 2-2d**) and 2,6-DCP (**Figure 2-2e**), the final models that gave the best fits for these compounds are different. The model for 2,4-DCP has three terms (equation 2-7), whereas the one for 2,6-DCP has four terms (equation 2-8). Equation 2-8 can also be used to fit the k_{obs} versus pH data for TCP (**Figure 2-2f**).

$$k_{obs} = k_{HOCl,\,ArO^-}[HOCl]\,f_{ArO^-} + k_{Cl_2O,\,ArOH}[Cl_2O]\,f_{ArOH} + k_{Cl_2,\,ArO^-}[Cl_2]\,f_{ArO^-} \quad (2\text{-}7)$$

$$k_{obs} = k_{HOCl,\,ArO^-}[HOCl]\,f_{ArO^-} + k_{Cl_2O,\,ArOH}[Cl_2O]\,f_{ArOH} + k_{Cl_2O,\,ArO^-}[Cl_2O]\,f_{ArO^-} + k_{Cl_2,\,ArO^-}[Cl_2]\,f_{ArO^-} \quad (2\text{-}8)$$

The best-fit estimates of the second-order rate constants are listed in **Table 2-1**. For each (chloro)phenol, the second-order rate constants for Cl_2 and Cl_2O are at least as large as, or in many cases orders of magnitude larger than, the rate constants for HOCl. The differences among the rate constants for Cl_2 and Cl_2O and those for HOCl become more pronounced as the (chloro)phenol becomes more highly chlorinated and, thus, less reactive towards electrophilic aromatic substitution. In general, the second-order rate constants for reactions with the ArO^- form of (chloro)phenols are larger than those for reactions with the ArOH form, which is poorly reactive towards HOCl.

To test the validity of the second-order rate constants in **Table 2-1**, we used the rate constants to predict the concentration of each (chloro)phenol as a function of time at selected pH values. The model predictions are in close agreement with the measured concentrations for all the (chloro)phenols investigated (**Figure 2-7**).

To delineate the influence of Cl_2 and Cl_2O at low pH and in the absence of added Cl^-, we compared the reaction order (n) in [HOCl] computed using the second-order rate constants in Table 1 with the values of n determined from the log k_{obs} versus log [HOCl] data. An expression for the computed n (n_{calc}) has been derived with the assumption that [HOCl] = [Cl^-] at pH < 6.5 for the experiments conducted in the absence of added chloride (see Appendix A for details). The close agreement between n_{calc} and the experimentally determined n (**Tables 2-2 and 2-3**) is consistent with Cl_2 representing the predominant chlorinating agent for (chloro)phenols at the acidic pH values tested.

Table 2-1. Second-Order Rate Constants for the Reactions of HOCl, Cl_2, and Cl_2O with the Conjugate Acid (ArOH) and Phenolate (ArO^-) Forms of (Chloro)phenols [a]

	$\Sigma\sigma_{o,p}$ [b]	pK_a [c]	Second-order rate constants (M^{-1} s^{-1}) [d]				
			k_{HOCl, ArO^-}	$k_{Cl_2, ArOH}$	k_{Cl_2, ArO^-}	$k_{Cl_2O, ArOH}$	k_{Cl_2O, ArO^-}
Phenol	0	9.99	2.61 (± 0.26) × 10^4	8.92 (± 0.98) × 10^4	2.61 (± 0.50) × 10^9	9.0 (± 3.1) × 10^4	—
2-CP	0.68	8.56	3.17 (± 0.33) × 10^3	1.76 (± 0.13) × 10^3	1.12 (± 0.06) × 10^9	5.9 (± 1.3) × 10^5	—
4-CP	0.23	9.43	3.58 (± 0.23) × 10^3	2.08 (± 0.17) × 10^3	1.71 (± 0.13) × 10^9	9.8 (± 0.6) × 10^4	—
2,4-DCP	0.91	7.85	3.09 (± 0.19) × 10^2	—	2.69 (± 0.13) × 10^8	9.9 (± 2.5) × 10^5	—
2,6-DCP	1.36	6.97	1.28 (± 0.09) × 10^2	—	1.58 (± 0.16) × 10^8	2.3 (± 0.3) × 10^6	8.6 (± 2.1) × 10^7
TCP	1.59	6.15	3.39 (± 0.47)	—	9.35 (± 0.67) × 10^6	9.2 (± 3.3) × 10^5	3.3 (± 1.0) × 10^6

[a] All uncertainties indicate 95% confidence intervals.

[b] Calculated using the σ_p and σ_o values for chlorine listed in ref. 44

[c] pK_a values taken from ref. 6

[d] Inclusion of a term for the HOCl/ArOH reaction did not improve model fits to the experimental data, so values of $k_{HOCl, ArOH}$ are not reported.

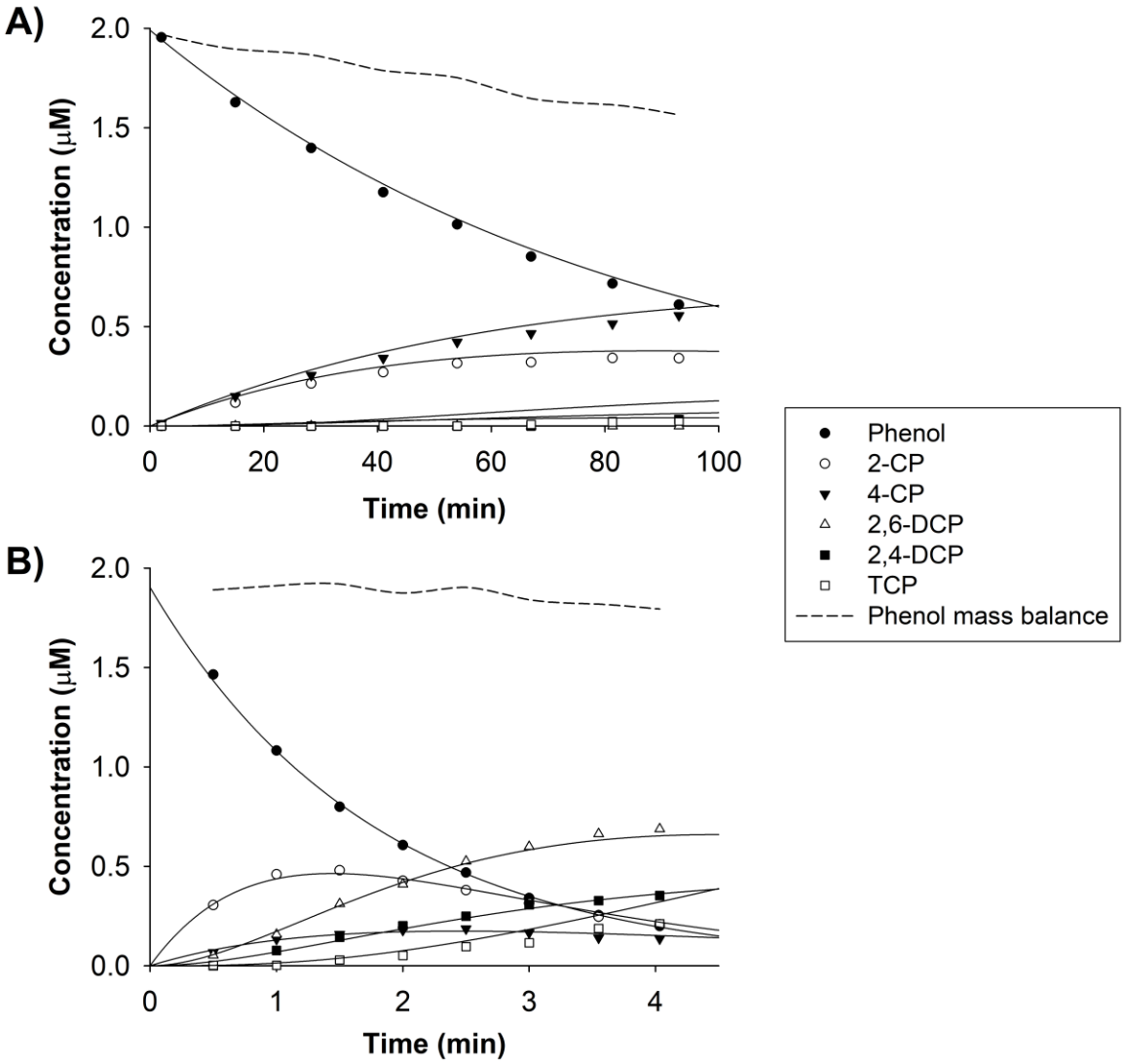

Figure 2-7. Typical reaction time courses for a reactor spiked with phenol at **(A)** pH 4.0 and **(B)** pH 8.4. Concentrations of the reaction products were also monitored. Experimental conditions: $[FAC]_o$ = 125 μM, $[phenol]_o$ = 2 μM, ionic strength = 0.1 M, [pH buffer] = 10 mM, T = 25 °C. No NaCl was added. Solid lines are model predictions based on the second-order rate constants in Table 2-1 and equation 2-6. Dashed lines represent the phenol mass balance (calculated as [phenol] + [2-CP] + [4-CP] + [2,6-DCP] + [2,4-DCP] + [TCP] measured in samples).

Table 2-2. Experimental Reaction Orders (n) and Calculated Reaction Orders (n_{calc}) in [HOCl] for Phenol in the Absence of Added Chloride [a]

pH	Range of $[FAC]_0$ (μM)	Experimental n	Range of n_{calc}	Average n_{calc}
4.7	125 – 640	1.71 ± 0.05	1.64 – 1.90	1.81
6.2	125 – 640	1.18 ± 0.15	1.02 – 1.11	1.07
10.8	125 – 640	0.907 ± 0.105	1.00 – 1.00	1.00

[a] Uncertainties indicate 95% confidence intervals.

Table 2-3. Experimental Reaction Orders (n) and Calculated Reaction Orders (n_{calc}) in [HOCl] for 4-CP in the Absence of Added Chloride [a]

pH	Range of $[FAC]_0$ (μM)	Experimental n	Range of n_{calc}	Average n_{calc}
4.1	160 – 805	1.94 ± 0.04	1.93 – 1.98	1.97
5.0	160 – 805	1.80 ± 0.09	1.59 – 1.88	1.78
6.0	120 – 610	1.34 ± 0.10	1.09 – 1.34	1.21
6.8	80 – 320	1.08 ± 0.06	1.01 – 1.04	1.02

[a] Uncertainties indicate 95% confidence intervals.

Comparisons with Previous Results. This is the first investigation on the roles of Cl_2, Cl_2O, and HOCl in the chlorination of all six (chloro)phenols. Our experimental results highlight the role of Cl^- as a catalyst for the reactions of (chloro)phenols at low pH and reveal the importance of Cl_2 as a chlorinating agent. Although Lee and Morris[32] previously speculated that Cl_2 could influence the reaction kinetics of (chloro)phenols, they did not conduct experiments specifically designed to reveal the importance of Cl_2. Grimley and Gordon[45] demonstrated that the rate of phenol chlorination at $[H^+] = 0.023$ M (pH < 2) increased with varying $[Cl^-]$ (2.1–100 mM) while the ionic strength was maintained at 1.00 M, but the data set is limited to a single pH value. Our experiments conducted at different values of $[Cl^-]_{added}$ and pH allowed us to compute robust second-order rate constants for Cl_2.

In their study on (chloro)phenol reactions, Gallard and von Gunten[6] considered reactions with both HOCl and H_2OCl^+ when developing kinetic models for phenol and 4-CP, whereas only the reactions with HOCl were considered for the other (chloro)phenols. The best-fit estimates of $k_{\mathrm{HOCl,\,ArO^-}}$ in this study are generally similar to those reported by Gallard and von Gunten. The exception is TCP; the previously reported $k_{\mathrm{HOCl,\,ArO^-}}$ (12.84 ± 0.69 M^{-1} s^{-1}) is more than three times larger than our estimate (3.39 ± 0.47 M^{-1} s^{-1}). Gallard and von Gunten might have overestimated $k_{\mathrm{HOCl,\,ArO^-}}$ by attributing reactivities of TCP towards Cl_2 and Cl_2O to reactions with HOCl. Although Gallard and von Gunten reported values of $k_{\mathrm{HOCl,\,ArOH}}$ for phenol and 4-CP, we found that it is not necessary to include a term for the HOCl/ArOH reaction in order for our model (equation 2-6) to fit our experimental data.

When we considered the presence of trace Cl^- in the no-NaCl-added reactors and included the $k_{Cl_2,\,ArOH}$ and $k_{Cl_2,\,ArO^-}$ terms in our model for phenol, 2-CP, and 4-CP (equation 2-6), we were able to fit the no-added-chloride data at low pH without invoking H_2OCl^+ as a reactive species. If H_2OCl^+ were the sole chlorinating agent for (chloro)phenols at low pH, varying $[Cl^-]_{added}$ under conditions of uniform ionic strength would not affect the value of k_{obs} because $[H_2OCl^+]$ depends only on [HOCl] and $[H^+]$. We recognize that the presence of Cl_2 does not necessarily preclude the involvement of H_2OCl^+ in (chloro)phenol reactions, since the speciations of Cl_2 and H_2OCl^+ parallel each other at low pH (**Figure 2-1**). In order to fully elucidate the importance of H_2OCl^+, we would need to conduct experiments at $[Cl^-] \ll [FAC]_o$ to minimize the influence of Cl_2. As so little chloride is required for appreciable quantities of Cl_2 to be generated, however, the relevance of H_2OCl^+ for (chloro)phenols is dubious. Therefore, while we cannot rule out H_2OCl^+ as a reactive chlorine species based on our experimental and modeling results, we have shown that it is not necessary to invoke H_2OCl^+ in order to explain the chlorination kinetics of (chloro)phenols.

In their study on the halogenation kinetics of 2,4-DCP, Vikesland et al.[33] considered the reactions with Cl_2, Cl_2O, and HOCl when modeling 2,4-DCP reactivity at pH 5–10. These researchers computed the following second-order rate constants from the log k_{obs} versus pH data collected at a single set of $[Cl^-]$ and $[FAC]_o$: $k_{Cl_2,\,ArOH}$ = 30 (± 17) $M^{-1}\,s^{-1}$, $k_{HOCl,\,ArOH}$ = 23 (± 13) $M^{-1}\,s^{-1}$, and $k_{HOCl,\,ArO^-}$ = 660 (± 130) $M^{-1}\,s^{-1}$. Vikesland et al. were not able to obtain an estimate of k_{Cl_2O}, but our modeling results suggest that the influence of Cl_2O on 2,4-DCP reactivity should be insignificant at the low $[FAC]_o$ (10 μM) used in their experiments. In contrast, our findings reveal that Cl_2

reacts primarily with the ArO^- form—rather than with the ArOH form—of 2,4-DCP. The $k_{HOCl,\,ArO^-}$ computed by Vikesland et al. is about twice as large as our estimate (309 ± 19 M^{-1} s^{-1}), suggesting that the authors might have overestimated $k_{HOCl,\,ArO^-}$ because they did not consider the reaction of Cl_2 with ArO^-. The discrepancies between the findings of Vikesland et al.[33] and this study underscore the need to systematically vary solution pH, $[FAC]_o$, and $[Cl^-]$ in order to obtain robust estimates of the second-order rate constants for HOCl, Cl_2O, and Cl_2.

Linear Free Energy Relationships. Hammett-type correlations were constructed for $k_{HOCl,\,ArO^-}$, $k_{Cl_2,\,ArO^-}$, and $k_{Cl_2O,\,ArOH}$ using the substituent constants in ref. 44 (**Table 2-1**). As shown in **Figure 2-8a**, the Hammett plots for both the HOCl/ArO^- and Cl_2/ArO^- reactions have negative slopes (ρ), as expected if the rate-determining step involved electrophilic aromatic substitution. Furthermore, the value of ρ for the HOCl/ArO^- reaction (–2.09 ± 1.00) is not significantly different from that computed by Gallard and von Gunten[6] (–3.00 ± 0.22). Although our ρ value has a relatively large uncertainty, we would expect it to be similar to that determined by Gallard and von Gunten since our estimates of $k_{HOCl,\,ArO^-}$ are generally quite similar.

The Hammett plot for the Cl_2O/ArOH reaction is distinct from those for the HOCl/ArO^- and Cl_2/ArO^- reactions. As shown in **Figure 2-8b**, the Cl_2O/ArOH Hammett plot has a small positive ρ value (0.829 ± 0.568), suggesting that the rate-determining step may not be electrophilic aromatic substitution. Small ρ values are often associated with free-radical reactions, as in the case of hydroxyl radicals ($^{\bullet}OH$),[46] and some researchers have proposed that Cl_2O reacts with organic compounds in solution via free-radical pathways, with $Cl^{\bullet}$ and $ClO^{\bullet}$ from the photolysis of Cl_2O implicated in those

reactions.[47] Our use of amber glass vials as reactors, however, would reduce the likelihood of photocatalyzed reactions.

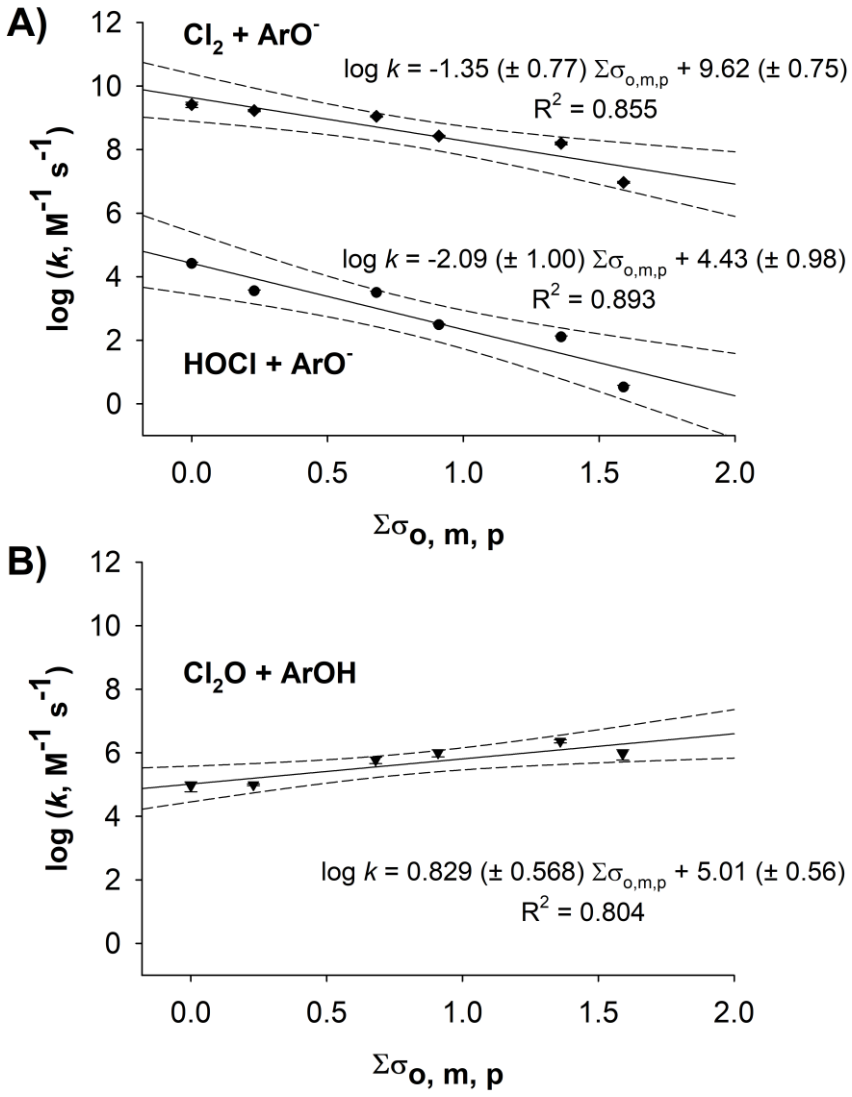

Figure 2-8. Hammett-type linear free energy relationships for (chloro)phenol reactions in FAC correlating **(A)** $k_{Cl_2,\ ArO^-}$ and $k_{HOCl,\ ArO^-}$ as well as **(B)** $k_{Cl_2O,\ ArOH}$. ArOH and ArO^- denote the conjugate acid and phenolate forms, respectively. Error bars (smaller than symbols if not shown) and uncertainties in the equations indicate 95% confidence intervals.

In addition, analysis of our FAC solutions using electron paramagnetic resonance (EPR) spectroscopy did not provide compelling evidence for the presence of radical species. Even though an EPR signal was observed (**Figure 2-9a**) upon adding the spin trap agent 5,5-dimethyl-1-pyrroline-*N*-oxide (DMPO) to a FAC solution at pH < 3, simulation of the experimental EPR spectrum using *WinSim 2002* (**Figure 2-9b**) yielded hyperfine splitting constants that are consistent with the one-electron oxidation product of DMPO.[48] Therefore, the observed EPR signal was due to an experimental artifact (possibly the oxidation of DMPO by FAC) rather than to the genuine trapping of a radical species.

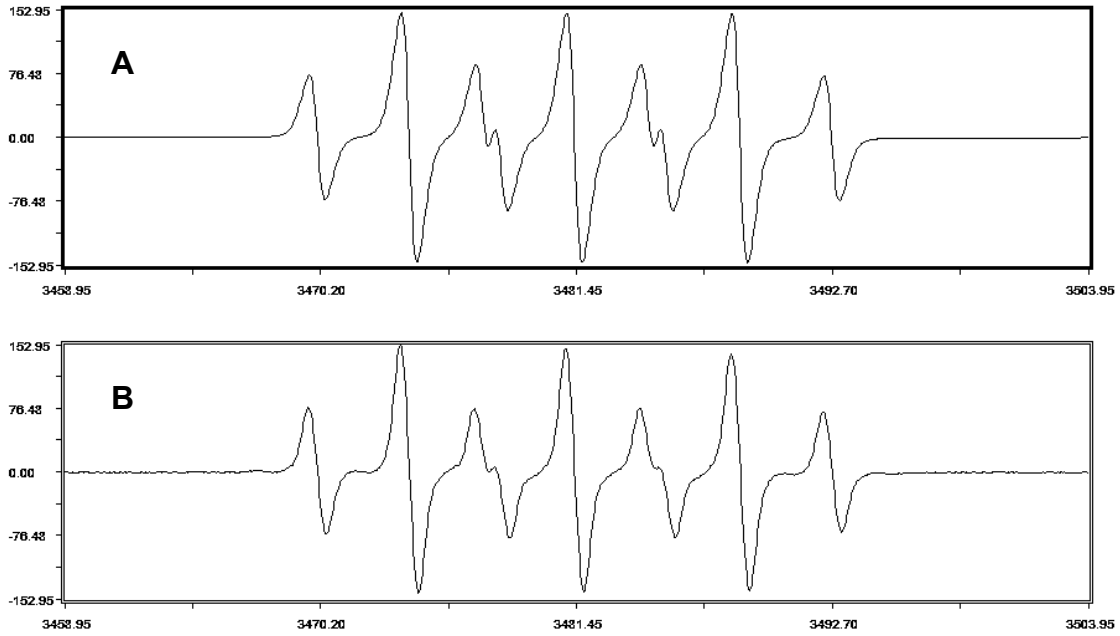

Figure 2-9. (A) EPR spectrum of an FAC solution (~100 μM) adjusted to pH < 3 with HNO_3 and mixed with 5,5-dimethyl-1-pyrroline-*N*-oxide (DMPO). EPR conditions: room temperature (~22 °C), microwave frequency 9.78 GHz, microwave power 10 mW, modulation amplitude 1.0 G, time constant 81.9 ms, and conversion time 41 s. No signal was observed in the absence of DMPO. **(B)** Simulation of (A) in *WinSim 2002* using two radical species. Species 1 consists of one atom with spin 1 and a^H = 7.26 G. Species 2 consists of two atoms with spin ½ and a^H = 4.04 G.

Environmental Implications. Using the second-order rate constants in **Table 2-1**, we calculated the pseudo-first-order rate coefficients (k_{calc}) that would result if we assumed $[FAC]_o$ values that are closer to the chlorine doses typically used in drinking water and wastewater treatments. We then calculated the contributions of different reactions to the overall reactivities of the (chloro)phenols as fractions of k_{calc}. The results for phenol and TCP are shown in **Figures 2-10 and 2-11**, respectively. For phenol, the Cl_2/ArOH reaction predominates at low pH and the HOCl/ArO^- reaction predominates at circum-neutral and high pH under typical drinking water treatment conditions (**Figure 2-10a**), in the presence of excess Cl^- (**Figure 2-10b**), and under typical wastewater treatment conditions (**Figure 2-10c**). The importance of the Cl_2/ArO^- reaction increases in the presence of high [Cl^-], a situation that is likely to occur when chlorinating desalinated water or water with $FeCl_3$ added as a coagulant. The Cl_2O/ArOH reaction remains unimportant for phenol in all the assumed scenarios. The situation for TCP is different; reactions with Cl_2 and Cl_2O represent significant fractions of k_{calc} at circum-neutral pH in all situations (**Figure 2-11**).

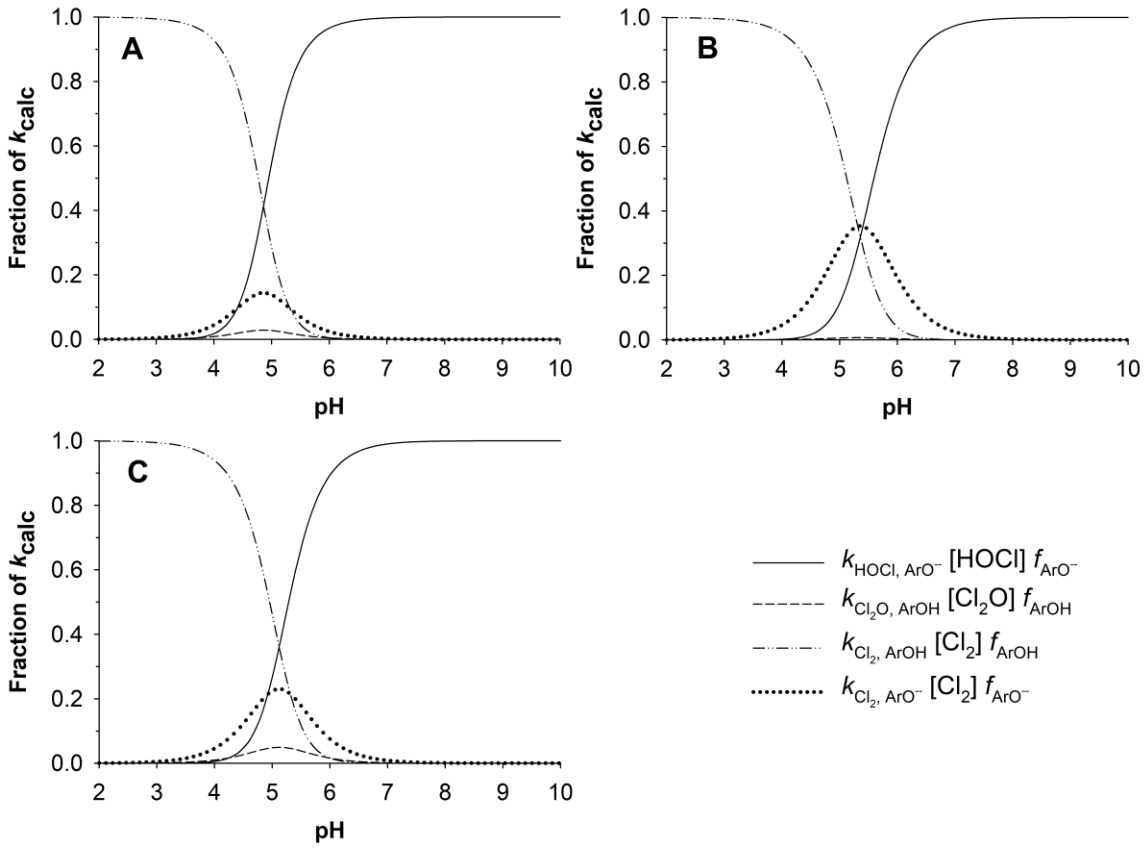

Figure 2-10. Contributions of Cl_2, Cl_2O, and HOCl to phenol reactivity (represented as fractions of k_{calc}) **(A)** under typical drinking water treatment conditions ([FAC] = 28 μM, [Cl^-] = 0.3 mM), **(B)** in the presence of excess chloride ([FAC] = 28 μM, [Cl^-] = 3 mM), and **(C)** under typical wastewater treatment conditions ([FAC] = 100 μM, [Cl^-] = 1 mM). ArOH and ArO^- denote the conjugate acid and phenolate forms, respectively.

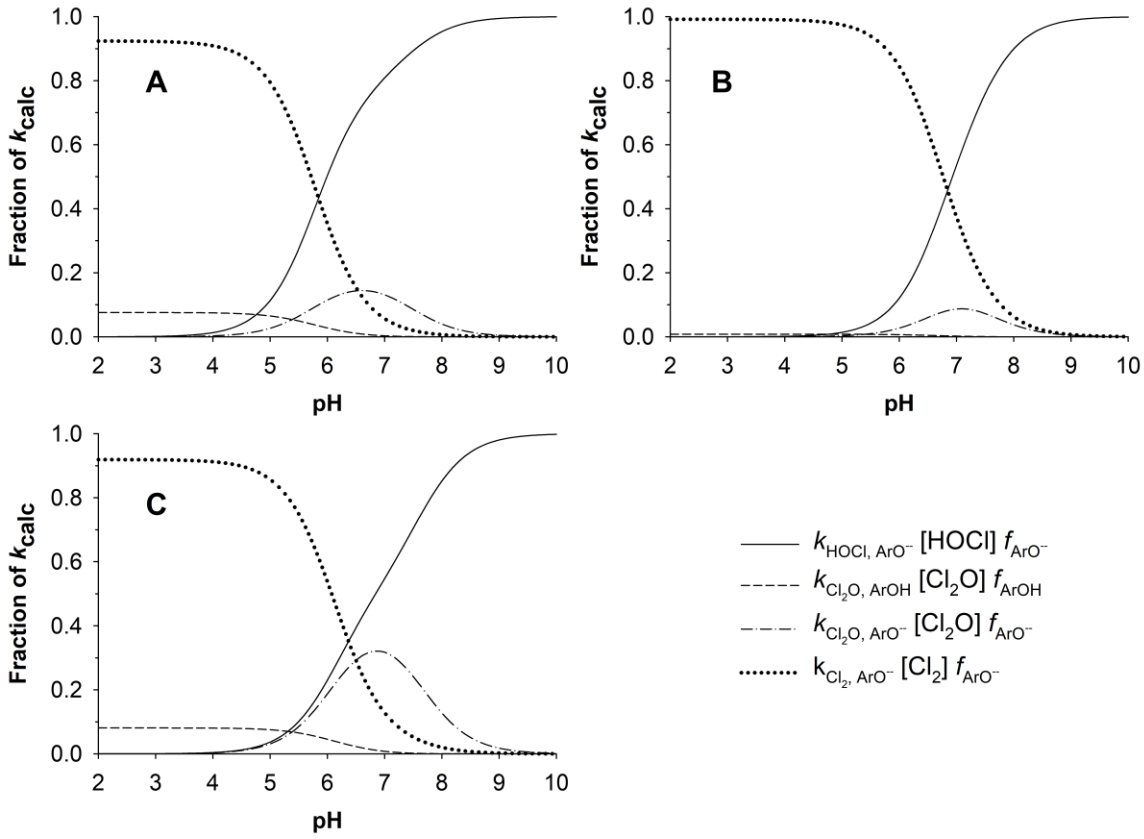

Figure 2-11. Contributions of Cl_2, Cl_2O, and HOCl to 2,4,6-trichlorophenol (TCP) reactivity (represented as fractions of k_{calc}) **(A)** under typical drinking water treatment conditions ([FAC] = 28 μM, [Cl^-] = 0.3 mM), **(B)** in the presence of excess chloride ([FAC] = 28 μM, [Cl^-] = 3 mM), and **(C)** under typical wastewater treatment conditions ([FAC] = 100 μM, [Cl^-] = 1 mM). ArOH and ArO^- denote the conjugate acid and phenolate forms, respectively.

In accordance with the reactivity-selectivity principle,[49] we hypothesized that the less reactive (i.e., the more highly chlorinated) (chloro)phenols would be more selective towards Cl_2 and Cl_2O. Our results show that, at a fixed pH, the contributions of Cl_2 and Cl_2O towards k_{calc} relative to the contribution of HOCl increase as the overall reactivity of the (chloro)phenol decreases (**Figure 2-12a**). At a higher [Cl^-], the reactions with Cl_2 contribute substantially more towards k_{calc} than they do at a lower [Cl^-], and the importance of Cl_2 as a chlorinating agent is the greatest for the most highly chlorinated/least reactive compound (**Figure 2-12b**). The contribution of Cl_2O, on the other hand, is trivial for most of the (chloro)phenols. The insignificance of Cl_2O for (chloro)phenols is in contrast to the findings from previous studies on the chlorination kinetics of dimethenamid,[22] aromatic ethers,[23] and antipyrine.[19]

One consequence of the tradeoff between reactivity and selectivity is that Cl_2 and Cl_2O are expected to be more important for the slow-reacting NOM fraction than for a fast-reacting one. The kinetics of DBP formation from NOM can be divided into two phases. The "fast" reactions occur within seconds to minutes; the "slow" reactions occur on the order of hours to days, much longer than the time scale of Cl_2 and Cl_2O regeneration in aqueous chlorine solutions (see discussion of Cl_2 regeneration in Appendix A). One study has demonstrated that the fast-reacting trihalomethane (THM) precursors account for only 15–30% of all THM precursors in natural waters.[27] As most precursors of THMs and perhaps other DBPs belong to the slow-reacting NOM fraction, Cl_2 (and possibly Cl_2O) may have more influence on the kinetics of DBP formation than is presently recognized.

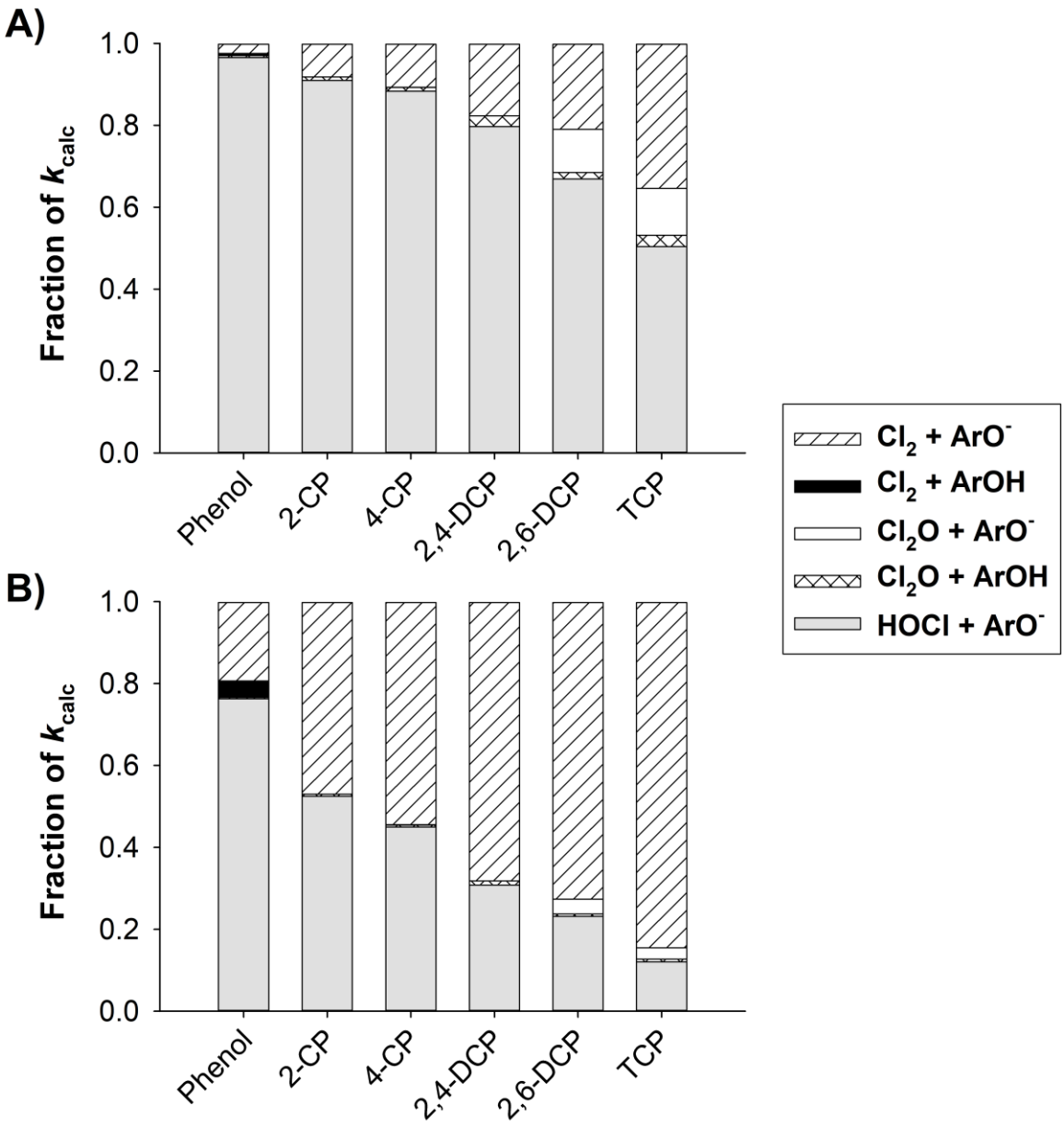

Figure 2-12. Contributions of Cl_2, Cl_2O, and HOCl to overall (chloro)phenol reactivities in FAC (represented as fractions of k_{calc}) **(A)** under drinking water treatment conditions (pH 6, [FAC] = 28 μM, [Cl^-] = 0.3 mM) and **(B)** in the presence of excess chloride (pH 6, [FAC] = 28 μM, [Cl^-] = 3 mM). ArOH and ArO^- denote the conjugate acid and phenolate forms, respectively.

The roles of Cl_2 and Cl_2O as chlorinating agents are often overlooked because of the low concentrations of these chlorine species under typical water treatment conditions. In most studies, second-order rate constants were computed by dividing the experimental pseudo-first-order rate coefficients by $[HOCl]_T$ or $[FAC]_o$, thus assuming that HOCl is the only chlorinating agent present and that the reactions are first-order in [FAC]. Nonetheless, laboratory experiments often employ reaction conditions that favor Cl_2 and Cl_2O formation, so researchers may need to take these chlorinating agents into account when interpreting their experimental results. In addition, activities such as desalination, water recycling, and hydraulic fracturing can increase $[Cl^-]$ in raw water supplies. Chloride can also accumulate in swimming pools.[50] Therefore, Cl_2 could become an important chlorinating agent when water of impaired quality or water for recreation is chlorinated.

2. 5. Acknowledgements

We thank the late Dr. Justine Roth (Johns Hopkins University) for helpful discussions on EPR analysis and for the use of quartz flat cells. We thank Dr. Jung Yoon Lee for help with running the EPR spectrometer at JHU. We are also grateful to Dr. Neil Blough (University of Maryland, College Park) for his help on interpreting EPR spectra. This material is based upon work supported by the U.S. National Science Foundation (CBET-1067391 and the Graduate Research Fellowship to S.S.L. under Grant No. 123825).

2. 6. References

1. Richardson, S. D.; Plewa, M. J.; Wagner, E. D.; Schoeny, R.; DeMarini, D. M. Occurrence, genotoxicity, and carcinogenicity of regulated and emerging disinfection by-products in drinking water: A review and roadmap for research. *Mutat. Res.* **2007,** *636*, 178-242.

2. Deborde, M.; von Gunten, U. Reactions of chlorine with inorganic and organic compounds during water treatment – Kinetics and mechanisms: A critical review. *Water Res.* **2008,** *42*, 13-51.

3. Morris, J. C. The acid ionization constant of HOCl from 5 to 35°. *J. Phys. Chem.* **1966,** *70*, 3798-3805.

4. Swain, C. G.; Crist, D. R. Mechanisms of chlorination by hypochlorous acid. The last of chlorinium ion, Cl^+. *J. Am. Chem. Soc.* **1972,** *94*, 3195-3200.

5. Rebenne, L. M.; Gonzalez, A. C.; Olson, T. M. Aqueous chlorination kinetics and mechanism of substituted dihydroxybenzenes. *Environ. Sci. Technol.* **1996,** *30*, 2235-2242.

6. Gallard, H.; Von Gunten, U. Chlorination of phenols: Kinetics and formation of chloroform. *Environ. Sci. Technol.* **2002,** *36*, 884-890.

7. Deborde, M.; Rabouan, S.; Gallard, H.; Legube, B. Aqueous chlorination kinetics of some endocrine disruptors. *Environ. Sci. Technol.* **2004,** *38*, 5577-5583.

8. Gallard, H.; Leclercq, A.; Croué, J.-P. Chlorination of bisphenol A: kinetics and by-products formation. *Chemosphere* **2004,** *56*, 465-473.

9. Pinkston, K. E.; Sedlak, D. L. Transformation of aromatic ether- and amine-containing pharmaceuticals during chlorine disinfection. *Environ. Sci. Technol.* **2004,** *38*, 4019-4025.

10. Chusaksri, S.; Sutthivaiyakit, S.; Sedlak, D. L.; Sutthivaiyakit, P. Reactions of phenylurea compounds with aqueous chlorine: Implications for herbicide transformation during drinking water disinfection. *J. Hazard. Mater.* **2012,** *209–210*, 484-491.

11. Qin, L.; Lin, Y.-L.; Xu, B.; Hu, C.-Y.; Tian, F.-X.; Zhang, T.-Y.; Zhu, W.-Q.; Huang, H.; Gao, N.-Y. Kinetic models and pathways of ronidazole degradation by chlorination, UV irradiation and UV/chlorine processes. *Water Res.* **2014,** *65*, 271-281.

12. Lane, R. F.; Adams, C. D.; Randtke, S. J.; Carter Jr, R. E. Chlorination and chloramination of bisphenol A, bisphenol F, and bisphenol A diglycidyl ether in drinking water. *Water Res.* **2015,** *79*, 68-78.

13. Arotsky, J.; Symons, M. C. R. Halogen cations. *Q. Rev. Chem. Soc.* **1962,** *16*, 282-297.

14. Morris, J. C. The chemistry of aqueous chlorine in relation to water chlorination. In *Water Chlorination: Environmental Impact and Health Effects*, Jolley, R. L., Ed. Ann Arbor Science Publishers: Ann Arbor, Michigan, 1978; Vol. 1, pp 21-35.

15. Wang, T. X.; Margerum, D. W. Kinetics of reversible chlorine hydrolysis: Temperature dependence and general-acid/base-assisted mechanisms. *Inorg. Chem.* **1994,** *33*, 1050-1055.

16. Cherney, D. P.; Duirk, S. E.; Tarr, J. C.; Collette, T. W. Monitoring the speciation of aqueous free chlorine from pH 1 to 12 with Raman spectroscopy to determine the identity of the potent low-pH oxidant. *Appl. Spectrosc.* **2006,** *60*, 764-772.

17. Dodd, M. C.; Huang, C. H. Aqueous chlorination of the antibacterial agent trimethoprim: Reaction kinetics and pathways. *Water Res.* **2007,** *41*, 647-655.

18. Wang, P.; He, Y.-L.; Huang, C.-H. Reactions of tetracycline antibiotics with chlorine dioxide and free chlorine. *Water Res.* **2011,** *45*, 1838-1846.

19. Cai, M.-Q.; Feng, L.; Jiang, J.; Qi, F.; Zhang, L.-Q. Reaction kinetics and transformation of antipyrine chlorination with free chlorine. *Water Res.* **2013,** *47*, 2830-2842.

20. Soufan, M.; Deborde, M.; Delmont, A.; Legube, B. Aqueous chlorination of carbamazepine: Kinetic study and transformation product identification. *Water Res.* **2013,** *47*, 5076-5087.

21. Cheng, H.; Song, D.; Chang, Y.; Liu, H.; Qu, J. Chlorination of tramadol: Reaction kinetics, mechanism and genotoxicity evaluation. *Chemosphere* **2015,** *141*, 282-289.

22. Sivey, J. D.; McCullough, C. E.; Roberts, A. L. Chlorine monoxide (Cl_2O) and molecular chlorine (Cl_2) as active chlorinating agents in reaction of dimethenamid with aqueous free chlorine. *Environ. Sci. Technol.* **2010,** *44*, 3357-3362.

23. Sivey, J. D.; Roberts, A. L. Assessing the reactivity of free chlorine constituents Cl_2, Cl_2O, and HOCl toward aromatic ethers. *Environ. Sci. Technol.* **2012,** *46*, 2141-2147.

24. Abdallah, P.; Deborde, M.; Dossier Berne, F.; Karpel Vel Leitner, N. Kinetics of chlorination of benzophenone-3 in the presence of bromide and ammonia. *Environ. Sci. Technol.* **2015,** *49*, 14359-14367.

25. Tawk, A.; Deborde, M.; Labanowski, J.; Gallard, H. Chlorination of the β-triketone herbicides tembotrione and sulcotrione: Kinetic and mechanistic study, transformation products identification and toxicity. *Water Res.* **2015,** *76*, 132-142.

26. Gao, Y.; Pang, S.-Y.; Jiang, J.; Ma, J.; Zhou, Y.; Li, J.; Wang, L.-H.; Lu, X.-T.; Yuan, L.-P. Transformation of flame retardant tetrabromobisphenol A by aqueous chlorine and the effect of humic acid. *Environ. Sci. Technol.* **2016,** *50*, 9608-9618.

27. Gallard, H.; von Gunten, U. Chlorination of natural organic matter: kinetics of chlorination and of THM formation. *Water Res.* **2002,** *36*, 65-74.

28. Czaplicka, M. Sources and transformations of chlorophenols in the natural environment. *Sci. Total Environ.* **2004,** *322*, 21-39.

29. Burttschell, R. H.; Rosen, A. A.; Middleton, F. M.; Ettinger, M. B. Chlorine derivatives of phenol causing taste and odor. *J. Am. Water Works Assoc.* **1959,** *51*, 205-214.

30. Arnold, W. A.; Bolotin, J.; Von Gunten, U.; Hofstetter, T. B. Evaluation of functional groups responsible for chloroform formation during water chlorination using compound specific isotope analysis. *Environ. Sci. Technol.* **2008,** *42*, 7778-7785.

31. Guo, G.; Chen, X. Halogenating reaction activity of aromatic organic compounds during disinfection of drinking water. *J. Hazard. Mater.* **2009,** *163*, 1207-1212.

32. Lee, G. F.; Morris, J. C. Kinetics of chlorination of phenol – Chlorophenolic tastes and odors. *Int. J. Air Water Pollut.* **1962,** *6*, 419-431.

33. Vikesland, P. J.; Fiss, E. M.; Wigginton, K. R.; McNeill, K.; Arnold, W. A. Halogenation of bisphenol-A, triclosan, and phenols in chlorinated waters containing iodide. *Environ. Sci. Technol.* **2013,** *47*, 6764-6772.

34. Roth, W. A. Note on thermo-chemistry of chlorine monoxide. *Z. Phys. Chem. Abt. A* **1942,** *191*, 248-250.

35. American Public Health Association (APHA). *Standard Methods for the Examination of Water and Wastewater*, 18th ed.; American Public Health Association, American Water Works Association, Water Environment Federation: Washington, DC, 1992.

36. Zumdahl, S. S. Chemical Principles. 6 ed.; Houghton Mifflin: 2009; pp 723-726.

37. Bichsel, Y.; von Gunten, U. Determination of iodide and iodate by ion chromatography with postcolumn reaction and UV/visible detection. *Anal. Chem.* **1999,** *71*, 34-38.

38. Georgi, A.; Reichl, A.; Trommler, U.; Kopinke, F.-D. Influence of sorption to dissolved humic substances on transformation reactions of hydrophobic organic compounds in water. I. Chlorination of PAHs. *Environ. Sci. Technol.* **2007,** *41*, 7003-7009.

39. Israel, G. C. The kinetics of chlorohydrin formation. Part II. The reaction between hypochlorous acid and allyl alcohol in the presence of sodium acetate-acetic acid buffers of constant pH. *J. Chem. Soc.* **1950**, 1286-1289.

40. Anbar, M.; Dostrovsky, I. Ultra-violet absorption spectra of some organic hypohalites. *J. Chem. Soc.* **1954**, 1105-1108.

41. Chung, A.; Israel, G. C. The kinetics of chlorohydrin formation. Part VIII. The reaction between hypochlorous acid and allyl acetate in the presence of sodium acetate-acetic acid buffers of constant pH. *J. Chem. Soc.* **1955**, 2667-2673.

42. de la Mare, P. B. D.; Hilton, I. C.; Varma, S. The kinetics and mechanisms of aromatic halogen substitution. Part IX. Mixtures of acetic acid and aqueous hypochlorous acid. *J. Chem. Soc.* **1960**, 4044-4054.

43. Jia, Z.; Margerum, D. W.; Francisco, J. S. General-acid-catalyzed reactions of hypochlorous acid and acetyl hypochlorite with chlorite ion. *Inorg. Chem.* **2000,** *39*, 2614-2620.

44. Barlin, G. B.; Perrin, D. D. Prediction of the strengths of organic acids. *Q. Rev. Chem. Soc.* **1966,** *20*, 75-101.

45. Grimley, E.; Gordon, G. Kinetics and mechanism of reaction between chlorine and phenol in acidic aqueous solution. *J. Phys. Chem.* **1973,** *77*, 973-978.

46. Gligorovski, S.; Strekowski, R.; Barbati, S.; Vione, D. Environmental implications of hydroxyl radicals (•OH). *Chem. Rev.* **2015,** *115*, 13051-13092.

47. Renard, J. J.; Bolker, H. I. The chemistry of chlorine monoxide (dichlorine monoxide). *Chem. Rev.* **1976,** *76*, 487-508.

48. Evans, J. C.; Jackson, S. K.; Rowlands, C. C.; Barratt, M. D. An electron spin resonance study of radicals from chloramine-T — 1 : Spin trapping of radicals produced in acid media. *Tetrahedron* **1985,** *41*, 5191-5194.

49. Anslyn, E. V.; Dougherty, D. A. Modern Physical Organic Chemistry. University Science: 2006.

50. E, Y.; Bai, H.; Lian, L.; Li, J.; Blatchley, E. R., III. Effect of chloride on the formation of volatile disinfection byproducts in chlorinated swimming pools. *Water Res.* **2016,** *105*, 413-420.

3. Quenching and Quantifying Free Chlorine and Free Bromine Using 1,3,5-Trimethoxybenzene (TMB) *

3. 1. Abstract

Choosing an appropriate quencher for free chlorine and free bromine is a critical part of disinfection byproduct (DBP) research. The ideal quencher needs to react rapidly with free halogens, be inert with analytes of interest, and not interfere with the quantitation of those analytes. Commonly used quenchers, such as sodium sulfite, sodium thiosulfate, and ascorbic acid, are known to rapidly covert free chlorine and free bromine into chloride and bromide, respectively. The reducing capabilities of these quenchers, however, can lead to the degradation of some redox-labile analytes. Ammonium chloride, often used to quench free chlorine via the formation of monochloramine, would be inappropriate for analytes that are susceptible to chloramination. We propose an alternative approach using 1,3,5-trimethoxybenzene (TMB) to quench free chlorine and free bromine. The chlorination of 2,4-dichlorophenol and the bromination of anisole were chosen to explore the feasibility of TMB serving as a free halogen quencher. Although TMB does not react with free chlorine as quickly as do traditional quenchers, we found that there was generally no significant difference in the experimental rate constants (k_{obs}) with TMB versus sodium thiosulfate as the quencher. By monitoring the chlorination and bromination products of TMB, we were also able to quantify residual free halogens in the quenched samples. Furthermore, our results indicate that TMB does not affect the

* A version of this chapter has been submitted to *Water Research* as: Lau, S.S., Dias, R.P., Martin-Culet, K.R., Race, N.A., Roberts, A.L., and Sivey, J.D. Quenching and Quantifying Free Chlorine and Free Bromine Using 1,3,5-Trimethoxybenzene (TMB). S.S.L. collected approximately 65% of the experimental data and did 75% of the writing.

stabilities of selected DBPs (chloropicrin, chloral hydrate, tribromoacetaldehyde, and haloacetonitriles) that otherwise degrade in the presence of traditional quenchers. TMB could, therefore, be an appropriate quencher for free chlorine and free bromine in aqueous halogenation experiments involving redox-labile analytes and/or when selective quantification of residual free halogens is desired.

3. 2. Introduction

Quenching residual oxidants is indispensable for identifying and quantifying disinfection byproducts (DBPs), which are often produced when a chemical disinfectant (an oxidant) is applied to treat water containing organic matter. Various methods exist for quenching free chlorine, which is the most widely used disinfectant for drinking water treatment in the United States.[1] When choosing an appropriate quencher, previous researchers usually sought the following characteristics: "(1) rapid and complete reaction with residual oxidants; (2) chemical inertness towards the analytes; (3) negligible effects on quantitation; and (4) undetectable signal (for itself or its reaction products)".[2] The first three characteristics are especially important for researchers who wish to determine the kinetics of DBP (trans)formation. The fourth characteristic is considered desirable because a quencher that cannot be detected by the analytical instrument employed would not be expected to interfere with analyte signals.

Reagents that are commonly used to quench free chlorine can be divided into two major categories. The first category of quenchers reduces free chlorine (Cl(+I) or Cl(0)) to chloride (Cl^-).[3] Examples of such quenchers are sodium thiosulfate ($Na_2S_2O_3$), sodium sulfite (Na_2SO_3), and ascorbic acid. The high redox reactivities of these compounds

towards free chlorine lead to rapid quenching; the downside is that these compounds can transform analytes that are redox active. Sodium sulfite, for instance, can dehalogenate chloropicrin, trichloroacetonitrile, and dibromoacetonitrile.[4-5] Sodium thiosulfate can reduce *N*-acetyl-*p*-benzoquinone imine and 1,4-benzoquinone to acetaminophen and 1,4-hydroquinone, respectively.[6] Ascorbic acid can convert the chlorination product of the antiretroviral drug nevirapine back into the parent compound.[7] Moreover, sodium sulfite, sodium thiosulfate, and ascorbic acid can reduce *N*-chloro-2,2-dichloroacetamide to 2,2-dichloroacetamide, leading to erroneous identification of the latter as a drinking water DBP.[8]

The other major category of quenchers reacts with free chlorine to form monochloramine (NH_2Cl), which generally reacts with organic compounds more slowly than does free chlorine.[3] Ammonium chloride (NH_4Cl) is the most commonly encountered quencher in this category; it is considered to be a "soft" quencher since it does not reduce/transform redox-labile organic compounds such as sulfamethoxazole[9] and tramadol.[10] Nonetheless, some organic compounds (e.g., phenols) can react with monochloramine.[11] Although chloramination reactions tend to be slower than chlorination reactions, using ammonium chloride to quench free chlorine may affect the quantitation of analytes if the sample storage time is prolonged. Ammonium chloride may be particularly problematic for water samples that contain free bromine because bromamines are relatively potent brominating agents for organic compounds.[12]

We propose that 1,3,5-trimethoxybenzene (TMB) could serve as an effective quencher for free chlorine and free bromine without the limitations of traditional quenchers. Unlike traditional quenchers, TMB reacts with free chlorine to form a

chlorinated product (**Scheme 3-1**) that can be readily analyzed via gas chromatography-mass spectrometry (GC-MS). As such, when present in sufficient excess, TMB can both quench and rapidly convert free chlorine into a single, stable product (2-chloro-1,3,5-trimethoxybenzene).[13] When free bromine is present, as in the case of chlorinating bromide-containing waters, TMB also reacts rapidly with free bromine to form a single, stable product (2-bromo-1,3,5-trimethoxybenzene).[14] Quantifying the monohalogenated products of TMB could, therefore, allow researchers to selectively determine the concentrations of free chlorine and free bromine in aqueous solutions.

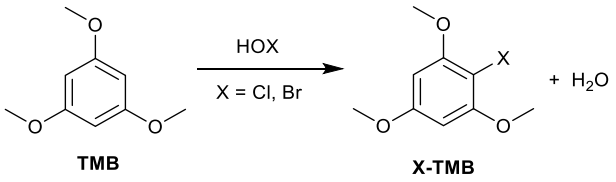

Scheme 3-1. Reactions of free chlorine and free bromine with excess 1,3,5-trimethoxybenzene (TMB) form monochlorinated and monobrominated products (X-TMB).

The objective of this study was to evaluate TMB as a quencher for free chlorine and free bromine in aqueous halogenation experiments. Rate constants for the chlorination of 2,4-dichlorophenol and the bromination of anisole were determined with TMB as the free halogen quencher and compared to values obtained using sodium thiosulfate as the quencher. We chose to examine these halogenation reactions because their rate constants have previously been reported in the literature.[15-16] Unreacted TMB and its monohalogenated products were also analyzed to quantify residual free chlorine

and free bromine in quenched samples. Furthermore, the stabilities of several DBPs in the presence of TMB were assessed in batch reactors over 7 days. Findings from our work could expand the choice of free halogen quenchers for future DBP studies and related experiments involving redox-labile analytes.

3. 3. Materials and Methods

All aqueous solutions were prepared using deionized water further purified with a Nanopure Analytical UV system (Thermo Scientific) or distilled water purified with a Milli-Q Advantage A10 system (EMD Millipore) to a resistivity of 18.2 MΩ•cm. Laboratory-grade sodium hypochlorite (NaOCl, ~6% w/w, Fisher Scientific) served as the source of free chlorine and was standardized via iodometric titration.[17] Working solutions of free chlorine were prepared daily by diluting the NaOCl stock solution with water and were standardized via UV-vis spectrophotometry.[18] Additional reagents are described in Appendix B; the procedure for synthesizing 2,4-dichloro-1,3,5-trimethoxybenzene is also provided in Appendix B.

Stoichiometry of TMB Reactions with Free Chlorine and Free Bromine. The ability of TMB to stoichiometrically convert residual free chlorine and free bromine into unique halogenated products was investigated via halogenation reactions performed at room temperature (21 ± 1 ºC). Chlorination reactors (total volume = 25 mL) were prepared in 40-mL amber glass vials and contained borate buffer (20 mM, adjusted to pH 8.00 using HNO_3), $NaNO_3$ (0.1 M), and NaOCl (5.0–46 μM). Following NaOCl dosing, vials were capped and shaken vigorously for 10 seconds. Bromination reactors were prepared in 40-mL amber glass vials and contained borate buffer (20 mM, adjusted to pH 8.00 using

HNO_3), $NaNO_3$ (0.1 M), NaBr (5.0–60 μM), and NaOCl (65 μM). Following NaOCl addition, reactors were capped, shaken vigorously for 10 seconds, and allowed to stand for 5 minutes to permit bromide oxidation by excess free chlorine. Three aliquots (1.00 mL each) were obtained from each reactor and transferred to a 4-mL amber glass vial pre-amended with TMB (0.150 mL at 360 μM, dissolved in methanol). Molar ratios of [TMB]-to-[free chlorine] ranged from 8:1 to 72:1; molar ratios of [TMB]-to-[free bromine] ranged from 6:1 to 72:1. The 4-mL vials were capped and shaken manually for 10 seconds and allowed to stand for 5 minutes for complete quenching. After all the samples from halogenation reactors were quenched with TMB, toluene (1.00 mL, containing 2-chlorobenzonitrile at 10.2 μM as the internal standard) was added to each 4-mL vial as the extraction solvent. Vials were capped and shaken manually. An aliquot of the toluene phase (0.20 mL) was transferred to a 0.3-mL glass insert seated inside an amber glass 2-mL autosampler vial. These vials were capped with a screw-top plastic cap fitted with a PFTE-lined septum. The concentrations of TMB, Cl-TMB, and Br-TMB in the toluene samples were determined using GC-MS (see Appendix B for method details).

TMB as a Quencher for Free Chlorine. The effectiveness of TMB in quenching free chlorine was assessed by determining rate constants for the chlorination of 2,4-dichlorophenol (2,4-DCP) at pH 7.08 and 9.14 using either TMB or sodium thiosulfate as the quencher. At each pH, two identical reactors (40-mL amber glass vials) were set up with 31 mL of reaction solution in each. The reaction solution consisted of phosphate buffer (10 mM, adjusted to pH 7.08 using NaOH) or carbonate buffer (10 mM, adjusted to pH 9.14 using NaOH), NaCl (5 mM), $NaNO_3$ (0.095 M), and NaOCl (128 μM). The reactors were kept in the dark inside a stainless-steel constant-temperature

water bath set at 25.00 ± 0.01 °C for ~8 minutes for temperature equilibration to occur. Previous work in our laboratory showed that free chlorine decay in the absence of 2,4-DCP was negligible at this timescale.[16] To initiate the reactions, each vial was spiked with 0.30 mL of 2,4-DCP solution (219 μM in water) using a glass syringe to yield an initial concentration of 2.1 μM. The vial was then capped, shaken vigorously, and returned to the water bath. At each sampling time, 2.0 mL of the reaction solution was transferred to a 4-mL amber glass vial pre-amended with 0.20 mL of either TMB (2.77 mM in 50 vol% water and 50 vol% methanol) or sodium thiosulfate (2.77 mM in water). For the experiment conducted at pH 9.14, the TMB quencher solution contained 0.1 M HNO_3 so as to lower the solution pH to 6–7 once reactor aliquots were added to the vials (because chlorination rate of TMB decreases as the pH increases). In all quenched samples, $[quencher]_o/[NaOCl]_o \geq 2.2$.

Liquid-liquid extractions were carried out after all samples were obtained and quenched. Toluene (0.80 mL with 2-chlorobenzonitrile at 97.6 μM as the internal standard) served as the extraction solvent and was added to each quenched sample. The 4-mL vials were then capped and shaken manually for 10 seconds. After waiting ≥ 3 minutes for phase separation to re-establish, a portion of the toluene phase (~ 0.5 mL) was transferred to a 2-mL amber glass autosampler vial and analyzed using GC-MS. Details of the analytical method for 2,4-DCP, TMB, and their chlorination products are in Appendix B.

TMB as a Quencher for Free Bromine. The performance of TMB as a quencher for kinetic experiments involving the bromination of anisole was examined via batch reactors. The experimental setup has been described previously.[15] Briefly, batch reactors

(total volume = 25 mL) were prepared in 40-mL amber glass vials and contained NaBr (130 μM), carbonate buffer (20 mM, adjusted to pH 7.48 using HNO_3) or borate buffer (20 mM, adjusted to pH 8.02, 8.50, or 9.02 using HNO_3), $NaNO_3$ (90 mM), NaCl (10 mM), and anisole (6.0 μM). The reactors were incubated in a circulating water bath at 20.00 ± 0.01 ºC for several minutes prior to dosing with NaOCl (305 μM) at t = 0. Following addition of NaOCl, vials were capped, shaken manually for 10 seconds, and returned to the water bath. Aliquots from the reactors (0.90 mL) were obtained periodically and transferred to 4-mL amber glass vials pre-amended with TMB. For the reactor at pH 7.48, 1.00 mL of TMB solution (938 μM dissolved in 80 vol% water and 20 vol% methanol) was present in each 4-mL glass vial. For reactors at pH ≥ 8.02, 0.210 mL of TMB solution (2.62 mM in methanol) was present in each 4-mL glass vial. The 4-mL vials were capped and shaken manually after aliquots from the reactors were added.

Once all samples were obtained and quenched, toluene (0.45 mL, containing 2-chlorobenzonitrile at 10.2 μM as the internal standard) was added to each 4-mL vial as the extraction solvent. Vials were capped and shaken manually. After phase separation was re-established, a portion of the toluene phase (0.2 mL) from each sample was transferred to a 0.3-mL glass insert seated inside an amber glass 2-mL autosampler vial. Autosampler vials were secured with a screw-top plastic cap fitted with a PTFE-lined septum. Anisole, TMB, as well as their monochlorinated and monobrominated products were analyzed concurrently via GC-MS. Details of the GC-MS analytical method are in Appendix B.

The experimental designs described in the preceding sections are consistent with the general approach of several previous studies of organic compound halogenation kinetics,[13, 15-16, 19-20] except that our prior studies employed sodium thiosulfate rather than TMB as a quencher. Solution conditions (e.g., temperature, pH range, and ionic strength) employed herein were selected to permit comparisons to prior studies.[15-16]

Competitive Quenching Experiments. The rate at which TMB reacts with free chlorine relative to four traditional quenchers (sodium sulfite, sodium thiosulfate, ascorbic acid, and ammonium chloride) was assessed via competitive quenching experiments. Each reactor (60-mL clear glass vials wrapped in aluminum foil) contained 50 mL of reaction solution, which consisted of phosphate buffer (10 mM, adjusted to pH 7.10 with NaOH), $NaNO_3$ (0.1 M), and NaOCl (52 μM). The reactors were kept in the dark inside a stainless-steel constant-temperature water bath set at 25.00 ± 0.01 °C. After waiting ~8 minutes for the reaction solution to achieve temperature equilibration, each reactor was spiked with 0.50 mL of a solution that contained equimolar concentrations of TMB and a non-TMB quencher (nominally 52 μM of each in 50 vol% water and 50 vol% methanol). The reactor was then capped, shaken vigorously, and returned to the water bath. After 5 minutes, 3.0 mL of the reaction solution from each reactor was transferred to a clear glass 15-mL centrifuge tube containing 1 mL of toluene (with 2-chlorobenzonitrile at 40.6 μM as the internal standard). The contents of the centrifuge tubes were mixed vigorously using a vortex mixer for 2 minutes. The toluene phase was then transferred to a 2-mL amber glass autosampler vial. The concentrations of TMB and its monochlorinated product in the toluene extract were analyzed using GC-MS (see Appendix B for method details).

Influence of Quenchers on the Stabilities of DBPs. The stabilities of eight DBPs (chloropicrin, chloral hydrate, chloroacetonitrile, dichloroacetonitrile, trichloroacetonitrile, bromoacetonitrile, dibromoacetonitrile, and tribromoacetaldehyde) were assessed individually in the presence of TMB, sodium sulfite, sodium thiosulfate, ascorbic acid, and ammonium chloride. Sodium sulfite solutions were made fresh daily as the sulfite oxidized rapidly when headspace was present. Spiking solutions of DBPs were prepared in either methanol (chloropicrin) or acetonitrile (all other DBPs). Each reactor (clear glass bottle with ground-glass stopper, actual volume ≈ 315 mL) contained 300 mL of phosphate buffer (10 mM, adjusted to pH 7.0 using NaOH) and one quencher at an initial concentration of 60 μM. The reactor was then spiked with a DBP to give an initial concentration of 6.0 μM and shaken vigorously. A control reactor, to which no quencher was added, was set up for each DBP to determine whether processes such as volatilization and hydrolysis could affect the stability of the DBP. All reactors were kept in a constant-temperature incubator set at 25 ± 1 °C and were sampled once a day for 7 days. At each sampling time, 4.0 mL of the reaction solution were transferred to a clear glass 15-mL centrifuge tube containing 1.5 mL of methyl *tert*-butyl ether (MTBE, with 1,2-dibromopropane at 10 μM as the internal standard). Although the volume of headspace in the reactor increased over the course of the experiment, the percentage of each DBP in the aqueous solution (calculated using Henry's Law constants obtained from the program HENRYWIN, ref. 21) never dropped below 98%. Some of the sulfite, however, might have decayed through oxidation by molecular oxygen.[22] The centrifuge tube was then vortexed for 2 minutes, and ~ 1 mL of the MTBE phase was subsequently transferred to a 2-mL amber glass autosampler vial. The concentrations of DBPs in the

MTBE extracts were analyzed using GC with micro-electron capture detection (μ-ECD). Details of the analytical methods are in Appendix B.

Chloramination of TMB. To assess whether the presence of monochloramine could interfere with the quantification of free chlorine using TMB, a batch reactor was set up to examine the chloramination kinetics of TMB. The reactor (60-mL clear glass vial) contained 50 mL of reaction solution that consisted of phosphate buffer (10 mM, adjusted to pH 7.03 with NaOH) and ammonium chloride (NH_4Cl; 385 μM). The reactor was placed inside a stainless-steel constant-temperature water bath set at 25.00 ± 0.01 °C. After several minutes of temperature equilibration, 1 mL of NaOCl (7.86 mM) was added to the reactor, yielding an initial concentration of 154 μM ($[NH_4Cl]_o/[NaOCl]_o = 2.5$). The reactor was capped, shaken vigorously, and returned to the water bath. After waiting ~7 minutes to permit formation of monochloramine, the reactor was spiked with 0.10 mL of a TMB solution (5.50 mM in methanol) such that $[TMB]_o = 10.8$ μM. The reactor was again capped, shaken vigorously, and returned to the water bath. At each sampling time, 3.0 mL of the reaction solution was transferred to a clear glass 15-mL centrifuge tube containing 1.0 mL of toluene (with 2-chlorobenzonitrile at 40.0 μM as the internal standard). The centrifuge tube was vortexed for 2 minutes, and ~ 0.5 mL of the toluene layer was then transferred to a 2-mL amber glass autosampler vial. The concentrations of TMB and Cl-TMB in the toluene extracts were analyzed using GC-MS. Details of the GC-MS method are in Appendix B.

3. 4. Results and Discussion

Commonly used quenchers for free chlorine and free bromine can potentially reduce/transform analytes of interest in aqueous samples, leading to inaccurate quantitation of the analytes. This sparked our desire to develop an alternative method for quenching free halogens using 1,3,5-trimethoxybenzene (TMB). In addition, by measuring the concentrations of the monochlorinated and monobrominated products of TMB in the quenched samples, we can determine the free chlorine and free bromine concentrations present at the time of quenching. The effectiveness of using TMB to quench and quantify free halogens are demonstrated and discussed in the following sections.

TMB as a Dual-Purpose Quencher for Kinetic Experiments. Solutions of free chlorine or free bromine were quenched with excess TMB ($[TMB]_o/[HOX]_{tot,o} \geq 6$, X = Cl or Br) to evaluate the conversion efficiency of free chlorine and free bromine into Cl-TMB and Br-TMB, respectively. A plot of [Cl-TMB] as a function of total free chlorine dose (**Figure 3-1a**) is linear with a slope not significantly different from 1.00 (at the 95% confidence level). An analogous plot of [Br-TMB] as a function of total free bromine concentration (**Figure 3-1b**) is also linear with a slope not significantly different from 1.00 (at the 95% confidence level). These results indicate that, under the examined conditions, TMB reacts stoichiometrically with free chlorine and with free bromine to form the respective monochlorinated and monobrominated products.

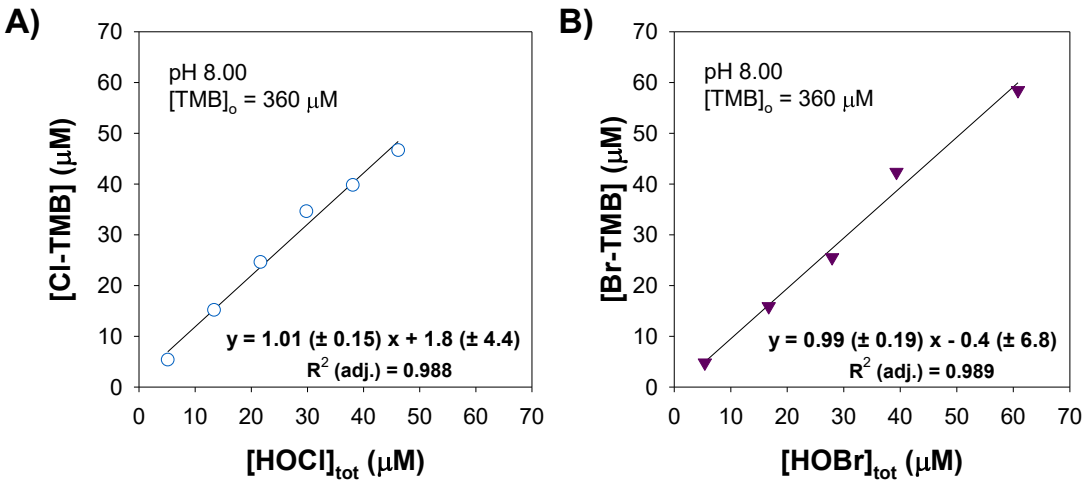

Figure 3-1. **(A)** Yields of 2-chloro-1,3,5-trimethoxybenzene (Cl-TMB) as a function of chlorine dose. Reaction conditions: $[TMB]_o$ = 360 μM, $[NaOCl]_o$ = 5.0–46 μM, $[NaNO_3]$ = 0.1 M, pH = 8.00, $[borate]_{tot}$ = 20 mM, T = 21 ± 1°C. **(B)** Yields of 2-bromo-1,3,5-trimethoxybenzene (Br-TMB) as a function of free bromine (generated via oxidation of bromide by free chlorine) concentration. Conditions: $[TMB]_o$ = 360 μM, $[NaOCl]_o$ = 65 μM, $[Br^-]$ = 5.0–60 μM, $[NaNO_3]$ = 0.1 M, pH = 8.00, $[borate]_{tot}$ = 20 mM, T = 21 ± 1°C. Cl-TMB was detected but its concentrations are not shown. Error estimates in both frames denote 95% confidence intervals.

Chlorination of 2,4-Dichlorophenol. The chlorination of 2,4-dichlorophenol (2,4-DCP) was carried out at pH 7.08 under pseudo-first-order conditions ($[HOCl]_{tot} \approx [HOCl]_{tot,o} \gg [2,4\text{-DCP}]_{tot,o}$) with TMB as the free chlorine quencher. The overall rate of 2,4-DCP chlorination in our experiments can be described by equation 3-1:

$$\frac{d[2,4\text{-DCP}]_{tot}}{dt} = -k_{obs}\,[2,4\text{-DCP}]_{tot} \qquad (3\text{-}1)$$

where k_{obs} represents the pseudo-first-order rate constant and $[2,4\text{-DCP}]_{tot}$ denotes the sum of the concentrations of the acid and conjugate base forms of 2,4-DCP (pK_a = 7.85, ref. 23). The disappearance of 2,4-DCP was accompanied by the formation of 2,4,6-trichlorophenol (TCP) (**Figure 3-2a**; concentrations were corrected for the dilution that

resulted from adding aliquots of the reaction solution to autosampler vials pre-amended with TMB). The decrease in the carbon mass balance, calculated as $[2,4\text{-DCP}]_{tot}$ + $[TCP]_{tot}$, can be attributed to the reaction of TCP with free chlorine.[16] The value of k_{obs} was computed from linear regression of $\ln[2,4\text{-DCP}]_{tot}$ vs. time data (**Figure 3-3a**). With TMB as the quencher, k_{obs} = 8.5 (± 0.4) × 10^{-3} s^{-1} (all uncertainties herein indicate 95% confidence intervals). In a parallel 2,4-DCP chlorination experiment in which sodium thiosulfate was used to quench free chlorine, k_{obs} = 8.0 (± 0.3) × 10^{-3} s^{-1} (**Figure 3-3b**). The difference between the two k_{obs} values is not significant at the 95% confidence level, showing that under our experimental conditions TMB and sodium thiosulfate are equally effective in quenching free chlorine.

When TMB was used as the quencher, the concentrations of unreacted TMB and Cl-TMB in the quenched samples were also monitored (**Figure 3-2b**; concentrations not corrected for dilution). Recoveries of free chlorine, computed as ([Cl-TMB] + [TCP])/$[HOCl]_{tot,o}$, remained constant at 96% to 102% with an average of 99% ± 2% (**Figure 3-2c**), as expected if pseudo-first-order conditions were maintained throughout the experiment. The amount of free chlorine that was incorporated into TMB—quantified as [Cl-TMB]—was within 5% of $[HOCl]_{tot,o}$ (data not shown). There were undoubtedly other products besides TCP that were formed from the chlorination of 2,4-DCP; however, under our reaction conditions in which $[HOCl]_{tot,o} \gg [2,4\text{-DCP}]_o$, other reactions that contribute to the loss of 2,4-DCP or its daughter products would not represent significant losses of free chlorine.

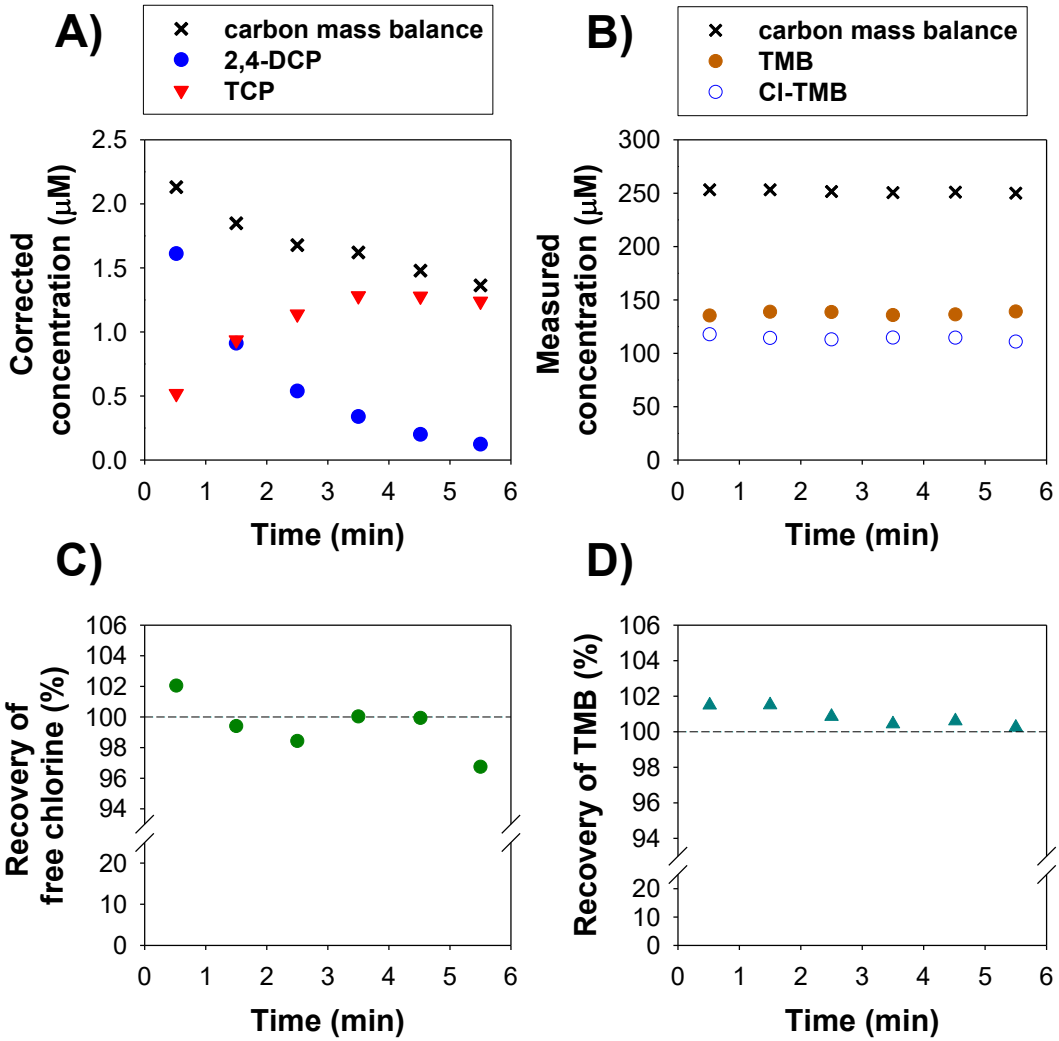

Figure 3-2. Reaction of 2,4-DCP with excess free chlorine, quenched using 1,3,5-trimethoxybenzene (TMB). Reaction conditions: pH 7.08, $[2,4\text{-DCP}]_o$ = 2.1 μM, $[NaOCl]_o$ = 128 μM, [phosphate buffer] = 10 mM, $[NaCl]_{added}$ = 5 mM, ionic strength (i.e., [NaCl] + $[NaNO_3]$) = 0.1 M, T = 25.0 °C. **(A)** The concentrations of the parent compound (2,4-DCP) and its chlorination product (TCP) over the course of the experiments. The mass balance was calculated as $[2,4\text{-DCP}]_{tot}$ + $[TCP]_{tot}$ at each time point. **(B)** Measured concentrations of TMB and its major chlorination product, Cl-TMB, over the course of the experiments. The mass balance was calculated as [TMB] + [Cl-TMB] at each time point. **(C)** The recovery of chlorine at each sampling time; % recovery of Cl = ([Cl-TMB] + [TCP])/$[HOCl]_{tot,o}$. **(D)** The recovery of TMB at each sampling time; % recovery of TMB = ([TMB] + [Cl-TMB])/$[TMB]_o$, where $[TMB]_o$ = 252 μM at the time of quenching.

Recoveries of TMB, computed as ([TMB] + [Cl-TMB])/$[TMB]_o$, ranged from 100% to 102% with an average of 101% ± 1% (**Figure 3-2d**). As effectively all the TMB mass can be accounted for by considering TMB and Cl-TMB only, the formation of additional chlorination products of TMB (e.g., dichlorinated and trichlorinated TMB) was insignificant in our experiment. Monitoring 2,4-dichloro-1,3,5-trimethoxybenzene in the quenched samples confirmed that dichlorinated TMB accounted for < 0.1% of the total [TMB] under our reaction conditions.

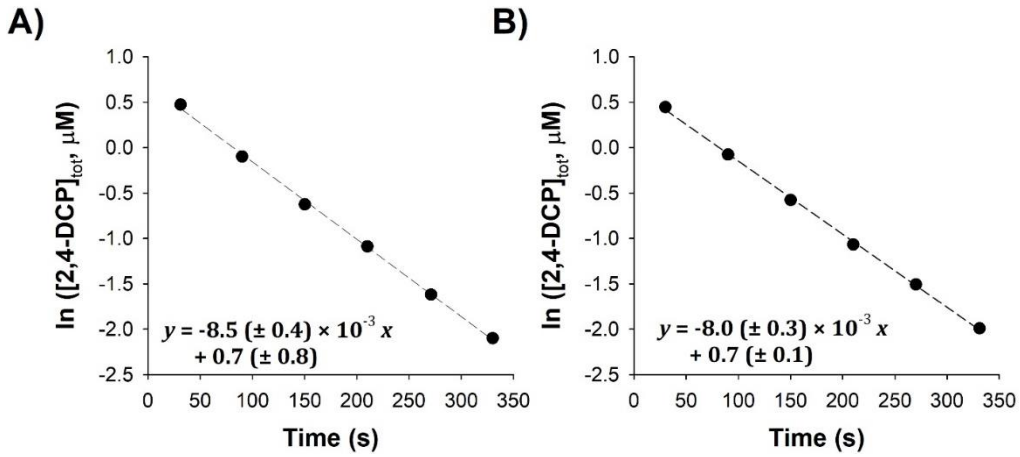

Figure 3-3. Linear regressions of $\ln[2,4\text{-DCP}]_{tot}$ versus time data from 2,4-DCP chlorination experiments using **(A)** TMB or **(B)** sodium thiosulfate to quench free chlorine. Reaction conditions: $[2,4\text{-DCP}]_{tot,o}$ = 2 µM, $[NaOCl]_o$ = 128 µM, pH = 7.08 (buffered with 10 mM phosphate), $[NaNO_3]$ = 95 mM, [NaCl] = 5 mM. Uncertainties in the equations indicate 95% confidence intervals.

As the chlorination rate of TMB decreases with increasing pH,[13] we also assessed the ability of TMB to quench free chlorine in a 2,4-DCP chlorination experiment conducted at pH 9.14. The quenching was carried out using a TMB solution that

contained 0.1 M HNO_3, and the pH of the reactor aliquots after thorough mixing with the TMB solution was 6–7. With TMB as the quencher, k_{obs} = 6.4 (± 0.2) × 10^{-4} s^{-1}. In a parallel experiment with sodium thiosulfate as the quencher, k_{obs} = 6.1 (± 0.3) × 10^{-4} s^{-1}. The close agreement between the k_{obs} values indicates that TMB can be an effective quencher for free chlorine at high pH as long as steps are taken to lower the solution pH to ~7 at the time of quenching.

Bromination of Anisole. TMB was employed as a quencher in kinetic experiments involving bromination of anisole in the presence of excess free bromine (generated via NaBr + excess NaOCl) at pH 7.48. As the bromination of anisole is much more rapid than the analogous chlorination reaction, only brominated products were observed to form in our experiments (**Figure 3-4a**; concentrations were corrected for the dilution that occurred when adding aliquots of the reaction solution to autosampler vials pre-amended with TMB). Concentrations of unreacted TMB, Cl-TMB, and Br-TMB were measured in the toluene extract obtained at each sampling time (**Figure 3-4b**; concentrations not corrected for dilution). Recoveries of free chlorine and free bromine ranged from 97 – 104% with averages of 100% ± 3% and 103% ± 2%, respectively (**Figure 3-4c**). These results suggest that TMB was converted quantitatively into Cl-TMB and Br-TMB upon reaction with residual free chlorine and free bromine, respectively. Recoveries of TMB ranged from 97% to 100% (average = 99% ± 1%; **Figure 3-4d**), which suggests that formation of additional products (e.g., dihalogenated forms of TMB) was negligible.

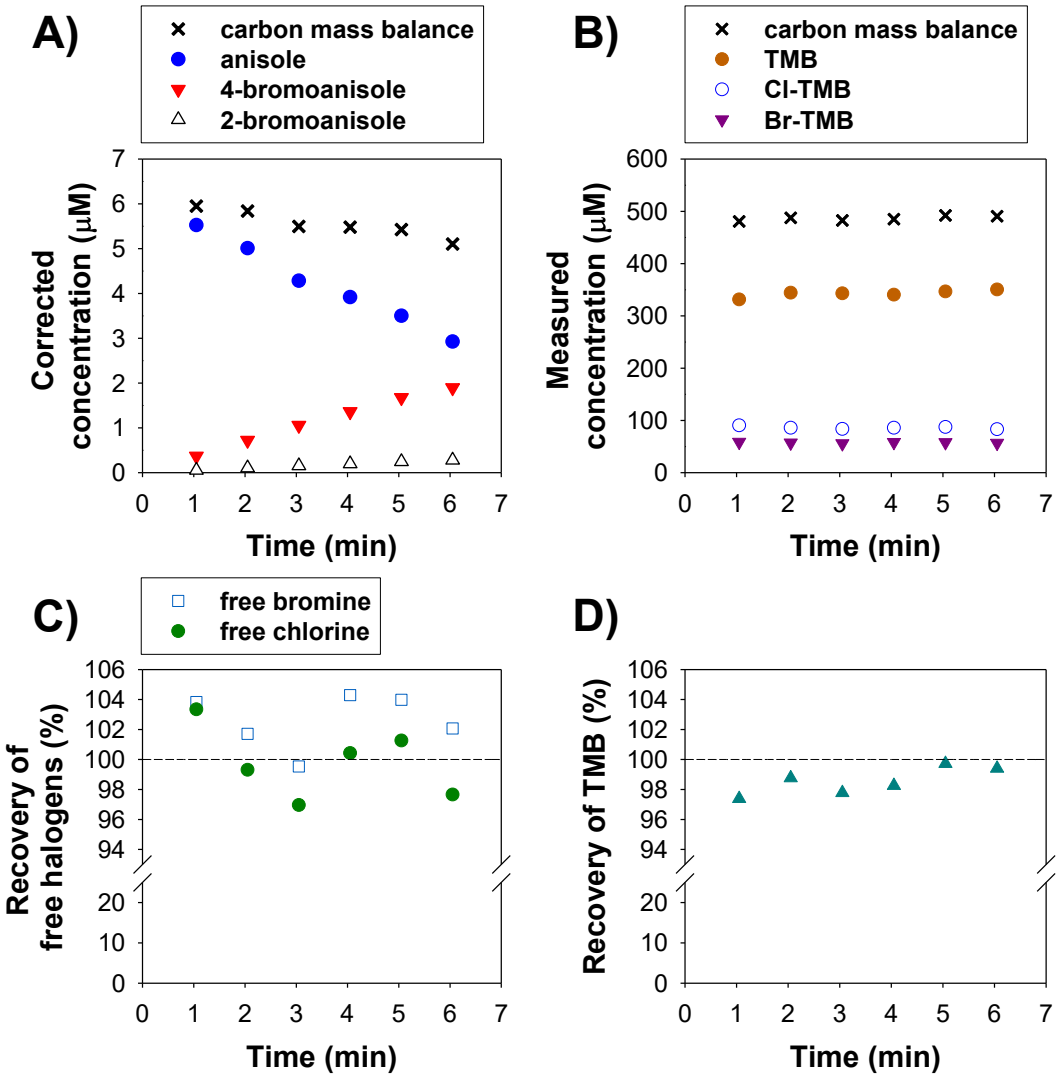

Figure 3-4. Reaction of anisole with solutions amended with bromide + excess NaOCl, periodically quenched using 1,3,5-trimethoxybenzene (TMB). Reaction conditions: $[anisole]_o$ = 6.0 μM, $[NaBr]_o$ = 130 μM, $[NaOCl]_o$ = 305 μM, pH = 7.48, $[NaHCO_3]$ = 20 mM, $[NaNO_3]$ = 90 mM, [NaCl] = 10 mM, T = 20.0 °C. **(A)** Time course depicting anisole transformation into brominated products; carbon mass balance = [anisole] + [4-bromoanisole] + [2-bromoanisole]; chlorination of anisole was sufficiently slow as to preclude detection of chlorinated products. **(B)** Measured concentrations of the quencher (TMB) and its monochlorinated (Cl-TMB) and monobrominated (Br-TMB) products; carbon mass balance = [TMB] + [Cl-TMB] + [Br-TMB]. **(C)** Recovery of free chlorine and free bromine for each sampling time; recovery of chlorine = $[Cl\text{-}TMB]/[HOCl]_{tot,o}$; recovery of bromine = $([4\text{-}bromoanisole] + [2\text{-}bromoanisole] + [Br\text{-}TMB])/[Br^-]_o$; **(D)** Recovery of TMB = $([TMB] + [Cl\text{-}TMB] + [Br\text{-}TMB])/[TMB]_o$, where $[TMB]_o$ = 494 μM at the time of quenching.

Under pseudo-first-order conditions in which $[HOBr]_{tot} \approx [HOBr]_{tot,o} \gg [anisole]_o$, the overall rate of anisole bromination can be expressed as equation 3-2:

$$\frac{d[\text{anisole}]}{dt} = -k_{\text{obs}}[\text{anisole}] = -(k_{\text{I,obs}} + k_{\text{II,obs}})[\text{anisole}] \quad (3\text{-}2)$$

where k_{obs}, $k_{\text{I,obs}}$, and $k_{\text{II,obs}}$ are the pseudo-first-order rate constants for the disappearance of anisole, the formation of 4-bromoanisole, and the formation of 2-bromoanisole, respectively. Using TMB as a quencher at pH 7.48, $k_{\text{I,obs}}$ = 8.6 (± 0.7) × 10^{-4} s^{-1} and $k_{\text{II,obs}}$ = 1.33 (± 0.11) × 10^{-4} s^{-1}. These experimental rate constants are in reasonable agreement with the predicted $k_{\text{I,obs}}$ and $k_{\text{II,obs}}$ values (7.3 (± 0.9) × 10^{-4} s^{-1} and 1.03 (± 0.14) × 10^{-4} s^{-1}, respectively) determined via equation 3-3:

$$k_{\text{obs}} = k_{\text{BrCl}}[\text{BrCl}] + k_{\text{BrOCl}}[\text{BrOCl}] + k_{\text{Br}_2\text{O}}[\text{Br}_2\text{O}] + k_{\text{HOBr}}[\text{HOBr}] \quad (3\text{-}3)$$

where k_{BrCl}, k_{BrOCl}, $k_{\text{Br}_2\text{O}}$, and k_{HOBr} denote second-order rate constants (M^{-1} s^{-1}) for bromination by BrCl, BrOCl, Br_2O, and HOBr, respectively, from experiments conducted using sodium thiosulfate as the quencher.[15] Molar concentrations of various brominating agents were determined using the solution conditions reported in **Figure 3-4** and the equilibrium constants compiled in ref. 15. Pseudo-first-order rate constants for the bromination of anisole ($k_{\text{I,obs}}$ and $k_{\text{II,obs}}$) were also determined at pH 8.02, 8.50, and 9.02 (**Table 3-1**). Of the eight rate constants obtained using TMB as the quencher, seven were not significantly different (at the 95% confidence level) from those calculated via equation 3-3 (based on data obtained using sodium thiosulfate as the quencher). In all cases, rate constants obtained using TMB as a quencher differed by ≤ 23% relative to values calculated via equation 3-3 (**Table 3-1**). Together with the data reported for 2,4-

DCP chlorination, these findings demonstrate the ability of TMB to facilitate concurrent quenching and halogen-specific quantification of free chlorine and free bromine residuals in batch reactors simulating water disinfection conditions.

Competitive Quenching of Free Chlorine. To assess the rate at which TMB reacts with free chlorine relative to four traditional quenchers, competitive quenching experiments were conducted at pH 7.10 in batch reactors that initially contained approximately equimolar concentrations (~52 μM each) of free chlorine, TMB, and one non-TMB quencher (sodium sulfite, sodium thiosulfate, ascorbic acid, or ammonium chloride). A reactor containing equimolar concentrations (~52 μM each) of free chlorine and TMB only served as the control. The concentrations of unreacted TMB and Cl-TMB in each reactor after quenching are reported in **Table 3-2**. In the control reactor, most of the initial TMB was converted into Cl-TMB via reaction with free chlorine ([Cl-TMB]/([Cl-TMB] + [TMB]) = 89%). When a non-TMB quencher was present, however, only a small percentage of the initial TMB was converted into Cl-TMB. Values of [Cl-TMB]/([Cl-TMB] + [TMB]) were ≤ 0.70% for sodium sulfite, sodium thiosulfate, and ascorbic acid, while that for ammonium chloride was 13%.

Table 3-1. Pseudo-first-order Rate Constants for the Formation of 4-Bromoanisole ($k_{\mathrm{I,obs}}$) and 2-Bromoanisole ($k_{\mathrm{II,obs}}$) in Solutions of Free Bromine + Anisole Measured Using Thiosulfate or TMB as Quenchers [a]

Product	pH	Pseudo-first-order rate constant ± 95% confidence interval (s^{-1})		Percent Difference [d]	Significantly Different at 95% CI?
		Quencher = TMB [b]	Quencher = Thiosulfate [c]		
4-bromo-anisole	7.48	$(8.6 \pm 0.7) \times 10^{-4}$	$(7.3 \pm 1.5) \times 10^{-4}$	18%	No
	8.02	$(1.85 \pm 0.13) \times 10^{-4}$	$(2.0 \pm 0.4) \times 10^{-4}$	–9%	No
	8.50	$(6.34 \pm 0.13) \times 10^{-5}$	$(5.7 \pm 1.2) \times 10^{-5}$	12%	No
	9.02	$(1.19 \pm 0.02) \times 10^{-5}$	$(1.1 \pm 0.2) \times 10^{-5}$	8%	No
2-bromo-anisole	7.48	$(1.27 \pm 0.15) \times 10^{-4}$	$(1.03 \pm 0.12) \times 10^{-4}$	23%	Yes
	8.02	$(2.42 \pm 0.17) \times 10^{-5}$	$(2.7 \pm 0.3) \times 10^{-5}$	–10%	No
	8.50	$(7.25 \pm 0.09) \times 10^{-6}$	$(6.7 \pm 0.7) \times 10^{-6}$	8%	No
	9.02	$(1.13 \pm 0.03) \times 10^{-6}$	$(1.12 \pm 0.13) \times 10^{-6}$	0.7%	No

[a] Reaction conditions: $[NaBr]_o = 130$ μM, $[anisole]_o = 6.0$ μM, $[HOCl]_{tot,o} = 305$ μM, $[NaHCO_3$ or $Na_2B_4O_7] = 20$ mM, $[NaCl] = 10$ mM, $[NaNO_3] = 90$ mM, T = 20.00 ± 0.01 °C.

[b] Determined experimentally in this study.

[c] Calculated using equation 3-3 and second-order rate constants reported in ref. 15. Confidence intervals were determined by propagating uncertainties associated with second-order rate constants and assuming an average uncertainty of ± 0.1 for log(K) values (i.e., equilibrium constants used to calculate concentrations of brominating agents). This assumed average uncertainty for log(K) values is consistent with uncertainties reported for the pK_a of HOBr and the log(K) values associated with the hydrolysis of BrCl and Br_2 (see ref. 24 and references therein).

[d] % difference = $\left(\frac{k_{\mathrm{obs,TMB}} - k_{\mathrm{obs,thiosulfate}}}{k_{\mathrm{obs,thiosulfate}}}\right) \times 100\%$

Table 3-2. Results from Competitive Quenching Experiments [a]

Non-TMB quencher	Concentration (μM)			$\frac{[\text{Cl-TMB}]}{([\text{Cl-TMB}] + [\text{TMB}])}$
	TMB	Cl-TMB	Mass balance [b]	
Sodium sulfite	59.38	0.36	59.74	0.61%
Sodium thiosulfate	52.49	0.23	52.71	0.43%
Ascorbic acid	55.32	0.37	55.69	0.67%
Ammonium chloride	49.52	7.15	56.67	13%
Control	6.03	48.11	54.14	89%

[a] Reaction conditions: pH 7.10, $[HOCl]_{tot,o} \approx [TMB]_o \approx$ [non-TMB quencher]$_o \approx 52$ μM, [phosphate buffer] = 10 mM, ionic strength = 0.1 M

[b] TMB mass balance was calculated as the sum of [TMB] and [Cl-TMB]

The value of [Cl-TMB]/([Cl-TMB] + [TMB]) is indicative of the relative competitiveness of TMB for free chlorine. If TMB were to react with free chlorine more quickly than did the non-TMB quencher, we would expect the value of [Cl-TMB]/([Cl-TMB] + [TMB]) to approach 89% (the value of [Cl-TMB]/([Cl-TMB] + [TMB]) in the control reactor in which TMB was the only quencher present). In our experiments, the values of [Cl-TMB]/([Cl-TMB] + [TMB]) were close to zero when sodium sulfite, sodium thiosulfate, or ascorbic acid was present, indicating that these quenchers reacted with free chlorine much more rapidly than did TMB. The value of [Cl-TMB]/([Cl-TMB] + [TMB]) with ammonium chloride was higher (13%), but ammonium chloride still reacted with free chlorine more quickly than did TMB. We note that the TMB mass balances (computed as [TMB] + [Cl-TMB]) in these experiments ranged from 52.7 to 59.7 μM and somewhat exceeded the nominal $[TMB]_o$ (52 μM). The variation in TMB mass balances should not, however, affect our interpretation of the trends in

[Cl-TMB]/([Cl-TMB] + [TMB]) values. Despite its more modest reactivity towards free chlorine relative to traditional quenchers, the kinetic experiments reported above for 2,4-DCP chlorination (**Figure 3-2**) and anisole bromination (**Figure 3-4**) indicate that TMB can serve as an effective quencher for free chlorine and free bromine for reactions with half-times ≥ 0.5 minute.

Influence of Quenchers on DBP Stability. While high reactivity with free chlorine and free bromine is a defining trait of an effective quencher, inertness towards the analytes of interest is equally important. To assess the stabilities of eight DBPs in the presence of TMB, we conducted week-long experiments in batch reactors at pH 7.0 with $[TMB]_o \geq 10 \times [DBP]_o$. We also evaluated the stabilities of the DBPs in the presence of sodium sulfite, sodium thiosulfate, ascorbic acid, and ammonium chloride under similar conditions. We chose to study these eight DBPs because the influence of various quenchers on their stabilities has been examined in the literature,[2, 4-5] thus allowing us to compare our findings with those of previous researchers. Our results are presented in **Figures 3-5 and 3-6** and summarized in **Table 3-3**, with check marks in the latter denoting negligible differences in DBP concentrations from those in the control reactors after 7 days.

Chloropicrin was stable in the presence of TMB, in the presence of ammonium chloride, and when no quencher was present (**Figure 3-5a**). On the other hand, the concentration of chloropicrin decreased substantially in the presence of sodium sulfite, ascorbic acid, and sodium thiosulfate. Sodium sulfite and ascorbic acid led to no detectable chloropicrin after 1 day and 3 days, respectively. Sodium thiosulfate led to a more gradual degradation of chloropicrin, with 42% of the initial chloropicrin

concentration remaining after 7 days. Previous researchers found that dichloronitromethane was the major transformation product of chloropicrin, also known as trichloronitromethane, in the presence of sodium sulfite.[4] The degradation of chloropicrin in the presence of ascorbic acid has also been documented,[5] but to our knowledge the adverse impact of sodium thiosulfate on chloropicrin stability has not been previously reported.

TMB did not have any discernable effect on the stabilities of chloroacetonitriles, although the effect of other quenchers depended on the identity of the DBP. Chloroacetonitrile (MCAN) was stable at pH 7.0 regardless of which quencher was present (**Figure 3-5b**). Dichloroacetonitrile (DCAN) concentrations decreased by ~23% over 7 days in all reactors (**Figure 3-5c**), ostensibly due to base-catalyzed hydrolysis to form dichloroacetamide.[25] The presence of quenchers did not have any appreciable effect on the rate of DCAN hydrolysis. Trichloroacetonitrile (TCAN) is inherently unstable at pH 7.0, as evidenced by its disappearance from the control reactor within 4 days (**Figure 3-5d**). Previous researchers found that TCAN undergoes base-catalyzed hydrolysis to form trichloroacetamide and trichloroacetic acid.[26] Of the quenchers we tested, sodium sulfite and ascorbic acid were the only ones that enhanced the rate of TCAN disappearance, causing TCAN to become undetectable after 1 day and 2 days, respectively. The disappearance of TCAN in the reactor containing sodium sulfite was accompanied by the generation of DCAN (data not shown), and our observation agrees with previous research showing that TCAN is converted into DCAN in the presence of sodium sulfite.[4] We did not observe any DCAN formation when ascorbic acid was

present; accordingly, the product of reaction between TCAN and ascorbic acid merits further investigation.

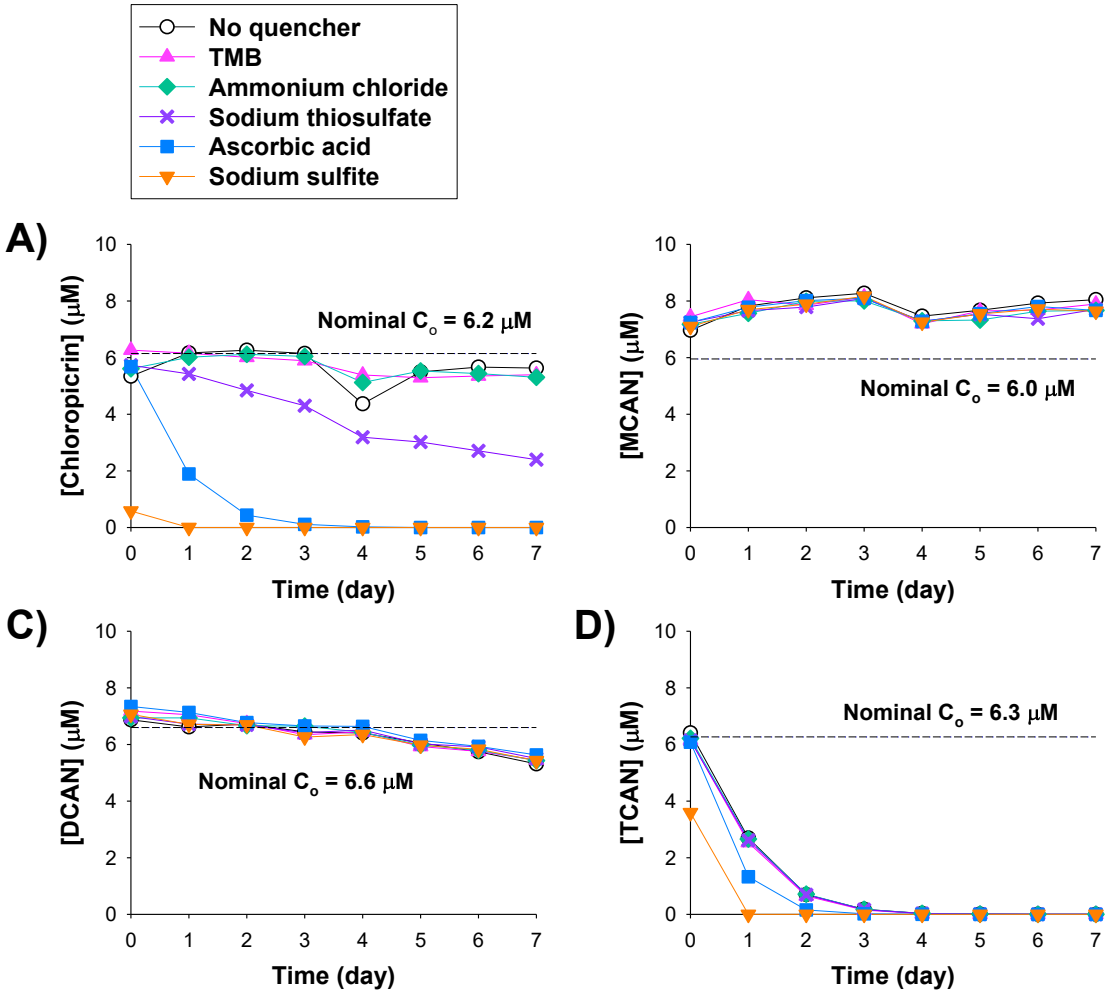

Figure 3-5. The stability of **(A)** chloropicrin, **(B)** chloroacetonitrile (MCAN), **(C)** dichloroacetonitrile (DCAN), and **(D)** trichloroacetonitrile (TCAN) in the presence of various quenchers at pH 7.0. Reaction conditions: $[DBP]_o$ = 6 μM, $[quencher]_o$ = 60 μM, $[phosphate\ buffer]_o$ = 10 mM, T = 25 °C.

TMB did not affect the stabilities of the bromoacetonitriles examined herein, but certain other quenchers did affect their stabilities. Bromoacetonitrile (MBAN) was stable in the absence of quenchers as well as in presence of TMB, ammonium chloride, ascorbic acid, or sodium sulfite (**Figure 3-6a**). Sodium thiosulfate, however, led to a 67% decrease in [MBAN] over 7 days. No degradation products of MBAN were detected using our analytical method. Dibromoacetonitrile (DBAN) concentrations decreased by ~15% over 7 days in the absence of quenchers (**Figure 3-6b**), most likely due to the hydrolysis of DBAN to form dibromoacetamide.[25] TMB, ammonium chloride, ascorbic acid, and sodium thiosulfate did not enhance DBAN hydrolysis. Sodium sulfite, on the other hand, caused DBAN to become undetectable within 1 day. The major degradation product was previously reported to be MBAN;[4] we observed the conversion of DBAN into MBAN in our experiment, and mass balances (computed as [MBAN] + [DBAN]) did not vary appreciably over 7 days (data not shown).

The stability of chloral hydrate was not affected by TMB or by any of the other quenchers tested (**Figure 3-6c**). Our results are in contrast with previous work showing that when ascorbic acid was present, the concentration of chloral hydrate decreased by 11% in 1 day and then decreased further by 6% after 18 days.[2] Low recoveries of chloral hydrate in the presence of ammonium chloride have also been reported.[27] The discrepancy between our findings and those in previous studies may be explained by differences in experimental conditions, although further investigation is warranted.

Tribromoacetaldehyde (TBAL), like TCAN, was inherently unstable in aqueous solutions at pH 7.0 (**Figure 3-6d**). TBAL became undetectable after 2 days in the absence of any quencher, and the presence of TMB, ammonium chloride, and ascorbic acid did

not affect its degradation rate appreciably. When sodium thiosulfate was present, the concentration of TBAL fell below the detection limit after only 10 minutes of reaction time. Previous researchers identified bromoform as the major product of TBAL hydrolysis, although the incomplete mass balance indicated that additional products were formed.[28]

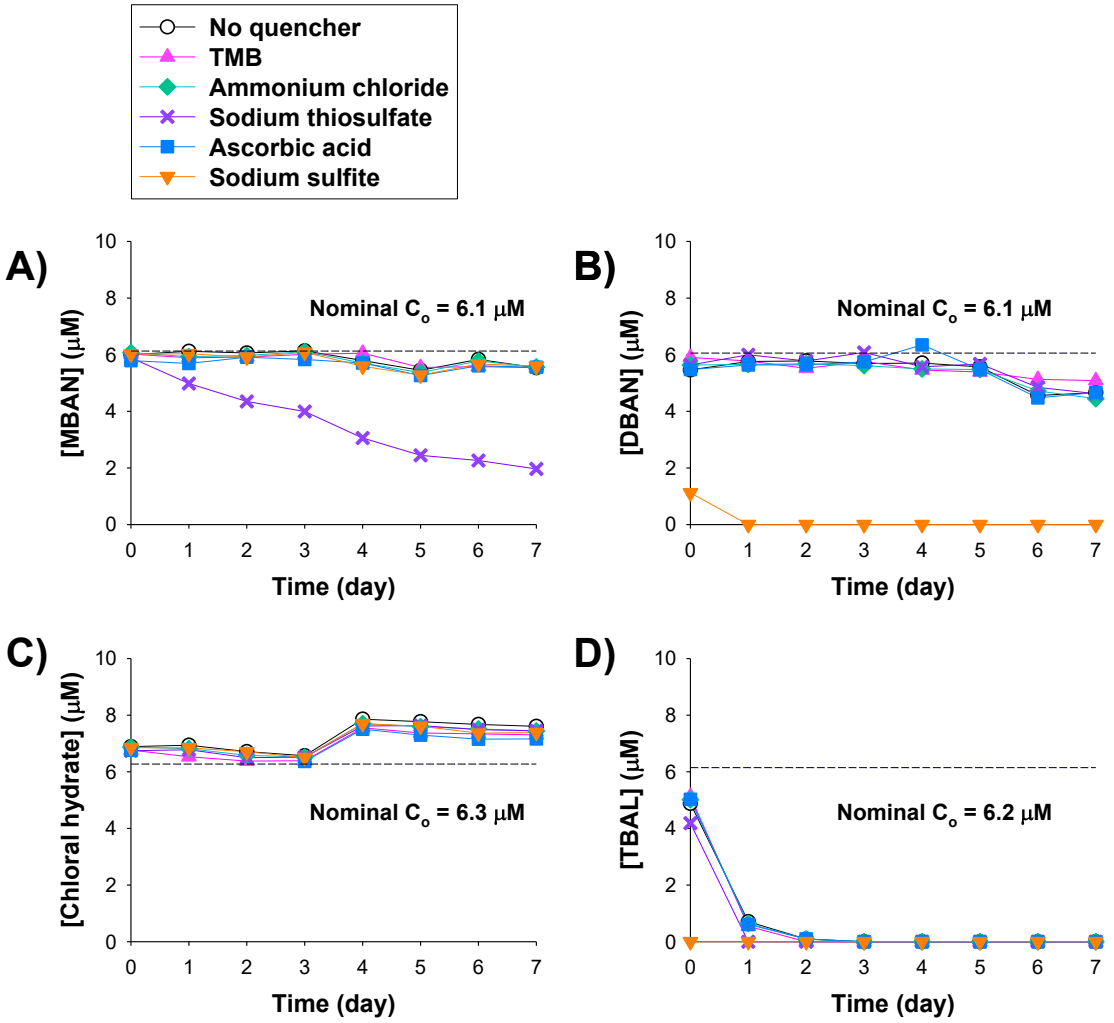

Figure 3-6. The stability of **(A)** bromoacetonitrile (MBAN), **(B)** dibromoacetonitrile (DBAN), **(C)** chloral hydrate, and **(D)** tribromoacetaldehyde (TBAL) in the presence of various quenchers at pH 7.0. Reaction conditions: $[DBP]_o$ = 6 µM, $[quencher]_o$ = 60 µM, $[phosphate\ buffer]_o$ = 10 mM, T = 25 °C.

Table 3-3. Influence of Quenchers on the Stabilities of DBPs [a]

DBP	TMB	Ammonium chloride	Sodium thiosulfate	Ascorbic acid	Sodium sulfite
Chloropicrin	✓	✓			
Chloral hydrate	✓	✓	✓	✓	✓
Chloroacetonitrile (MCAN)	✓	✓	✓	✓	✓
Dichloroacetonitrile (DCAN)	✓	✓	✓	✓	✓
Trichloroacetonitrile (TCAN)	Inherently unstable in water, so quenchers make little difference				
Bromoacetonitrile (MBAN)	✓	✓		✓	✓
Dibromoacetonitrile (DBAN)	✓	✓	✓	✓	
Tribromoacetaldehyde (TBAL)	Inherently unstable in water, so quenchers make little difference				

[a] Check marks indicate that changes in DBP concentrations are not appreciably different from those in the control reactor without any quencher

As shown in **Table 3-3**, sodium thiosulfate, ascorbic acid, and sodium sulfite would not be appropriate quenchers for chloropicrin. In addition, sodium sulfite should not be used when analyzing DBAN, while sodium thiosulfate should be avoided for MBAN. TCAN and TBAL are inherently unstable in water at pH 7.0, so the presence of quenchers has little influence on their stabilities. TMB and ammonium chloride did not adversely affect the stabilities of any of the DBPs tested since they do not serve as facile reducing agents for organic compounds. Thus, both TMB and ammonium chloride could serve as quenchers for free chlorine, with the caveat that ammonium chloride should only be used if the analytes of interest do not react with monochloramine (formed via free chlorine + excess NH_4Cl). When free bromine is present, using ammonium chloride to quench free halogens is not recommended due to the formation of bromamines, which are more reactive towards organic compounds than are chloramines.[12]

Chloramination of TMB. To assess whether monochloramine could interfere with the effectiveness of TMB as a selective quencher for free chlorine, we added TMB to an aqueous solution containing free chlorine and a molar excess of ammonium chloride (NH_4Cl) at pH 7.03. Monochloramine formation from free chlorine + NH_4Cl should be rapid under our experimental conditions.[29] Our results show that [TMB] decreased by ~7% over 7 hours, accompanied by an approximately stoichiometric increase in [Cl-TMB] over the same period (**Figure 3-7**). In a control reactor to which NH_4Cl—but not free chlorine—was added, no Cl-TMB was detected after 7 hours (data not shown). The low reactivity of TMB towards monochloramine indicates that TMB is a selective nucleophile. In water samples that contain both free chlorine and monochloramine,

monitoring [TMB] and [Cl-TMB] should allow researchers to selectively quantify free chlorine as long as free chlorine is present in excess of monochloramine.

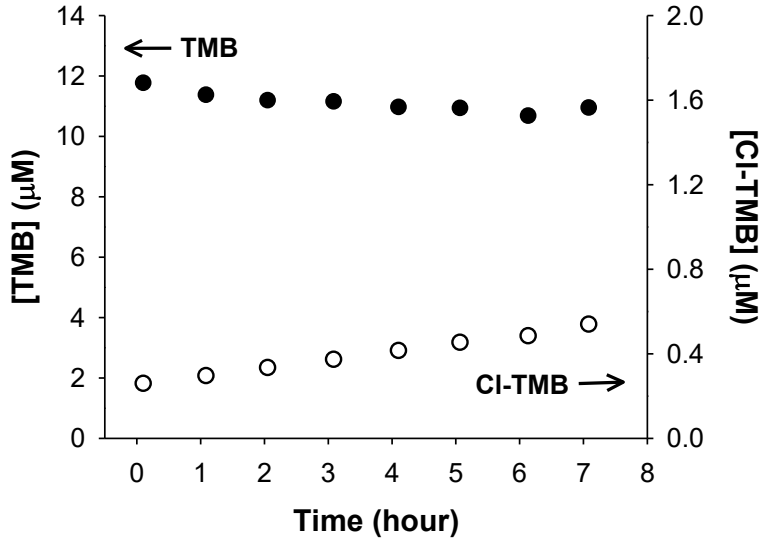

Figure 3-7. The stability of TMB in the presence of monochloramine formed via free chlorine + excess NH_4Cl. Reaction conditions: pH 7.03, $[TMB]_o$ = 12 μM, $[NaOCl]_o$ = 154 μM, $[NH_4Cl]_o$ = 385 μM, [phosphate buffer] = 10 mM, T = 25 °C.

3. 5. Conclusions

To circumvent the problem of analyte decomposition in the presence of traditional quenchers, we have developed a novel method for quenching free chlorine and free bromine with TMB. We assessed the efficacy of TMB as a quencher in halogenation kinetics experiments as well as the effect of TMB on the stabilities of a range of DBPs. Our findings are as follows:

- TMB is quantitatively converted into Cl-TMB and Br-TMB when present in sufficient (≥ 2-fold molar) excess relative to free chlorine and free bromine, respectively.
- For the chlorination of 2,4-dichlorophenol (2,4-DCP), there was no significant difference in the experimental pseudo-first-order rate constants (k_{obs}) for reactions quenched with TMB versus those quenched with sodium thiosulfate.
- For the bromination of anisole, experimental k_{obs} values with TMB as the quencher agreed with values predicted for reactions quenched with sodium thiosulfate.
- Although TMB does not react with free chlorine as quickly as do traditional quenchers, TMB is able to serve as an effective quencher for halogenation reactions with half-times ≥ 0.5 minute.
- TMB did not degrade DBPs that were otherwise unstable in the presence of traditional quenchers. Ammonium chloride similarly did not destabilize the examined DBPs, but its utility as a quencher is limited to analytes that would not react with monochloramine.
- Using TMB as a quencher offers the additional benefit of being able to quantify residual free chlorine and free bromine via measurements of [Cl-TMB] and [Br-TMB], respectively, in quenched samples.
- The reaction of TMB with monochloramine is slow (relative to reactions with free chlorine) and thus is unlikely to interfere with the use of Cl-TMB as surrogate for residual free chlorine.

3. 6. Acknowledgements

The authors acknowledge Dr. Keith Reber (Towson University) for synthesis of 2,4-dichloro-1,3,5-trimethoxybenzene. Funding to A.L.R. and S.S.L. was received from the U.S. National Science Foundation (CBET-1067391) with additional support to S.S.L from the Whiting School of Engineering at Johns Hopkins University. Funding to J.D.S. was received from the ACS Petroleum Research Fund (54560-UNI4), the U.S. National Science Foundation (CBET-1651536), and a Jess and Mildred Fisher Endowed Professorship. Funding to R.P.D. and K.R.M. was received from the Fisher College of Science and Mathematics and the Office of Undergraduate Research and Creative Inquiry at Towson University. Any views reported herein are those of the authors and do not necessary reflect the views of the U.S. National Science Foundation or the ACS Petroleum Research Fund.

3. 7. References

1. Crittenden, J. C.; Trussell, R. R.; Hand, D. W.; Howe, K. J.; Tchobanoglous, G. *MWH's Water Treatment: Principles and Design* 3rd ed.; John Wiley & Sons: Hoboken, New Jersey, 2012.

2. Urbansky, E. T. Ascorbic acid treatment to reduce residual halogen-based oxidants prior to the determination of halogenated disinfection byproducts in potable water. *J. Environ. Monit.* **1999,** *1*, 471-476.

3. Black & Veatch Corporation. *White's Handbook of Chlorination and Alternative Disinfectants*, 5th ed.; John Wiley & Sons: Hoboken, New Jersey, 2010.

4. Croue, J.-P.; Reckhow, D. A. Destruction of chlorination byproducts with sulfite. *Environ. Sci. Technol.* **1989,** *23*, 1412-1419.

5. Kristiana, I.; Lethorn, A.; Joll, C.; Heitz, A. To add or not to add: The use of quenching agents for the analysis of disinfection by-products in water samples. *Water Res.* **2014,** *59*, 90-98.

6. Bedner, M.; MacCrehan, W. A. Transformation of acetaminophen by chlorination produces the toxicants 1,4-benzoquinone and N-acetyl-p-benzoquinone imine. *Environ. Sci. Technol.* **2006,** *40*, 516-522.

7. Wood, T. P.; Basson, A. E.; Duvenage, C.; Rohwer, E. R. The chlorination behaviour and environmental fate of the antiretroviral drug nevirapine in South African surface water. *Water Res.* **2016,** *104*, 349-360.

8. Yu, Y.; Reckhow, D. A. Formation and occurrence of *N*-chloro-2,2-dichloroacetamide, a previously overlooked nitrogenous disinfection byproduct in chlorinated drinking waters. *Environ. Sci. Technol.* **2017,** *51*, 1488-1497.

9. Dodd, M. C.; Huang, C. H. Transformation of the antibacterial agent sulfamethoxazole in reactions with chlorine: Kinetics, mechanisms, and pathways. *Environ. Sci. Technol.* **2004,** *38*, 5607-5615.

10. Cheng, H.; Song, D.; Chang, Y.; Liu, H.; Qu, J. Chlorination of tramadol: Reaction kinetics, mechanism and genotoxicity evaluation. *Chemosphere* **2015,** *141*, 282-289.

11. Heasley, V. L.; Fisher, A. M.; Herman, E. E.; Jacobsen, F. E.; Miller, E. W.; Ramirez, A. M.; Royer, N. R.; Whisenand, J. M.; Zoetewey, D. L.; Shellhamer, D. F. Investigations of the reactions of monochloramine and dichloramine with selected phenols: Examination of humic acid models and water contaminants. *Environ. Sci. Technol.* **2004,** *38*, 5022-5029.

12. Duirk, S. E.; Valentine, R. L. Bromide oxidation and formation of dihaloacetic acids in chloraminated water. *Environ. Sci. Technol.* **2007,** *41*, 7047-7053.

13. Sivey, J. D.; Roberts, A. L. Assessing the reactivity of free chlorine constituents Cl_2, Cl_2O, and HOCl toward aromatic ethers. *Environ. Sci. Technol.* **2012,** *46*, 2141-2147.

14. Mayeno, A. N.; Curran, A. J.; Roberts, R. L.; Foote, C. S. Eosinophils preferentially use bromide to generate halogenating agents. *J. Biol. Chem.* **1989,** *264*, 5660-5668.

15. Sivey, J. D.; Bickley, M. A.; Victor, D. A. Contributions of BrCl, Br_2, BrOCl, Br_2O, and HOBr to regiospecific bromination rates of anisole and bromoanisoles in aqueous solution. *Environ. Sci. Technol.* **2015,** *49*, 4937-4945.

16. Lau, S. S.; Abraham, S. M.; Roberts, A. L. Chlorination revisited: Does Cl^- serve as a catalyst in the chlorination of phenols? *Environ. Sci. Technol.* **2016,** *50*, 13291-13298.

17. Rice, E. W.; Baird, R. B.; Clesceri, L. S.; Eaton, A. D. *Standard Methods for the Examination of Water and Wastewater*. 22nd ed.; American Public Health

Association, American Water Works Association, Water Environment Federation: Washington, D.C., 2012.

18. Joo, S. H.; Mitch, W. A. Nitrile, aldehyde, and halonitroalkane formation during chlorination/chloramination of primary amines. *Environ. Sci. Technol.* **2007,** *41*, 1288-1296.

19. Sivey, J. D.; McCullough, C. E.; Roberts, A. L. Chlorine monoxide (Cl_2O) and molecular chlorine (Cl_2) as active chlorinating agents in reaction of dimethenamid with aqueous free chlorine. *Environ. Sci. Technol.* **2010,** *44*, 3357-3362.

20. Sivey, J. D.; Arey, J. S.; Tentscher, P. R.; Roberts, A. L. Reactivity of BrCl, Br_2, BrOCl, Br_2O, and HOBr toward dimethenamid in solutions of bromide + aqueous free chlorine. *Environ. Sci. Technol.* **2013,** *47*, 1330-1338.

21. US EPA. *Estimation Programs Interface Suite™ for Microsoft® Windows, v 4.11*, United States Environmental Protection Agency: Washington, DC, USA, 2012.

22. Zhang, J.-Z.; Millero, F. J. The rate of sulfite oxidation in seawater. *Geochim. Cosmochim. Acta* **1991,** *55*, 677-685.

23. Gallard, H.; Von Gunten, U. Chlorination of phenols: Kinetics and formation of chloroform. *Environ. Sci. Technol.* **2002,** *36*, 884-890.

24. Heeb, M. B.; Criquet, J.; Zimmermann-Steffens, S. G.; von Gunten, U. Oxidative treatment of bromide-containing waters: Formation of bromine and its reactions with inorganic and organic compounds — A critical review. *Water Res.* **2014,** *48*, 15-42.

25. Krasner, S. W.; Weinberg, H. S.; Richardson, S. D.; Pastor, S. J.; Chinn, R.; Sclimenti, M. J.; Onstad, G. D.; Thruston, A. D. Occurrence of a new generation of disinfection byproducts. *Environ. Sci. Technol.* **2006,** *40*, 7175-7185.

26. Yu, Y.; Reckhow, D. A. Kinetic analysis of haloacetonitrile stability in drinking waters. *Environ. Sci. Technol.* **2015,** *49*, 11028–11036.

27. U.S. Environmental Protection Agency (EPA). *Method 551.1: Determination of Chlorination Disinfection Byproducts, Chlorinated Solvents, and Halogenated Pesticides/Herbicides in Drinking Water by Liquid-Liquid Extraction and Gas Chromatography With Electron-Capture Detection (Revision 1.0)*, Washington, D.C., 1995.

28. Koudjonou, B. K.; LeBel, G. L. Halogenated acetaldehydes: Analysis, stability and fate in drinking water. *Chemosphere* **2006,** *64*, 795-802.

29. Qiang, Z.; Adams, C. D. Determination of monochloramine formation rate constants with stopped-flow spectrophotometry. *Environ. Sci. Technol.* **2004,** *38*, 1435-1444.

4. Roles of Cl_2, Cl_2O, and HOCl on the Kinetics of Ionone Chlorination

4. 1. Abstract

Although Cl_2 and Cl_2O have gained recognition in recent years as highly reactive constituents of free available chlorine (FAC), robust second-order rate constants for Cl_2 and Cl_2O remain scarce in the environmental literature. In this work, we explored the chlorination kinetics of three structurally related alkenes (α-ionone, β-ionone, and dehydro-β-ionone), a class of compounds whose reactivities with Cl_2 and Cl_2O under environmentally-relevant conditions have not been previously investigated. Second-order rate constants for Cl_2, Cl_2O, and HOCl were computed from experimental rate constants obtained at various pH, $[Cl^-]$, and [FAC]. Our results show that HOCl is the predominant chlorinating agent for the most reactive of the alkenes (i.e., dehydro-β-ionone), whereas Cl_2 and Cl_2O can strongly influence the chlorination kinetics of the less reactive alkenes (i.e., α- and β-ionones) at high $[Cl^-]$ and high [FAC], respectively. The tradeoff between overall reactivity with FAC and selectivity for Cl_2 and Cl_2O observed in previous studies involving aromatic compounds also applies to the alkenes examined. In laboratory experiments in which high [FAC] may be used, omission of Cl_2O in data modeling could yield second-order rate constants of dubious validity. In chlorinating real waters with elevated $[Cl^-]$, formation of Cl_2 may enhance the formation kinetics of chlorinated disinfection byproducts (DBPs) and exacerbate the burden of DBP control for water utilities.

4. 2. Introduction

Despite advances in water disinfection technologies over the past decades, aqueous chlorine (also known as free available chlorine, or FAC) remains the most commonly used disinfectant for drinking water treatment in the United States and Canada.[1] FAC is known to form potentially toxic disinfection byproducts (DBPs) upon reactions with organic compounds.[2] According to conventional wisdom, HOCl (pK_a = 7.54 at 25 °C, ref. 3) is regarded as the predominant chlorinating agent in FAC under typical drinking water treatment conditions. Over the past several years, however, studies have emerged to show that molecular chlorine (Cl_2) and chlorine monoxide (Cl_2O), which are minor constituents of FAC, can also influence the chlorination kinetics of some organic compounds. Cl_2 and Cl_2O exist in equilibrium with HOCl (equations 4-1 and 4-2):

$$HOCl + Cl^- + H^+ \rightleftharpoons Cl_2 + H_2O \qquad \log K_{Cl_2} = 2.72 \qquad (4\text{-}1)$$

(ref. 4, 25 °C, corrected to 0 M ionic strength using the Davies equation)

$$2\,HOCl \rightleftharpoons Cl_2O + H_2O \qquad \log K_{Cl_2O} = -2.06 \qquad (4\text{-}2)$$

(ref. 5, corrected to 25 °C according to ref. 6)

It has been shown that Cl_2 and Cl_2O can play important roles in the chlorination of aromatic compounds including dimethenamid,[6] 3-methylanisole,[7] 1,3-dimethoxy-benzene,[7] and (chloro)phenols.[8] Reactivities of FAC with heterocyclic nitrogen compounds such as antipyrine[9] and aminopyrine[10] similarly cannot be explained unless Cl_2 and Cl_2O are considered. Nevertheless, robust second-order rate constants for Cl_2 and Cl_2O are only available for a limited number of compounds, and the importance of these

chlorinating agents for compounds that do not possess aromatic moieties has not been investigated. Alkenes are particularly under-examined in the aqueous chlorination literature, with apparent rate constants (k_{app}) for reactions with HOCl reported for fewer than five compounds.[11] To our knowledge, no robust second-order rate constants for the reactions of alkenes with Cl_2 and Cl_2O are available. To address the knowledge gaps in the literature, we chose to examine the chlorination kinetics of three structurally related alkenes: α-ionone, β-ionone, and dehydro-β-ionone. All three compounds consist of a methyl-substituted cyclohexene (or cyclohexadiene) and an α,β-unsaturated carbonyl, which is also called an enone (**Figure 4-1**). In α-ionone, the alkene in the cyclohexene is not conjugated with the enone. In β-ionone, the alkene is conjugated with the enone. In dehydro-β-ionone, the two alkenes in the cyclohexadiene are conjugated with the enone. As the number and location of alkenes differ in the three ionones, these compounds are anticipated to have different reactivities in the presence of FAC.

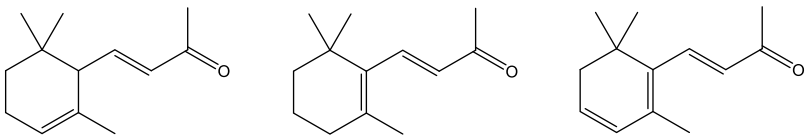

Figure 4-1. Structures of the alkene-containing compounds investigated in this study.

Ionones are aroma compounds in flowers[12] and can be found as fragrance ingredients in cosmetics, toiletries, and cleaning products.[13-14] Despite their pleasant scents, ionones (particularly β-ionone) can contribute to taste and odor problems in drinking water. β-Ionone is produced by some cyanobacteria[15-16] and algae[17-18] via

oxidative cleavage of β-carotene.[19] Concentrations of β-ionone have been reported to reach as high as 27 ng/L in Lake Zurich, Switzerland[18] and 50 ng/L in Lake Taihu, China[20] during algal bloom events. These measured concentrations of β-ionone exceed the compound's odor threshold of 7 ng/L.[21]

Ionones are expected to be efficient precursors of trihalomethanes (THMs) due to their methyl ketone functional groups, which are known to produce THMs via the haloform reaction.[22] Indeed, one study found that the yield of total THMs from β-ionone chlorination was 35% (on a molar basis) after 7 days.[23] *Trans*-β-ionone-5,6-epoxide (or simply β-ionone epoxide) has been hypothesized to be a reaction intermediate that leads to THM formation, while β-cyclocitral is proposed to be an intermediate leading to non-THM DBPs (**Figure 4-2**). The chlorination pathways of α-ionone and dehydro-β-ionone have not been explored, although formation of chlorohydrins and non-chlorinated compounds (e.g., epoxides) seems likely given the chlorination mechanisms of other alkenes in aqueous solutions.[24-26]

The objective of this work is to investigate the influence of Cl_2, Cl_2O, and HOCl on the chlorination kinetics of three ionones. Solution pH, [Cl^-], and [FAC] were systematically varied in kinetic experiments conducted in batch reactors. Second-order rate constants for Cl_2, Cl_2O, and HOCl computed from experimental rate constants allows us to determine the contributions of various chlorine species to overall reactivities of the ionones. Comparisons of the relative importance of various chlorinating agents, in turn, enables us to elucidate the relationship between alkene structure and alkene reactivity in the presence of FAC.

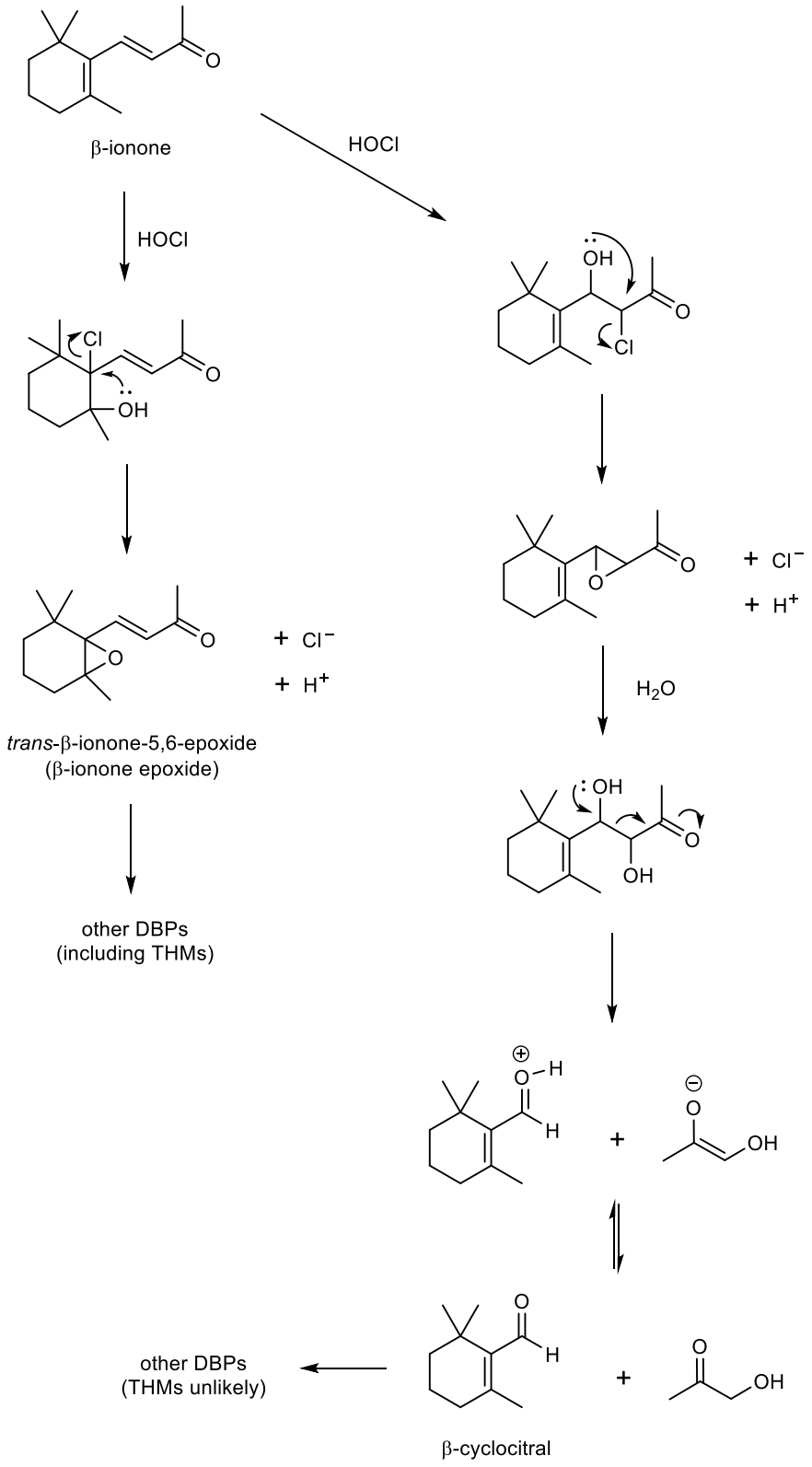

Figure 4-2. Proposed reaction pathways for the chlorination of β-ionone (adapted from ref. 23).

4. 3. Materials and Methods

All aqueous solutions were prepared using distilled water that was further purified in a Milli-Q Advantage A10 system (EMD Millipore) to a resistivity of 18.2 MΩ•cm. Sodium hypochlorite (NaOCl) solutions (laboratory grade, 5.65–6%) purchased from Fisher Scientific served as the source of FAC in all experiments. NaOCl solutions were standardized weekly via iodometric titrations (Standard Methods 4500-Cl B, ref. 27). All glassware was soaked in concentrated FAC solutions (≥ 0.5 M) for at least 8 hours and subsequently rinsed with Milli-Q water before use. α-Ionone (racemate, 94%), β-ionone (predominantly *trans*, ≥ 97%), 1,3,5-trimethoxybenzene (≥ 99.0%), 2-chloro-1,3,5-trimethoxybenzene (98%), and sodium nitrate (≥ 99.0%) were purchased from Sigma-Aldrich. Methanol (99.9%), nitric acid (70%), sodium chloride (ACS grade), and sodium hydroxide (ACS grade) were obtained from Fisher Scientific. Potassium phosphate monobasic, sodium phosphate dibasic, and sodium bicarbonate (all ACS grade) were purchased from J. T. Baker. Aside from sodium chloride, commercially available reagents were used without further purification. Sodium chloride was recrystallized twice to reduce bromide contamination by ≥ 97% using a procedure described in ref. 8 and also in Appendix A. Dehydro-β-ionone was synthesized according to ref. 28. Details of dehydro-β-ionone synthesis, as well as the syntheses of hypothesized products of β-ionone chlorination, are described in Appendix C.

Kinetic Experiments. Experiments were conducted in batch reactors (40-mL amber glass vials with PTFE-lined plastic caps) kept in the dark inside a stainless-steel constant-temperature water bath set at 25.00 ± 0.01 °C. Reaction solutions (30 mL) consisted of 10 mM of phosphate buffer (pH 5.5–8.5) or carbonate buffer (> pH 8.5) as well as 0.1 M

$NaNO_3$ (to set the ionic strength). In our previous study[8] that employed an identical reactor setup, we found that the presence of headspace in the reactor did not affect chlorination kinetics, suggesting that partitioning of chlorine species into the headspace was minimal. Furthermore, control experiments done in this study at pH 6–7 without FAC addition revealed that the concentrations of ionones did not change appreciably after ≥ 5 hours, indicating that volatilization or hydrolysis did not contribute significantly to the loss of these compounds under our reaction conditions.

The pH of reaction solutions was adjusted using small volumes of HNO_3 or NaOH. Measurements showed that solution pH did not vary by more than 0.05 unit throughout the experiments. Working solutions of FAC were prepared by diluting the NaOCl stock with water shortly before each experiment. In most experiments, $[FAC]_o$ = 130 μM. Stock solutions of ionones were made by dissolving the neat compounds in methanol; these were subsequently diluted with a solution consisting of 20 vol% methanol and 80 vol% water to make spiking solutions. Control experiments were carried out at selected pH values to assess the effect of methanol in the spiking solution on β-ionone chlorination kinetics. Except for experiments in which the initial ionone concentration was varied, nominal $[ionone]_o$ = 5 μM.

At the start of each kinetic experiment, 1.0 mL of the working FAC solution was added to the reactor using a glass pipet. The reactor was capped, shaken vigorously, and returned to the water bath. After waiting approximately 8 minutes for temperature equilibration to occur, the reaction was initiated by spiking the reactor with 0.40 mL of ionone spiking solution. The final methanol content in the reactor was approximately 0.25% (v/v). The reactor was again capped, shaken vigorously, and returned to the water

bath. Aliquots (2.0 mL) of the reaction solution were periodically collected using a 2-mL glass syringe fitted with a stainless-steel needle. The aliquots were transferred to 4-mL amber glass autosampler vials pre-amended with 0.20 mL of 1,3,5-trimethoxybenzene (TMB) dissolved in 50 vol% methanol and 50 vol% water ($[TMB]_o/[FAC]_o \geq 3.5$). For experiments conducted at pH > 7.5, the TMB quenching solution contained 0.1 M HNO_3 so as to lower the pH of the sample to ≤ 7 at the time of quenching. We have previously demonstrated that TMB can serve as an effective quencher for FAC under similar reaction conditions (see Chapter 3). Rate constants for the chlorination of ionones obtained from experiments using TMB as the quencher are not significantly different (at the 95% confidence interval) from those obtained using sodium thiosulfate as the quencher (data not shown). Efforts were made to follow the disappearance of the parent compound for at least three half-lives. Concentrations of TMB and its monochlorinated product, Cl-TMB, were also monitored in selected experiments to ensure that pseudo-first-order conditions ($[FAC] \approx [FAC]_o$ = constant) were maintained throughout the reaction time courses.

In experiments designed to elucidate the influence of varying $[Cl^-]$ on kinetics of ionone chlorination, sufficient NaCl was added such that $[Cl^-]_{added}$ in the reactor = 1, 3, or 10 mM. $[NaNO_3]$ was adjusted to maintain constant ionic strength (i.e., [NaCl] + $[NaNO_3]$ = 0.1 M). To investigate the reaction order in [HOCl], $[FAC]_o$ was varied (97–320 μM for α-ionone, 85–380 μM for β-ionone, and 94–310 μM for dehydro-β-ionone) at selected pH values while keeping all other reaction conditions constant. The reaction order in [ionone] was assessed by varying the initial ionone concentration at a fixed [FAC] at pH 7.0. $[Ionone]_o$ was varied from 2.5 to 6.8 μM (for β-ionone) or from 2.1 to

6.2 μM (for α-ionone and dehydro-β-ionone). Effects of varying ionic strength and pH buffer concentration were also investigated in separate experiments.

Analytical Method for Kinetic Experiments. After all the samples were collected and quenched, they were analyzed using high-performance liquid chromatography (HPLC). The HPLC system consisted of a Waters 1525 binary pump, Waters 2996 photodiode array (PDA) detector, and XBridge Shield reversed-phase C18 column (5-μm particles, 4.6 × 150 mm). The mobile phase consisted of (A) water and (B) methanol. Gradient elution was used to analyze the ionones (70% B at t = 0, increased to 80% B over 8 minutes; total run time = 8 minutes; flow rate = 1 mL/min). The ionones, TMB, and Cl-TMB were quantified at their respective wavelengths of maximum absorbance (λ_{max}). Although some products of ionone chlorination were detected, only the parent compounds were quantified. In selected experiments, the samples were analyzed a second time using an isocratic method (50% B; total run time = 14 minutes; flow rate = 1 mL/min) to monitor [TMB] and [Cl-TMB]. By quantifying [TMB] and [Cl-TMB] in our quenched samples, we confirmed that [FAC] did not decrease by ≥ 9% throughout the course of those experiments.

Identification of Intermediates/Products of β-Ionone Chlorination. In a separate experiment, gas chromatography-mass spectrometry (GC-MS) was used to detect the intermediates/products of β-ionone chlorination. The chlorination experiment was carried out in a batch reactor (40-mL amber glass vial with PTFE-lined plastic cap) at room temperature (22 ± 1 °C). The reaction solution (30 mL) consisted of 10 mM of phosphate buffer (pH 6.24) and 0.1 M $NaNO_3$. At the start of the experiment, 1.0 mL of a working FAC solution (4.0 mM) was added to the reactor using a glass pipet, resulting in $[FAC]_o$

= 130 μM. The reactor was capped and shaken vigorously. After waiting approximately 8 minutes for temperature equilibration to occur, 0.50 mL of a β-ionone spiking solution (710 μM) was added to the reactor (nominal $[\beta\text{-ionone}]_o$ = 11 μM). The reaction was allowed to proceed for 20 minutes, after which 5.0 mL of the reaction solution was collected using a 5-mL glass syringe fitted with a stainless-steel needle and then transferred to a 15-mL glass centrifuge tube pre-amended with 0.30 mL of sodium thiosulfate dissolved in water ($[S_2O_3^{2-}]_o/[FAC]_o$ = 1.5). Ethyl acetate (1.0 mL) was added to the centrifuge tube as the extraction solvent. The contents of the centrifuge tube were mixed vigorously for 1 minute using a vortex mixer. The ethyl acetate layer was subsequently transferred to a 2-mL amber glass autosampler vial and analyzed by GC-MS.

The GC-MS system consisted of an Agilent 7890B gas chromatograph interfaced with an Agilent 5977A mass spectrometer with electron ionization (EI). An Agilent HP-5MS UI column (30 m × 0.25 mm, film thickness = 0.25 μm) was used. The GC inlet was set to 150 °C and operated in splitless mode. The total column flow was constant at 1 mL/min. The oven temperature program included an initial temperature of 60 °C (no hold), ramp at 10 °C/min to 100 °C (hold for 0.5 min), ramp at 5 °C/min to 160 °C (hold for 0.5 min), and ramp at 20 °C/min to 280 °C (no hold); the total analysis time was 23 minutes. The transfer line temperature was fixed at 280 °C. An aliquot (1 μL) of the ethyl acetate sample was injected onto the GC/MS, and mass spectra were obtained in full scan (*m/z* 50–350) mode.

Data Modeling. Pseudo-first-order rate constants (k_{obs}) for the loss of ionones were computed from linear regressions of experimental $\ln[\text{ionone}]$ versus time data. Second-

order rate constants for Cl_2, Cl_2O, and HOCl were computed via nonlinear least-squares regressions in *SigmaPlot 12.5* (Systat Software). Details of the data modeling process are in Appendix C.

4. 4. Results and Discussion

Kinetic experiments were conducted under pseudo-first-order conditions in which [FAC] ≈ $[FAC]_o$ (≫ $[ionone]_o$) in order to elucidate the roles of Cl_2, Cl_2O, and HOCl in the aqueous chlorination of three ionones. Pseudo-first-order rate constants (k_{obs}) for the loss of α-ionone, β-ionone, and dehydro-β-ionone were determined from linear regressions of ln[ionone] versus time data (example data for β-ionone are shown in **Figure 4-3**). Under our reaction conditions, the overall rate expression for the loss of ionones can be described by equation 4-3:

$$-\frac{d[\text{ionone}]}{dt} = k_{obs}[\text{ionone}] \tag{4-3}$$

where k_{obs} is represented by equation 4-4:

$$k_{obs} = k_{Cl_2}[Cl_2] + k_{Cl_2O}[Cl_2O] + k_{HOCl}[HOCl] \tag{4-4}$$

where k_{Cl_2}, k_{Cl_2O}, and k_{HOCl} are the second-order rate constants for reactions with Cl_2, Cl_2O, and HOCl, respectively. Results from our chlorination kinetic experiments are described and discussed in the following sections.

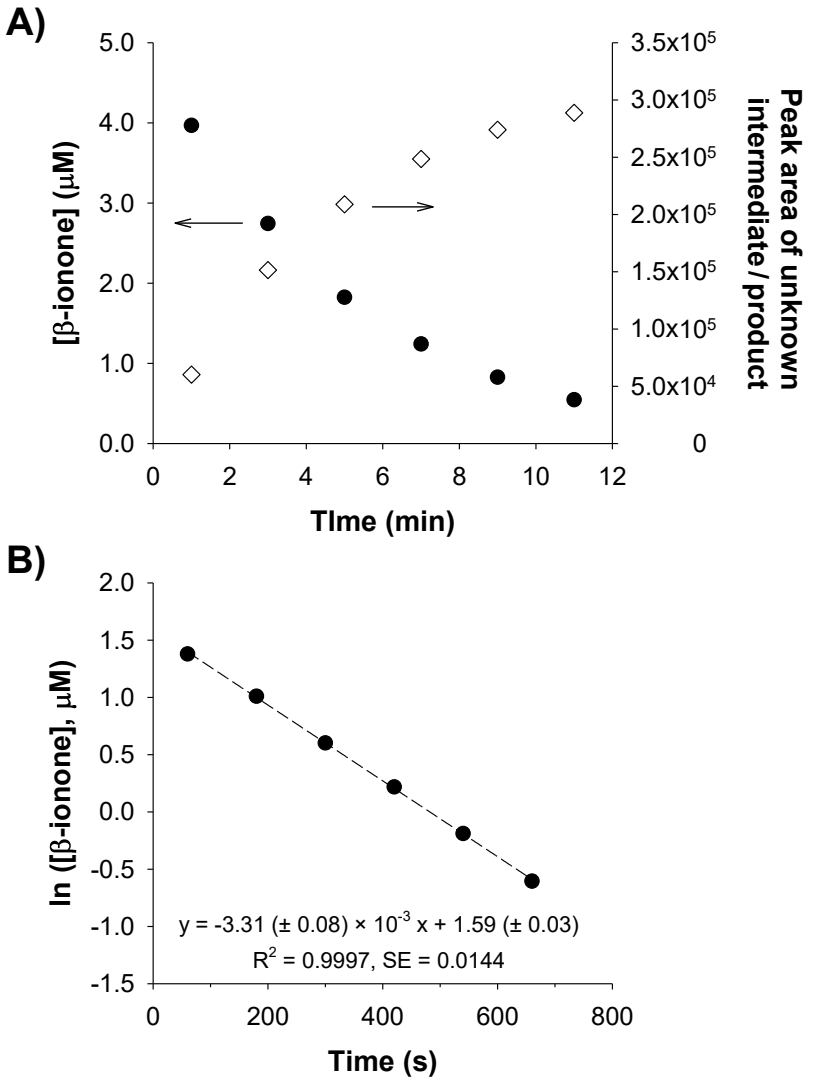

Figure 4-3. Typical data from β-ionone chlorination experiments showing **(A)** [β-ionone] and peak areas of an unknown intermediate/product versus time and **(B)** linear regressions of ln[β-ionone] versus time data. Reaction conditions: pH 6.74, $[\beta\text{-ionone}]_o$ = 5 μM, $[FAC]_o$ = 130 μM, no NaCl added, [phosphate buffer] = 10 mM, $[NaNO_3]$ = 0.1 M, T = 25 °C. Uncertainties in the slope and y-intercept indicate 95% confidence intervals.

Effects of Varying pH and [Cl^-]. Chlorination experiments were conducted at pH 5.5–9.2 and at various concentrations of added NaCl. The resulting $\log k_{obs}$ versus pH data for α-ionone, β-ionone, and dehydro-β-ionone are shown in **Figure 4-4**. α-Ionone and β-ionone generally reacted with FAC more slowly than did dehydro-β-ionone under similar reaction conditions. Adding 1, 3, or 10 mM of Cl^- while maintaining constant ionic strength led to an increase in k_{obs} at pH ≤ 7 for all three compounds. The increase in k_{obs} with increasing $[Cl^-]_{added}$ can be attributed to reactions with Cl_2, the concentration of which depends on both $[Cl^-]$ and $[H^+]$ (equation 4-1). At pH > 7.5, Cl^- addition did not have any appreciable effect on k_{obs}, indicating that Cl_2 is not an important chlorinating agent at high pH. Although some previous researchers have suggested that reactions with H_2OCl^+ can cause k_{obs} to increase with decreasing pH,[29-32] $[H_2OCl^+]$ does not depend on $[Cl^-]$ and thus cannot explain the increase in k_{obs} with added NaCl.

α-Ionone and β-ionone are more sensitive to the effect of Cl^- addition than is dehydro-β-ionone; adding 1 mM of Cl^- to reactors with α- and β-ionones produced a qualitatively similar enhancement in k_{obs} as adding 3 mM of Cl^- to reactors with dehydro-β-ionone. This observation implies that Cl_2 exerts a greater influence on the chlorination kinetics of the less reactive alkenes.

The distinction between $[Cl^-]_{added}$ and actual $[Cl^-]$ in the reactor is important because we have previously shown that the NaOCl stock solutions used in our experiments contained approximately equimolar concentrations of Cl^- and OCl^-.[8] The total $[Cl^-]$ in the reactor was considered in modeling the data from ionone chlorination experiments.

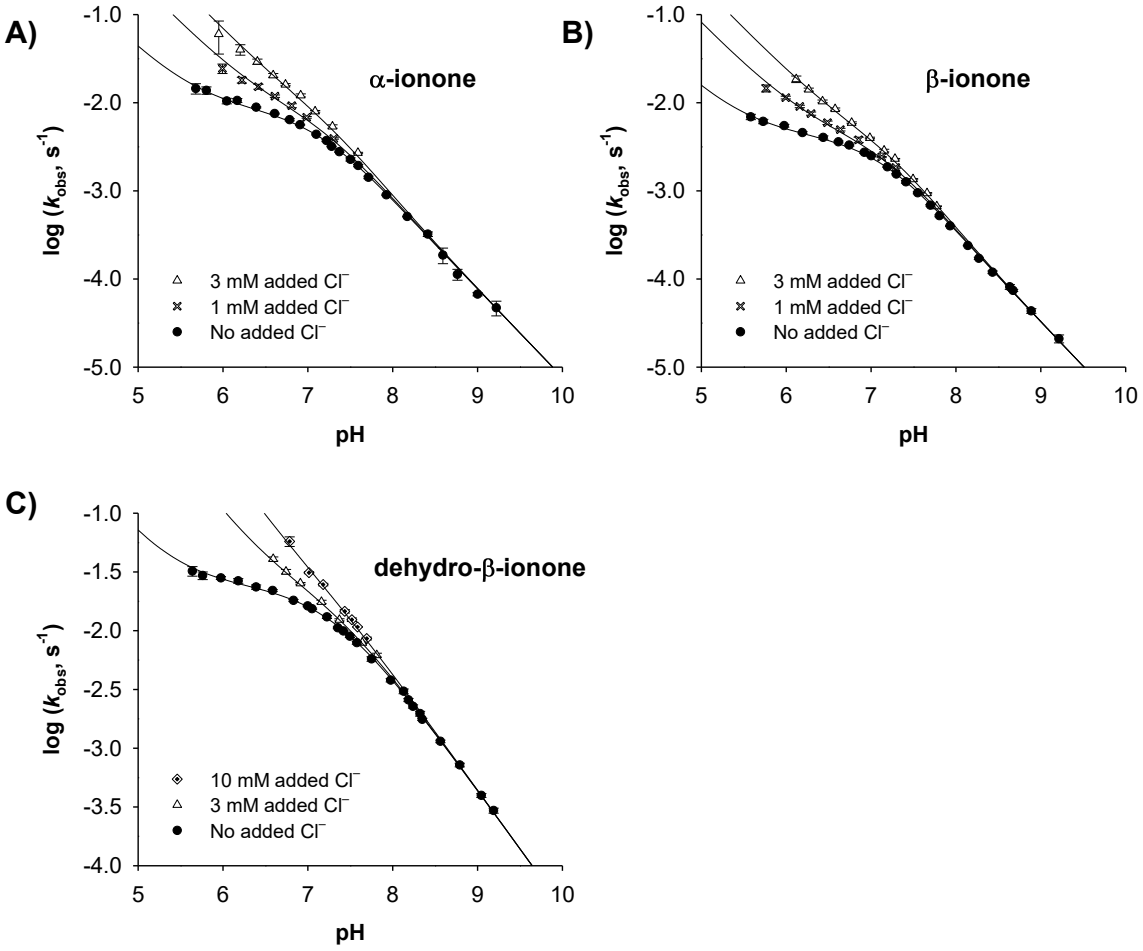

Figure 4-4. Pseudo-first-order rate constants (k_{obs}) versus pH at varying chloride concentrations for **(A)** α-ionone, **(B)** β-ionone, and **(C)** dehydro-β-ionone. Solid lines are model fits to the form of equation 4-4. Reaction conditions: $[\text{ionone}]_o$ = 5 μM, $[\text{FAC}]_o$ = 130 μM, $[\text{NaCl}]_{\text{added}}$ = 0, 1, 3, or 10 mM, ionic strength (i.e., $[\text{NaCl}]_{\text{added}}$ + $[\text{NaNO}_3]$) = 0.1 M, [pH buffer] = 10 mM, T = 25 °C. Error bars denote 95% confidence intervals (smaller than symbols if not shown).

Effects of Varying [FAC] and [Ionone]. To investigate the reaction order (n) in [HOCl], $[FAC]_o$ was varied at selected pH values while maintaining all other reaction conditions constant. The resulting $\log k_{obs}$ versus $\log[HOCl]$ data, as well as the slopes (i.e., n) of the linear regressions, are shown in **Figure 4-5**. For α-ionone, the values of n at pH 7.3 and 7.6 without added Cl^- (1.52 ± 0.05 and 1.48 ± 0.07, respectively) are not significantly different from each other at the 95% confidence level (**Figure 4-5a**). For β-ionone, the largest n (1.71 ± 0.06) was observed at pH 7.0 without added Cl^-, and n decreased with increasing pH (**Figure 4-5b**). When 3 mM of Cl^- was present at pH 7.0, n decreased to 1.43 ± 0.08. The value of n for dehydro-β-ionone at pH 7.6 without added Cl^- (1.10 ± 0.02) was the lowest observed in our experiments (**Figure 4-5c**).

The influence of Cl_2O on reaction kinetics is anticipated to be most pronounced at high [HOCl] because $[Cl_2O]$ is proportional to $[HOCl]^2$ (equation 4-2). Accordingly, a reaction that is first-order in $[Cl_2O]$ will be second-order in [HOCl]. In such case, plotting $\log k_{obs}$ versus $\log[HOCl]$ will yield a slope of 2, with slopes that are between 1 and 2 reflecting contributions from both Cl_2O and HOCl. Complications arise when FAC solutions contain approximately equimolar concentrations of Cl^- and [HOCl]; a first-order dependence on $[Cl_2]$ can masquerade as a second-order dependence on [HOCl] because $[Cl_2] = K_{Cl_2}[H^+][HOCl][Cl^-]$ (equation 4-1). We have previously shown that both Cl_2 and Cl_2O must be considered in order to explain the $\log k_{obs}$ versus $\log[HOCl]$ data for (chloro)phenols at low pH.[8] In this study, however, the experiments with varying [FAC] were conducted at pH 7–8, and $[Cl^-]_{tot}$ in the reactor was ≤ 0.5 mM in the absence of added Cl^-. Under these conditions, the influence of Cl_2 should be minor relative to that

of Cl_2O. Nonetheless, the increase in [Cl^-] that would accompany the increase in [HOCl] was taken into account in modeling the experimental data.

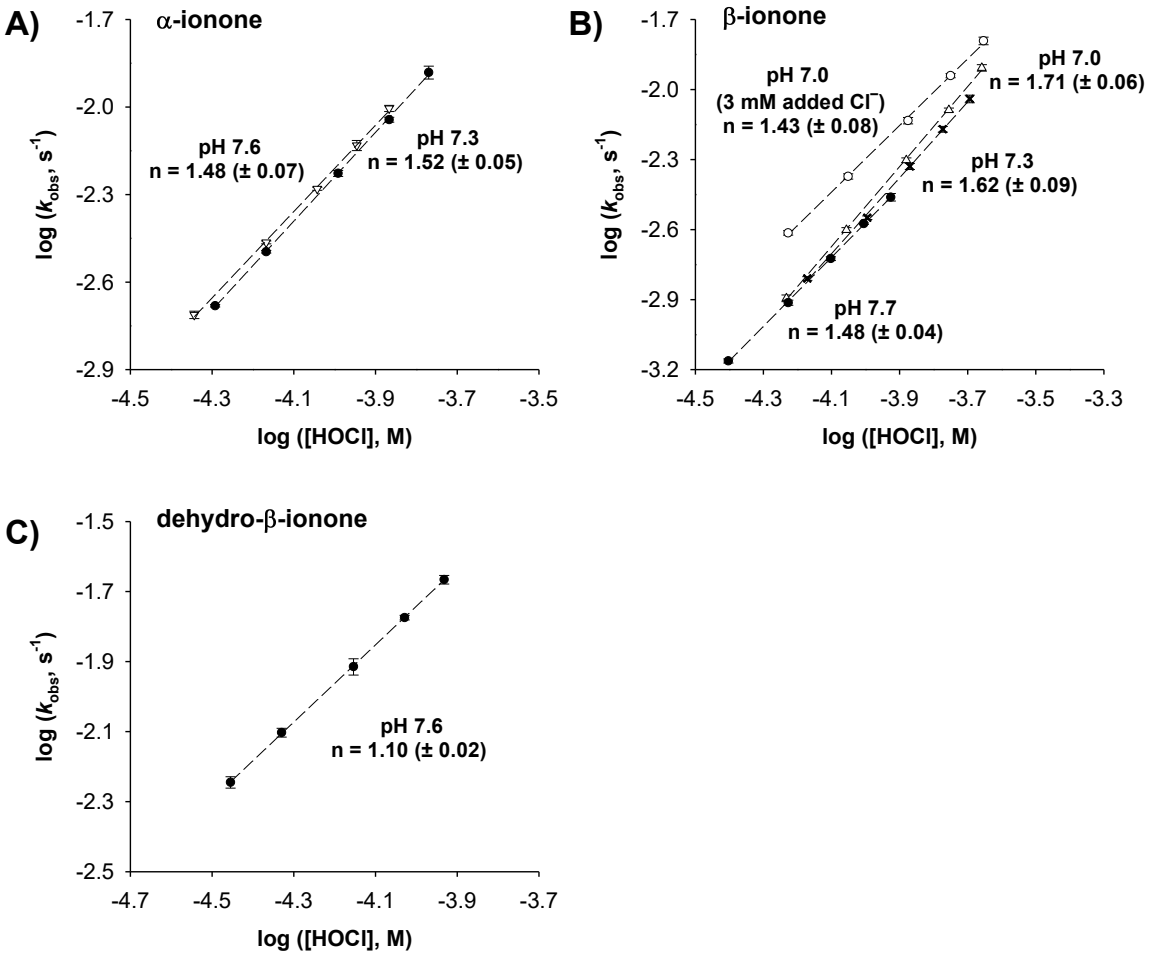

Figure 4-5. Pseudo-first-order rate constants (k_{obs}) as a function of [HOCl] for **(A)** α-ionone, **(B)** β-ionone, and **(C)** dehydro-β-ionone at selected pH values. Reaction conditions: $[ionone]_o$ = 5 μM; $[FAC]_o$ = 97–320 μM (α-ionone), 85–380 μM (β-ionone), or 94–310 μM (dehydro-β-ionone); no NaCl was added unless otherwise stated; ionic strength (i.e., $[NaCl]_{added}$ + $[NaNO_3]$) = 0.1 M; [pH buffer] = 10 mM; T = 25 °C. Error bars and uncertainties in the slopes denote 95% confidence intervals.

The initial concentration of each ionone was varied to determine the reaction order in [ionone]. Plots of log (rate) versus log $[ionone]_o$ for all compounds are linear with slopes close to 1.0 (**Figure 4-6**), indicating that reactions with FAC are first-order in [ionone].

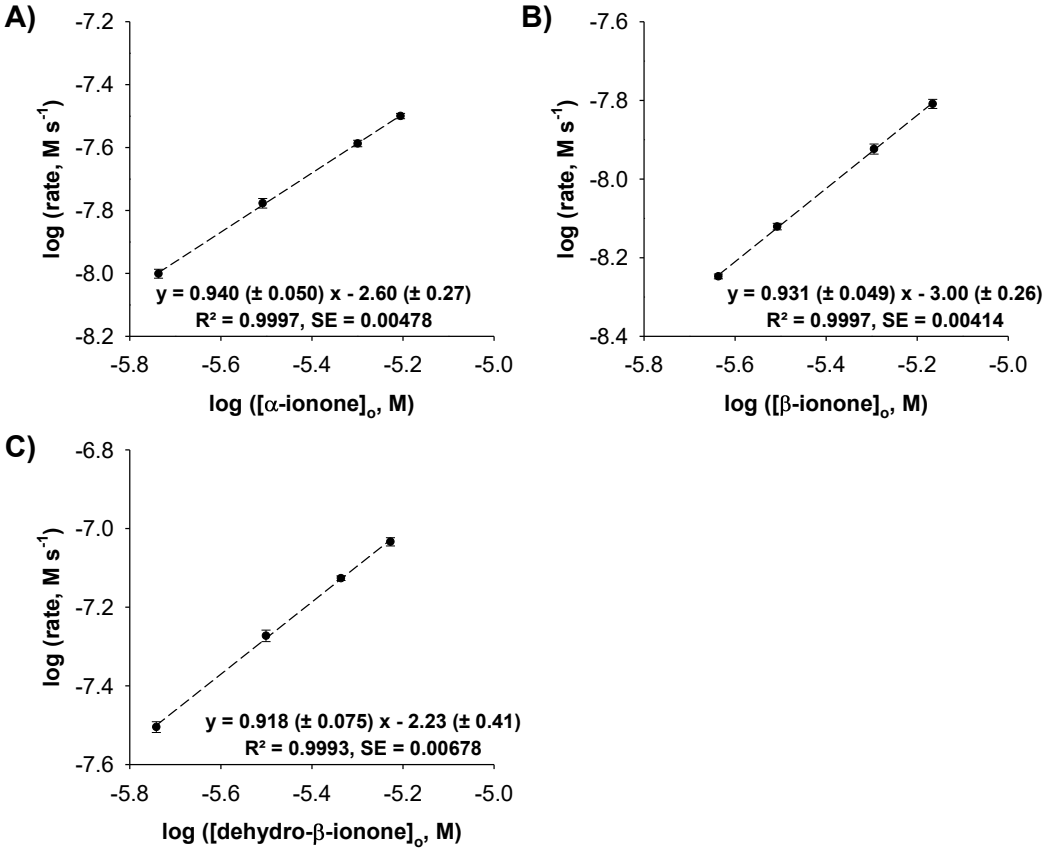

Figure 4-6. Chlorination rates as a function of initial ionone concentration for **(A)** α-ionone, **(B)** β-ionone, and **(C)** dehydro-β-ionone. Reaction conditions: pH 7.0, $[ionone]_o$ = 2.5–6.8 μM (β-ionone) or 2.1–6.2 μM (α-ionone and dehydro-β-ionone), $[FAC]_o$ = 130 μM, no NaCl added, $[NaNO_3]$ = 0.1 M, T = 25 °C. Dashed lines represent linear regressions of the data. Error bars on the symbols and uncertainties in the equations denote 95% confidence intervals. SE = standard errors of the regressions.

Effect of Other Reactor Constituents. The effect of ionic strength on chlorination kinetics was assessed by varying [$NaNO_3$]. We found that varying [$NaNO_3$] had no appreciable effect on k_{obs} for α- and β-ionones (**Figures 4-7a and 4-7b**, respectively). There is some scatter in the k_{obs} versus [$NaNO_3$] data for dehydro-β-ionone (**Figure 4-7c**), but the scatter is likely due to variations in pH across the four reactors.

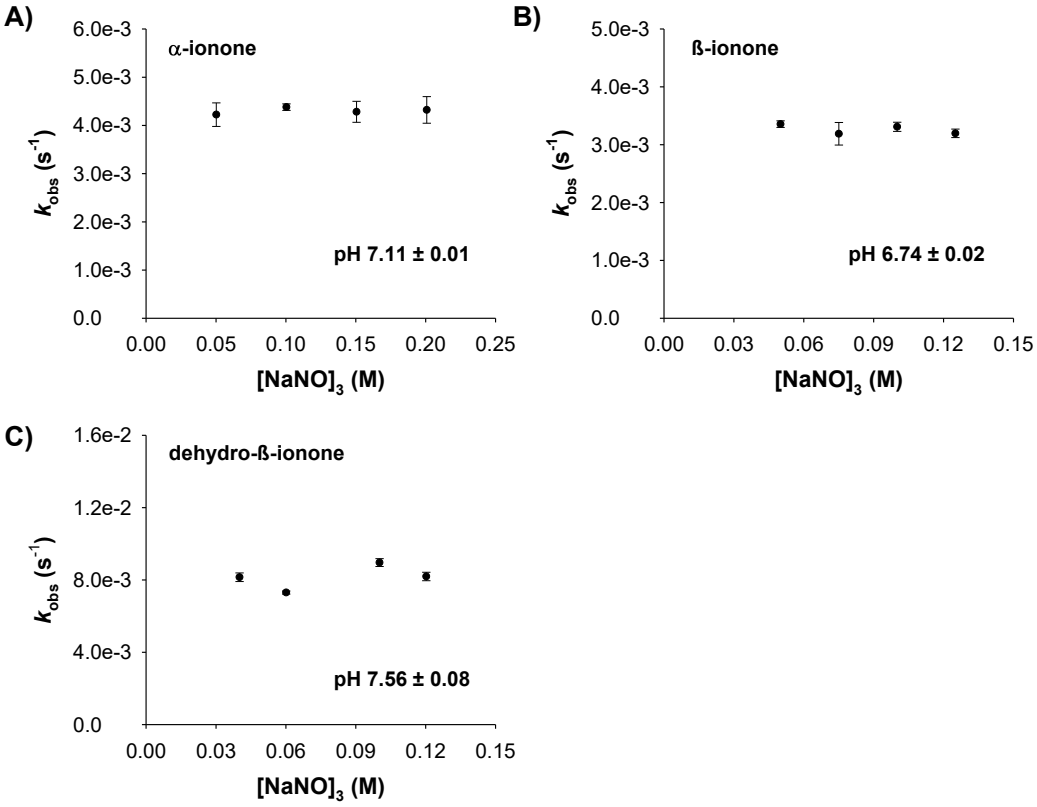

Figure 4-7. Pseudo-first-order rate constants (k_{obs}) as a function of [$NaNO_3$] for **(A)** α-ionone, **(B)** β-ionone, and **(C)** dehydro-β-ionone. Reaction conditions: $[ionone]_o$ = 5 μM, $[FAC]_o$ = 130 μM, no NaCl added, $[phosphate]_{tot}$ = 10 mM, T = 25 °C. Error bars denote 95% confidence intervals (smaller than symbols if not shown).

Some fluctuation exists in the k_{obs} versus [phosphate]$_{tot}$ data for α-ionone (**Figure 4-8a**), but the effect appears to be modest at [phosphate]$_{tot}$ ≤ 10 mM. As the concentration of pH buffer used in most experiments did not exceed 10 mM, we did not pursue the effect of phosphate buffer on α-ionone chlorination rates further. Phosphate buffer did not affect k_{obs} for β-ionone (**Figure 4-8b**) and dehydro-β-ionone (**Figure 4-8c**).

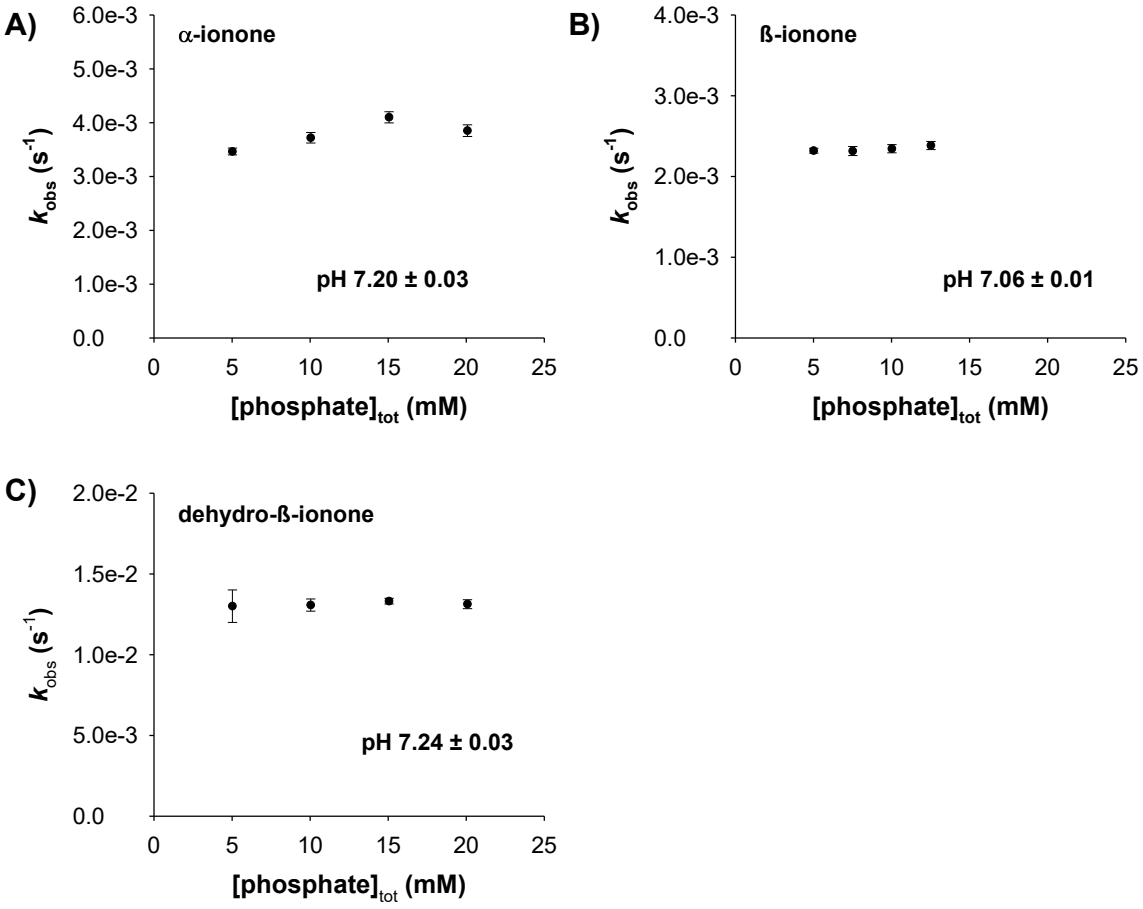

Figure 4-8. Pseudo-first-order rate constants (k_{obs}) as a function of phosphate buffer concentration for **(A)** α-ionone, **(B)** β-ionone, and **(C)** dehydro-β-ionone. Reaction conditions: [ionone]$_o$ = 5 μM, [FAC]$_o$ = 130 μM, no NaCl added, [$NaNO_3$] = 0.1 M, T = 25 °C. Error bars denote 95% confidence intervals (smaller than symbols if not shown).

Carbonate buffer did not affect k_{obs} for β-ionone (**Figure 4-9a**) and dehydro-β-ionone (**Figure 4-9b**), although it appreciably enhanced k_{obs} for α-ionone (**Figure 4-10**). For α-ionone, the degree to which carbonate buffer enhanced k_{obs} at pH 8.59–9.22 decreased slightly with increasing pH. As pK_{a2} of the carbonate buffer system is 10.31,[33] our results suggest that bicarbonate (HCO_3^-) has greater catalytic activity than does carbonate (CO_3^{2-}) in the chlorination of α-ionone. At each pH, we extrapolated the k_{obs} of α-ionone to $[carbonate]_{tot} = 0$ using linear regressions of the k_{obs} versus $[carbonate]_{tot}$ data, and the extrapolated k_{obs} values are the ones shown in **Figure 4-4a**.

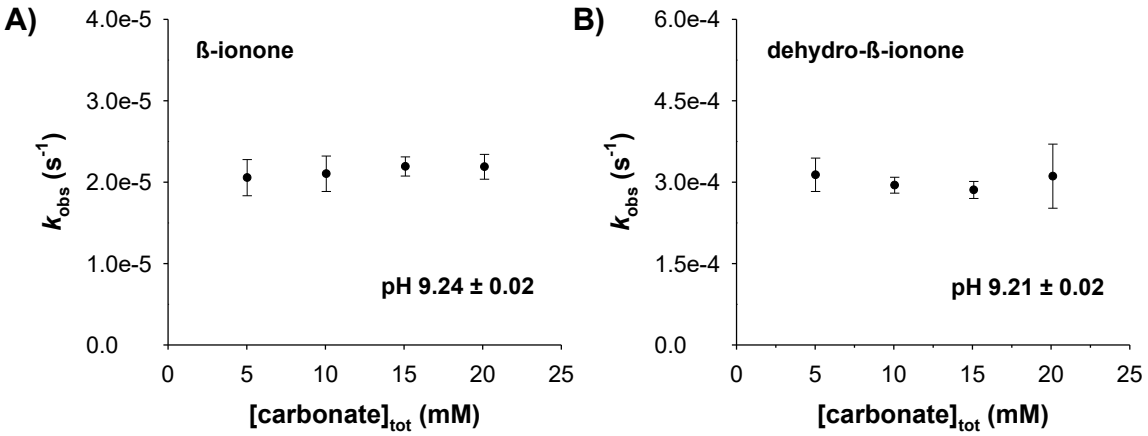

Figure 4-9. Pseudo-first-order rate constants (k_{obs}) as a function of carbonate buffer concentration for **(A)** β-ionone and **(B)** dehydro-β-ionone. Reaction conditions: $[ionone]_o = 5$ μM, $[FAC]_o = 130$ μM, no NaCl added, $[NaNO_3] = 0.1$ M, T = 25 °C. Error bars denote 95% confidence intervals.

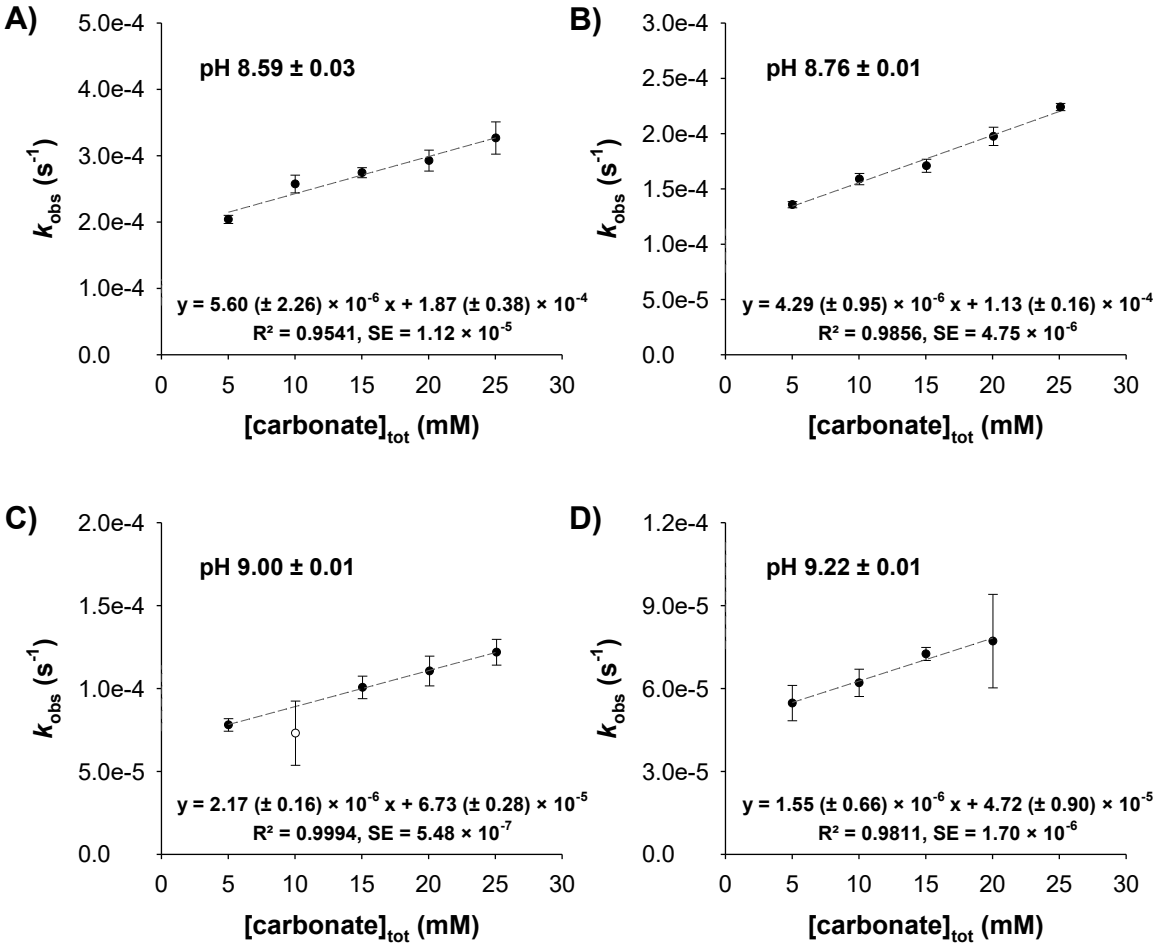

Figure 4-10. Pseudo-first-order rate constants (k_{obs}) as a function of carbonate buffer concentration for α-ionone at pH 8.59–9.22. Reaction conditions: $[\text{ionone}]_o$ = 5 μM, $[\text{FAC}]_o$ = 130 μM, no NaCl added, $[NaNO_3]$ = 0.1 M, T = 25 °C. Dashed lines represent linear regressions of the data. Error bars on the symbols and uncertainties in the equations denote 95% confidence intervals. SE = standard errors of the regressions.

The final methanol content in each reactor (0.25% (v/v)) was sufficiently low as to preclude cosolvent effect on the activity coefficients of ionones in aqueous solutions.[34] Nevertheless, at pH 5.56, the k_{obs} for β-ionone chlorination obtained when β-ionone was added from a methanolic spiking solution was smaller than the one obtained when β-ionone was added from an aqueous spiking solution (**Figure 4-11a**). At pH 7.43, there was no significant difference between the k_{obs} obtained with a methanolic spiking solution and that obtained with an aqueous spiking solution (**Figure 4-11b**). The difference in k_{obs} at pH 5.56 was perhaps due to methanol interfering with the mixing of β-ionone with other reactor constituents. At pH 7.43, the reaction time course was longer, so there was more time for the reagents to mix thoroughly before the first sample was collected from the reactor. At both pH 5.56 and 7.43, the value of extrapolated $[\beta\text{-ionone}]_o$ was lower with the aqueous spiking solution, most likely due to β-ionone being sparingly soluble in water. As a compromise, we prepared spiking solutions of all three ionones in 20 vol% methanol and 80% water to keep the compounds dissolved while minimizing the potential effect of methanol on mixing.

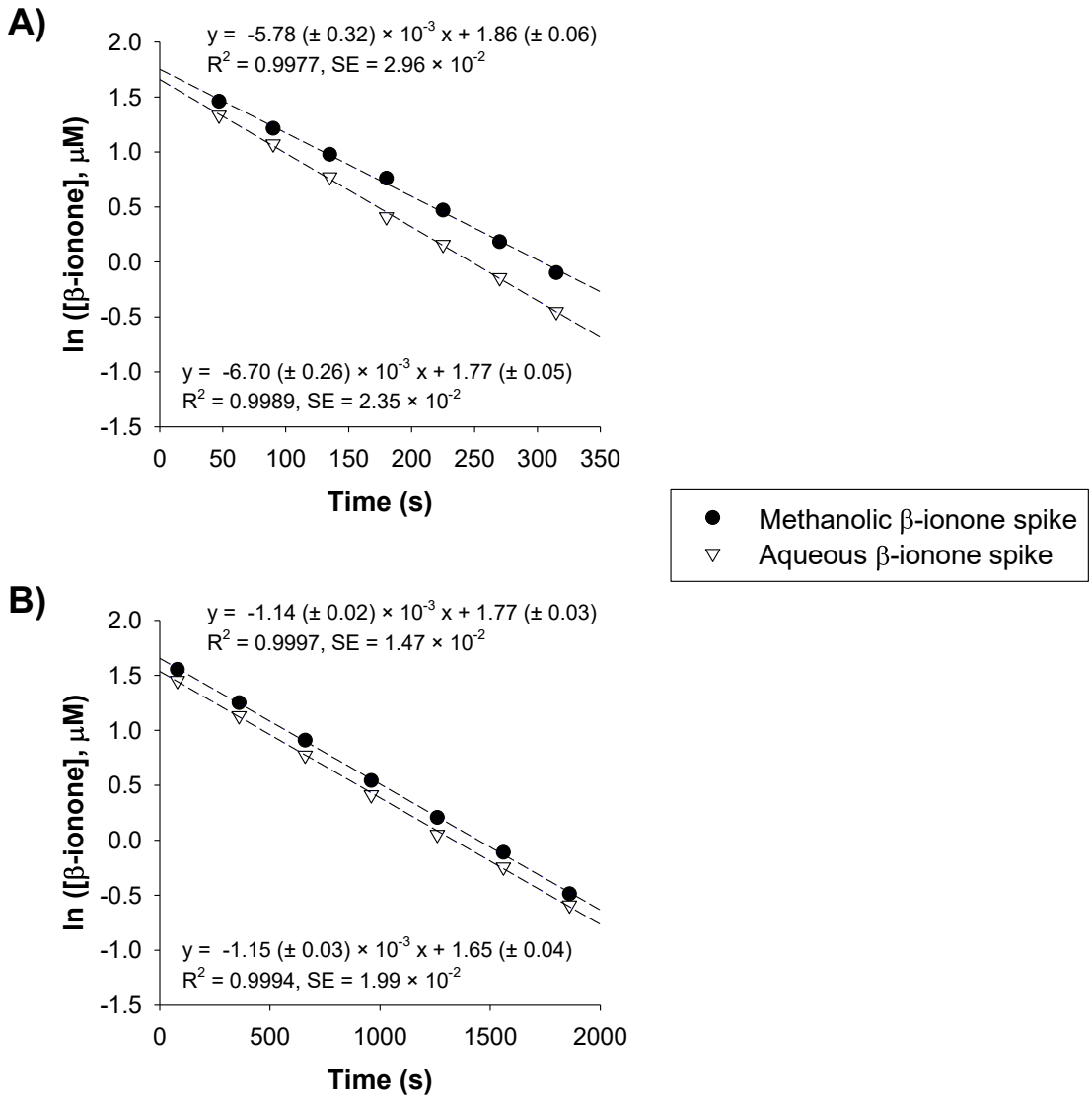

Figure 4-11. Effect of methanol in β-ionone spiking solutions on the ln[β-ionone] versus time data at **(A)** pH 5.56 and **(B)** pH 7.43. Reaction conditions: nominal $[\beta\text{-ionone}]_o$ = 5 μM, $[FAC]_o$ = 130 μM, no NaCl added, [phosphate buffer] = 10 mM, $[NaNO_3]$ = 0.1 M, T = 25 °C. SE = standard errors of the regressions.

Second-Order Rate Constants. Values of k_{Cl_2}, k_{Cl_2O}, and k_{HOCl} were computed using nonlinear least-squares regressions of the experimental $\log k_{obs}$ data in *SigmaPlot 12.5*. As **Figure 4-4** shows, a model of the form of equation 4-4 fits the data well at all values of $[Cl^-]_{added}$. We found that we did not need to include a term for H_2OCl^+ in order for our model to fit the data.

Best-fit estimates of k_{Cl_2}, k_{Cl_2O}, and k_{HOCl} are shown in **Table 4-1**. The overall reactivity of the ionone with FAC increases from β-ionone to α-ionone to dehydro-β-ionone. For all three compounds, k_{Cl_2} and k_{Cl_2O} are five to six orders of magnitude larger than k_{HOCl}. As the most reactive of the compounds examined, dehydro-β-ionone has the largest values of k_{HOCl} and k_{Cl_2}. The least reactive compound, β-ionone, has the smallest k_{HOCl} and k_{Cl_2}. α-Ionone has the largest k_{Cl_2O}, but the values of k_{Cl_2O} for all three ionones are similar when the uncertainties (reported as 95% confidence intervals) are considered.

Table 4-1. Second-Order Rate Constants for the Chlorination of Ionones [a]

	k_{Cl_2} (M^{-1} s^{-1})	k_{Cl_2O} (M^{-1} s^{-1})	k_{HOCl} (M^{-1} s^{-1})
α-ionone	1.88 (± 0.30) × 10^8	3.26 (± 0.23) × 10^7	28.1 (± 1.0)
β-ionone	6.25 (± 0.45) × 10^7	1.94 (± 0.13) × 10^7	12.0 (± 0.4)
dehydro-β-ionone	2.65 (± 0.44) × 10^8	2.33 (± 0.60) × 10^7	165 (± 3)

[a] Uncertainties represent 95% confidence intervals.

The high nucleophilicity of dehydro-β-ionone relative to α- and β-ionones can be rationalized by the differences in their structures. Dehydro-β-ionone has two alkenes that are conjugated in a cyclohexadiene. Assuming that the mechanism of ionone chlorination is electrophilic addition of chlorine to a cyclic alkene, then the carbocation that would form upon chlorine addition may be stabilized by the remaining cyclic alkene in dehydro-β-ionone through resonance (**Figure 4-12**). This form of resonance stabilization is not possible in α- and β-ionones.

For dehydro-β-ionone, the presence of a second cyclic alkene in a conjugated system leads to a pronounced enhancement in k_{HOCl} while having a modest (if any) effect on $k_{\mathrm{Cl_2}}$ and $k_{\mathrm{Cl_2O}}$. Variations in the extent to which the second cyclic alkene affects the values of k_{HOCl}, $k_{\mathrm{Cl_2}}$, and $k_{\mathrm{Cl_2O}}$ may be attributable to the difference in electrophilicity of the chlorinating agents. Cl_2 is more electrophilic than is HOCl because Cl^- (from Cl_2) is a better leaving group than is OH^- (from HOCl). If Cl_2O were to react by a heterolytic mechanism, it would also have a better leaving group (i.e., OCl^-) than does HOCl. The resonance stabilization that is available in the carbocation formed from dehydro-β-ionone is perhaps more important for HOCl, the weakest electrophile, than for Cl_2 and Cl_2O.

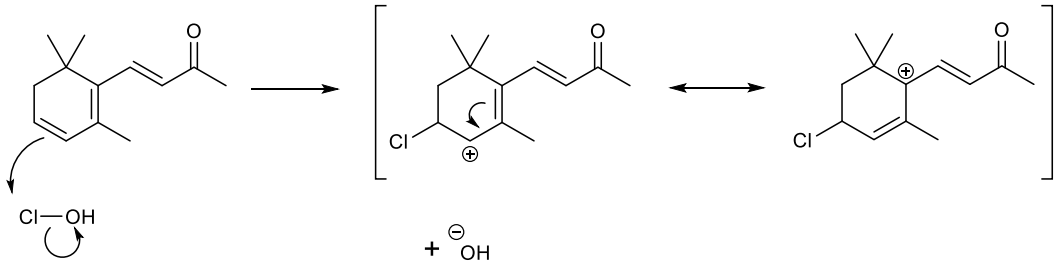

Figure 4-12. Partial reaction mechanism proposed for the chlorination of dehydro-β-ionone showing the resonance contributors that may explain the high reactivity of dehydro-β-ionone relative to α- and β-ionones.

β-Ionone is generally less reactive than is α-ionone in the presence of FAC. One possible reason for the lower reactivity of β-ionone with FAC is that the cyclohexene in β-ionone is conjugated with the enone. As a result, the electron density at the cyclic alkene in β-ionone is delocalized, and the nucleophilicity of the cyclic alkene in β-ionone is lowered. Because the electron density at the cyclic alkene in α-ionone is not delocalized in a conjugated system, the cyclic alkene in α-ionone ought to be more nucleophilic than is the one in β-ionone. Moreover, the cyclic alkene in α-ionone is less sterically hindered than that in β-ionone. Having an alkene that is not part of a conjugated system in a less sterically hindered position could explain the high chlorination rates of α-ionone compared with β-ionone.

Comparisons with Previous Results. There are very limited data on the kinetics of ionone chlorination. Zhang et al.[35] reported a pseudo-first-order rate constant of 1.86 ± 0.12 min^{-1} (equivalent to 0.031 ± 0.002 s^{-1}) for the loss of β-ionone at pH 7 and 25 °C when [FAC] was in large excess of [ionone] ($[FAC]_o$ = 100 mg/L as Cl_2 ≈ 1.41 mM, $[\beta\text{-ionone}]_o$ = 20 mg/L ≈ 104 μM). Using the second-order rate constants for β-ionone listed in **Table 4-1**, we predicted a pseudo-first-order rate constant (k_{calc}) of 0.174 s^{-1} at pH 7 (assuming that $[Cl^-] = [FAC]_o$ = 1.41 mM). Our k_{calc} is more than five times larger than the experimental rate constant determined by Zhang et al. The reason for this discrepancy is unclear, although we note that the rate constant reported by Zhang et al. might not be robust because it was determined using data from an experiment in which ~95% of $[\beta\text{-ionone}]_o$ had reacted by the third time point. Zhang et al.[35] also reported a "pseudo-second-order" rate constant of 3.39 × 10^{-4} ± 3.85 × 10^{-5} L μg^{-1} min^{-1} (equivalent

to 1.09 (± 0.12) × 10^{-3} M^{-1} s^{-1}) for the chlorination of β-ionone, but the meaning of this "pseudo-second-order" rate constant is uncertain.

Using values of k_{Cl_2}, k_{Cl_2O}, and k_{HOCl} for the three ionones obtained in this work as well as those for dimethenamid,[6] aromatic ethers,[7] and (chloro)phenols[8] (obtained under reaction conditions similar to those used in this study), we constructed log-log plots of (k_{Cl_2}/k_{HOCl}) versus k_{HOCl} and (k_{Cl_2O}/k_{HOCl}) versus k_{HOCl} (**Figures 4-13a and 4-13b**, respectively). For the (chloro)phenols, only second-order rate constants for the conjugate base (ArO^-) forms are included because a complete set of rate constants for the acid (ArOH) forms is not available. Even though estimates of $k_{Cl_2}$and k_{Cl_2O} for *p*-xylene are available, the reaction of *p*-xylene with HOCl was sufficiently slow as to preclude estimation of k_{HOCl}.[36] Values of k_{Cl_2}, k_{Cl_2O}, and k_{HOCl} have been reported by Cai et al.[9-10] for antipyrine and aminopyrine. For antipyrine, the second-order rate constants were fit to the k_{obs} versus pH data at only one set of [Cl^-] and [FAC].[9] For aminopyrine, a different estimate of k_{Cl_2} was reported for each of the $[Cl^-]_{added}$ used in kinetic experiments.[10] As the data modeling procedures employed in these studies entail questionable assumptions, the second-order rate constants reported for antipyrine and aminopyrine may not be robust and thus are excluded from our analysis.

Linear regression of $\log(k_{Cl_2}/k_{HOCl})$ versus $\log k_{HOCl}$ yields a slope of -0.341 ± 0.087 (uncertainty represents 95% confidence intervals; **Figures 4-13a**). Linear regression of $\log(k_{Cl_2O}/k_{HOCl})$ versus $\log k_{HOCl}$ yields a slope of -0.307 ± 0.155 (**Figures 4-13b**). Values of (k_{Cl_2}/k_{HOCl}) and (k_{Cl_2O}/k_{HOCl}) reflect the degree to which an organic compound will selectively react with Cl_2 and Cl_2O, respectively, rather than with HOCl. Values of k_{HOCl} are a measure of a compound's overall reactivity in the

presence of FAC. As the reactivity of a compound increases, selectivity for Cl_2 (**Figure 4-13a**) and Cl_2O (**Figure 4-13b**) decreases. Thus, the correlations shown in **Figure 4-13** are consistent with the reactivity-selectivity principle[37] in physical organic chemistry. There is more scatter in the selectivity versus reactivity plot for Cl_2O than in the one for Cl_2, perhaps reflecting the more complex mechanism involved in Cl_2O reactions relative to that in Cl_2 reactions.

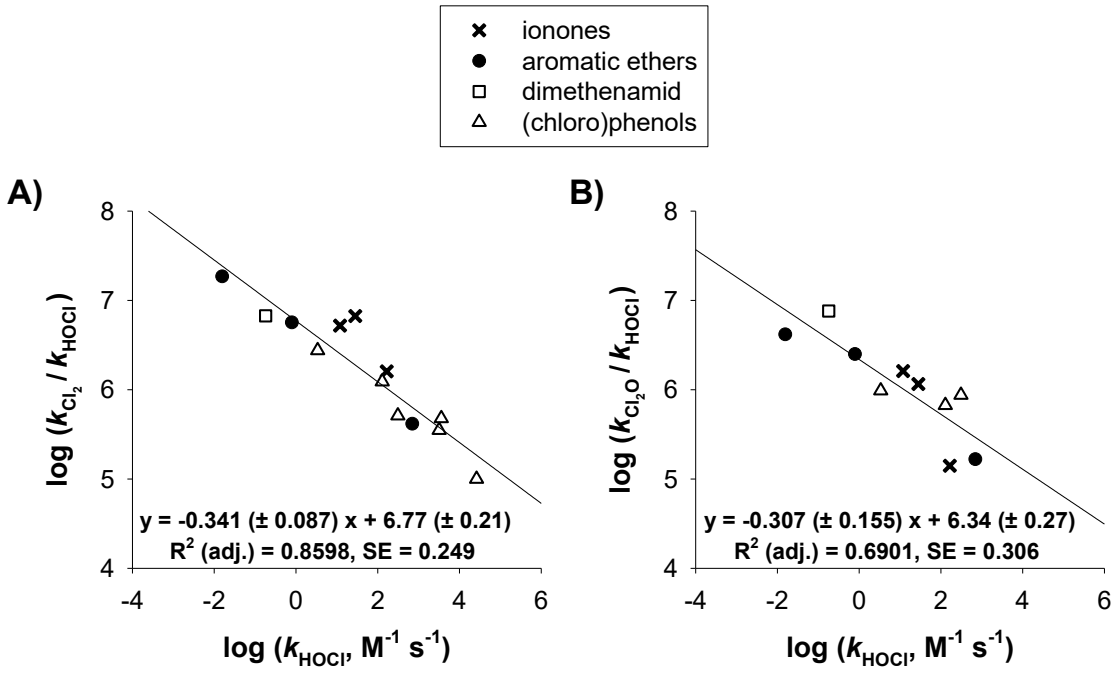

Figure 4-13. Selectivity versus reactivity for **(A)** Cl_2 and **(B)** Cl_2O. Second-order rate constants were obtained from this study as well as those from refs. 6-8. For (chloro)phenols, only rate constants for the conjugate base forms are included. Uncertainties in the equations denote 95% confidence intervals. SE = standard errors of the regressions.

Caution is advised when using the equations in **Figure 4-13** and k_{HOCl} values reported in the literature to predict k_{Cl_2} and k_{Cl_2O}. For instance, the reactivity of 2,4,6-trichlorophenol with Cl_2 and Cl_2O may have been misattributed to reactivity with HOCl, thus leading to overestimation of k_{HOCl} for this compound.[8] Conducting experiments in which pH, $[Cl^-]$, and $[FAC]_o$ are systematically varied is necessary for obtaining precise estimates of k_{Cl_2}, k_{Cl_2O}, and k_{HOCl}.

Pathway of Ionone Chlorination. While we only quantified the parent compounds in our experiments, some reaction intermediates/products were detected using HPLC. In the β-ionone chlorination experiments, the presence of an unknown compound was observed in nearly all samples. The increase in peak area of this unknown compound was concurrent with the decrease in [β-ionone] (**Figure 4-3**), suggesting that the unknown compound could be an intermediate or a product of β-ionone chlorination.

β-Ionone epoxide and β-cyclocitral have been hypothesized to form from the chlorination of β-ionone via the pathways shown in **Figure 4-2**.[23] We considered β-ionone epoxide to be the more likely candidate for the unknown compound detected in our samples because epoxide formation has been reported in the chlorination of α-terpineol,[24] which also contains a cyclohexene moiety. After synthesizing an authentic standard of β-ionone epoxide (see Appendix C for details) and then subjecting it to HPLC analysis, however, we found that the retention time and wavelength of maximum absorbance (λ_{max}) of β-ionone epoxide do not match those of the unknown compound.

β-Cyclocitral is proposed to form from β-ionone via a pathway that involves electrophilic addition of chlorine to the alkene in the enone (**Figure 4-2**), although this proposed mechanism is inconsistent with the known reactivity patterns of enones.

Carbonyls are electron-withdrawing groups; as such, alkenes that are conjugated with carbonyls are anticipated to be deactivated towards electrophilic additions. The low reactivities of enones with electrophiles is supported by evidence from the environmental literature showing that progesterone[32] and enone-containing androgenic steroids[38] are not transformed in the presence of FAC. Therefore, for the ionones examined in this study, the nucleophilic sites ought to be at the cyclic alkenes rather than at the enones. Analysis of an authentic standard of β-cyclocitral by HPLC showed that this compound was not "the" unknown intermediate/product we sought, and β-cyclocitral was not detected in any of the samples from our β-ionone chlorination experiments.

Two additional compounds were synthesized in an effort to identify the unknown intermediate/product of β-ionone chlorination (see Appendix C for synthesis procedures). To our disappointment, neither ε-chloro-β-ionone nor α-chloro-β-ionone (**Figure 4-14**) has the same retention time and λ_{max} as the unknown compound.

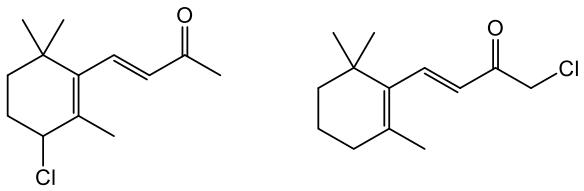

ε-chloro-β-ionone α-chloro-β-ionone

Figure 4-14. Hypothesized products of β-ionone chlorination synthesized in this study.

GC-MS with electron ionization (EI) was employed to analyze the sample from a β-ionone chlorination experiment conducted at pH 6.24. Two peaks were observed in the resulting total ion count chromatogram (**Figure 4-15**), and their mass spectra are shown in **Figure 4-16**. The major peak in the chromatogram has the same retention time and mass spectrum as those of an authentic standard of dehydro-β-ionone (**Figure 4-17**). The mass spectrum that corresponds to the minor peak appears to be a combination of the mass spectra of β-ionone (**Figure 4-18a**) and β-ionone epoxide (**Figure 4-18a**).

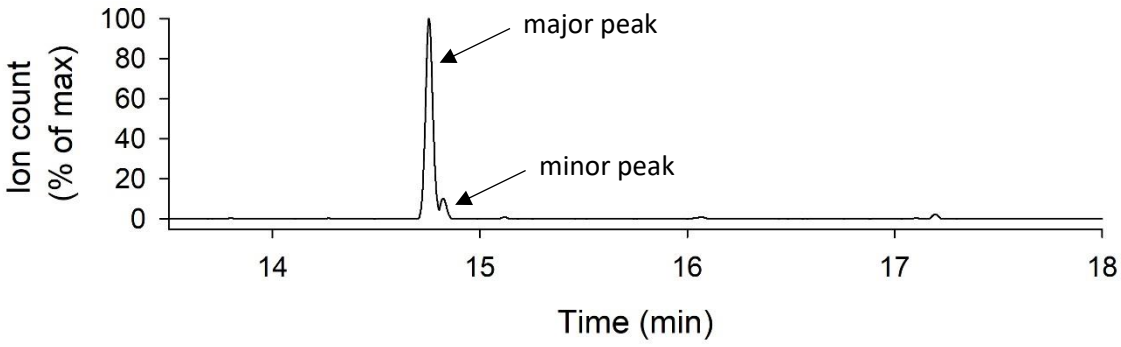

Figure 4-15. Total ion chromatogram (GC-MS) of the sample from a β-ionone chlorination experiment collected after 20 minutes of reaction time. Reaction conditions: $[\beta\text{-ionone}]_o$ = 11 μM, $[FAC]_o$ = 130 μM, no NaCl added, [phosphate buffer] = 10 mM, $[NaNO_3]$ = 0.1 M, T = 22 °C

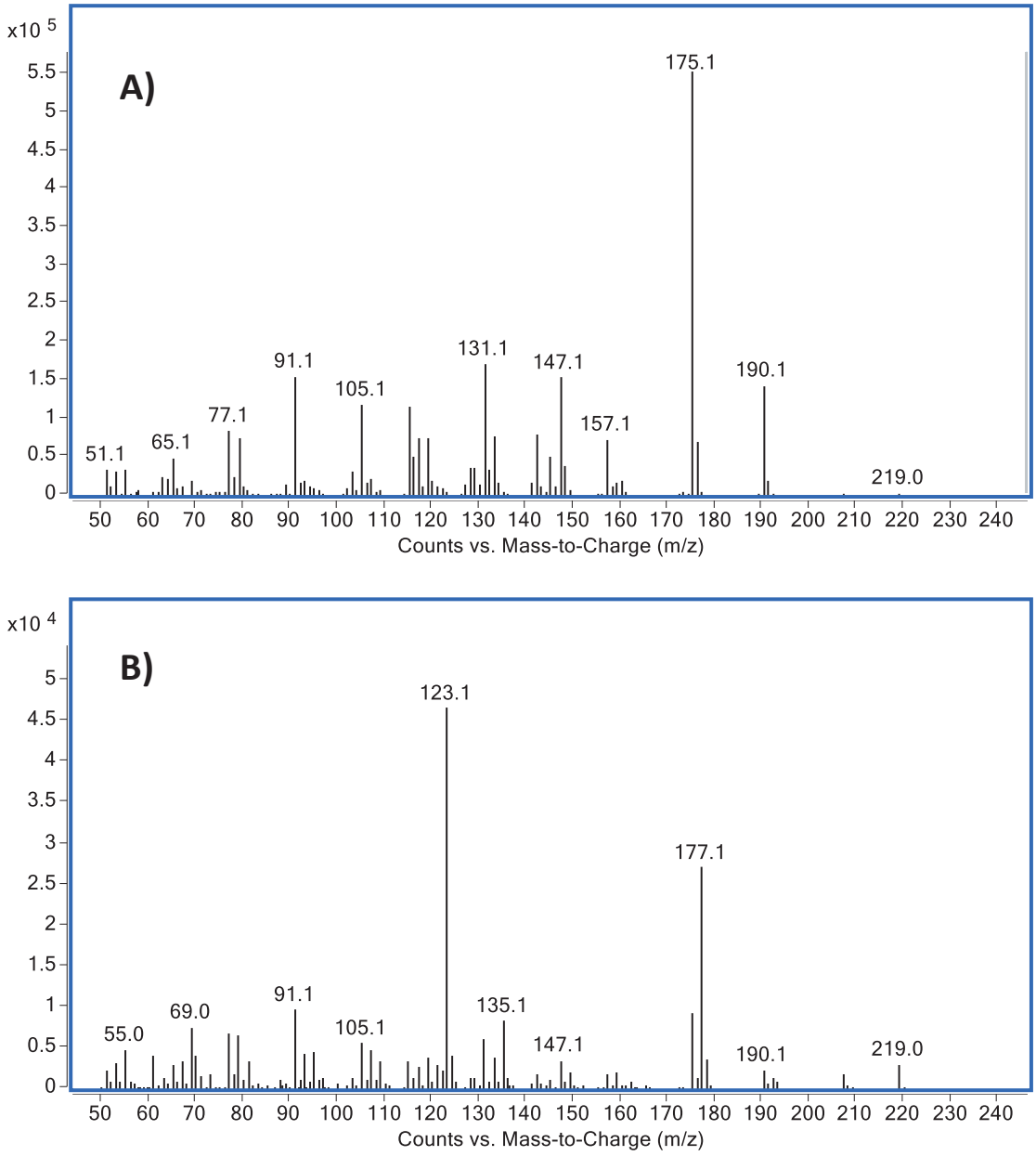

Figure 4-16. Mass spectra associated with the **(A)** major and **(B)** minor peak observed in the total ion chromatogram presented in **Figure 4-15**.

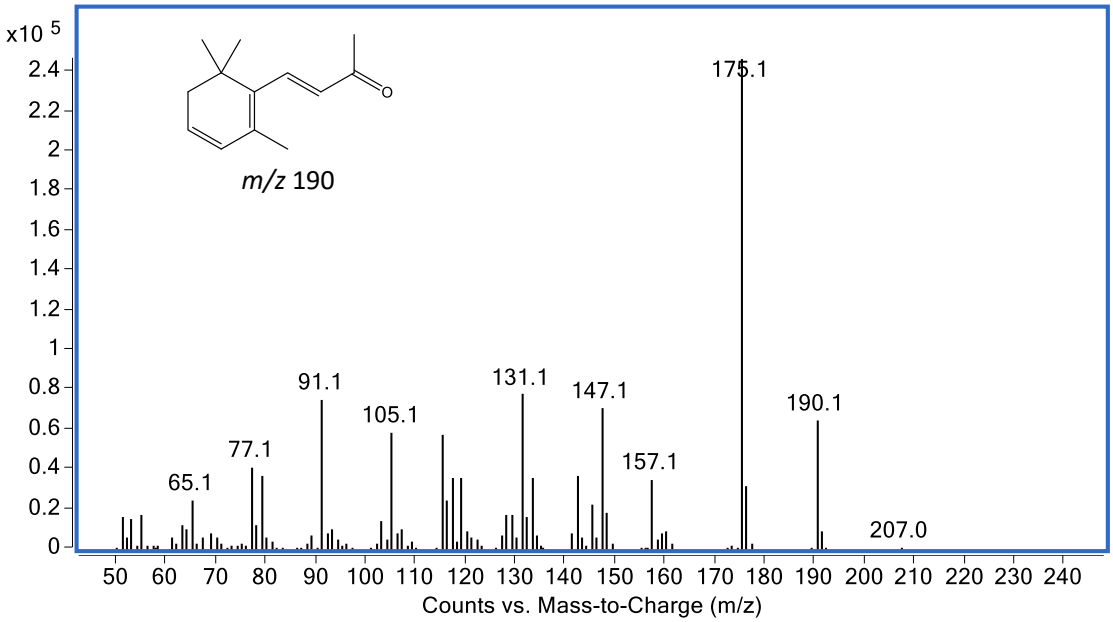

Figure 4-17. Mass spectrum (EI) of an authentic standard of dehydro-β-ionone.

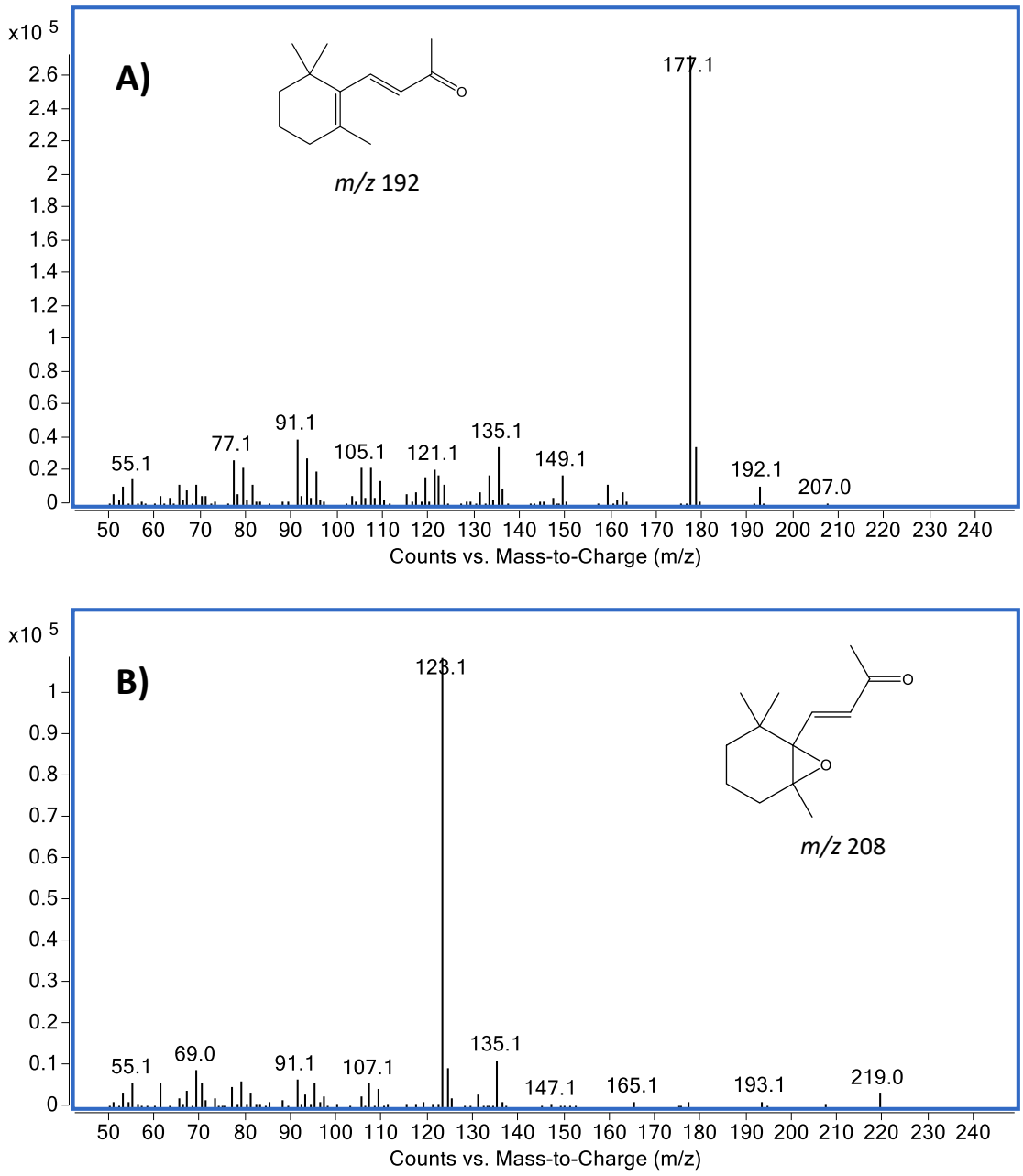

Figure 4-18. Mass spectra (EI) of authentic standards of **(A)** β-ionone and **(B)** β-ionone epoxide.

β-Ionone and β-ionone epoxide have very similar retention times under our GC-MS method. Thus, the presence of any unreacted β-ionone in the reactor could obscure the β-ionone epoxide peak. Interestingly, we found that β-ionone epoxide decomposed to form dehydro-β-ionone at GC injector temperatures > 175 °C. When we lowered the GC injector temperature to 150 °C, no appreciable formation of dehydro-β-ionone from the thermal decomposition of β-ionone epoxide was observed. We also found that β-ionone epoxide was stable in the presence of sodium thiosulfate, a reducing agent that was used to quench FAC in our β-ionone chlorination experiment at pH 6.24. As the presence of dehydro-β-ionone in our quenched sample could not be explained by thermal decomposition or reduction of β-ionone epoxide, it is likely that dehydro-β-ionone is indeed a reaction intermediate in the chlorination of β-ionone.

Previous researchers were able to detect β-ionone epoxide and β-cyclocitral in samples from β-ionone chlorination experiments using closed loop stripping analysis followed by GC-MS.[23] Although some β-ionone epoxide might have formed in our experiment, our analysis showed that it was not the major product under our experimental conditions. β-Cyclocitral, the mass spectrum of which we obtained using an authentic standard (**Figure 4-19**), was not detected in our sample. Instead, results of our GC-MS analysis support dehydro-β-ionone as a key intermediate of β-ionone chlorination. As neither dehydro-β-ionone nor β-ionone epoxide has the same retention time and λ_{max} as the unknown product of β-ionone chlorination detectable by HPLC, more work will be needed to elucidate the reaction pathway of ionone chlorination.

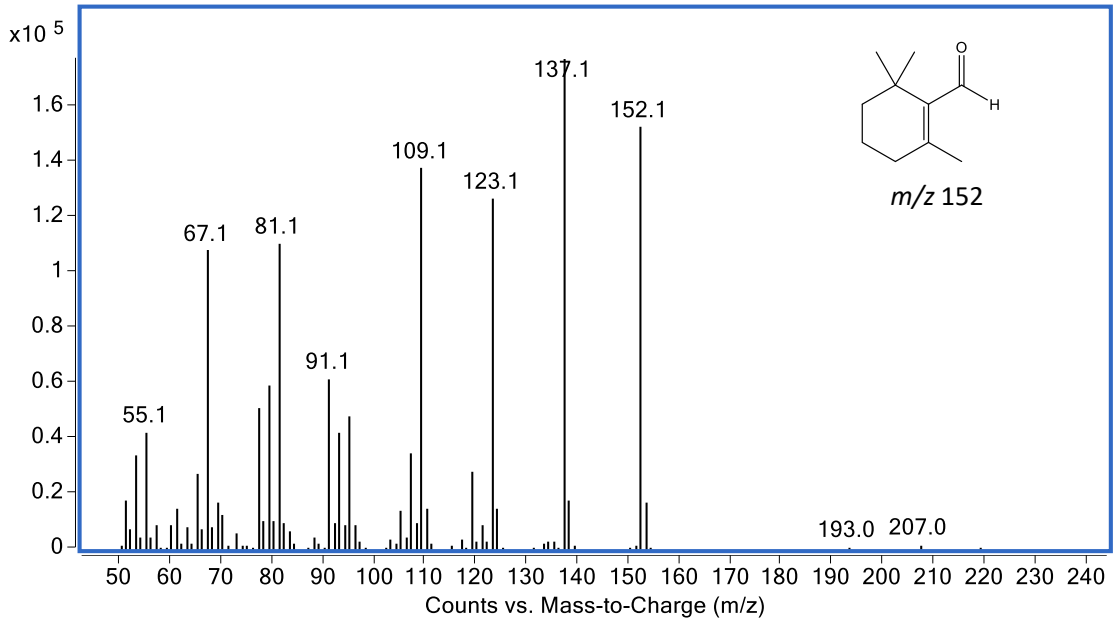

Figure 4-19. Mass spectrum (EI) of an authentic standard of β-cyclocitral.

Environmental Implications. Using the second-order rate constants listed in **Table 4-1**, we computed the pseudo-first-order rate constants (k_{calc}) at different values of [FAC] and [Cl^-] that may be encountered in various chlorination scenarios (**Table 4-2**). Fractional contributions of various chlorine species towards the overall k_{calc} can then be computed, and the results are presented in **Figures 4-20 to 4-22**.

Table 4-2. Values of [FAC] and [Cl^-] Used to Compute the Contributions of Various Chlorine Species Towards k_{calc} Under Different Chlorination Scenarios

Scenario	[FAC]	[Cl^-]
Drinking water treatment [a]	28 μM ≈ 2.0 mg/L as Cl_2	0.23 mM ≈ 8 mg/L
Disinfection of desalinated water [b]	28 μM ≈ 2.0 mg/L as Cl_2	3.0 mM ≈ 110 mg/L
Laboratory experiments [c]	140 μM ≈ 9.9 mg/L as Cl_2	0.14 mM ≈ 5.0 mg/L

[a] [FAC] = typical chlorine dose for drinking water treatment (ref. 1). [Cl^-] = mean Cl^- concentration in North American rivers (ref. 39).

[b] [FAC] = typical chlorine dose for disinfection of desalinated water (ref. 40). [Cl^-] in desalinated water was computed by assuming a best-case scenario of 99.4% salt rejection by reverse-osmosis membranes (ref. 41). These values of [FAC] and [Cl^-] may also be encountered when chlorinating freshwater that has been coagulated using ferric chloride ($FeCl_3$).

[c] [FAC] = chlorine dose often encountered in the environmental literature. [Cl^-] = concentration of Cl^- present in NaOCl solutions that are equimolar in [Cl^-] and [OCl^-].

For α-ionone, HOCl is the most important chlorinating agent at pH 6–8 and at a set of [FAC] and [Cl^-] representative of drinking water treatment (**Figure 4-20a**). When chlorinating water containing higher [Cl^-] (e.g., desalinated water or freshwater that has been coagulated using $FeCl_3$), the influence of Cl_2 at pH 6–8 increases substantially (**Figure 4-20b**). In laboratory studies in which the chlorine doses used are often higher than those employed in typical drinking water treatment, the influence of Cl_2O at pH 7–8 becomes pronounced while the influence of HOCl is diminished (**Figure 4-20c**).

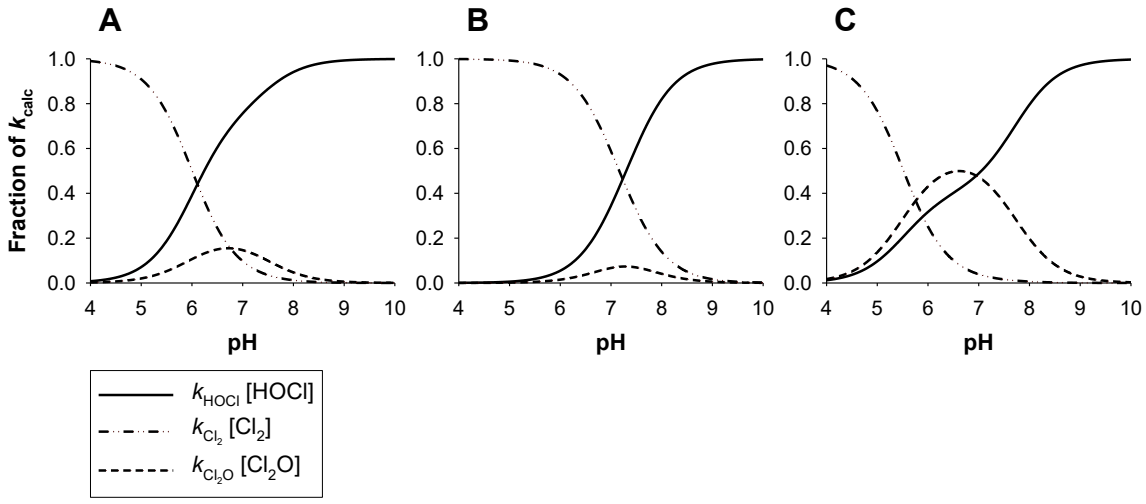

Figure 4-20. Contributions of Cl_2, Cl_2O, and HOCl towards k_{calc} for α-ionone at [FAC] and [Cl^-] typically encountered in **(A)** drinking water treatment, **(B)** chlorination of water with elevated [Cl^-], and **(C)** bench-scale laboratory experiments (see **Table 4-2** for the values of [FAC] and [Cl^-] used to construct this figure; T = 25 °C).

The contributions of various chlorinating agents towards the overall reactivity for β-ionone are similar to those for α-ionone. HOCl is the most important chlorinating agent for α-ionone under typical drinking water treatment conditions (**Figure 4-21a**), but the influence of Cl_2 will be significant in the presence of high [Cl^-] (**Figure 4-21b**). The influence of Cl_2O is most apparent in laboratory experiments employing high [FAC] (**Figure 4-21c**).

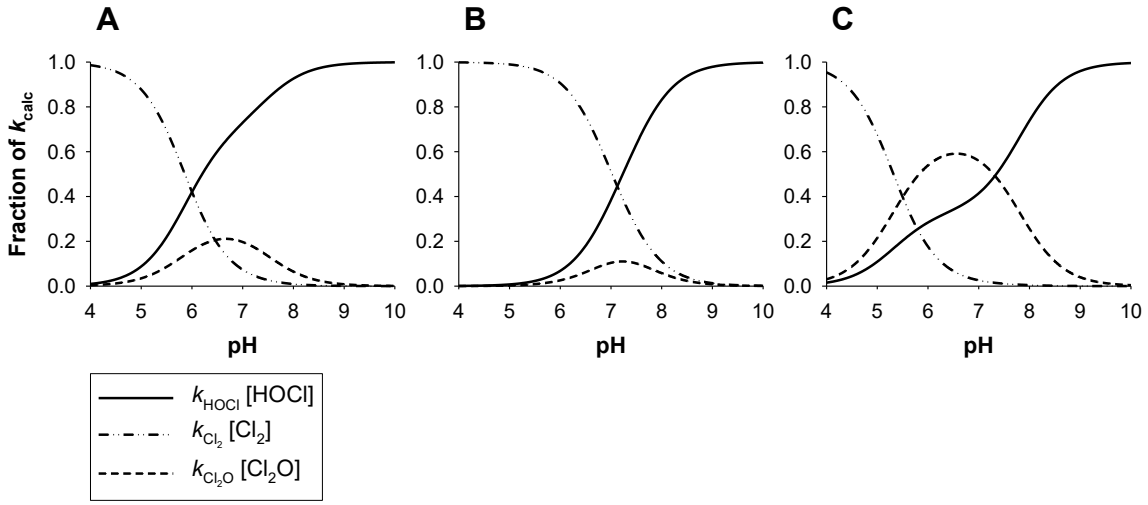

Figure 4-21. Contributions of Cl_2, Cl_2O, and HOCl towards k_{calc} for β-ionone at [FAC] and [Cl^-] typically encountered in **(A)** drinking water treatment, **(B)** chlorination of water with elevated [Cl^-], and **(C)** bench-scale laboratory experiments (see **Table 4-2** for the values of [FAC] and [Cl^-] used to construct this figure; T = 25 °C).

The results for dehydro-β-ionone are slightly different from those for the other two compounds. The role of Cl_2O is insignificant in all the chlorination scenarios considered (**Figure 4-22**), whereas Cl_2 can still exert a significant influence on dehydro-β-ionone kinetics at high [Cl^-] at pH 6–7 (**Figure 4-22b**). HOCl contributes the major fraction towards k_{calc} in all scenarios.

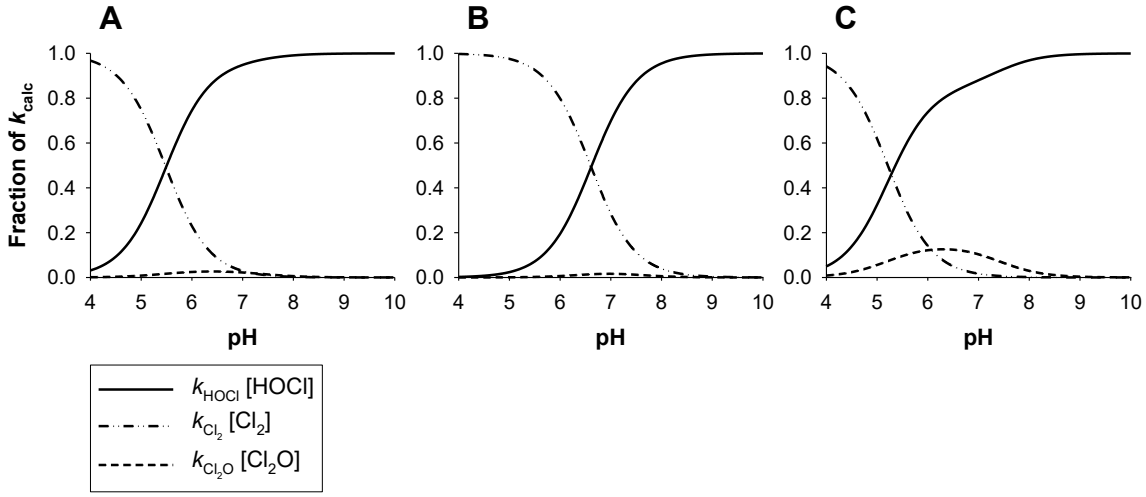

Figure 4-22. Contributions of Cl_2, Cl_2O, and HOCl towards k_{calc} for dehydro-β-ionone at [FAC] and [Cl^-] typically encountered in **(A)** drinking water treatment, **(B)** chlorination of water with elevated [Cl^-], and **(C)** bench-scale laboratory experiments (see **Table 4-2** for the values of [FAC] and [Cl^-] used to construct this figure; T = 25 °C).

In summary, the influence of Cl_2 and Cl_2O on chlorination kinetics is more apparent for α- and β-ionones than for dehydro-β-ionone. At a set of pH, [FAC], and [Cl^-] representative of drinking water treatment, reactions with Cl_2 and Cl_2O account for < 30% of k_{calc} for α- and β-ionones and < 10% of k_{calc} for dehydro-β-ionone (**Figure 4-23a**). When water with elevated [Cl^-] is chlorinated at pH 7, reactions with Cl_2 can contribute nearly 50% towards k_{calc} for α- and β-ionones and close to 30% towards k_{calc} for dehydro-β-ionone (**Figure 4-23b**). In laboratory settings where high chlorine doses may be used, reactions with Cl_2O can account for at least 50% of the reactivities of α- and β-ionones (**Figure 4-23c**). Consistent with the reactivity-selectivity principle, the most reactive of the three ionones (dehydro-β-ionone) is the least selective and will tend to react with the most abundant chlorine species present (i.e., HOCl). The less reactive ionones (α- and β-ionones) will be more selective and thus are more likely to react with Cl_2 and Cl_2O.

The tradeoff between reactivity and selectivity is significant because natural organic matter (NOM) can be divided into fast-reacting and slow-reacting fractions.[42] The majority of THM precursors in NOM are moderately reactive, and their reactions with FAC occur on the order of hours to days (rather than seconds to minutes). Findings from this work, as well as those from previous studies,[7-8] suggest that Cl_2 and possibly Cl_2O may be more important for the slow-reacting fraction of NOM. Furthermore, algal organic matter, of which β-ionone is a component, can also produce THMs upon chlorination.[43] Laboratory studies have shown that both algal cells and algal extracellular products can continue to form THMs after more than 48 hours.[44-45] The moderate

reactivities of DBP precursors in algal organic matter may predispose them to reactions with Cl_2 and Cl_2O as well.

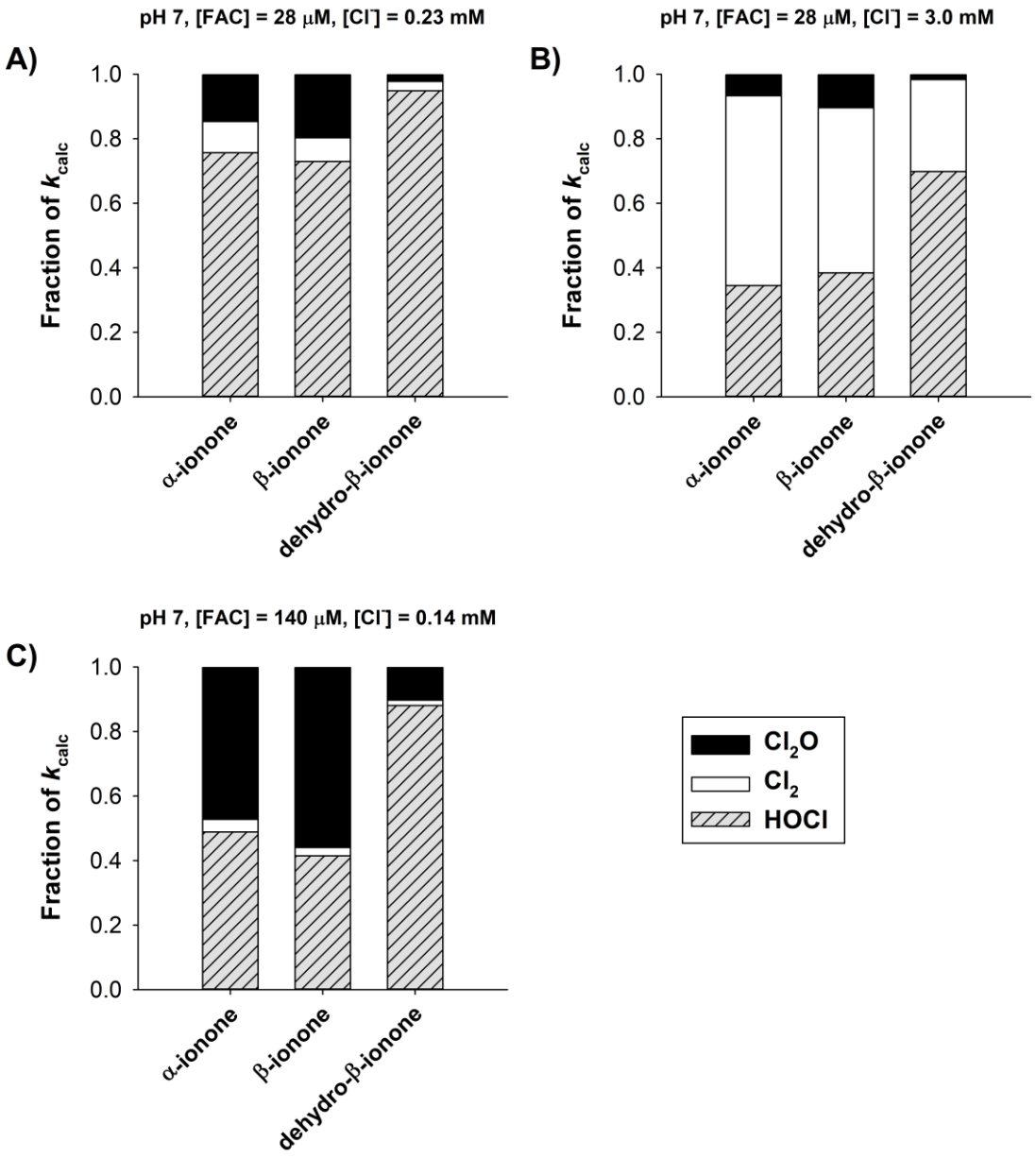

Figure 4-23. Contributions of Cl_2, Cl_2O, and HOCl towards k_{calc} under typical conditions for **(A)** drinking water treatment, **(B)** chlorination of water with high [Cl^-], and **(C)** bench-scale chlorination experiments.

In this work, we have shown that chloride can enhance the chlorination rates of moderately-reactive organic compounds at pH < 7.5 via the formation of Cl_2. Other studies have also noted the importance of chloride. Addition of chloride at the millimolar level can enhance THM formation from the chlorination of carbohydrates,[46] and chloride can promote the formation of several volatile DBPs in swimming pool water.[47] While chloride concentrations in most surface waters are low, chloride levels in many North American rivers and streams are expected to rise due to intensifying urbanization.[48-49] Moreover, as desalination becomes more widely adopted, the chloride concentrations in our drinking water supplies will likely increase. Seawater intrusion due to rising sea levels may also add appreciable amounts of Cl^- to drinking water supplies. Thus, the potential influence of Cl_2 in DBP (trans)formation should not be underestimated.

In the laboratory, chlorine doses that are higher than those encountered in typical drinking water treatment are often employed to maintain a detectable chlorine residual over hours or days. As a result, Cl_2O formation will be favored in these experimental systems. Researchers sometimes correct for variations in chlorination conditions by dividing the experimental k_{obs} values by [FAC]. We have shown, however, that chlorination reactions will not be first-order in [HOCl] when Cl_2O (and perhaps Cl_2 if FAC solutions are equimolar in [Cl^-] and [HOCl]) influences reaction kinetics. Therefore, the validity of normalizing k_{obs} values obtained in laboratory settings in this manner is dubious.

4. 5. Acknowledgements

This material is based upon work supported by the U.S. National Science Foundation (CBET-1067391). Additional funding for S.S.L. was received from the Whiting School of Engineering at the Johns Hopkins University. We are grateful to Keith Reber (Towson University), who will be a co-author on the manuscript derived from this chapter, for his assistance in synthesizing dehydro-β-ionone and other compounds related to β-ionone.

4. 6. References

1. Crittenden, J. C.; Trussell, R. R.; Hand, D. W.; Howe, K. J.; Tchobanoglous, G. *MWH's Water Treatment: Principles and Design*, 3rd ed.; John Wiley & Sons: Hoboken, New Jersey, 2012.

2. Richardson, S. D.; Plewa, M. J.; Wagner, E. D.; Schoeny, R.; DeMarini, D. M. Occurrence, genotoxicity, and carcinogenicity of regulated and emerging disinfection by-products in drinking water: A review and roadmap for research. *Mutat. Res.* **2007,** *636*, 178-242.

3. Morris, J. C. The acid ionization constant of HOCl from 5 to 35°. *J. Phys. Chem.* **1966,** *70*, 3798-3805.

4. Wang, T. X.; Margerum, D. W. Kinetics of reversible chlorine hydrolysis: Temperature dependence and general-acid/base-assisted mechanisms. *Inorg. Chem.* **1994,** *33*, 1050-1055.

5. Roth, W. A. Note on thermo-chemistry of chlorine monoxide. *Z. Phys. Chem. Abt. A* **1942,** *191*, 248-250.

6. Sivey, J. D.; McCullough, C. E.; Roberts, A. L. Chlorine monoxide (Cl_2O) and molecular chlorine (Cl_2) as active chlorinating agents in reaction of dimethenamid with aqueous free chlorine. *Environ. Sci. Technol.* **2010,** *44*, 3357-3362.

7. Sivey, J. D.; Roberts, A. L. Assessing the reactivity of free chlorine constituents Cl_2, Cl_2O, and HOCl toward aromatic ethers. *Environ. Sci. Technol.* **2012,** *46*, 2141-2147.

8. Lau, S. S.; Abraham, S. M.; Roberts, A. L. Chlorination revisited: Does Cl^- serve as a catalyst in the chlorination of phenols? *Environ. Sci. Technol.* **2016,** *50*, 13291-13298.

9. Cai, M.-Q.; Feng, L.; Jiang, J.; Qi, F.; Zhang, L.-Q. Reaction kinetics and transformation of antipyrine chlorination with free chlorine. *Water Res.* **2013,** *47*, 2830-2842.

10. Cai, M.-Q.; Feng, L.; Zhang, L.-Q. Transformation of aminopyrine in the presence of free available chlorine: Kinetics, products, and reaction pathways. *Chemosphere* **2017,** *171*, 625-634.

11. Deborde, M.; von Gunten, U. Reactions of chlorine with inorganic and organic compounds during water treatment – Kinetics and mechanisms: A critical review. *Water Res.* **2008,** *42*, 13-51.

12. Kaiser, R. Carotenoid-derived aroma compounds in flower scents. In *Carotenoid-Derived Aroma Compounds*, American Chemical Society: 2001; Vol. 802, pp 160-182.

13. Lalko, J.; Lapczynski, A.; Politano, V. T.; McGinty, D.; Bhatia, S.; Letizia, C. S.; Api, A. M. Fragrance material review on α-ionone. *Food Chem. Toxicol.* **2007,** *45*, S235-S240.

14. Lalko, J.; Lapczynski, A.; McGinty, D.; Bhatia, S.; Letizia, C. S.; Api, A. M. Fragrance material review on β-ionone. *Food Chem. Toxicol.* **2007,** *45*, S241-S247.

15. Jones, G. J.; Korth, W. *In situ* production of volatile odour compounds by river and reservoir phytoplankton populations in Australia. *Water Sci. Technol.* **1995,** *31*, 145-151.

16. Höckelmann, C.; Jüttner, F. Off-flavours in water: hydroxyketones and β-ionone derivatives as new odour compounds of freshwater cyanobacteria. *Flavour Fragrance J.* **2005,** *20*, 387-394.

17. Cotsaris, E.; Bruchet, A.; Mallevialle, J.; Bursill, D. B. The identification of odorous metabolites produced from algal monocultures. *Water Sci. Technol.* **1995,** *31*, 251-258.

18. Peter, A.; Köster, O.; Schildknecht, A.; von Gunten, U. Occurrence of dissolved and particle-bound taste and odor compounds in Swiss lake waters. *Water Res.* **2009,** *43*, 2191-2200.

19. Watson, S. B. Cyanobacterial and eukaryotic algal odour compounds: signals or by-products? A review of their biological activity. *Phycologia* **2003,** *42*, 332-350.

20. Chen, J.; Xie, P.; Ma, Z.; Niu, Y.; Tao, M.; Deng, X.; Wang, Q. A systematic study on spatial and seasonal patterns of eight taste and odor compounds with relation to various biotic and abiotic parameters in Gonghu Bay of Lake Taihu, China. *Sci. Total Environ.* **2010,** *409*, 314-325.

21. Buttery, R. G.; Teranishi, R.; Ling, L. C.; Turnbaugh, J. G. Quantitative and sensory studies on tomato paste volatiles. *J. Agric. Food. Chem.* **1990,** *38*, 336-340.

22. Morris, J. C. The chemistry of aqueous chlorine in relation to water chlorination. In *Water Chlorination: Environmental Impact and Health Effects*, Jolley, R. L., Ed. Ann Arbor Science Publishers: Ann Arbor, Michigan, 1978; Vol. 1, pp 21-35.

23. Joll, C. A.; Alessandrino, M. J.; Heitz, A. Disinfection by-products from halogenation of aqueous solutions of terpenoids. *Water Res.* **2010,** *44*, 232-242.

24. Kopperman, H. L.; Hallcher, R. C.; Riehl, A.; Carlson, R. M.; Caple, R. Aqueous chlorination of α-terpineol. *Tetrahedron* **1976,** *32*, 1621-1626.

25. Winterbourn, C. C.; van den Berg, J. J. M.; Roitman, E.; Kuypers, F. A. Chlorohydrin formation from unsaturated fatty acids reacted with hypochlorous acid. *Arch. Biochem. Biophys.* **1992,** *296*, 547-555.

26. Arnhold, J.; Panasenko, O. M.; Schiller, J.; Vladimirov, Y. A.; Arnold, K. The action of hypochlorous acid on phosphatidylcholine liposomes in dependence on the content of double bonds. Stoichiometry and NMR analysis. *Chem. Phys. Lipids* **1995,** *78*, 55-64.

27. American Public Health Association (APHA). *Standard Methods for the Examination of Water and Wastewater*, 18th ed.; American Public Health Association, American Water Works Association, Water Environment Federation: Washington, DC, 1992.

28. Liu, W.; Zhou, J.; Geng, G.; Lin, R.; Wu, J. H. Synthesis and in vitro characterization of ionone-based compounds as dual inhibitors of the androgen receptor and NF-κB. *Investigational New Drugs* **2014,** *32*, 227-234.

29. Swain, C. G.; Crist, D. R. Mechanisms of chlorination by hypochlorous acid. The last of chlorinium ion, Cl^+. *J. Am. Chem. Soc.* **1972,** *94*, 3195-3200.

30. Rebenne, L. M.; Gonzalez, A. C.; Olson, T. M. Aqueous chlorination kinetics and mechanism of substituted dihydroxybenzenes. *Environ. Sci. Technol.* **1996,** *30*, 2235-2242.

31. Gallard, H.; Von Gunten, U. Chlorination of phenols: Kinetics and formation of chloroform. *Environ. Sci. Technol.* **2002,** *36*, 884-890.

32. Deborde, M.; Rabouan, S.; Gallard, H.; Legube, B. Aqueous chlorination kinetics of some endocrine disruptors. *Environ. Sci. Technol.* **2004,** *38*, 5577-5583.

33. Perdue, E. M.; Wolfe, N. L. Prediction of buffer catalysis in field and laboratory studies of pollutant hydrolysis reactions. *Environ. Sci. Technol.* **1983,** *17*, 635-642.

34. Schwarzenbach, R. P.; Gschwend, P. M.; Imboden, D. M. *Environmental Organic Chemistry*, 2 ed.; John Wiley & Sons, Inc.: 2005.

35. Zhang, K.-j.; Gao, N.-y.; Deng, Y.; Zhang, T.; Li, C. Aqueous chlorination of algal odorants: Reaction kinetics and formation of disinfection by-products. *Sep. Purif. Technol.* **2012,** *92*, 93-99.

36. Voudrias, E. A.; Reinhard, M. A kinetic model for the halogenation of *p*-xylene in aqueous HOCl solutions containing Cl^- and Br^-. *Environ. Sci. Technol.* **1988,** *22*, 1056-1062.

37. Anslyn, E. V.; Dougherty, D. A. Modern Physical Organic Chemistry. University Science: 2006.

38. Mash, H.; Schenck, K.; Rosenblum, L. Hypochlorite oxidation of select androgenic steroids. *Water Res.* **2010,** *44*, 1950-1960.

39. Wetzel, R. G. *Limnology: Lake and River Ecosystems*. 3rd ed.; Academic Press: San Diego, 2001.

40. Kim, D.; Amy, G. L.; Karanfil, T. Disinfection by-product formation during seawater desalination: A review. *Water Res.* **2015,** *81*, 343-355.

41. Li, D.; Wang, H. Recent developments in reverse osmosis desalination membranes. *J. Mater. Chem.* **2010,** *20*, 4551-4566.

42. Gallard, H.; von Gunten, U. Chlorination of natural organic matter: kinetics of chlorination and of THM formation. *Water Res.* **2002,** *36*, 65-74.

43. Hoehn, R. C.; Barnes, D. B.; Thompson, B. C.; Randall, C. W.; Grizzard, T. J.; Shaffer, P. T. B. Algae as sources of trihalomethane precursors. *J. Am. Water Works Assoc.* **1980,** *72*, 344-350.

44. Oliver, B. G.; Shindler, D. B. Trihalomethanes from the chlorination of aquatic algae. *Environ. Sci. Technol.* **1980,** *14*, 1502-1505.

45. Graham, N. J. D.; Wardlaw, V. E.; Perry, R.; Jiang, J.-Q. The significance of algae as trihalomethane precursors. *Water Sci. Technol.* **1998,** *37*, 83-89.

46. Navalon, S.; Alvaro, M.; Garcia, H. Carbohydrates as trihalomethanes precursors. Influence of pH and the presence of Cl^- and Br^- on trihalomethane formation potential. *Water Res.* **2008,** *42*, 3990-4000.

47. E, Y.; Bai, H.; Lian, L.; Li, J.; Blatchley, E. R., III. Effect of chloride on the formation of volatile disinfection byproducts in chlorinated swimming pools. *Water Res.* **2016,** *105*, 413-420.

48. Kaushal, S. S.; Groffman, P. M.; Likens, G. E.; Belt, K. T.; Stack, W. P.; Kelly, V. R.; Band, L. E.; Fisher, G. T. Increased salinization of fresh water in the northeastern United States. *Proc. Natl. Acad. Sci. USA* **2005,** *102*, 13517-13520.

49. Mullaney, J. R.; Lorenz, D. L.; Arntson, A. D. Chloride in groundwater and surface water in areas underlain by the glacial aquifer system, northern United States. *U.S. Geological Survey Scientific Investigations Report (2009–5086).* 2009.

5. Conclusions

5. 1. Chloride as a Catalyst in the Chlorination of (Chloro)phenols

Phenol and chlorophenols are among the most extensively studied compounds in the aqueous chlorination literature. Previous researchers agree that HOCl is the most important chlorinating agent in free available chlorine (FAC) at circum-neutral and high pH,[1-2] although their views differ on the identity of the chlorine species responsible for the transformation of (chloro)phenols at low pH. Lee and Morris[1] hypothesized that Cl_2 could explain the chlorination kinetics of (chloro)phenols at pH < 6, while Gallard and von Gunten[2] argued that H_2OCl^+ is the more likely candidate. In Chapter 2, we attempted to lay this controversy to rest by revisiting the chlorination kinetics of (chloro)phenols with an updated understanding of aqueous chlorine chemistry derived from previous work on dimethenamid[3] and aromatic ethers.[4]

By conducting experiments in which solution pH, chloride concentration, and chlorine dose were systematically varied, we obtained pseudo-first-order rate constants that were subsequently used to compute second-order rate constants for Cl_2, Cl_2O, and HOCl. We found that chloride addition enhances chlorination rates at pH < 7 for all the (chloro)phenols examined, indicating that Cl_2 is important for these compounds at low pH. For each (chloro)phenol, the reaction order in [HOCl] is between 1 and 2 at low pH and approaches 1 as the pH increases. One interpretation of this result is that Cl_2O has a pronounced influence on the reaction kinetics of (chloro)phenols at low pH. Nonetheless, as the FAC solutions used in our experiments contained approximately equimolar concentrations of [Cl^-] and [HOCl] at pH < 6.5, the reaction order in [HOCl] will also be

greater than 1 if Cl_2 is the most important chlorinating agent. Additional analysis shows that, under our experimental conditions, Cl_2 has a greater influence on the reactivities of (chloro)phenols than does Cl_2O.

The second-order rate constants we computed for Cl_2 and Cl_2O are orders of magnitude larger than those for HOCl. Therefore, even though Cl_2 and Cl_2O are present at low concentrations compared with HOCl under typical drinking water treatment conditions, they are capable of influencing the chlorination kinetics of (chloro)phenols due to their high intrinsic reactivities. Even though we were not able to rule out H_2OCl^+ as a chlorinating agent for (chloro)phenols, we did not need to invoke H_2OCl^+ in order for our kinetic models to fit the experimental data.

Prior to our work, rate constants for Cl_2, Cl_2O, and HOCl have been reported for only a few organic compounds with ionizable functional groups.[5-7] The (chloro)phenols examined have pK_a values between 6.16 and 9.99,[2] so both the acid (ArOH) and conjugate base (ArO^-) forms would have been present in our experiments conducted at pH 2–12. Given that ArO^- is more nucleophilic than is ArOH, the two forms of (chloro)phenols are expected to have different reactivities with electrophilic chlorine. Cl_2 is more abundant at low pH, so one might expect Cl_2 to react mostly with ArOH. Our experimental results, however, suggest that Cl_2 is more likely to react with ArO^-. Cl_2O reacts predominantly with ArOH, although we were able to determine second-order rate constants for the Cl_2O/ArO^- reaction for two chlorophenols as well. Our findings show that, when studying organic compounds with ionizable functional groups, experiments must be conducted under various solution conditions in order to determine the most likely reaction partners for each chlorinating agent. Also, when constructing a kinetic model for

describing reactivities of compounds with ionizable functional groups, researchers need to determine whether all the terms in the model are needed to fit their experimental data.

Using the second-order rate constants determined for Cl_2, Cl_2O, and HOCl, we computed the contribution of each chlorine species towards the overall chlorination rate in different chlorination scenarios: drinking water treatment, disinfection of desalinated water, and wastewater treatment. At pH > 7, HOCl remains the most important chlorinating agent for (chloro)phenols. In contrast with previous investigations on the chlorination kinetics of dimethenamid[3] and aromatic ethers,[4] Cl_2O is not anticipated to be particularly significant in any of the scenarios examined. The influence of Cl_2, on the other hand, is apparent for all the (chloro)phenols. When high chloride concentrations are present at pH ≤ 7, Cl_2 can contribute a significant fraction towards the overall reactivities of (chloro)phenols.

In waters containing elevated chloride concentrations (e.g., desalinated water, water that has been coagulated using ferric chloride, and swimming pool water), the potential role of chloride in enhancing chlorination rates of some organic constituents has been underappreciated. As one mole of chloride is generated when one mole of (chloro)phenol reacts with one mole of Cl_2, chloride can thus be considered a catalyst in the chlorination of aromatic organic compounds. Any kinetic model that does not take into account the concentration of chloride may underestimate the rate of organic compound transformation in the presence of FAC.

5. 2. Using 1,3,5-Trimethoxybenzene to Quench and Quantify Free Chlorine and Free Bromine

In disinfection byproduct (DBP) research, investigators often need to quench residual free halogens before analyzing for the organic compounds of interest. Many of the traditional quenchers employed (e.g., sodium sulfite, sodium thiosulfate, and ascorbic acid) are reducing agents that are known to interact with some redox-labile analytes, potentially leading to inaccurate quantification of those analytes.[8] Ammonium chloride is also used to quench free chlorine, but the resulting monochloramine can transform some organic compounds if the sample storage time is prolonged or if free bromine is present (because bromamines are more reactive than are chloramines[9]).

In Chapter 3, we developed an alternative approach entailing the use of 1,3,5-trimethoxybenzene (TMB) to quench free chlorine and free bromine. When present in excess of free halogens, TMB rapidly forms stable monohalogenated products (i.e., Cl-TMB and Br-TMB). TMB and its halogenation products are not likely to participate in redox reactions under conditions that are relevant to DBP research, so using TMB as a quencher is not anticipated to affect the stabilities of redox-labile analytes. Furthermore, TMB, Cl-TMB, and Br-TMB can be detected using analytical instruments that are available in most environmental chemistry laboratories. By monitoring TMB, Cl-TMB, and Br-TMB in quenched samples, the concentration of free chlorine and free bromine at the time of quenching can be determined.

We demonstrated the feasibility of using TMB as a quencher in kinetic experiments involving the chlorination of 2,4-dichlorophenol and bromination of anisole. Our results show that there is generally no significant difference in the rate constants

determined from experiments employing TMB as the quencher versus those from experiments employing sodium thiosulfate as the quencher. Measurements of [TMB], [Cl-TMB], and [Br-TMB] in quenched samples revealed that the concentrations of free halogens in our reactors did not vary over the course of the experiments, consistent with the maintenance of pseudo-first-order conditions ([free halogen(s)] ≈ [free halogen(s)]$_o$). We assessed the rate at which TMB reacts with free chlorine relative to traditional quenchers in competitive quenching experiments. We found that TMB does not react with free chlorine as quickly as do traditional quenchers. Nonetheless, TMB can serve as an effective quencher for free chlorine and free bromine in halogenation kinetic experiments as long as it is present in sufficient excess of the free halogens.

Unlike traditional quenchers that are reducing agents, TMB does not affect the stabilities of the eight DBPs we examined (chloropicrin, chloral hydrate, tribromoacetaldehyde, and haloaceontriles). Even though ammonium chloride similarly does not participate in redox reactions with redox-labile analytes, it can only be used to quench free chlorine for compounds that do not react with monochloramine. TMB can undergo chloramination, but the reaction of TMB with excess monochloramine is generally slow. As a result, in water samples containing both free chlorine and monochloramine, the latter should not interfere with the reaction of free chlorine with TMB provided that free chlorine is present in large excess of monochloramine.

The approach of quenching with a highly reactive organic compound that can outcompete other analytes for available halogenating agents has not been rigorously tested prior to our work. The lack of systematic assessments on the effectiveness of this quenching approach may explain why this approach has not been widely adopted. Results

from our experiments described in Chapter 3 provide quantitative evidence that TMB can serve as a selective quencher for free chlorine and free bromine without the limitations associated with traditional quenchers. Findings from this work will expand the choice of quenchers available to future researchers conducting DBP research.

5. 3. Kinetics of Ionone Chlorination

Previous investigations on the kinetics of aqueous chlorination have largely focused on organic compounds with aromatic moieties. The chlorination of alkenes is particularly under-examined. A few apparent rate constants for alkenes are available in the literature,[10] but the paucity of experimental rate constants does not permit computation of robust second-order rate constants. In Chapter 4, we sought to address this knowledge gap by assessing the influence of Cl_2, Cl_2O, and HOCl on the chlorination kinetics of three structurally related alkenes: α-ionone, β-ionone, and dehydro-β-ionone.

Of the three alkenes, β-ionone is the least reactive in the presence of FAC, while dehydro-β-ionone is the most reactive. Differences in alkene reactivity with electrophilic chlorine can be rationalized by differences in alkene structure. Chloride addition led to an appreciable increase in experimental rate constants at pH < 7.5 for all compounds. The rate enhancement is, however, more apparent for α- and β-ionones than for dehydro-β-ionone, indicating that Cl_2 is more important for the less reactive ionones. The reaction order in [HOCl] at pH 7–8 is significantly greater than 1 for α- and β-ionones, whereas it is close to 1 for dehydro-β-ionone. The differences in reaction order in [HOCl] suggest that Cl_2O, similar to Cl_2, is more important for the less reactive ionones.

For all three compounds, the second-order rate constants for Cl_2 and Cl_2O are orders of magnitude larger than those for HOCl, underscoring the high intrinsic reactivities of Cl_2 and Cl_2O compared with HOCl. Using the second-order rate constants for Cl_2, Cl_2O, and HOCl determined in this study as well as those reported for dimethenamid,[3] aromatic ethers,[4] and (chloro)phenols,[11] we quantitatively showed that there is an inverse relationship between selectivity for Cl_2 and Cl_2O and reactivity of the nucleophile. Our results suggest that the reactivity-selectivity principle[12] may be applied to predict the likelihood of reactions with Cl_2 and Cl_2O for a diverse group of organic compounds.

For the ionones, we also used second-order rate constants for Cl_2, Cl_2O, and HOCl to compute the contributions of these chlorinating agents towards the overall reactivity of each compound. Under a set of chlorine dose and chloride concentration that are representative of drinking water treatment, HOCl is the predominant chlorinating agent for all ionones, with Cl_2 being important only at pH < 7 and Cl_2O having minor or negligible influence on reaction rates. When chlorinating waters that contain elevated concentrations of chloride, the influence of Cl_2 at pH 6–8 increases substantially for all three ionones. In laboratory settings in which the chlorine doses used may be higher than those encountered in drinking water treatment, Cl_2O may contribute more than 50% towards the overall reactivities of α- and β-ionones.

Our findings suggest that the importance of Cl_2 cannot be underestimated when the water being chlorinated contains elevated chloride concentrations. The role of chloride as a catalyst in chlorination reactions, first discussed in Chapter 2, is again highlighted by the results of this study. While Cl_2O may not be particularly important for

the ionones examined under typical drinking water treatment conditions, it can have a substantial influence on reaction kinetics in laboratory experiments employing high chlorine doses. Thus, researchers should not assume that chlorination reactions are first-order in [HOCl]. Conducting experiments in which solution pH, chloride concentration, and chlorine dose are systematically varied are necessary for computing robust second-order rate constants that truly reflect the reactivities of organic compounds in the presence of FAC.

5. 4. Future Work

Deducing the Mechanism of Cl_2O Reactions. In Chapter 2, we constructed Hammett plots using the second-order rate constants we computed for reactions of (chloro)phenols with Cl_2, Cl_2O, and HOCl. The Hammett plots for Cl_2 and HOCl have negative slopes (ρ). As the nucleophilicity of phenol decreases with increasing number of electron-withdrawing substituents, a Hammett plot with a negative slope is consistent with (chloro)phenols reacting via electrophilic aromatic substitutions. On the other hand, the Hammett plot for Cl_2O has a slight positive ρ value, suggesting that Cl_2O may react by a free-radical mechanism. We were not able to detect the presence of radicals in our FAC solutions using electron paramagnetic resonance (EPR) spectroscopy (the signals we detected were due to an experimental artifact). The absence of a radical signal, however, does not rule out the presence of radicals at concentrations below the detection limit of our EPR method. Furthermore, there is considerable scatter in the Hammett plot we constructed for Cl_2O. More data points (i.e., more second-order rate constants for the

reaction of Cl_2O with substituted phenols) will be needed to assess whether our Hammett plots are robust and to pinpoint the reaction mechanism of Cl_2O.

Elucidating the Chlorination Pathways of Phenols. It is well known that phenol is chlorinated successively to form mono-, di-, and trichlorophenols. It is also known that phenol can form chloroform and trichloroacetic acid. Nevertheless, identities of the reaction intermediates that form upon the chlorination of 2,4,6-trichlorophenol have not been determined. There is evidence that 2,6-dichloro-1,4-benzoquinone (2,6-DCBQ), a DBP that has been detected in effluents of drinking water treatment plants employing chlorination, can form from the chlorination of phenol.[13] Despite the widespread occurrence of 2,6-DCBQ in chlorinated waters, the reactivity of 2,6-DCBQ in the presence of FAC has not been thoroughly investigated. Future research efforts should examine whether 2,6-DCBQ is a "kinetically competent" intermediate in the formation of chloroform and trichloroacetic acid from phenol. The influence of Cl_2, Cl_2O, and HOCl on the (trans)formation of 2,6-DCBQ also merits investigation.

Using TMB as a Free Halogen Quencher in Various Water Matrices. We have demonstrated that TMB can be an effective quencher for free chlorine and free bromine in halogenation experiments conducted in the laboratory. Nevertheless, many investigations on the (trans)formation of DBPs employ real waters, and at this point it is not clear how the various constituents of real waters will affect the reactivity of TMB with free halogens. More assessments will be needed to determine whether TMB can serve as an effective quencher for free halogens in different water matrices.

Elucidating the Chlorination Pathways of Ionones. β-Ionone is known to produce trihalomethanes (THMs) upon chlorination, but the exact transformation pathway is unknown. While structures have been proposed for the reaction intermediates/products of β-ionone chlorination, they have not been confirmed with authentic standards. We synthesized a few compounds that seemed to be plausible reaction intermediates/ products. With the exception of dehydro-β-ionone and, perhaps, β-ionone epoxide, we have not identified all the reaction intermediates/products in the chlorination of β-ionone. Currently our analytical tools are limited to high-performance liquid chromatography (HPLC) with photodiode array (PDA) detection and gas-chromatography mass spectrometry (GC-MS). Additional analyses using liquid-chromatography mass spectrometry (LC-MS) will be needed to obtain more information on the structures of these reaction intermediates/products.

Is Chloride a Catalyst in the Formation of Chlorinated DBPs? In Chapter 2, we presented evidence that chloride can catalyze the chlorination of (chloro)phenols via formation of Cl_2. If the reaction of alkenes with free chlorine results in chlorohydrin formation, then chloride can also be considered a catalyst for alkene chlorination (as one mole of chloride would be generated when one mole of Cl_2 reacts with one mole of alkene). It is not clear, however, whether chloride can catalyze the formation of chlorinated DBPs upon chlorination of natural organic matter (NOM), the structure of which is much more complicated than those of the model compounds investigated in our work.

Trihalomethane (THM) formation is favored at high pH, while haloacetic acid (HAA) formation is favored at low pH.[14] As the influence of Cl_2 on chlorination kinetics

is most pronounced at pH < 7, the effect (if any) of chloride addition on the kinetics of DBP formation from the chlorination of NOM should be more appreciable for HAAs than for THMs. Future research efforts should be directed at examining the effect of chloride addition on the kinetics of HAA formation. Measuring the total organic halogen (TOX) that form upon chlorination of NOM may lead to additional insights on the potential role of chloride as a catalyst in the formation of unregulated DBPs.

5. 5. References

1. Lee, G. F.; Morris, J. C. Kinetics of chlorination of phenol – Chlorophenolic tastes and odors. *Int. J. Air Water Pollut.* **1962,** *6*, 419-431.

2. Gallard, H.; Von Gunten, U. Chlorination of phenols: Kinetics and formation of chloroform. *Environ. Sci. Technol.* **2002,** *36*, 884-890.

3. Sivey, J. D.; McCullough, C. E.; Roberts, A. L. Chlorine monoxide (Cl_2O) and molecular chlorine (Cl_2) as active chlorinating agents in reaction of dimethenamid with aqueous free chlorine. *Environ. Sci. Technol.* **2010,** *44*, 3357-3362.

4. Sivey, J. D.; Roberts, A. L. Assessing the reactivity of free chlorine constituents Cl_2, Cl_2O, and HOCl toward aromatic ethers. *Environ. Sci. Technol.* **2012,** *46*, 2141-2147.

5. Cai, M.-Q.; Feng, L.; Jiang, J.; Qi, F.; Zhang, L.-Q. Reaction kinetics and transformation of antipyrine chlorination with free chlorine. *Water Res.* **2013,** *47*, 2830-2842.

6. Cai, M.-Q.; Feng, L.; Zhang, L.-Q. Transformation of aminopyrine in the presence of free available chlorine: Kinetics, products, and reaction pathways. *Chemosphere* **2017,** *171*, 625-634.

7. Vikesland, P. J.; Fiss, E. M.; Wigginton, K. R.; McNeill, K.; Arnold, W. A. Halogenation of bisphenol-A, triclosan, and phenols in chlorinated waters containing iodide. *Environ. Sci. Technol.* **2013,** *47*, 6764-6772.

8. Kristiana, I.; Lethorn, A.; Joll, C.; Heitz, A. To add or not to add: The use of quenching agents for the analysis of disinfection by-products in water samples. *Water Res.* **2014,** *59*, 90-98.

9. Duirk, S. E.; Valentine, R. L. Bromide oxidation and formation of dihaloacetic acids in chloraminated water. *Environ. Sci. Technol.* **2007,** *41*, 7047-7053.

10. Deborde, M.; von Gunten, U. Reactions of chlorine with inorganic and organic compounds during water treatment – Kinetics and mechanisms: A critical review. *Water Res.* **2008,** *42*, 13-51.

11. Lau, S. S.; Abraham, S. M.; Roberts, A. L. Chlorination revisited: Does Cl^- serve as a catalyst in the chlorination of phenols? *Environ. Sci. Technol.* **2016,** *50*, 13291-13298.

12. Anslyn, E. V.; Dougherty, D. A. Modern Physical Organic Chemistry. University Science: 2006.

13. Zhao, Y. L.; Anichina, J.; Lu, X. F.; Bull, R. J.; Krasner, S. W.; Hrudey, S. E.; Li, X. F. Occurrence and formation of chloro- and bromo-benzoquinones during drinking water disinfection. *Water Res.* **2012,** *46*, 4351-4360.

14. Larson, R. A.; Weber, E. J. *Reaction Mechanisms in Environmental Organic Chemistry*. CRC Press: Boca Raton, Florida, 1994.

Appendix A: Supporting Information for Chapter 2

A. 1. List of Abbreviations

FAC: free available chlorine

2-CP: 2-chlorophenol

4-CP: 4-chlorophenol

2,4-DCP: 2,4-dichlorophenol

2,6-DCP: 2,6-dichlorophenol

TCP: 2,4,6-trichlorophenol

A. 2. Procedure for NaCl Recrystallization

To reduce bromide (Br^-) contamination, commercial sodium chloride (NaCl) was recrystallized in our laboratory using the following method: 35 g of NaCl was dissolved in 100 mL of Milli-Q water in a 500-mL beaker. The mixture was heated on a hot plate with occasional stirring until the NaCl had completely dissolved. The beaker was then removed from heat and the solution was allowed to cool to room temperature. NaCl crystals began to form as the solution cooled. Once the solution reached room temperature, the beaker was placed in an ice bath, where upon more NaCl crystals formed. After the solution reached temperature equilibrium with the ice slurry, acetone (100 mL) was slowly added to the beaker over 5 minutes. The NaCl solution turned cloudy as more crystals formed. The beaker was covered with aluminum foil and was stored at 4 °C for ≥ 8 hours. Vacuum filtration was then used to separate the NaCl crystals from the acetone-water mixture while the mixture was still cold. The NaCl

crystals were dried at 100 °C for 30 minutes before weighing. The NaCl was recrystallized for a second time to further reduce the Br^- content.

Ion chromatographic analysis revealed that 0.780 μM of Br^- was present in a 30 mM NaCl solution prepared by dissolving the original (non-recrystallized) NaCl in water. Bromide was not detected in a 30 mM NaCl solution made using the twice-recrystallized NaCl (Br^- detection limit = 0.02 μM). Thus, the recrystallization procedure was effective in reducing the Br^- content in NaCl by ≥ 97%.

IC measurements were carried out using a Dionex ICS-2100 ion chromatography system with a Dionex AERS 500 Suppressor and an IonPac® AS18 anion-exchange column (4 × 250 mm) from Thermo Fisher Scientific. The eluent was 30 mM KOH, and analyses were performed at a column temperature of 30 °C.

A. 3. Procedure for Data Modeling

Model Development. The modeling approach described herein is similar to the processes described in refs. 1 and 2. Second-order rate constants were estimated via nonlinear least-squares regressions of the experimental data (k_{obs}) for (chloro)phenol decay using the computer program *SigmaPlot 12.5* (Systat Software). Assuming that HOCl, Cl_2, and Cl_2O all influence the reaction kinetics of (chloro)phenols, the change in $[(\text{chloro})\text{phenol}]_T$ over time can be expressed as equation A-1.

$$-\frac{d[\text{ArOH}]_T}{dt} = -\left(\frac{d[\text{ArOH}]}{dt} + \frac{d[\text{ArO}^-]}{dt}\right) \quad \text{(A-1)}$$

Equation A-1 can be written as equation A-2.

$$-\frac{d[\mathrm{ArOH}]_\mathrm{T}}{dt} = k_{\mathrm{HOCl,\,ArOH}}[\mathrm{HOCl}][\mathrm{ArOH}] + k_{\mathrm{HOCl,\,ArO^-}}[\mathrm{HOCl}][\mathrm{ArO^-}] + k_{\mathrm{Cl_2,\,ArOH}}[\mathrm{Cl_2}][\mathrm{ArOH}] + k_{\mathrm{Cl_2,\,ArO^-}}[\mathrm{Cl_2}][\mathrm{ArO^-}] + k_{\mathrm{Cl_2O,\,ArOH}}[\mathrm{Cl_2O}][\mathrm{ArOH}] + k_{\mathrm{Cl_2O,\,ArO^-}}[\mathrm{Cl_2O}][\mathrm{ArO^-}] \quad \text{(A-2)}$$

where ArOH and ArO^- represent the conjugate acid and phenolate forms, respectively, and $[\mathrm{ArOH}]_\mathrm{T} = [\mathrm{ArOH}] + [\mathrm{ArO^-}]$. As our experiments were conducted under pseudo-first-order conditions in which $[\mathrm{FAC}] \approx [\mathrm{FAC}]_\mathrm{o} \gg [\text{(chloro)phenol}]_\mathrm{o}$, we can express the change in $[\text{(chloro)phenol}]_\mathrm{T}$ as equation A-3.

$$-\frac{d[\mathrm{ArOH}]_\mathrm{T}}{dt} = k_{\mathrm{obs}}[\mathrm{ArOH}]_\mathrm{T} \quad \text{(A-3)}$$

The pseudo-first-order coefficient (k_{obs}) can be written as equation A-4:

$$k_{\mathrm{obs}} = k_{\mathrm{HOCl,\,ArOH}}[\mathrm{HOCl}]f_{\mathrm{ArOH}} + k_{\mathrm{HOCl,\,ArO^-}}[\mathrm{HOCl}]f_{\mathrm{ArO^-}} + k_{\mathrm{Cl_2,\,ArOH}}[\mathrm{Cl_2}]f_{\mathrm{ArOH}} + k_{\mathrm{Cl_2,\,ArO^-}}[\mathrm{Cl_2}]f_{\mathrm{ArO^-}} + k_{\mathrm{Cl_2O,\,ArOH}}[\mathrm{Cl_2O}]f_{\mathrm{ArOH}} + k_{\mathrm{Cl_2O,\,ArO^-}}[\mathrm{Cl_2O}]f_{\mathrm{ArO^-}} \quad \text{(A-4)}$$

where f_{ArOH} and $f_{\mathrm{ArO^-}}$ represent the fractions of (chloro)phenol in the phenol (ArOH) and phenolate (ArO^-) forms, respectively, and $f_{\mathrm{ArO^-}} = (1 - f_{\mathrm{ArOH}})$.

$$f_{\mathrm{ArOH}} = \frac{[\mathrm{ArOH}]}{[\mathrm{ArOH}]+[\mathrm{ArO^-}]} = \frac{1}{1+(K_\mathrm{a}/[\mathrm{H^+}])} \quad \text{(A-5)}$$

$[Cl_2]$ and $[Cl_2O]$ in equation A-4 can be rewritten in terms of [HOCl]:

$$k_{\mathrm{obs}} = k_{\mathrm{HOCl,\,ArOH}}[\mathrm{HOCl}]f_{\mathrm{ArOH}} + k_{\mathrm{HOCl,\,ArO^-}}[\mathrm{HOCl}]f_{\mathrm{ArO^-}} + k_{\mathrm{Cl_2,\,ArOH}}K_{\mathrm{Cl_2}}[\mathrm{HOCl}][\mathrm{Cl^-}][\mathrm{H^+}]f_{\mathrm{ArOH}} + k_{\mathrm{Cl_2,\,ArO^-}}K_{\mathrm{Cl_2}}[\mathrm{HOCl}][\mathrm{Cl^-}][\mathrm{H^+}]f_{\mathrm{ArO^-}} + k_{\mathrm{Cl_2O,\,ArOH}}K_{\mathrm{Cl_2O}}[\mathrm{HOCl}]^2 f_{\mathrm{ArOH}} + k_{\mathrm{Cl_2O,\,ArO^-}}K_{\mathrm{Cl_2O}}[\mathrm{HOCl}]^2 f_{\mathrm{ArO^-}} \quad \text{(A-6)}$$

where K_{Cl_2} and K_{Cl_2O} are the equilibrium constants for the formation of Cl_2 and Cl_2O, respectively. The values of K_{Cl_2} and K_{Cl_2O} are given in Chapter 2.

Equation A-6 reflects all the reactions between FAC and (chloro)phenols considered in this study. It is necessary to check whether all the terms are needed to fit the experimental data to avoid over-parameterizing the model. The fitting procedure minimizes the sums of squares between the experimental log k_{obs} data and the model predictions, and only one parameter (i.e., one second-order rate constant) is fitted at any given time. Uncertainties in the second-order rate constants indicate the 95% confidence intervals calculated by *SigmaPlot 12.5*.

Data Modeling for Phenol. The modeling procedure for phenol will be described in detail to illustrate our data fitting approach. We first modeled the no-added-chloride data at pH > 9 (where k_{obs} decreases with increasing pH) with the assumption that the HOCl/ArO^- reaction is the only one important at high pH. We fixed all other second-order rate constants in equation A-6 at zero and computed $k_{HOCl,\,ArO^-}$, which we estimated to be 2.61 (± 0.26) × 10^4 M^{-1} s^{-1} (**Figure A-1a**). With $k_{HOCl,\,ArO^-}$ constrained to this value, we modeled the log k_{obs} versus log $[HOCl]_o$ data from reaction order experiments at pH 4.7 by assuming that Cl_2O/ArOH is the dominant reaction. Our initial estimate for $k_{Cl_2O,\,ArOH}$ was 3.61 (± 0.31) × 10^5 M^{-1} s^{-1} (**Figure A-1b**).

Next, we constrained both $k_{HOCl,\,ArO^-}$ and $k_{Cl_2O,\,ArOH}$ to their estimated values while modeling the 5 mM added Cl^- data at pH < 5.5 to compute $k_{Cl_2,\,ArOH}$. Our initial estimate of $k_{Cl_2,\,ArOH}$ was 8.47 (± 1.40) × 10^4 M^{-1} s^{-1} (**Figure A-1c**). As ion chromatographic measurements revealed that 0.17 mM Cl^- was present in reactors

without added NaCl for phenol (see later discussion in Section A-5), we expect that the Cl_2/ArOH reaction would be important even in the absence of added Cl^-. Thus, we might have overestimated $k_{Cl_2O,\,ArOH}$ by not considering the Cl_2/ArOH reaction when modeling the log k_{obs} versus log $[HOCl]_o$ data at pH 4.7. We modeled the same data set again, but this time we constrained $k_{Cl_2,\,ArOH}$ = 8.47 (± 1.40) × 10^4 M^{-1} s^{-1} and $[Cl^-]$ = 0.17 mM while computing a new estimate for $k_{Cl_2O,\,ArOH}$ (**Figure A-1d**).

Afterwards, we modeled the entire 5 mM added Cl^- data set to compute $k_{Cl_2,\,ArO^-}$ with $k_{HOCl,\,ArO^-}$, $k_{Cl_2O,\,ArOH}$, and $k_{Cl_2,\,ArOH}$ constrained to their previously estimated values. The initial estimate for $k_{Cl_2,\,ArO^-}$ was 1.31 (± 0.78) × 10^9 M^{-1} s^{-1} (**Figure A-1e**). With $k_{Cl_2,\,ArO^-}$ constrained, we then sequentially estimated $k_{Cl_2O,\,ArOH}$ and $k_{Cl_2,\,ArOH}$ again. We repeated the process a few more times until we obtained the best qualitative fit to the log k_{obs} versus pH data (**Figure A-1f**).

The best-fit estimates of second-order rate constants are as follows: $k_{HOCl,\,ArO^-}$ = 2.61 (± 0.26) × 10^4 M^{-1} s^{-1}, $k_{Cl_2,\,ArOH}$ = 8.92 (± 0.98) × 10^4 M^{-1} s^{-1}, $k_{Cl_2,\,ArO^-}$ = 2.61 (± 0.50) × 10^9 M^{-1} s^{-1}, and $k_{Cl_2O,\,ArOH}$ = 9.02 (± 3.06) × 10^4 M^{-1} s^{-1}. We did not include terms for $k_{HOCl,\,ArOH}$ and $k_{Cl_2O,\,ArO^-}$ in the final model for phenol (equation 2-6) because they did not provide any improvement to the fit to the experimental data.

The iterative data fitting processes for the other chlorophenols are similar to the one described for phenol. Although the final models for the six (chloro)phenols are different, we followed these general data fitting principles:

1. $k_{\mathrm{HOCl,\,ArO^-}}$ is estimated from no-added-chloride data at high pH
2. $k_{\mathrm{Cl_2O,\,ArOH}}$ is estimated from log k_{obs} versus log $[\mathrm{HOCl}]_o$ data at low pH without added Cl^-
3. $k_{\mathrm{Cl_2,\,ArOH}}$ (if included) is estimated from 3 or 5 mM added Cl^- at low pH
4. $k_{\mathrm{Cl_2,\,ArO^-}}$ is estimated from the entire 3 or 5 mM added Cl^- data set
5. $k_{\mathrm{Cl_2O,\,ArO^-}}$ (if included) is estimated from the entire no-added-chloride data set
6. $k_{\mathrm{HOCl,\,ArOH}}$ (if included) is estimated from no-added-chloride data at low pH

Using our model for phenol (equation 2-6 in Chapter 2), we also calculated a value for $[Cl^-]$ in no-NaCl-added reactors that is independent of ion chromatographic measurements. After computing the initial estimates of $k_{\mathrm{HOCl,\,ArO^-}}$, $k_{\mathrm{Cl_2O,\,ArOH}}$, and $k_{\mathrm{Cl_2,\,ArOH}}$, we constrained these rate constants and used $[Cl^-]$ as a fitting parameter for the no-added-chloride data at pH < 4.5 (where k_{obs} increases with decreasing pH). When computing $k_{\mathrm{Cl_2O,\,ArOH}}$ for a second time, we fixed $[Cl^-]$ at the previously estimated value. The iterative data fitting proceeded as described above. For phenol ($[\mathrm{FAC}]_o$ = 125 μM), the final estimate of $[Cl^-]$ in reactors without added NaCl is 0.22 ± 0.03 mM. This calculated value of $[Cl^-]$ is close to the measured $[Cl^-]$ value (0.17 mM).

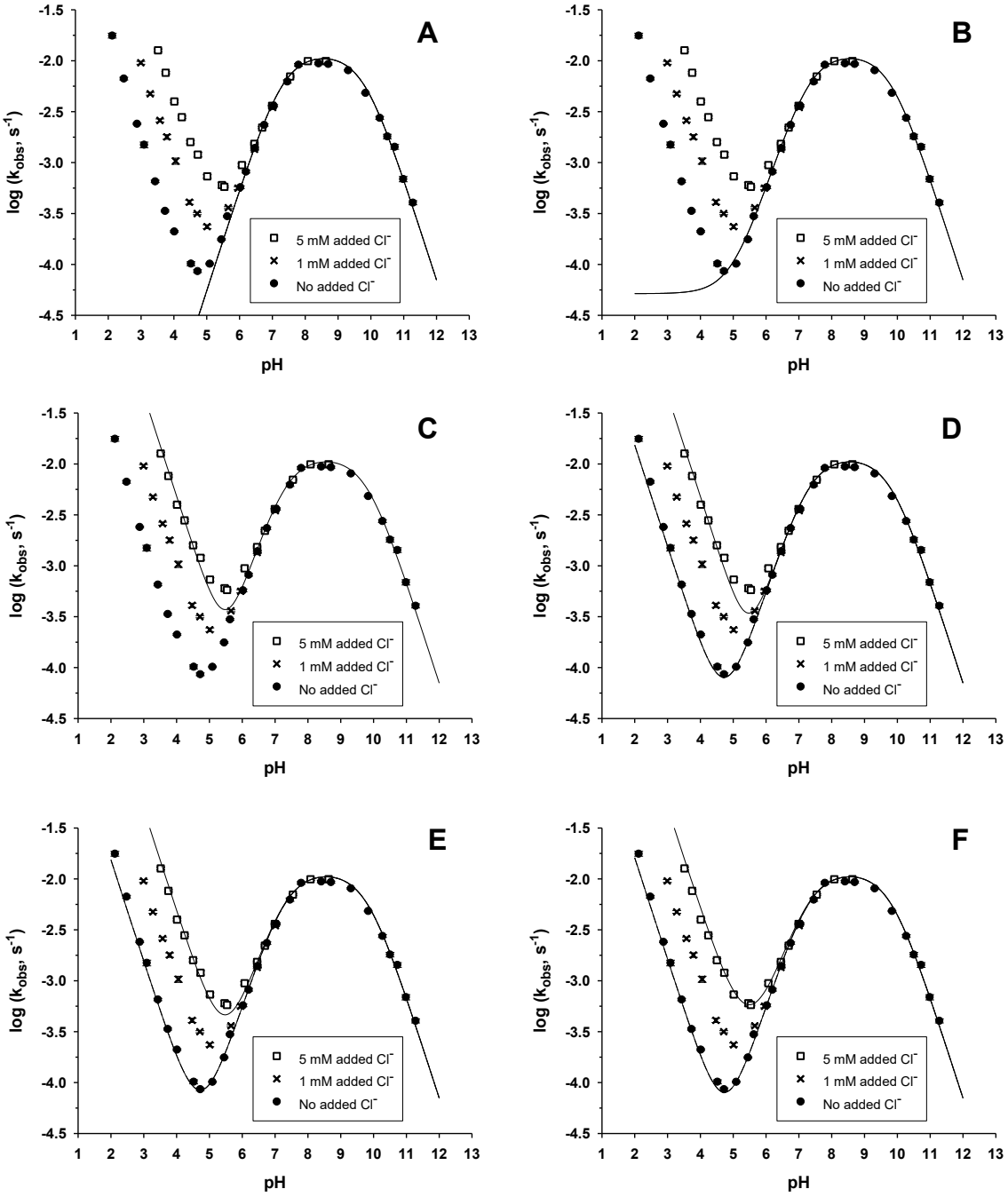

Figure A-1. Plots of log k_{obs} versus pH for phenol showing the model fit at various stages of the iterative data fitting process: **(A)** HOCl/ArO⁻-only model; **(B)** both HOCl and Cl_2O were considered; **(C)** fitting $k_{\mathrm{Cl_2,\,ArOH}}$ while constraining $k_{\mathrm{HOCl,\,ArO^-}}$ and $k_{\mathrm{Cl_2O,\,ArOH}}$; **(D)** fitting $k_{\mathrm{Cl_2O,\,ArOH}}$ while $k_{\mathrm{Cl_2,\,ArOH}}$ and $k_{\mathrm{HOCl,\,ArO^-}}$ were constrained; **(E)** fitting $k_{\mathrm{Cl_2,\,ArO^-}}$ while all other second-order rate constants were constrained; and **(F)** the final model fit. Note that the 1 mM added Cl^- data were not used in the data fitting process.

We also used the program *Scientist 3.0* (Micromath) to predict the concentrations of all six (chloro)phenols (parent compounds and products alike) as a function of time. We input the differential rate laws for all (chloro)phenols according to **Figure A-2**, and we used the best-fit estimates of second-order rate constants listed in **Table 2-1** (Chapter 2) to calculate the pseudo-first-order rate coefficients (k_{calc}) we would expect for a given value of $[FAC]_o$. Those k_{calc} values are represented by k_A, k_B, k_C, k_D, k_E, and k_F in the *Scientist* model. Phenol can be chlorinated to form either 2-CP or 4-CP, while 2-CP can be chlorinated to form 2,4-DCP or 2,6-DCP. As we were unable to determine k_{AB}, k_{AC}, k_{BD}, k_{BE} experimentally, we treated them as fitting parameters (keeping in mind that $k_{AB} + k_{AC} = k_A$ and $k_{BD} + k_{BE} = k_B$) while all the other rate coefficients were constrained. The concentration profiles of the (chloro)phenols predicted by our model from the chlorination of phenol are illustrated in **Figure 2-7** (Chapter 2).

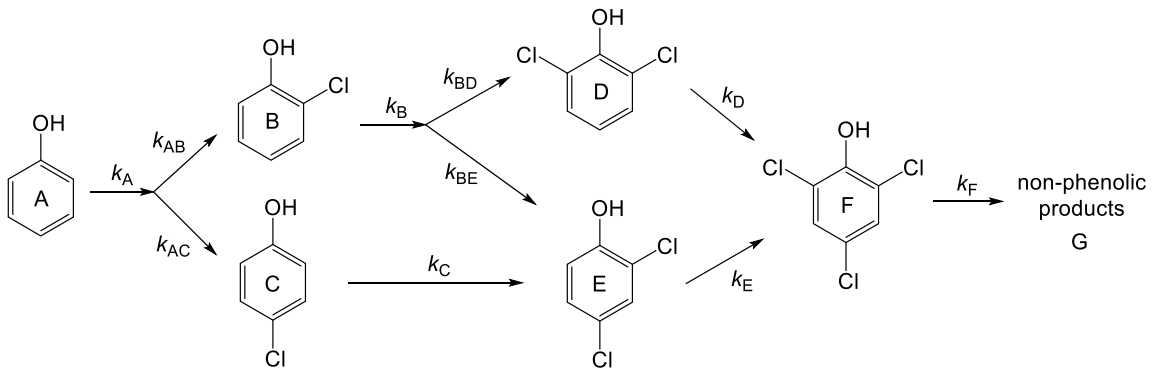

Figure A-2. Reaction pathway for the chlorination of phenol.

A. 4. Sample Data from Phenol Chlorination Experiments

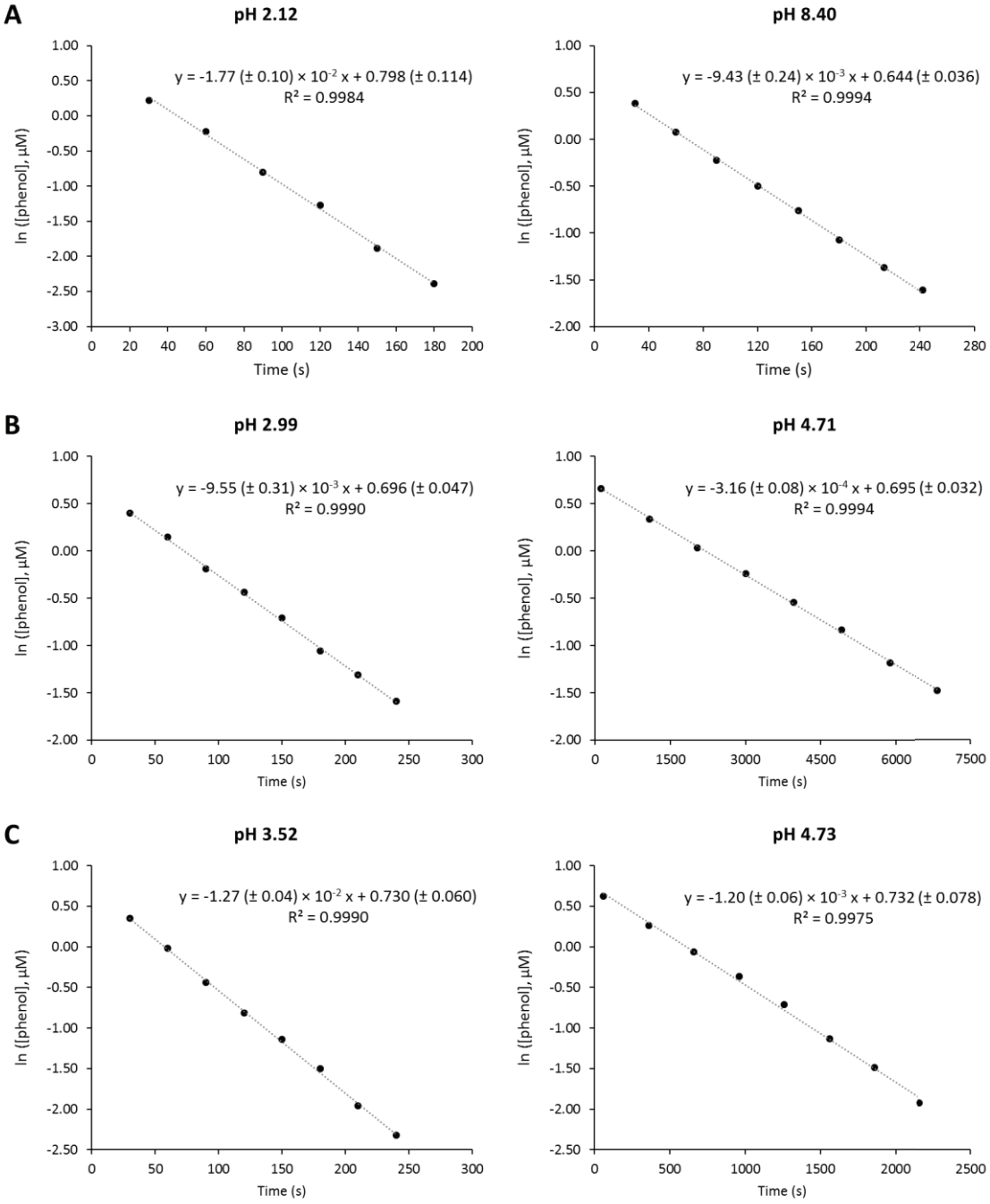

Figure A-3. Linear regressions of $\ln[\text{phenol}]_T$ versus time data for selected reactors with **(A)** no Cl^- added, **(B)** $[Cl^-]_{added}$ = 1 mM, and **(C)** $[Cl^-]_{added}$ = 5 mM. Reaction conditions: $[FAC]_o$ = 125 µM, $[phenol]_o$ = 2 µM, [pH buffer] = 10 mM, ionic strength = 0.1 M, T = 25 °C. Uncertainties in the slopes and y-intercepts indicate 95% confidence intervals.

A. 5. Chloride in FAC Solutions: Origin and Measurement via Ion Chromatography

Sodium hypochlorite (NaOCl) is typically manufactured by bubbling gaseous Cl_2 into water and then adding two moles of NaOH for every mole of Cl_2:

$$Cl_{2\,(aq)} + 2\,NaOH \rightarrow NaOCl + NaCl + H_2O \quad \text{(A-7)}$$

A solution of NaOCl made via the above process ought to contain equimolar concentrations of $[Cl^-]$ and $[OCl^-]_T$. Nonetheless, sodium hypochlorite is known to degrade over a time scale of months, even when the concentrated stock solution is stored in the dark at 4 °C. Rather than relying on deduction to assess the chloride concentration in our FAC solutions, we opted to measure it via ion chromatography (IC).

Our approach to Cl^- measurements was similar to that used by Cherney et al.[3] First, the commercial NaOCl stock solution was standardized iodometrically according to Standard Methods 4500-Cl B.[4] After diluting the NaOCl stock solution with Milli-Q water to the desired concentration, a molar excess of sodium sulfite (Na_2SO_3) was added to reduce all chlorinating agents to Cl^-. Then, the total chloride ($[Cl^-]_{total}$) in the solution was determined by IC. The concentration of Cl^- in a reagent blank containing only sodium sulfite (i.e., $[Cl^-]_{sulfite}$) was also measured. As the concentration of FAC initially present in the FAC solution ($[FAC]_o$) was known, we could calculate the concentration of chloride contributed by the NaOCl stock solution by difference: $[Cl^-]$ in FAC solution = $[Cl^-]_{total} - [FAC]_o - [Cl^-]_{sulfite}$. The concentration of Cl^- in our FAC solutions as a function of $[FAC]_o$ is shown in **Figure 2-3** (Chapter 2).

IC measurements were carried out using a Dionex ICS-2100 ion chromatography system with a Dionex AERS 500 Suppressor and an IonPac® AS18 anion-exchange

column (4 × 250 mm) from Thermo Fisher Scientific. The eluent was 30 mM KOH, and analyses were performed at a column temperature of 30 °C.

A. 6. Reaction Order in [HOCl]

The reaction order (n) in [HOCl] can be calculated using the second-order rate constants listed in **Table 2-1** (Chapter 2). The derivation of calculated n (n_{calc}) for phenol, 2-CP, and 4-CP is shown herein, and the approach is similar to that shown in ref. 1. The final model for phenol, 2-CP, and 4-CP reactivity in the presence of FAC is

$$k_{\mathrm{obs}} = k_{\mathrm{HOCl,\,ArO^-}}[\mathrm{HOCl}]\, f_{\mathrm{ArO^-}} + k_{\mathrm{Cl_2O,\,ArOH}}\,[\mathrm{Cl_2O}]\, f_{\mathrm{ArOH}} + k_{\mathrm{Cl_2,\,ArOH}}\,[\mathrm{Cl_2}]\, f_{\mathrm{ArOH}} + k_{\mathrm{Cl_2,\,ArO^-}}[\mathrm{Cl_2}]\, f_{\mathrm{ArO^-}} \quad \text{(A-8)}$$

where k_{obs} represents the pseudo-first-order rate constant determined from kinetic experiments; f_{ArOH} and $f_{\mathrm{ArO^-}}$ represent the fractions of (chloro)phenol in the conjugate acid (ArOH) and phenolate (ArO^-) forms, respectively.

Substituting known quantities for $[Cl_2]$ and $[Cl_2O]$ into equation A-8:

$$k_{\mathrm{obs}} = k_{\mathrm{HOCl,\,ArO^-}}[\mathrm{HOCl}]\, f_{\mathrm{ArO^-}} + k_{\mathrm{Cl_2O,\,ArOH}}\left(K_{\mathrm{Cl_2O}}\,[\mathrm{HOCl}]^2\right) f_{\mathrm{ArOH}} + k_{\mathrm{Cl_2,\,ArOH}}\left(K_{\mathrm{Cl_2}}[\mathrm{HOCl}][\mathrm{Cl^-}][\mathrm{H^+}]\right) f_{\mathrm{ArOH}} + k_{\mathrm{Cl_2,\,ArO^-}}\left(K_{\mathrm{Cl_2}}[\mathrm{HOCl}][\mathrm{Cl^-}][\mathrm{H^+}]\right) f_{\mathrm{ArO^-}} \quad \text{(A-9)}$$

Measurements by ion chromatography (IC) showed that the FAC solutions in our experiments contained roughly equimolar concentrations of [FAC] and $[Cl^-]$. As [HOCl] ≈ [FAC] at pH ≤ 6.5, we can substitute $[Cl^-]$ for [HOCl] in equation A-9 to obtain the following:

$$k_{obs} = k_{HOCl,\,ArO^-}[HOCl]\,f_{ArO^-} + k_{Cl_2O,\,ArOH}\left(K_{Cl_2O}\,[HOCl]^2\right) f_{ArOH} + k_{Cl_2,\,ArOH}\left(K_{Cl_2}\,[HOCl]^2[H^+]\right) f_{ArOH} + k_{Cl_2,\,ArO^-}\left(K_{Cl_2}\,[HOCl]^2[H^+]\right) f_{ArO^-} \quad \text{(A-10)}$$

Factoring out [HOCl] yields equation A-11:

$$k_{obs} = [HOCl]\,(k_{HOCl,\,ArO^-}f_{ArO^-} + k_{Cl_2O,\,ArOH}\,K_{Cl_2O}[HOCl]\,f_{ArOH} + k_{Cl_2,\,ArOH}\,K_{Cl_2}[HOCl][H^+]\,f_{ArOH} + k_{Cl_2,\,ArO^-}K_{Cl_2}[HOCl][H^+]\,f_{ArO^-}) \quad \text{(A-11)}$$

Taking the log of both sides of equation A-11:

$$\log k_{obs} = \log [HOCl] + \log (k_{HOCl,\,ArO^-}f_{ArO^-} + k_{Cl_2O,\,ArOH}\,K_{Cl_2O}[HOCl]\,f_{ArOH} + k_{Cl_2,\,ArOH}\,K_{Cl_2}[HOCl][H^+]\,f_{ArOH} + k_{Cl_2,\,ArO^-}\,K_{Cl_2}[HOCl][H^+]\,f_{ArO^-}) \quad \text{(A-12)}$$

Grouping the constants in equation A-12 together yields the following:

$$\log k_{obs} = \log [HOCl] + \log (C_1[HOCl] + C_2) \quad \text{(A-13)}$$

where $C_1 = k_{Cl_2O,\,ArOH}\,K_{Cl_2O}\,f_{ArOH} + k_{Cl_2,\,ArOH}\,K_{Cl_2}[H^+]\,f_{ArOH} + k_{Cl_2,\,ArO^-}\,K_{Cl_2}[H^+]\,f_{ArO^-}$

and $C_2 = k_{HOCl,\,ArO^-}\,f_{ArO^-}$

The definition of n_{calc} is the derivative of log k_{obs} with respect to the derivative of log [FAC]:

$$n_{\text{calc}} = \frac{d(\log k_{\text{obs}})}{d(\log [\text{FAC}])} \tag{A-14}$$

Under the reaction conditions employed in this study, [FAC] can be approximated as the sum of [HOCl] and [OCl^-]:

$$[\text{FAC}] \approx [\text{HOCl}] + [\text{OCl}^-] = [\text{HOCl}]\left(1 + \frac{K_a}{[\text{H}^+]}\right) \tag{A-15}$$

Taking the log of both sides of equation A-15:

$$\log [\text{FAC}] = \log [\text{HOCl}] + \log\left(1 + \frac{K_a}{[\text{H}^+]}\right) \tag{A-16}$$

Taking the derivative of both sides of equation A-16 with respect to log [HOCl]:

$$\frac{d(\log [\text{FAC}])}{d(\log [\text{HOCl}])} = 1 \tag{A-17}$$

which is equivalent to equation A-18:

$$d(\log\ [\text{FAC}]) = d(\log\ [\text{HOCl}]) \tag{A-18}$$

Thus, equation A-14 can be written as the following:

$$n_{\text{calc}} = \frac{d(\log\ k_{\text{obs}})}{d(\log [\text{FAC}])} = \frac{d(\log\ k_{\text{obs}})}{d(\log [\text{HOCl}])} \tag{A-19}$$

Substituting equation A-13 into equation A-19 leads to these expressions for n_{calc}:

$$\begin{aligned} n_{\text{calc}} &= \frac{d(\log\ k_{\text{obs}})}{d(\log [\text{HOCl}])} \\ &= \frac{d(\log [\text{HOCl}])}{d(\log [\text{HOCl}])} + \frac{d}{d(\log [\text{HOCl}])}(\log (C_1[\text{HOCl}] + C_2)) \end{aligned} \tag{A-20}$$

$$n_{\text{calc}} = 1 + \frac{d}{d(\log [\text{HOCl}])}(\log (C_1[\text{HOCl}] + C_2)) \quad \text{(A-21)}$$

Use the chain rule to evaluate $\frac{d}{d(\log [\text{HOCl}])}(\log (C_1[\text{HOCl}] + C_2))$ in equation A-21:

$$\frac{d}{d(\log [\text{HOCl}])}(\log (C_1[\text{HOCl}] + C_2))$$

$$= \frac{d([\text{HOCl}])}{d(\log [\text{HOCl}])} \frac{d}{d([\text{HOCl}])}(\log (C_1[\text{HOCl}] + C_2))$$

$$= [\text{HOCl}]\left(\frac{C_1}{C_1[\text{HOCl}] + C_2}\right) \quad \text{(A-22)}$$

Substituting equation A-22 into equation A-21:

$$n_{\text{calc}} = 1 + \frac{d}{d(\log [\text{HOCl}])}(\log (C_1[\text{HOCl}] + C_2))$$

$$= 1 + [\text{HOCl}]\left(\frac{C_1}{C_1[\text{HOCl}] + C_2}\right) \quad \text{(A-23)}$$

Rearranging equation A-23 yields the following expression for n_{calc}:

$$n_{\text{calc}} = \frac{2\,C_1[\text{HOCl}] + C_2}{C_1[\text{HOCl}] + C_2} \quad \text{(A-24)}$$

Multiplying the numerator and denominator in equation A-24 by [HOCl] leads to equation A-25:

$$n_{\text{calc}} = \frac{2\,C_1[\text{HOCl}]^2 + C_2[\text{HOCl}]}{C_1[\text{HOCl}]^2 + C_2[\text{HOCl}]} \quad \text{(A-25)}$$

Replacing C_1 and C_2 in equation A-25 with their actual values:

$$n_{\text{calc}} = \frac{2\left(k_{Cl_2O,\,ArOH}\,K_{Cl_2O}\,f_{ArOH} + k_{Cl_2,\,ArOH}\,K_{Cl_2}[H^+]\,f_{ArOH} + k_{Cl_2,\,ArO^-}\,K_{Cl_2}[H^+]\,f_{ArO^-}\right)[HOCl]^2 + k_{HOCl,\,ArO^-}\,f_{ArO^-}\,[HOCl]}{\left(k_{Cl_2O,\,ArOH}\,K_{Cl_2O}\,f_{ArOH} + k_{Cl_2,\,ArOH}\,K_{Cl_2}[H^+]\,f_{ArOH} + k_{Cl_2,\,ArO^-}\,K_{Cl_2}[H^+]\,f_{ArO^-}\right)[HOCl]^2 + k_{HOCl,\,ArO^-}\,f_{ArO^-}\,[HOCl]} \quad \text{(A-26)}$$

Substituting $[Cl_2]$ and $[Cl_2O]$ into equation A-26 (and noting that $[Cl^-] \approx [HOCl]$ at pH $\leq$ 6.5):

$$n_{\text{calc}} = \frac{2\,k_{Cl_2O,\,ArOH}\,[Cl_2O]\,f_{ArOH} + 2\,k_{HOCl,\,ArO^-}[HOCl]\,f_{ArO^-} + 2\,k_{Cl_2,\,ArOH}\,[Cl_2]\,f_{ArOH} + k_{Cl_2,\,ArO^-}[Cl_2]\,f_{ArO^-}}{k_{Cl_2O,\,ArOH}\,[Cl_2O]\,f_{ArOH} + k_{HOCl,\,ArO^-}[HOCl]\,f_{ArO^-} + k_{Cl_2,\,ArOH}\,[Cl_2]\,f_{ArOH} + k_{Cl_2,\,ArO^-}[Cl_2]\,f_{ArO^-}} \quad \text{(A-27)}$$

As can be seen from equations A-26 and A-27, k_{obs} will show a second-order dependence on [HOCl] when either Cl_2 or Cl_2O is the dominant chlorinating agent. This is due to the FAC solutions used in our experiments being close to equimolar in [HOCl] and [Cl^-]. The close agreement between the experimental *n* values and the calculated *n* values (n_{calc}) for phenol and 4-CP (**Tables 2-2 and 2-3**, respectively) supports our assertion that Cl_2 is the predominant chlorinating agent for these compounds at low pH.

A. 7. Kinetics of Cl_2 Regeneration

Cl_2 and HOCl can be assumed to be in equilibrium in solutions of FAC:

$$\mathrm{HOCl} + \mathrm{H^+} + \mathrm{Cl^-} \rightleftharpoons \mathrm{Cl_2} + \mathrm{H_2O} \qquad \text{(A-28)}$$

with k_1 as the rate constant of the forward reaction and k_{-1} as that of the reverse reaction. The equilibrium constant is represented by $K_{\mathrm{Cl_2}}$.

The change in [Cl_2] over time can be written as the following:

$$\frac{d[\mathrm{Cl_2}]}{dt} = k_1\,[\mathrm{HOCl}][\mathrm{H^+}][\mathrm{Cl^-}] - k_{-1}\,[\mathrm{Cl_2}] \qquad \text{(A-29)}$$

Assuming that the pH remains constant, the mass balance can be represented by equation A-30:

$$[\mathrm{HOCl}] + [\mathrm{Cl_2}] = [\mathrm{HOCl}]_{\mathrm{eq}} + [\mathrm{Cl_2}]_{\mathrm{eq}} \qquad \text{(A-30)}$$

Rearranging equation A-30 leads to equation A-31:

$$[\mathrm{HOCl}] = [\mathrm{HOCl}]_{\mathrm{eq}} + [\mathrm{Cl_2}]_{\mathrm{eq}} - [\mathrm{Cl_2}] \tag{A-31}$$

where $[\mathrm{HOCl}]_{\mathrm{eq}}$ and $[\mathrm{Cl_2}]_{\mathrm{eq}}$ represent the equilibrium concentrations of HOCl and Cl_2, respectively.

Substituting equation A-31 into equation A-29:

$$\frac{d[\mathrm{Cl_2}]}{dt} = k_1 \left([\mathrm{HOCl}]_{\mathrm{eq}} + [\mathrm{Cl_2}]_{\mathrm{eq}} - [\mathrm{Cl_2}]\right)[\mathrm{H^+}][\mathrm{Cl^-}] - k_{-1}[\mathrm{Cl_2}] \tag{A-32}$$

Expanding equation A-32 leads to the following:

$$\begin{aligned}\frac{d[\mathrm{Cl_2}]}{dt} = {} & k_1[\mathrm{H^+}][\mathrm{Cl^-}][\mathrm{HOCl}]_{\mathrm{eq}} + k_1[\mathrm{H^+}][\mathrm{Cl^-}][\mathrm{Cl_2}]_{\mathrm{eq}} \\ & - k_1[\mathrm{H^+}][\mathrm{Cl^-}][\mathrm{Cl_2}] - k_{-1}[\mathrm{Cl_2}]\end{aligned} \tag{A-33}$$

The equilibrium constant $K_{\mathrm{Cl_2}}$ can be written as the following:

$$K_{\mathrm{Cl_2}} = \frac{[\mathrm{Cl_2}]_{\mathrm{eq}}}{[\mathrm{HOCl}]_{\mathrm{eq}}\,[\mathrm{H^+}][\mathrm{Cl^-}]} \tag{A-34}$$

Rearranging equation A-34:

$$[\mathrm{HOCl}]_{\mathrm{eq}} = \frac{[\mathrm{Cl_2}]_{\mathrm{eq}}}{\mathrm{K_{Cl_2}}[\mathrm{H^+}][\mathrm{Cl^-}]} \tag{A-35}$$

Substituting equation A-35 into equation A-33:

$$\begin{aligned}\frac{d[\mathrm{Cl_2}]}{dt} = {} & k_1\,[\mathrm{H^+}][\mathrm{Cl^-}]\left(\frac{[\mathrm{Cl_2}]_{\mathrm{eq}}}{K_{\mathrm{Cl_2}}[\mathrm{H^+}][\mathrm{Cl^-}]}\right) + k_1\,[\mathrm{H^+}][\mathrm{Cl^-}][\mathrm{Cl_2}]_{\mathrm{eq}} \\ & - k_1\,[\mathrm{H^+}][\mathrm{Cl^-}][\mathrm{Cl_2}] - k_{-1}\,[\mathrm{Cl_2}]\end{aligned} \tag{A-36}$$

Canceling $[H^+]$ and $[Cl^-]$ in the first term of equation A-36:

$$\frac{d[Cl_2]}{dt} = \left(\frac{k_1}{K_{Cl_2}}\right)[Cl_2]_{eq} + k_1[H^+][Cl^-][Cl_2]_{eq} - k_1[H^+][Cl^-][Cl_2] - k_{-1}[Cl_2] \quad \text{(A-37)}$$

Since $K_{Cl_2} = \frac{k_1}{k_{-1}}$, equation A-37 can be written as the following:

$$\frac{d[Cl_2]}{dt} = k_{-1}[Cl_2]_{eq} + k_1[H^+][Cl^-][Cl_2]_{eq} - k_1[H^+][Cl^-][Cl_2] - k_{-1}[Cl_2] \quad \text{(A-38)}$$

The right side of equation A-38 is the product of two binomials:

$$\frac{d[Cl_2]}{dt} = (k_1[H^+][Cl^-] + k_{-1})\left([Cl_2]_{eq} - [Cl_2]\right) \quad \text{(A-39)}$$

At constant $[H^+]$ and $[Cl^-]$, the reaction becomes a reversible pseudo-first order reaction. Equation A-39 can then be written as the following:

$$\frac{d[Cl_2]}{dt} = k'\left([Cl_2]_{eq} - [Cl_2]\right) \quad \text{(A-40)}$$

where $k' = k_1[H^+][Cl^-] + k_{-1}$

A half-time for Cl_2 formation can then be defined as the following:

$$t_{1/2} = \frac{\ln 2}{k'} \quad \text{(A-41)}$$

Wang and Margerum[5] reported the following values for k_1 and k_{-1}:

$k_1 = 2.14\ (\pm\ 0.08) \times 10^4\ \ M^{-2}\ s^{-1}$

$k_{-1} = 22.3\ (\pm\ 0.6)\ \ s^{-1}$

Assuming $[Cl^-]$ = 0.17 mM (the lowest $[Cl^-]$ encountered in our experiments), $t_{1/2}$ = 0.03 s at pH 2–12. As this characteristic time is much shorter than the duration of our experiments, Cl_2 should not become depleted, even though its concentration is much lower than the initial concentrations of our (chloro)phenols.

A. 8. Summary of Pseudo-First-Order Rate Constants (k_{obs})

The pseudo-first-order rate constants (k_{obs}) determined from linear regressions of $[(chloro)phenol]_T$ versus time data are listed in the following tables:

Tables A1–A3	phenol
Tables A4–A6	2-chlorophenol (2-CP)
Tables A7–A9	4-chlorophenol (4-CP)
Tables A10–A12	2,4-dichlorophenol (2,4-DCP)
Tables A13–A15	2,6-dichlorophenol (2,6-DCP)
Tables A16–A19	2,4,6-trichlorophenol (TCP)

Values of $[(chloro)phenol]_{o,T}$ were obtained from y-intercepts of the linear regressions of $\ln[(chloro)phenol]_T$ versus time data. All uncertainties in k_{obs} values denote 95% confidence intervals.

Table A-1. Experimental Rate Constants from Variable pH Experiments Without Added Chloride for Phenol

pH	$[FAC]_o$ (μM)	$[Cl^-]_{added}$ (mM)	Extrapolated $[phenol]_{T,o}$ (μM)	k_{obs} (s^{-1})	Uncertainty in k_{obs} (s^{-1}) [a]
2.12	128	0	2.22	1.77×10^{-2}	9.77×10^{-4}
2.47	128	0	2.03	6.68×10^{-3}	2.08×10^{-4}
2.87	128	0	2.06	2.41×10^{-3}	4.02×10^{-5}
3.09	128	0	2.11	1.50×10^{-3}	9.67×10^{-5}
3.43	128	0	2.09	6.54×10^{-4}	1.72×10^{-5}
3.73	128	0	1.99	3.35×10^{-4}	7.69×10^{-6}
4.01	128	0	1.99	2.11×10^{-4}	4.03×10^{-6}
4.52	128	0	1.96	1.02×10^{-4}	4.69×10^{-6}
4.72	128	0	1.99	8.60×10^{-5}	2.65×10^{-6}
5.09	128	0	1.97	1.02×10^{-4}	1.69×10^{-6}
5.45	128	0	2.05	1.76×10^{-4}	2.73×10^{-6}
5.62	128	0	1.89	2.97×10^{-4}	5.74×10^{-6}
6.02	128	0	1.97	5.73×10^{-4}	1.76×10^{-5}
6.19	128	0	1.98	8.16×10^{-4}	2.49×10^{-5}
6.46	128	0	2.01	1.39×10^{-3}	4.16×10^{-5}
6.75	128	0	1.95	2.34×10^{-3}	6.41×10^{-5}
7.04	128	0	1.93	3.62×10^{-3}	9.06×10^{-5}
7.45	128	0	2.04	6.25×10^{-3}	2.35×10^{-4}
7.79	128	0	1.91	9.13×10^{-3}	2.83×10^{-4}
8.40	128	0	1.90	9.43×10^{-3}	2.39×10^{-4}
8.70	128	0	1.95	9.30×10^{-3}	2.02×10^{-4}
9.31	128	0	1.96	8.06×10^{-3}	1.26×10^{-4}
9.84	128	0	1.95	4.83×10^{-3}	6.18×10^{-5}
10.27	128	0	2.01	2.75×10^{-3}	9.03×10^{-5}
10.50	128	0	1.98	1.80×10^{-3}	9.22×10^{-5}
10.72	128	0	2.03	1.43×10^{-3}	7.65×10^{-5}
10.98	128	0	1.89	6.90×10^{-4}	4.11×10^{-5}
11.28	128	0	1.90	4.04×10^{-4}	1.89×10^{-5}

[a] Uncertainties in k_{obs} denote 95% confidence intervals.

Table A-2. Experimental Rate Constants from Variable pH Experiments with Added Chloride for Phenol

pH	$[FAC]_o$ (μM)	$[Cl^-]_{added}$ (mM)	Extrapolated $[phenol]_{T,o}$ (μM)	k_{obs} (s^{-1})	Uncertainty in k_{obs} (s^{-1}) [a]
2.99	128	1.01	2.01	9.55×10^{-3}	3.09×10^{-4}
3.28	128	1.01	1.97	4.74×10^{-3}	1.48×10^{-4}
3.57	128	1.01	1.95	2.60×10^{-3}	9.15×10^{-5}
3.79	128	1.01	2.00	1.79×10^{-3}	9.08×10^{-5}
4.05	128	1.01	1.98	1.04×10^{-3}	7.09×10^{-5}
4.71	128	1.01	2.00	3.16×10^{-4}	7.82×10^{-6}
6.45	128	1.01	1.98	1.35×10^{-3}	3.20×10^{-5}
7.01	128	1.01	1.87	3.47×10^{-3}	7.24×10^{-5}
4.47	128	1.01	1.96	4.09×10^{-4}	1.99×10^{-5}
5.01	128	1.01	1.98	2.35×10^{-4}	9.76×10^{-6}
5.66	128	1.01	2.00	3.61×10^{-4}	7.95×10^{-6}
5.95	128	1.01	1.92	5.62×10^{-4}	1.99×10^{-5}
3.52	128	5.02	2.08	1.27×10^{-2}	3.96×10^{-4}
3.75	128	5.02	1.98	7.63×10^{-3}	1.89×10^{-4}
4.01	128	5.02	1.97	3.99×10^{-3}	1.17×10^{-4}
4.24	128	5.02	2.02	2.79×10^{-3}	7.37×10^{-5}
4.50	128	5.02	2.00	1.59×10^{-3}	5.85×10^{-5}
4.73	128	5.02	2.08	1.20×10^{-3}	5.99×10^{-5}
5.02	128	5.02	1.98	7.33×10^{-4}	2.94×10^{-5}
5.46	128	5.02	2.04	6.01×10^{-4}	3.74×10^{-5}
5.54	128	5.02	1.91	5.78×10^{-4}	1.17×10^{-5}
6.07	128	5.02	1.96	9.45×10^{-4}	3.53×10^{-5}
6.45	128	5.02	2.04	1.53×10^{-3}	2.94×10^{-5}
6.69	128	5.02	1.95	2.21×10^{-3}	4.77×10^{-5}
6.99	128	5.02	2.00	3.61×10^{-3}	5.06×10^{-5}
7.54	128	5.02	2.01	7.01×10^{-3}	1.24×10^{-4}
8.08	128	5.02	2.02	9.92×10^{-3}	2.24×10^{-4}
8.63	128	5.02	1.99	9.93×10^{-3}	2.36×10^{-4}

[a] Uncertainties in k_{obs} denote 95% confidence intervals.

Table A-3. Experimental Rate Constants from Variable [FAC] Experiments for Phenol

pH	$[FAC]_o$ (μM)	$[Cl^-]_{added}$ (mM)	Extrapolated $[phenol]_{T,o}$ (μM)	k_{obs} (s^{-1})	Uncertainty in k_{obs} (s^{-1}) [a]
4.72	128	0	1.99	8.60×10^{-5}	2.65×10^{-6}
4.72	256	0	2.02	2.79×10^{-4}	6.91×10^{-6}
4.72	383	0	1.99	5.41×10^{-4}	1.07×10^{-5}
4.72	511	0	1.97	9.07×10^{-4}	1.66×10^{-5}
4.72	639	0	1.96	1.35×10^{-3}	5.80×10^{-5}
6.19	128	0	1.98	8.16×10^{-4}	2.49×10^{-5}
6.19	256	0	1.93	1.71×10^{-3}	2.68×10^{-5}
6.19	383	0	1.93	2.69×10^{-3}	3.81×10^{-5}
6.19	511	0	1.92	4.04×10^{-3}	4.39×10^{-5}
6.19	639	0	1.90	5.54×10^{-3}	9.95×10^{-5}
10.77	128	0	2.09	1.16×10^{-3}	5.80×10^{-5}
10.77	256	0	1.99	2.02×10^{-3}	8.12×10^{-5}
10.77	383	0	2.10	3.21×10^{-3}	1.13×10^{-4}
10.77	511	0	1.93	4.03×10^{-3}	1.26×10^{-4}
10.77	639	0	1.96	4.84×10^{-3}	3.40×10^{-4}
4.67	127	1.00	2.05	3.30×10^{-4}	1.40×10^{-5}
4.67	254	1.00	2.04	7.34×10^{-4}	2.49×10^{-5}
4.67	509	1.00	2.09	1.82×10^{-3}	7.21×10^{-5}
4.67	636	1.00	1.97	2.46×10^{-3}	8.16×10^{-5}
4.67	127	5.02	2.14	1.29×10^{-3}	5.82×10^{-5}
4.67	191	5.02	2.13	1.96×10^{-3}	4.71×10^{-5}
4.67	254	5.02	2.08	2.56×10^{-3}	6.92×10^{-5}
4.67	339	5.02	2.07	3.46×10^{-3}	1.16×10^{-4}
4.67	424	5.02	2.07	4.24×10^{-3}	7.26×10^{-5}

[a] Uncertainties in k_{obs} denote 95% confidence intervals.

Table A-4. Experimental Rate Constants from Variable pH Experiments Without Added Chloride for 2-Chlorophenol (2-CP)

pH	$[FAC]_o$ (μM)	$[Cl^-]_{added}$ (mM)	Extrapolated $[2\text{-}CP]_{T,o}$ (μM)	k_{obs} (s^{-1})	Uncertainty in k_{obs} (s^{-1}) [a]
2.02	128	0	2.04	6.54×10^{-4}	1.79×10^{-5}
2.25	128	0	2.06	4.60×10^{-4}	1.51×10^{-5}
2.48	128	0	1.97	3.51×10^{-4}	8.42×10^{-6}
2.71	128	0	2.05	2.76×10^{-4}	4.14×10^{-6}
3.05	127	0	1.99	2.32×10^{-4}	5.45×10^{-6}
3.58	128	0	1.97	2.21×10^{-4}	9.58×10^{-6}
4.04	128	0	1.91	2.20×10^{-4}	5.13×10^{-6}
4.54	128	0	1.96	2.76×10^{-4}	4.33×10^{-6}
4.99	127	0	2.02	4.14×10^{-4}	1.25×10^{-5}
5.53	129	0	1.96	9.20×10^{-4}	2.17×10^{-5}
6.04	129	0	1.94	2.38×10^{-3}	6.35×10^{-5}
6.48	129	0	1.90	5.18×10^{-3}	2.28×10^{-4}
6.97	127	0	2.28	1.40×10^{-2}	2.19×10^{-4}
7.48	127	0	2.34	2.46×10^{-2}	2.19×10^{-4}
7.97	127	0	1.98	2.41×10^{-2}	2.32×10^{-3}
8.48	127	0	2.04	1.58×10^{-2}	2.19×10^{-4}
9.03	127	0	1.92	6.90×10^{-3}	2.19×10^{-4}
9.41	129	0	1.91	2.84×10^{-3}	1.59×10^{-4}
9.74	129	0	2.01	1.35×10^{-3}	2.71×10^{-5}
10.02	127	0	1.96	7.65×10^{-4}	2.00×10^{-5}
10.35	129	0	1.90	3.27×10^{-4}	1.31×10^{-5}

[a] Uncertainties in k_{obs} denote 95% confidence intervals.

Table A-5. Experimental Rate Constants from Variable pH Experiments with Added Chloride for 2-Chlorophenol (2-CP)

pH	$[FAC]_o$ (μM)	$[Cl^-]_{added}$ (mM)	Extrapolated $[2\text{-}CP]_{T,o}$ (μM)	k_{obs} (s^{-1})	Uncertainty in k_{obs} (s^{-1}) [a]
2.03	128	5.02	2.17	1.24×10^{-2}	4.09×10^{-4}
2.23	129	5.02	2.00	9.05×10^{-3}	1.49×10^{-4}
2.45	129	5.02	2.00	6.41×10^{-3}	9.44×10^{-5}
2.67	129	5.02	2.01	4.88×10^{-3}	1.49×10^{-4}
2.88	129	5.02	2.04	4.05×10^{-3}	1.31×10^{-4}
3.32	128	5.02	1.98	3.25×10^{-3}	4.94×10^{-5}
3.87	129	5.02	2.00	3.11×10^{-3}	8.09×10^{-5}
4.48	129	5.02	1.99	3.22×10^{-3}	9.40×10^{-5}
4.97	129	5.02	2.08	3.11×10^{-3}	1.24×10^{-4}
5.51	129	5.02	1.99	3.44×10^{-3}	1.58×10^{-4}
6.04	129	5.02	2.06	4.94×10^{-3}	1.61×10^{-4}
6.54	129	5.02	2.05	8.42×10^{-3}	2.88×10^{-4}
6.99	127	5.02	2.08	1.51×10^{-2}	2.19×10^{-4}
7.50	129	5.02	2.11	2.33×10^{-2}	6.04×10^{-4}

[a] Uncertainties in k_{obs} denote 95% confidence intervals.

Table A-6. Experimental Rate Constants from Variable [FAC] Experiments for 2-Chlorophenol (2-CP)

pH	$[FAC]_o$ (μM)	$[Cl^-]_{added}$ (mM)	Extrapolated $[2\text{-}CP]_{T,o}$ (μM)	k_{obs} (s^{-1})	Uncertainty in k_{obs} (s^{-1}) [a]
3.51	129	0	2.01	2.00×10^{-4}	8.16×10^{-6}
3.51	258	0	2.01	7.35×10^{-4}	2.17×10^{-5}
3.51	387	0	1.96	1.53×10^{-3}	2.93×10^{-5}
3.51	516	0	1.94	2.72×10^{-3}	1.21×10^{-4}
3.51	645	0	1.94	4.08×10^{-3}	2.03×10^{-4}
6.02	64	0	1.90	1.10×10^{-3}	3.49×10^{-5}
6.02	86	0	1.92	1.43×10^{-3}	8.27×10^{-5}
6.02	129	0	1.94	2.21×10^{-3}	5.59×10^{-5}
6.02	258	0	2.01	5.28×10^{-3}	1.12×10^{-4}
6.02	344	0	2.03	7.93×10^{-3}	2.32×10^{-4}
9.74	129	0	2.01	1.35×10^{-3}	2.71×10^{-5}
9.74	258	0	2.04	2.46×10^{-3}	4.62×10^{-5}
9.74	387	0	2.00	3.50×10^{-3}	2.16×10^{-4}
9.74	516	0	1.97	4.69×10^{-3}	1.44×10^{-4}

[a] Uncertainties in k_{obs} denote 95% confidence intervals.

Table A-7. Experimental Rate Constants from Variable pH Experiments Without Added Chloride for 4-Chlorophenol (4-CP)

pH	$[FAC]_o$ (μM)	$[Cl^-]_{added}$ (mM)	Extrapolated $[4\text{-CP}]_{T,o}$ (μM)	k_{obs} (s^{-1})	Uncertainty in k_{obs} (s^{-1}) [a]
2.03	164	0	2.10	8.67×10^{-4}	2.58×10^{-5}
2.25	163	0	2.04	5.11×10^{-4}	1.72×10^{-5}
2.47	164	0	2.07	3.15×10^{-4}	7.89×10^{-6}
2.66	163	0	2.05	2.08×10^{-4}	5.78×10^{-6}
2.88	164	0	2.06	1.38×10^{-4}	3.66×10^{-6}
3.16	163	0	2.04	9.91×10^{-5}	3.54×10^{-6}
3.51	164	0	2.04	7.36×10^{-5}	2.51×10^{-6}
3.98	164	0	2.08	6.35×10^{-5}	1.81×10^{-6}
4.11	161	0	1.96	6.28×10^{-5}	1.73×10^{-6}
4.43	164	0	2.01	6.66×10^{-5}	1.99×10^{-6}
4.94	164	0	2.02	8.40×10^{-5}	3.30×10^{-6}
5.02	161	0	1.94	8.77×10^{-5}	3.10×10^{-6}
5.27	163	0	2.03	1.22×10^{-4}	3.73×10^{-6}
5.47	164	0	2.02	1.65×10^{-4}	4.20×10^{-6}
5.66	163	0	1.95	2.37×10^{-4}	9.18×10^{-6}
6.05	163	0	1.95	4.64×10^{-4}	2.90×10^{-5}
6.43	163	0	2.00	9.54×10^{-4}	4.91×10^{-5}
6.71	164	0	1.93	1.49×10^{-3}	4.76×10^{-5}
6.99	163	0	1.85	2.30×10^{-3}	9.76×10^{-5}
7.43	163	0	1.97	4.24×10^{-3}	1.77×10^{-4}
7.80	163	0	1.99	5.42×10^{-3}	1.54×10^{-4}
8.49	163	0	1.93	5.63×10^{-3}	1.17×10^{-4}
8.98	163	0	1.89	4.29×10^{-3}	2.01×10^{-4}
9.51	163	0	2.02	2.74×10^{-3}	8.45×10^{-5}
9.70	164	0	2.04	1.82×10^{-3}	3.88×10^{-5}
9.99	163	0	2.05	1.03×10^{-3}	2.84×10^{-5}
10.49	163	0	2.00	3.91×10^{-4}	1.69×10^{-5}
10.94	164	0	2.04	1.47×10^{-4}	7.82×10^{-6}

[a] Uncertainties in k_{obs} denote 95% confidence intervals.

Table A-8. Experimental Rate Constants from Variable pH Experiments with Added Chloride for 4-Chlorophenol (4-CP)

pH	$[FAC]_o$ (μM)	$[Cl^-]_{added}$ (mM)	Extrapolated $[4\text{-}CP]_{T,o}$ (μM)	k_{obs} (s^{-1})	Uncertainty in k_{obs} (s^{-1}) [a]
1.99	161	5.01	2.14	1.73×10^{-2}	1.22×10^{-3}
2.21	163	5.02	2.10	1.04×10^{-2}	3.82×10^{-4}
2.41	161	5.01	1.95	6.07×10^{-3}	9.22×10^{-5}
2.62	163	5.02	2.22	4.26×10^{-3}	1.68×10^{-4}
3.01	161	5.01	2.07	2.37×10^{-3}	5.28×10^{-5}
3.23	163	5.02	2.06	1.54×10^{-3}	4.69×10^{-5}
3.43	161	5.01	2.02	1.22×10^{-3}	2.55×10^{-5}
4.05	161	5.01	2.02	9.43×10^{-4}	2.46×10^{-5}
4.44	161	5.01	2.00	8.46×10^{-4}	2.12×10^{-5}
4.92	161	5.01	2.02	8.58×10^{-4}	1.95×10^{-5}
5.47	161	5.01	2.05	9.15×10^{-4}	2.42×10^{-5}
6.09	161	5.01	2.03	1.14×10^{-3}	4.99×10^{-5}
6.48	161	5.01	1.99	1.54×10^{-3}	1.60×10^{-5}
6.68	163	5.02	1.91	2.07×10^{-3}	7.69×10^{-5}
7.01	163	5.02	2.05	3.45×10^{-3}	1.21×10^{-4}
7.49	163	5.02	2.01	5.53×10^{-3}	2.72×10^{-4}
7.83	163	5.02	1.88	6.15×10^{-3}	1.76×10^{-4}
8.43	163	5.02	1.92	6.19×10^{-3}	1.92×10^{-4}
8.98	163	5.02	2.03	4.92×10^{-3}	3.44×10^{-4}
9.52	163	5.02	2.01	2.39×10^{-3}	6.13×10^{-5}
2.02	171	1.01	1.95	4.64×10^{-3}	1.24×10^{-4}
2.51	171	1.01	2.07	1.70×10^{-3}	4.97×10^{-5}
2.97	171	1.01	1.96	6.18×10^{-4}	1.92×10^{-5}
3.55	171	1.01	2.02	3.69×10^{-4}	9.99×10^{-6}
4.08	171	1.01	1.92	2.95×10^{-4}	1.01×10^{-5}
4.51	171	1.01	2.07	2.78×10^{-4}	7.43×10^{-6}
4.99	171	1.01	1.94	2.95×10^{-4}	1.23×10^{-5}
5.49	171	1.01	1.96	3.90×10^{-4}	1.40×10^{-5}
6.00	171	1.01	1.89	6.58×10^{-4}	3.67×10^{-5}
6.52	171	1.01	1.91	1.32×10^{-3}	3.65×10^{-5}

[a] Uncertainties in k_{obs} denote 95% confidence intervals.

Table A-9. Experimental Rate Constants from Variable [FAC] Experiments for 4-Chlorophenol (4-CP)

pH	$[FAC]_o$ (μM)	$[Cl^-]_{added}$ (mM)	Extrapolated $[4\text{-CP}]_{T,o}$ (μM)	k_{obs} (s^{-1})	Uncertainty in k_{obs} (s^{-1}) [a]
4.11	161	0	1.96	6.28×10^{-5}	1.73×10^{-6}
4.11	322	0	1.91	2.32×10^{-4}	6.30×10^{-6}
4.11	483	0	1.99	5.17×10^{-4}	1.09×10^{-5}
4.11	604	0	1.96	8.13×10^{-4}	1.43×10^{-5}
4.11	805	0	2.01	1.40×10^{-3}	7.65×10^{-5}
5.02	161	0	1.94	8.77×10^{-5}	3.10×10^{-6}
5.02	322	0	1.96	2.91×10^{-4}	6.37×10^{-6}
5.02	483	0	1.97	5.93×10^{-4}	2.40×10^{-5}
5.02	644	0	2.01	1.07×10^{-3}	2.49×10^{-5}
5.02	805	0	1.94	1.58×10^{-3}	5.10×10^{-5}
6.03	122	0	1.99	3.26×10^{-4}	1.10×10^{-5}
6.03	163	0	1.96	4.40×10^{-4}	1.32×10^{-5}
6.03	326	0	2.01	1.12×10^{-3}	2.82×10^{-5}
6.03	489	0	1.95	2.00×10^{-3}	5.94×10^{-5}
6.03	611	0	1.91	2.76×10^{-3}	1.40×10^{-4}
6.79	80	0	1.95	8.69×10^{-4}	5.76×10^{-5}
6.79	119	0	1.93	1.31×10^{-3}	2.91×10^{-5}
6.79	159	0	1.96	1.77×10^{-3}	6.76×10^{-5}
6.79	239	0	1.98	2.78×10^{-3}	1.17×10^{-4}
6.79	319	0	1.98	3.88×10^{-3}	1.89×10^{-4}

[a] Uncertainties in k_{obs} denote 95% confidence intervals.

Table A-10. Experimental Rate Constants from Variable pH Experiments Without Added Chloride for 2,4-Dichlorophenol (2,4-DCP)

pH	$[FAC]_o$ (μM)	$[Cl^-]_{added}$ (mM)	Extrapolated $[2,4\text{-DCP}]_{T,o}$ (μM)	k_{obs} (s^{-1})	Uncertainty in k_{obs} (s^{-1}) [a]
1.98	123	0	1.93	2.56×10^{-4}	5.71×10^{-6}
2.41	123	0	2.00	2.53×10^{-4}	6.89×10^{-6}
3.04	119	0	1.87	2.57×10^{-4}	5.08×10^{-6}
3.43	123	0	2.00	2.51×10^{-4}	7.05×10^{-6}
3.96	123	0	2.26	2.49×10^{-4}	6.52×10^{-6}
4.50	123	0	2.20	2.81×10^{-4}	8.87×10^{-6}
4.94	123	0	2.30	3.69×10^{-4}	1.87×10^{-5}
5.47	123	0	2.32	5.68×10^{-4}	2.52×10^{-5}
5.97	121	0	1.85	1.08×10^{-3}	3.15×10^{-5}
6.10	123	0	2.20	1.39×10^{-3}	2.10×10^{-5}
6.41	119	0	1.90	2.67×10^{-3}	1.10×10^{-4}
6.65	122	0	2.26	3.40×10^{-3}	1.21×10^{-4}
7.13	123	0	2.21	5.80×10^{-3}	1.67×10^{-4}
7.64	123	0	2.16	6.25×10^{-3}	2.69×10^{-4}
7.99	122	0	2.10	4.64×10^{-3}	1.97×10^{-4}
8.28	123	0	1.83	2.82×10^{-3}	8.65×10^{-5}
8.67	122	0	2.25	1.41×10^{-3}	7.79×10^{-5}
9.07	119	0	1.94	6.48×10^{-4}	1.74×10^{-5}
9.16	123	0	2.21	5.05×10^{-4}	8.32×10^{-6}
9.32	119	0	1.90	3.83×10^{-4}	1.06×10^{-5}
9.67	123	0	1.93	1.71×10^{-4}	3.03×10^{-6}
9.86	123	0	2.25	1.25×10^{-4}	3.77×10^{-6}

[a] Uncertainties in k_{obs} denote 95% confidence intervals.

Table A-11. Experimental Rate Constants from Variable pH Experiments with Added Chloride for 2,4-Dichlorophenol (2,4-DCP)

pH	$[FAC]_o$ (μM)	$[Cl^-]_{added}$ (mM)	Extrapolated $[2,4\text{-DCP}]_{T,o}$ (μM)	k_{obs} (s^{-1})	Uncertainty in k_{obs} (s^{-1}) [a]
1.99	121	5.01	1.90	2.86×10^{-3}	8.29×10^{-5}
2.52	119	5.01	1.99	3.36×10^{-3}	5.69×10^{-5}
2.89	121	5.01	1.93	3.37×10^{-3}	9.75×10^{-5}
3.46	119	5.01	2.03	3.48×10^{-3}	3.78×10^{-5}
3.94	121	5.01	1.87	3.25×10^{-3}	1.52×10^{-4}
4.46	119	5.01	2.01	3.51×10^{-3}	1.07×10^{-4}
4.92	121	5.01	1.98	3.57×10^{-3}	1.06×10^{-4}
5.47	119	5.01	1.96	3.61×10^{-3}	1.69×10^{-4}
6.08	121	5.01	1.98	4.31×10^{-3}	4.19×10^{-5}
6.52	119	5.01	1.95	5.08×10^{-3}	3.75×10^{-4}
7.01	119	5.01	1.92	6.64×10^{-3}	2.15×10^{-4}
7.49	119	5.01	1.85	7.44×10^{-3}	2.91×10^{-4}
8.03	119	5.01	1.81	4.46×10^{-3}	1.41×10^{-4}
8.50	119	5.01	1.82	2.29×10^{-3}	5.69×10^{-5}
8.98	119	5.01	1.83	8.14×10^{-4}	2.42×10^{-5}

[a] Uncertainties in k_{obs} denote 95% confidence intervals.

Table A-12. Experimental Rate Constants from Variable [FAC] Experiments for 2,4-Dichlorophenol (2,4-DCP)

pH	$[FAC]_o$ (µM)	$[Cl^-]_{added}$ (mM)	Extrapolated $[2,4\text{-DCP}]_{T,o}$ (µM)	k_{obs} (s^{-1})	Uncertainty in k_{obs} (s^{-1}) [a]
3.04	119	0	1.87	2.57×10^{-4}	5.08×10^{-6}
3.04	239	0	1.89	9.64×10^{-4}	1.41×10^{-5}
3.04	358	0	1.75	1.91×10^{-3}	7.01×10^{-5}
3.04	478	0	1.72	3.20×10^{-3}	9.69×10^{-5}
3.04	597	0	1.97	5.01×10^{-3}	7.57×10^{-5}
5.98	80	0	1.82	6.86×10^{-4}	2.44×10^{-5}
5.98	120	0	1.90	1.25×10^{-3}	4.92×10^{-5}
5.98	159	0	1.97	1.81×10^{-3}	3.52×10^{-5}
5.98	239	0	1.93	3.21×10^{-3}	1.06×10^{-4}
5.98	299	0	2.03	4.14×10^{-3}	1.24×10^{-4}
9.11	163	0	1.97	7.91×10^{-4}	3.31×10^{-5}
9.11	245	0	1.79	1.13×10^{-3}	2.43×10^{-5}
9.11	367	0	1.83	1.71×10^{-3}	4.30×10^{-5}
9.11	489	0	1.87	2.30×10^{-3}	4.98×10^{-5}

[a] Uncertainties in k_{obs} denote 95% confidence intervals.

Table A-13. Experimental Rate Constants from Variable pH Experiments Without Added Chloride for 2,6-Dichlorophenol (2,6-DCP)

pH	$[FAC]_o$ (μM)	$[Cl^-]_{added}$ (mM)	Extrapolated $[2,6\text{-DCP}]_{T,o}$ (μM)	k_{obs} (s^{-1})	Uncertainty in k_{obs} (s^{-1}) [a]
2.01	129	0	2.08	8.97×10^{-4}	1.92×10^{-5}
2.52	127	0	2.14	8.09×10^{-4}	1.20×10^{-5}
2.99	127	0	2.16	8.42×10^{-4}	5.37×10^{-5}
3.49	129	0	1.98	8.72×10^{-4}	3.20×10^{-5}
4.04	127	0	2.06	8.89×10^{-4}	2.96×10^{-5}
4.51	126	0	2.05	1.05×10^{-3}	2.29×10^{-5}
4.95	126	0	2.11	1.47×10^{-3}	2.41×10^{-5}
5.32	128	0	2.16	2.00×10^{-3}	5.90×10^{-5}
5.50	126	0	2.14	2.63×10^{-3}	8.08×10^{-5}
5.70	128	0	2.09	3.42×10^{-3}	1.17×10^{-4}
6.00	122	0	2.11	4.77×10^{-3}	2.01×10^{-4}
6.23	128	0	2.02	6.08×10^{-3}	1.69×10^{-4}
6.48	122	0	2.31	7.98×10^{-3}	1.49×10^{-4}
7.01	122	0	2.09	9.76×10^{-3}	3.97×10^{-4}
7.26	128	0	1.88	8.65×10^{-3}	5.20×10^{-4}
7.51	122	0	1.96	5.98×10^{-3}	1.28×10^{-4}
7.70	128	0	1.82	4.51×10^{-3}	3.39×10^{-4}
7.80	128	0	1.96	3.74×10^{-3}	2.11×10^{-4}
8.02	122	0	1.88	2.75×10^{-3}	9.95×10^{-5}
8.13	128	0	1.91	1.94×10^{-3}	1.29×10^{-4}
8.32	129	0	1.80	1.65×10^{-3}	4.05×10^{-5}
8.45	126	0	1.95	9.78×10^{-4}	4.48×10^{-5}
8.68	129	0	1.99	6.40×10^{-4}	3.54×10^{-5}
9.00	126	0	2.03	3.25×10^{-4}	1.16×10^{-5}

[a] Uncertainties in k_{obs} denote 95% confidence intervals.

Table A-14. Experimental Rate Constants from Variable pH Experiments with Added Chloride for 2,6-Dichlorophenol (2,6-DCP)

pH	$[FAC]_o$ (μM)	$[Cl^-]_{added}$ (mM)	Extrapolated $[2,6\text{-DCP}]_{T,o}$ (μM)	k_{obs} (s^{-1})	Uncertainty in k_{obs} (s^{-1}) [a]
1.98	128	3.01	2.14	9.30×10^{-3}	3.36×10^{-4}
2.48	128	3.01	2.08	1.01×10^{-2}	3.00×10^{-4}
2.92	128	3.01	2.12	1.02×10^{-2}	4.10×10^{-4}
3.59	128	3.01	2.11	1.01×10^{-2}	3.53×10^{-4}
4.03	128	3.01	2.05	9.98×10^{-2}	3.40×10^{-4}
4.51	128	3.01	2.14	1.03×10^{-2}	3.45×10^{-4}
4.93	128	3.01	2.16	1.03×10^{-2}	3.89×10^{-4}
5.54	128	3.01	2.23	1.03×10^{-2}	4.90×10^{-4}
6.01	128	3.01	2.24	1.20×10^{-2}	6.26×10^{-4}
6.50	128	3.01	2.14	1.17×10^{-2}	2.22×10^{-4}
6.99	128	3.01	2.08	1.15×10^{-2}	3.40×10^{-4}
7.52	128	3.01	1.97	5.63×10^{-3}	3.38×10^{-4}
8.23	128	3.01	1.90	1.44×10^{-3}	9.27×10^{-5}

[a] Uncertainties in k_{obs} denote 95% confidence intervals.

Table A-15. Experimental Rate Constants from Variable [FAC] Experiments for 2,6-Dichlorophenol (2,6-DCP)

pH	$[FAC]_o$ (μM)	$[Cl^-]_{added}$ (mM)	Extrapolated $[2,6\text{-DCP}]_{T,o}$ (μM)	k_{obs} (s^{-1})	Uncertainty in k_{obs} (s^{-1}) [a]
3.00	128	0	1.90	7.95×10^{-4}	1.90×10^{-5}
3.00	192	0	2.11	1.97×10^{-3}	8.39×10^{-5}
3.00	256	0	2.02	3.27×10^{-3}	2.12×10^{-4}
3.00	320	0	1.93	5.16×10^{-3}	2.27×10^{-4}
3.00	384	0	2.15	7.58×10^{-3}	1.23×10^{-3}
6.01	43	0	1.95	1.43×10^{-3}	4.61×10^{-5}
6.01	86	0	1.98	3.09×10^{-3}	8.04×10^{-5}
6.01	107	0	2.06	4.20×10^{-3}	7.72×10^{-5}
6.01	129	0	2.01	5.20×10^{-3}	1.81×10^{-4}
6.01	172	0	2.18	7.95×10^{-3}	3.97×10^{-4}
8.99	129	0	1.97	3.30×10^{-4}	2.24×10^{-5}
8.99	258	0	1.97	6.50×10^{-4}	3.06×10^{-5}
8.99	387	0	2.00	9.80×10^{-4}	3.08×10^{-5}
8.99	516	0	2.01	1.28×10^{-3}	5.23×10^{-5}

[a] Uncertainties in k_{obs} denote 95% confidence intervals.

Table A-16. Experimental Rate Constants from Variable pH Experiments Without Added Chloride for 2,4,6-Trichlorophenol (TCP)

pH	$[FAC]_o$ (μM)	$[Cl^-]_{added}$ (mM)	Extrapolated $[TCP]_{T,o}$ (μM)	k_{obs} (s^{-1})	Uncertainty in k_{obs} (s^{-1}) [a]
1.98	187	0	2.08	7.81×10^{-4}	2.60×10^{-5}
2.78	183	0	2.17	9.12×10^{-4}	5.06×10^{-5}
2.86	186	0	2.09	8.12×10^{-4}	1.65×10^{-5}
3.04	183	0	2.15	9.29×10^{-4}	3.76×10^{-5}
3.56	185	0	1.98	8.92×10^{-4}	1.83×10^{-5}
4.00 [b]	187	0	N/A	8.94×10^{-4}	8.21×10^{-5}
4.50 [b]	183	0	N/A	9.39×10^{-4}	7.85×10^{-5}
5.07 [b]	187	0	N/A	1.00×10^{-3}	1.12×10^{-4}
5.53 [b]	187	0	N/A	1.11×10^{-3}	1.39×10^{-4}
6.05	183	0	1.98	1.19×10^{-3}	2.24×10^{-5}
6.12	186	0	2.08	1.19×10^{-3}	3.38×10^{-5}
6.18	182	0	2.01	1.15×10^{-3}	2.38×10^{-5}
6.40	183	0	1.99	1.16×10^{-3}	2.74×10^{-5}
6.82	183	0	1.99	1.01×10^{-3}	5.88×10^{-5}
6.82	182	0	1.95	9.45×10^{-4}	4.64×10^{-5}
7.24	182	0	1.93	5.29×10^{-4}	3.23×10^{-5}
7.54	182	0	1.85	2.86×10^{-4}	2.00×10^{-5}
7.94	182	0	1.77	1.40×10^{-4}	1.31×10^{-5}
8.26	185	0	2.03	5.93×10^{-5}	3.88×10^{-6}
8.53	185	0	2.00	3.88×10^{-5}	4.73×10^{-6}
9.01	185	0	2.13	1.84×10^{-5}	5.31×10^{-6}
9.51	185	0	2.11	8.00×10^{-6}	4.17×10^{-6}

[a] Uncertainties in k_{obs} denote 95% confidence intervals.

[b] Value of k_{obs} at $[acetate]_{tot} = 0$ extrapolated from k_{obs} versus $[acetate]_{tot}$ data at each pH. Uncertainty denotes 95% confidence intervals of the slope of linear regression.

Table A-17. Experimental Rate Constants from Variable pH Experiments with Added Chloride for 2,4,6-Trichlorophenol (TCP)

pH	$[FAC]_o$ (μM)	$[Cl^-]_{added}$ (mM)	Extrapolated $[TCP]_{T,o}$ (μM)	k_{obs} (s^{-1})	Uncertainty in k_{obs} (s^{-1}) [a]
1.97	187	5.01	1.94	7.84×10^{-3}	2.45×10^{-4}
2.46	185	5.01	1.97	8.51×10^{-3}	4.94×10^{-4}
2.96	186	5.01	1.83	8.41×10^{-3}	5.32×10^{-4}
3.57	185	5.01	1.88	8.87×10^{-3}	2.56×10^{-4}
3.99	186	5.01	1.86	8.97×10^{-3}	4.01×10^{-4}
4.44	185	5.01	1.94	8.92×10^{-3}	2.40×10^{-4}
5.04	186	5.01	2.04	8.76×10^{-3}	2.87×10^{-4}
5.58	186	5.01	2.19	7.00×10^{-3}	2.41×10^{-4}
6.15	187	5.01	2.11	4.92×10^{-3}	1.50×10^{-4}
6.49	185	5.01	2.06	3.10×10^{-3}	1.74×10^{-4}
6.82	182	5.01	1.97	1.84×10^{-3}	6.06×10^{-5}
7.25	187	5.01	1.90	9.02×10^{-4}	4.70×10^{-5}
7.49	186	5.01	1.85	4.75×10^{-4}	2.80×10^{-5}
7.87	185	5.01	1.92	1.80×10^{-4}	1.16×10^{-5}

[a] Uncertainties in k_{obs} denote 95% confidence intervals.

Table A-18. Experimental Rate Constants from Variable [FAC] Experiments for 2,4,6-Trichlorophenol (TCP)

pH	$[FAC]_o$ (μM)	$[Cl^-]_{added}$ (mM)	Extrapolated $[TCP]_{T,o}$ (μM)	k_{obs} (s^{-1})	Uncertainty in k_{obs} (s^{-1}) [a]
2.86	186	0	2.09	8.12×10^{-4}	1.65×10^{-5}
2.86	371	0	2.03	2.80×10^{-3}	4.14×10^{-5}
2.86	495	0	1.88	4.46×10^{-3}	2.17×10^{-4}
2.86	619	0	1.87	6.69×10^{-3}	4.56×10^{-4}
2.86	825	0	1.96	1.39×10^{-2}	6.47×10^{-4}
6.12	186	0	2.08	1.19×10^{-3}	3.38×10^{-5}
6.12	371	0	2.08	3.65×10^{-3}	4.14×10^{-5}
6.12	495	0	2.13	6.07×10^{-3}	1.82×10^{-4}
6.12	619	0	2.18	9.32×10^{-3}	4.00×10^{-4}
6.12	825	0	2.04	1.50×10^{-2}	5.17×10^{-4}
8.53	185	0	2.00	3.88×10^{-5}	4.73×10^{-6}
8.53	308	0	2.07	5.58×10^{-5}	7.74×10^{-6}
8.53	493	0	2.06	7.99×10^{-5}	8.12×10^{-6}
8.53	616	0	2.05	1.07×10^{-4}	7.07×10^{-6}
8.53	821	0	2.12	1.46×10^{-4}	4.57×10^{-6}

[a] Uncertainties in k_{obs} denote 95% confidence intervals.

Table A-19. Experimental Rate Constants from Variable $[Acetate]_{tot}$ Experiments Without Added Chloride for 2,4,6-Trichlorophenol (TCP) [a]

pH	$[carbonate]_{tot}$ (mM)	$[FAC]_o$ (μM)	Extrapolated $[TCP]_{T,o}$ (μM)	k_{obs} (s^{-1})	Uncertainty in k_{obs} (s^{-1}) [b]
3.97	2.6	187	2.02	9.09×10^{-4}	4.29×10^{-5}
4.01	5.2	187	2.05	1.00×10^{-3}	3.06×10^{-5}
4.01	7.8	187	2.19	1.03×10^{-3}	4.89×10^{-5}
4.00	10.4	187	2.07	1.07×10^{-3}	3.09×10^{-5}
4.00	13.0	187	2.05	1.08×10^{-3}	4.13×10^{-5}
4.51	2.6	183	2.09	1.01×10^{-3}	1.33×10^{-5}
4.50	5.2	183	2.21	1.15×10^{-3}	6.20×10^{-5}
4.50	7.8	183	2.11	1.21×10^{-3}	6.58×10^{-5}
4.50	10.4	183	2.17	1.30×10^{-3}	5.27×10^{-5}
4.51	13.0	183	2.18	1.39×10^{-3}	6.24×10^{-5}
5.07	2.6	187	2.15	1.13×10^{-3}	4.82×10^{-5}
5.08	5.2	187	2.09	1.24×10^{-3}	5.82×10^{-5}
5.06	7.8	187	2.17	1.43×10^{-3}	7.18×10^{-5}
5.07	10.4	187	2.19	1.56×10^{-3}	7.87×10^{-5}
5.08	13.0	187	2.12	1.64×10^{-3}	7.70×10^{-5}
5.53	7.8	187	2.16	1.42×10^{-3}	4.81×10^{-5}
5.53	10.4	187	2.15	1.51×10^{-3}	3.29×10^{-5}
5.53	13.0	187	2.18	1.65×10^{-3}	6.03×10^{-5}
5.53	15.7	187	2.18	1.70×10^{-3}	3.49×10^{-5}
5.54	18.3	187	2.20	1.84×10^{-3}	3.85×10^{-5}

[a] At each pH, k_{obs} was extrapolated to $[acetate]_{tot} = 0$. The extrapolated k_{obs} values are the ones shown in **Figure 2-2f** (Chapter 2) and **Table A-16**.

[b] Uncertainties in k_{obs} denote 95% confidence intervals.

A. 9. References

1. Sivey, J. D.; McCullough, C. E.; Roberts, A. L. Chlorine monoxide (Cl_2O) and molecular chlorine (Cl_2) as active chlorinating agents in reaction of dimethenamid with aqueous free chlorine. *Environ. Sci. Technol.* **2010,** *44*, 3357-3362.

2. Sivey, J. D.; Roberts, A. L. Assessing the reactivity of free chlorine constituents Cl_2, Cl_2O, and HOCl toward aromatic ethers. *Environ. Sci. Technol.* **2012,** *46*, 2141-2147.

3. Cherney, D. P.; Duirk, S. E.; Tarr, J. C.; Collette, T. W. Monitoring the speciation of aqueous free chlorine from pH 1 to 12 with Raman spectroscopy to determine the identity of the potent low-pH oxidant. *Appl. Spectrosc.* **2006,** *60*, 764-772.

4. American Public Health Association (APHA). *Standard Methods for the Examination of Water and Wastewater*, 18th ed.; American Public Health Association, American Water Works Association, Water Environment Federation: Washington, DC, 1992.

5. Wang, T. X.; Margerum, D. W. Kinetics of reversible chlorine hydrolysis: Temperature dependence and general-acid/base-assisted mechanisms. *Inorg. Chem.* **1994,** *33*, 1050-1055.

Appendix B: Supporting Information for Chapter 3

B. 1. List of Reagents

Chemical	Purity / Grade	Vendor
1,2-dibromopropane	98%	TCI America
1,3,5-trimethoxybenzene (TMB)	≥ 99.0 %	Aldrich or Fisher Scientific
2-bromo-1,3,5-trimethoxybenzene (Br-TMB)	98%	Oakwood Chemical
2-chloro-1,3,5-trimethoxybenzene (Cl-TMB)	98%	Sigma-Aldrich
2,4-dichlorophenol (2,4-DCP)	99%	Acros Organics
2,4,6-trichlorophenol (TCP)	98%	Aldrich
2-bromoanisole	97%	Sigma-Aldrich
2-chlorobenzonitrile	≥ 98%	Aldrich or Acros Organic
4-bromoanisole	99%	Sigma-Aldrich
acetonitrile	Optima	Fisher Scientific
ammonium chloride	99.5%	Sigma-Aldrich
anisole	99.7%	Sigma-Aldrich
bromoacetonitrile	97%	Sigma-Aldrich
chloral hydrate	99%	Supelco
chloroacetonitrile	99%	Sigma-Aldrich
chloropicrin	97%	Supelco
dibromoacetonitrile	93%	Supelco
dichloroacetonitrile	98%	Supelco
L-ascorbic acid	reagent grade	Sigma
methanol	99.9%	Fisher Scientific
methyl tert-butyl ether (MTBE)	CHROMASOLV Plus	Sigma-Aldrich
nitric acid	70%	Fisher Scientific
potassium phosphate monobasic	ACS reagent	J. T. Baker
sodium bicarbonate	≥ 99.7%	Acros Organics
sodium bromide	99.5%	Acros Organics
sodium chloride	99.999%	Acros Organics
sodium hydroxide	certified ACS pellets	Fisher Scientific
sodium hypochlorite solution	5.65-6%	Fisher Scientific
sodium nitrate	≥ 99.0 %	Sigma-Aldrich
sodium phosphate dibasic	ACS reagent	J. T. Baker
sodium sulfite	99.99%	Aldrich
sodium tetraborate decahydrate	99.5%	Acros
sodium thiosulfate pentahydrate	99.5–101.0%	Alfa Aesar
toluene	99.9%	Fisher Scientific

B. 2. Synthesis of 2,4-Dichloro-1,3,5-trimethoxybenzene

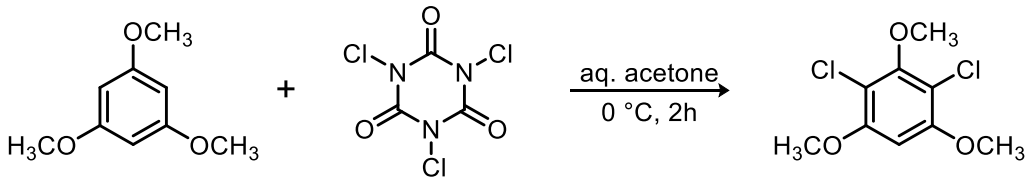

The synthesis was carried out according to the procedure reported in ref. 1. To a 50-mL round bottom flask equipped with a magnetic stirring bar was added a solution of 1,3,5-trimethyoxybenzene (500 mg, 2.97 mmol, 1.00 eq.) in 3.5 mL of acetone and 6 mL of water. This solution was cooled to 0 °C in an ice bath, and a solution of trichloroisocyanuric acid (482 mg, 2.08 mmol, 0.70 eq.) in 4 mL of acetone was added dropwise over five minutes. The reaction was stirred at 0 °C for two hours before the addition of 9 mL of 3% aqueous sodium hydroxide solution. After stirring for ten minutes, the liquid phase had turned bright yellow. The precipitated solids were collected by vacuum filtration and washed with three 25 mL portions of water to give the crude product as a white solid. This compound was purified by recrystallization from absolute ethanol to give 2,4-dichloro-1,3,5-trimethoxybenzene as white crystals (489 mg, 70% yield). Purity as determined by GC-MS was > 98%.

^{1}H–NMR (400 MHz, $CDCl_3$): δ 3.89 (3H, s), 3.91 (6H, s), 6.38 (1H, s)

B. 3. Analytical Methods

TMB as a quencher for free chlorine. Toluene samples (1.0 μL) containing 2,4-dichlorophenol, TMB, as well as their chlorination products (with 2-chlorobenzonitrile as the internal standard) were analyzed on an Agilent 7890B gas chromatograph (GC) interfaced with an Agilent 5977A mass spectrometer (MS). An Agilent HP-5MS UI column (30 m × 0.25 mm, film thickness = 0.25 μm) was used. The GC inlet was set to 280°C and operated in split mode (split ratio = 15:1). The total column flow was constant at 1 mL/min. The oven temperature program included an initial temperature of 70°C (no hold), ramp at 10°C/min to 100°C (no hold), ramp at 30°C/min to 290°C (1.667 min final hold); the total analysis time was 11 min. The transfer line temperature was fixed at 290°C. Retention times and ions detected in selected ion monitoring mode for each analyte are shown in **Table B-1**.

TMB as a quencher for free bromine. Toluene samples (1.0 μL) containing anisole, TMB, as well as their monochlorinated and monobrominated products were analyzed on an Agilent 7890A GC interfaced with an Agilent 5975C MS. An Agilent DB-5MS+DG column (30 m + 10 m DuraGuard, 0.250 mm inner diameter, 0.25 μm film thickness) was used. The GC inlet was set to 280°C and operated in splitless mode. The total column flow was constant at 1 mL/min. The oven temperature program included an initial temperature of 70°C (no hold), ramp at 10°C/min to 125°C (no hold time), ramp at 32°C/min to 285°C (1 min final hold); the total analysis time was 17 min. The transfer line was fixed at 290°C. Retention times and ions detected in selected ion monitoring mode for each analyte are shown in **Table B-2**.

Table B-1. GC-MS Selected Ion Monitoring (SIM) Method Details for Analyzing 2,4-Dichlorophenol, TMB, and their Chlorination Products

Analyte	**SIM Group**	**Retention time (min)**	**Quantitation Ion**	**Monitoring Ion**
2,4-dichlorophenol	A	5.11	162 $M^{+\bullet}$	126 $(M - H - Cl)^+$
2-chlorobenzonitrile (internal standard)		5.15	137 $M^{+\bullet}$	102 $(M - Cl)^+$
2,4,6-trichlorophenol	B	6.22	196 $M^{+\bullet}$	160 $(M - H - Cl)^+$
1,3,5-trimethoxybenzene		6.46	168 $M^{+\bullet}$	137 $(M - OCH_3)^+$
2-chloro-1,3,5-trimethoxybenzene	C	7.45	202 $M^{+\bullet}$	204 $M^{+\bullet}$ (^{37}Cl)
2,4-dichloro-1,3,5-trimethoxybenzene		7.87	236 $M^{+\bullet}$	238 $M^{+\bullet}$ (^{37}Cl)

Table B-2. GC-MS Selected Ion Monitoring (SIM) Method Details for Analyzing Anisole, TMB, and their Halogenation Products

Analyte	SIM Group	Retention time (min)	Quantitation Ion	Monitoring Ion
anisole	A	5.35	108 $M^{+\bullet}$	none [a]
4-chloroanisole	B	8.47	142 $M^{+\bullet}$	127 $(M - CH_3)^+$
2-chloroanisole		8.71	142 $M^{+\bullet}$	127 $(M - CH_3)^+$
2-chlorobenzonitrile (internal standard)	C	9.85	137 $M^{+\bullet}$	102 $(M - Cl)^+$
4-bromoanisole	D	10.47	186 $M^{+\bullet}$	171 $(M - CH_3)^+$
2-bromoanisole		10.59	186 $M^{+\bullet}$	171 $(M - CH_3)^+$
1,3,5-trimethoxybenzene	E	13.43	168 $M^{+\bullet}$	137 $(M - OCH_3)^+$
2-chloro-1,3,5-trimethoxybenzene	F	14.74	202 $M^{+\bullet}$	204 $M^{+\bullet}$ (^{37}Cl)
2-bromo-1,3,5-trimethoxybenzene		15.14	346 $M^{+\bullet}$	331 $(M - CH_3)^+$

[a] Background ions (likely originating from the solvent toluene) were detected with mass-to-charge ratios identical to the major daughter ions of anisole; therefore, no monitoring ions were recorded for this analyte. Interfering ions did not, however, preclude accurate quantitation of the molecular ion of anisole.

Influence of quenchers on the stability of DBPs. MTBE samples (1.0 μL) containing different disinfection byproducts (DBPs) and 1,2-dibromopropane as the internal standard were analyzed on an Agilent 7890B GC interfaced with a micro-electron capture detector (μ-ECD). An Agilent HP-5 column (30 m × 0.32 mm, film thickness = 0.25 μm) was used. The methods used to analyze different DBPs are described in **Tables B-3 and B4**.

Table B-3. GC-ECD Method Details for Analyzing Chloropicrin, Chloral Hydrate, and Tribromoacetaldehyde

	Chloropicrin	**Chloral Hydrate**	**Tribromoacetaldehyde**
Injection mode	splitless	splitless	splitless
Inlet temperature	117 °C	250 °C	250 °C
Detector temperature	297 °C	250 °C	250 °C
Carrier gas flow	1 mL/min	1 mL/min	1 mL/min
Oven temperature program	35 °C for 6 min 30 °C/min to 190 °C, hold for 1.5 min 40 °C/min to 280 °C, hold for 2.333 min	35 °C for 2 min 10 °C/min to 100 °C, no hold time 35 °C/min to 285 °C, no hold time	35 °C for 2 min 10 °C/min to 100 °C, no hold time 35 °C/min to 285 °C, hold for 3 min
Total run time	17.250 min	13.786 min	16.786 min

Table B-4. GC-ECD Method Details for Analyzing Chloroacetonitriles and Bromoacetonitriles

	Chloroacetonitriles	**Bromoacetonitriles**
Injection mode	split (15:1)	split (15:1)
Inlet temperature	175°C	175°C
Detector temperature	275°C	275°C
Carrier gas flow	0.8 mL/min	1 mL/min
Oven temperature program	27 °C for 4 min 15 °C/min to 75 °C, no hold time 35 °C/min to 185 °C, no hold time	35 °C for 2 min 15 °C/min to 100 °C, no hold time 20 °C/min to 185 °C, no hold time
Total run time	10.343 min	10.583 min

B. 4. Reference

1. Maraš, N.; Kočevar, M. Effects of tertiary amine catalysis on the regioselectivity of anisole chlorination with trichloroisocyanuric acid. *Monatsh. Chem.* **2015,** *146*, 697-704.

Appendix C: Supporting Information for Chapter 4

C. 1. Synthesis of Dehydro-β-ionone

Dehydro-β-ionone was synthesized using a procedure adapted from ref. 1. Details of the procedure are described herein.

Step 1

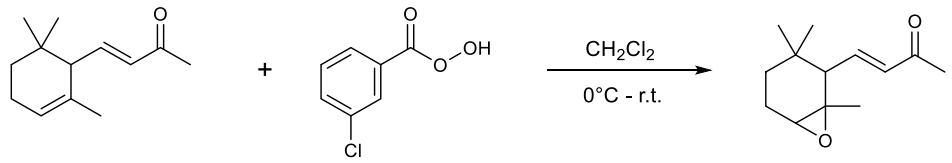

α-ionone | MCPBA, 77% | α-ionone epoxide

Step 2

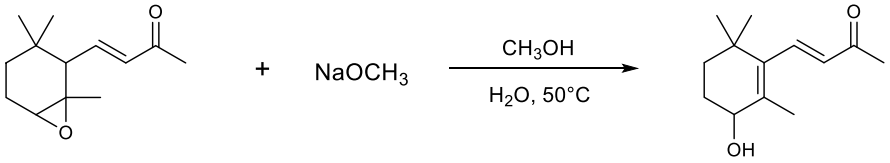

α-ionone epoxide | 4-hydroxy-β-ionone

Step 3

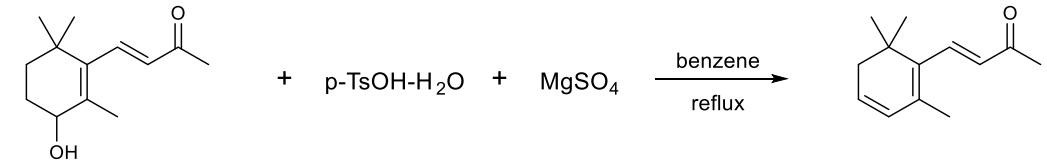

4-hydroxy-β-ionone | dehydro-β-ionone

Step 1: Synthesis of α-ionone epoxide from α-ionone

To a 100-mL flask under argon equipped with a magnetic stirring bar was added a solution of α-ionone (3 mL) in 10 mL CH_2Cl_2. This colorless solution was cooled to 0 °C in an ice bath, and a solution of 77% MCPBA in ~20 mL of CH_2Cl_2 was added dropwise via an addition funnel over 30 minutes. During the addition, a thick white precipitate formed, and after the addition was complete, the funnel was rinsed with an additional 5 mL of CH_2Cl_2. TLC (3:1 hexanes/ethyl acetate, UV/anisaldehyde) showed ~50% conversion of the starting material (R_f = 0.57, stained brown) to a major new spot of R_f = 0.34 (also stained brown). The cooling bath was removed, and the reaction mixture was allowed to rise slowly to room temperature. After one hour, TLC still showed some unreacted starting material, so an additional 0.5 g of MCPBA was added. After 30 minutes, TLC showed almost complete conversion to the product. The reaction was quenched with 20 mL of sodium metabisulfite (10%) and 20 mL of 2 M NaOH and diluted with H_2O and CH_2Cl_2. The layers had separated, and the organic phase was washed once with H_2O before being dried over Na_2SO_4. The solids were then removed by vacuum filtration and washed with ethyl acetate. The solvent was removed under reduced pressure, and the residue was purified by column chromatography (9:1 → 4:1 hexanes/ethyl acetate) to give 2.95 g of the product as a colorless oil (85:15 ratio of diastereomers by ^{1}H-NMR).

Step 2: Synthesis of 4-hydroxy-β-ionone from α-ionone epoxide

To a 200-mL flask under argon equipped with a magnetic stir bar was added a solution of KR-I-260 in 85 mL of CH_3OH and 3 mL H_2O. Solid sodium methoxide (1.01 g) was added, and the slightly yellow solution was heated to 50 °C overnight with a

reflux condenser. After 15 hours, TLC (1:1 hexanes/ethyl acetate, UV/anisaldehyde) of the orange reaction mixture showed almost complete consumption of the starting material ($R_f = 0.63$, stained brown) and formation of the product of $R_f = 0.40$ (stained black). Most of the methanol was removed under reduced pressure, and the residue was washed with 20 mL of 1M aqueous HCl and diluted with water and ethyl acetate. The layers were separated, and the aqueous phase was extracted with two additional portions of ethyl acetate before the combined organics were dried over Na_2SO_4. The solvent was removed under reduced pressure, and the yellow residue was purified by column chromatography (3:1 → 2:1 → 1.1 hexanes/ethyl acetate) to give 2.69 g of the product as a pale yellow oil.

Step 3: Synthesis of dehydro-β-ionone from 4-hydroxy-β-ionone

To a flame-dried 200-mL flask under argon equipped with a magnetic stirring bar was added a solution of KR-I-261 (2.69 g) in 68 mL of benzene. Solid p-TsOH and $MgSO_4$ were added, and the resulting mixture was heated to reflux. After 1.5 hours, the reaction mixture had turned bright yellow, and TLC (9:1 hexanes/ethyl acetate, UV/anisaldehyde) showed complete consumption of the starting material ($R_f = 0.04$) and formation of the product of $R_f = 0.34$. After cooling to r.t., the solids were removed by vacuum filtration and washed with ethyl acetate. The solvent was removed under reduced pressure, and the resulting brown oil was purified by column chromatography (9:1 hexanes/ethyl acetate) to give 1.93 g of the product as a bright yellow oil. Purity as determined by GC-MS was > 98%.

C. 2. Synthesis of β-Ionone Epoxide

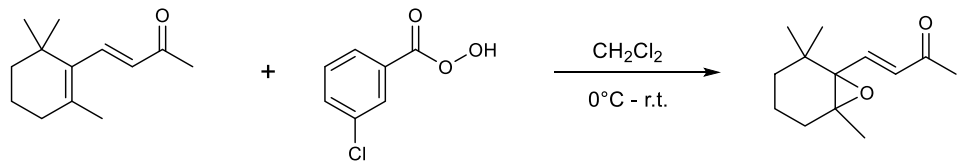

β-ionone MCPBA, 77% β-ionone epoxide

β-Ionone epoxide was synthesized using a procedure adapted from ref. 1. To a 100-mL flask under argon equipped with a magnetic stirring bar was added a solution of β-ionone (2.14 mL, 10.5 mmol, 1.00 eq.) in 10 mL of dichloromethane. This solution was cooled to 0 °C in an ice bath, and a solution of commercial 77% *m*-chloroperoxybenzoic acid (2.35 g, 10.5 mmol, 1.00 eq.) in 20 mL of dichloromethane was added dropwise via an addition funnel over the course of 30 minutes. During the addition, a thick white precipitate formed; and after the addition was complete, the addition funnel was rinsed with 5 mL of dichloromethane, which was also added to the reaction mixture. After warming to room temperature, thin layer chromatography (9:1 hexanes / ethyl acetate, UV / anisaldehyde stain) showed ~80% consumption of the β-ionone (R_f = 0.36) and clean formation of the epoxide (R_f = 0.23, stains brown). An additional portion of 77% *m*-chloroperoxybenzoic acid (350 mg, 1.56 mmol, 0.15 eq.) was added, and the reaction was stirred at room temperature for 15 minutes, at which point thin layer chromatography showed that the reaction was complete. The reaction mixture was quenched with 20 mL of 10% aqueous sodium metabisulfite solution and 20 mL of 2M aqueous sodium hydroxide solution. The layers were separated, and the organic phase was washed once with water before drying over anhydrous sodium sulfate.

After removal of the drying agent via filtration, the solvent was removed under reduced pressure, and the crude product was purified by column chromatography on silica gel (9:1 hexanes / ethyl acetate) to give 1.74 g (79%) of the epoxide as a colorless oil. Purity as determined by GC-MS was > 98%.

C. 3. Synthesis of α-Chloro-β-ionone and ε-Chloro-β-ionone

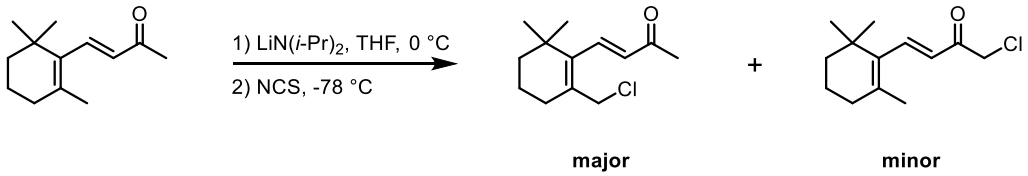

To a flame-dried 50 mL flask under argon equipped with a magnetic stirring bar was added a solution of diisopropylamine (273 μL, 1.95 mmol, 1.50 eq.) in 15 mL of anhydrous tetrahydrofuran. This solution was cooled to 0 °C in an ice bath, and a 2.5M solution of *n*-butyllithium in hexanes (624 μL, 1.56 mmol, 1.20 eq.) was added dropwise. The resulting solution of lithium diisopropylamide was stirred at 0 °C for 15 minutes, and a solution of β-ionone (265 μL, 1.30 mmol, 1.00 eq.) in 5 mL of anhydrous tetrahydrofuran was then added dropwise over 15 minutes. After an additional 30 minutes at 0 °C, the resulting orange enolate solution was cooled to -78 °C in a dry ice / isopropanol bath, and a solution of *N*-chlorosuccinimide (226 mg, 1.69 mmol, 1.30 eq.) in 5 mL of THF was added rapidly, discharging the orange color to light yellow. After 2 minutes at -78 °C, the reaction was quenched with saturated aqueous sodium bicarbonate solution and saturated aqueous sodium chloride solution before warming slowly to room temperature. After diluting with ethyl acetate, the layers were separated, and the organic phase was washed once with 1M aqueous hydrochloric acid solution and once with

saturated aqueous sodium chloride solution before drying over anhydrous sodium sulfate. Thin layer chromatography (9:1 hexanes / ethyl acetate, UV / anisaldehyde stain) showed unreacted β-ionone ($R_f = 0.44$), the α-chloro compound ($R_f = 0.50$), and the endocyclic ε-chloro compound ($R_f = 0.31$). The solvent was removed under reduced pressure, and the crude product mixture was purified by column chromatography on silica gel (9:1 hexanes / ethyl acetate) to give 14.6 mg of the α-chloro isomer (5%) and 20.5 mg of the ε-chloro isomer (7%) as yellow oils.

C. 4. Synthesis of Endocyclic and Exocyclic ε-Chloro-β-ionone

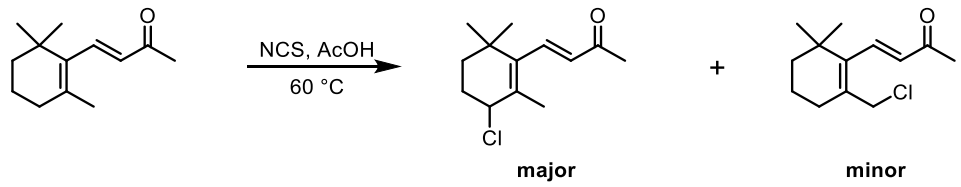

To a flame-dried 40 mL vial under argon equipped with a magnetic stirring bar was added a solution of β-ionone (500 μL, 2.46 mmol, 1.00 eq.) in 12 mL of glacial acetic acid. Solid *N*-chlorosuccinimide (361 mg, 2.70 mmol, 1.10 eq.) was added in a single portion, and the tightly capped vial was heated to 60 °C on an aluminum heating block for 40 minutes. After this time, a small aliquot of the reaction mixture was partitioned between ethyl acetate and saturated aqueous sodium bicarbonate solution for analysis by thin layer chromatography (9:1 hexanes / ethyl acetate, UV / anisaldehyde stain). This showed almost complete consumption of the β-ionone ($R_f = 0.44$, stains red) and formation of two new products: the endocyclic ε-chloro compound ($R_f = 0.31$, stains brown) and the exocyclic ε-chloro compound ($R_f = 0.40$, stains blue). The reaction mixture was diluted with ethyl acetate, and the acetic acid was quenched by the dropwise

addition of saturated aqueous potassium carbonate solution until no more gas evolution was observed. The layers were separated, and the organic phase was dried over anhydrous sodium sulfate before removal of the solvent under reduced pressure. The crude product was purified by repeated column chromatography on silica gel (19:1 hexanes / ethyl acetate) to give 394 mg of the endocyclic ε-chloro compound (71%) and 24 mg of the exocyclic ε-chloro compound (4%) as yellow oils.

C. 5. Computation of Second-Order Rate Constants

A similar data modeling approach has been described in great detail previously.[2] In the case of ionone chlorination, the overall reaction rate can be expressed as the following:

$$-\frac{d[\text{ionone}]}{dt} = k_{\text{Cl}_2}[\text{Cl}_2][\text{ionone}] + k_{\text{Cl}_2\text{O}}[\text{Cl}_2\text{O}][\text{ionone}] + k_{\text{HOCl}}[\text{HOCl}][\text{ionone}] \quad \text{(C-1)}$$

where k_{Cl_2}, $k_{\text{Cl}_2\text{O}}$, and k_{HOCl} represent second-order rate constants for Cl_2, Cl_2O, and HOCl, respectively. Under pseudo-first-order conditions in which $[\text{FAC}] \approx [\text{FAC}]_o \gg [\text{ionone}]_o$, equation C-1 can be written as:

$$-\frac{d[\text{ionone}]}{dt} = k_{\text{obs}}[\text{ionone}] \quad \text{(C-2)}$$

where the pseudo-first-order rate constant (k_{obs}) is equal to equation C-3:

$$k_{\text{obs}} = k_{\text{Cl}_2}[\text{Cl}_2] + k_{\text{Cl}_2\text{O}}[\text{Cl}_2\text{O}] + k_{\text{HOCl}}[\text{HOCl}] \quad \text{(C-3)}$$

Writing [Cl_2] and [Cl_2O] in terms of [HOCl] leads to equation C-4:

$$k_{obs} = k_{Cl_2}K_{Cl_2}[HOCl][Cl^-][H^+] + k_{Cl_2O}K_{Cl_2O}[HOCl]^2 + k_{HOCl}[HOCl] \qquad (C\text{-}4)$$

where K_{Cl_2} and K_{Cl_2O} represent equilibrium constants for the formation of Cl_2 and Cl_2O, respectively. The values of equilibrium constants are listed in equations 4-1 and 4-2 (Chapter 4).

When computing best-fit estimates of k_{Cl_2}, k_{Cl_2O}, and k_{HOCl}, nonlinear least squares regressions in *SigmaPlot 12.5* (Systat Software) minimizes the sums of squares between the experimental $\log k_{obs}$ data and the model predictions. Only one second-order rate constant is fitted at any given time. Uncertainties in the second-order rate constants denote 95% confidence intervals as determined by *SigmaPlot 12.5*. The order in which the second-order rate constants were fitted are described in the following sections. Best-fit estimates of k_{Cl_2}, k_{Cl_2O}, and k_{HOCl} are listed in **Table 4-1** (Chapter 4).

Data fitting procedure for β-ionone:

1. Fit k_{HOCl} to $\log k_{obs}$ versus pH data without added Cl^- at $6.4 \leq pH \leq 8.9$.
2. With k_{HOCl} constrained to the value estimated in (1), fit k_{Cl_2O} to $\log k_{obs}$ versus log [HOCl] data without added Cl^- at pH 7.0 and 7.3.
3. With k_{HOCl} and k_{Cl_2O} constrained to the values estimated in (1) and (2), fit k_{Cl_2} to $\log k_{obs}$ versus pH data at $[Cl^-]_{added}$ = 3 mM and $pH \leq 6.8$. The $\log k_{obs}$ versus pH data with $[Cl^-]_{added}$ = 1 mM were not used.

4. With k_{Cl_2} and k_{Cl_2O} constrained to the values estimated in (2) and (3), re-estimate k_{HOCl} according to (1).
5. Re-estimate k_{Cl_2} and k_{Cl_2O} individually using the steps described above. Repeat the process several times until the estimates of k_{Cl_2}, k_{Cl_2O}, and k_{HOCl} do not change appreciably from one iteration to another.

Data fitting procedure for α-ionone:

1. Fit k_{HOCl} to $\log k_{obs}$ versus pH data without added Cl^- at $6.2 \leq pH \leq 8.9$.
2. With k_{HOCl} constrained to the value estimated in (1), fit k_{Cl_2O} to $\log k_{obs}$ versus log [HOCl] data without added Cl^- at pH 7.3 and 7.6.
3. With k_{HOCl} and k_{Cl_2O} constrained to the values estimated in (1) and (2), fit k_{Cl_2} to all the $\log k_{obs}$ versus pH data at $[Cl^-]_{added}$ = 3 mM. The $\log k_{obs}$ versus pH data with $[Cl^-]_{added}$ = 1 mM are not used.
4. With k_{Cl_2} and k_{Cl_2O} constrained to the values estimated in (2) and (3), re-estimate k_{HOCl} according to (1).
5. Re-estimate k_{Cl_2} and k_{Cl_2O} individually using the steps described above. Repeat the process several times until the estimates of k_{Cl_2}, k_{Cl_2O}, and k_{HOCl} do not change appreciably from one iteration to another.

Data fitting procedure for dehydro-β-ionone:

1. Fit k_{HOCl} to $\log k_{obs}$ versus pH data without added Cl^- at $7.5 \leq pH \leq 9.2$.

2. With k_{HOCl} constrained to the value estimated in (1), fit $k_{\mathrm{Cl_2}}$ to the $\log\ k_{\mathrm{obs}}$ versus pH data at $[Cl^-]_{added}$ = 10 mM and 7.0 ≤ pH ≤ 7.6. The $\log\ k_{\mathrm{obs}}$ versus pH data with $[Cl^-]_{added}$ = 3 mM are not used.
3. With k_{HOCl} and $k_{\mathrm{Cl_2}}$ constrained to the values estimated in (1) and (2), fit $k_{\mathrm{Cl_2O}}$ to $\log\ k_{\mathrm{obs}}$ versus [HOCl] data at pH 7.6 and $\log\ k_{\mathrm{obs}}$ versus pH data without added Cl^- at 6.2 ≤ pH ≤ 7.2.
4. With $k_{\mathrm{Cl_2}}$ and $k_{\mathrm{Cl_2O}}$ constrained to the values estimated in (2) and (3), re-estimate k_{HOCl} according to (1).
5. Re-estimate $k_{\mathrm{Cl_2}}$ and $k_{\mathrm{Cl_2O}}$ individually using the steps described above. Repeat the process several times until the estimates of $k_{\mathrm{Cl_2}}$, $k_{\mathrm{Cl_2O}}$, and k_{HOCl} do not change appreciably from one iteration to another.

C. 6. Summary of Pseudo-First-Order Rate Constants (k_{obs})

The pseudo-first-order rate constants (k_{obs}) determined from linear regressions of ln[ionone] versus time data are listed in the following tables:

Tables C1–C3	β-ionone
Tables C4–C7	α-ionone
Tables C8–C10	dehydro-β-ionone

Values of $[ionone]_o$ were obtained from y-intercepts of the linear regressions of ln[ionone] versus time data. All uncertainties in k_{obs} values denote 95% confidence intervals.

Table C-1. Experimental Rate Constants from Variable pH Experiments Without Added Chloride for β-Ionone

pH	$[FAC]_o$ (μM)	$[Cl^-]_{added}$ (mM)	Extrapolated $[ionone]_o$ (μM)	k_{obs} (s^{-1})	Uncertainty in k_{obs} (s^{-1}) [a]
5.58	127	0	5.49	6.92×10^{-3}	4.89×10^{-4}
5.73	127	0	5.46	6.13×10^{-3}	3.48×10^{-4}
5.98	127	0	5.06	5.49×10^{-3}	1.97×10^{-4}
6.19	127	0	4.88	4.58×10^{-3}	1.23×10^{-4}
6.44	127	0	4.79	4.04×10^{-3}	1.74×10^{-4}
6.62	127	0	4.86	3.59×10^{-3}	8.82×10^{-5}
6.74	127	0	4.92	3.31×10^{-3}	7.97×10^{-5}
6.92	127	0	4.93	2.74×10^{-3}	8.10×10^{-5}
7.00	127	0	4.43	2.50×10^{-3}	5.70×10^{-5}
7.19	127	0	4.77	1.87×10^{-3}	2.96×10^{-5}
7.30	127	0	4.82	1.55×10^{-3}	2.80×10^{-5}
7.41	127	0	4.74	1.27×10^{-3}	4.29×10^{-5}
7.55	127	0	4.79	9.51×10^{-4}	2.35×10^{-5}
7.70	127	0	4.90	6.88×10^{-4}	1.42×10^{-5}
7.81	127	0	4.79	5.22×10^{-4}	1.35×10^{-5}
7.93	127	0	4.70	4.00×10^{-4}	6.20×10^{-6}
8.14	127	0	4.80	2.40×10^{-4}	1.80×10^{-6}
8.27	127	0	4.76	1.72×10^{-4}	5.02×10^{-6}
8.43	127	0	4.83	1.20×10^{-4}	4.19×10^{-6}
8.64	127	0	4.65	8.15×10^{-5}	5.17×10^{-6}
8.67	127	0	4.78	7.43×10^{-5}	2.00×10^{-6}
8.89	127	0	5.08	4.35×10^{-5}	2.69×10^{-6}
9.21	127	0	4.95	2.10×10^{-5}	2.18×10^{-6}

[a] Uncertainties in k_{obs} denote 95% confidence intervals.

Table C-2. Experimental Rate Constants from Variable pH Experiments with Added Chloride for β-Ionone

pH	$[FAC]_o$ (μM)	$[Cl^-]_{added}$ (mM)	Extrapolated $[ionone]_o$ (μM)	k_{obs} (s^{-1})	Uncertainty in k_{obs} (s^{-1}) [a]
6.12	127	2.99	5.63	1.85×10^{-2}	1.58×10^{-3}
6.27	127	2.99	5.11	1.41×10^{-2}	5.58×10^{-4}
6.43	127	2.99	4.83	1.04×10^{-2}	3.62×10^{-4}
6.58	127	2.99	4.98	8.48×10^{-3}	2.59×10^{-4}
6.77	127	2.99	4.87	5.94×10^{-3}	1.33×10^{-4}
6.99	127	2.99	4.76	3.99×10^{-3}	7.89×10^{-5}
7.15	127	2.99	4.76	2.87×10^{-3}	9.59×10^{-5}
7.28	127	2.99	4.43	2.32×10^{-3}	1.48×10^{-5}
7.49	127	2.99	4.83	1.36×10^{-3}	2.13×10^{-5}
7.66	127	2.99	4.40	9.42×10^{-4}	1.42×10^{-5}
7.77	127	2.99	4.81	6.70×10^{-4}	6.49×10^{-6}
5.76	127	0.99	5.49	1.46×10^{-2}	1.34×10^{-3}
5.99	127	0.99	5.46	1.15×10^{-2}	4.03×10^{-4}
6.16	127	0.99	4.97	9.09×10^{-3}	2.85×10^{-4}
6.29	127	0.99	4.90	7.54×10^{-3}	3.22×10^{-4}
6.49	127	0.99	4.79	5.94×10^{-3}	2.66×10^{-4}
6.64	127	0.99	4.84	4.96×10^{-3}	1.71×10^{-4}
6.85	127	0.99	4.82	3.80×10^{-3}	2.68×10^{-4}
7.12	127	0.99	4.65	2.42×10^{-3}	3.49×10^{-5}
7.29	127	0.99	4.74	1.84×10^{-3}	3.18×10^{-5}

[a] Uncertainties in k_{obs} denote 95% confidence intervals.

Table C-3. Experimental Rate Constants from Variable [FAC] Experiments for β-Ionone

pH	$[FAC]_o$ (μM)	$[Cl^-]_{added}$ (mM)	Extrapolated $[ionone]_o$ (μM)	k_{obs} (s^{-1})	Uncertainty in k_{obs} (s^{-1}) [a]
7.27	127	0	4.82	1.55×10^{-3}	2.80×10^{-5}
7.27	191	0	4.64	2.82×10^{-3}	5.06×10^{-5}
7.27	254	0	4.75	4.68×10^{-3}	1.40×10^{-4}
7.27	318	0	4.59	6.76×10^{-3}	1.95×10^{-4}
7.27	382	0	4.51	9.12×10^{-3}	3.45×10^{-4}
6.98	85	0	4.39	1.28×10^{-3}	4.18×10^{-5}
6.98	127	0	4.43	2.50×10^{-3}	5.70×10^{-5}
6.98	191	0	4.48	4.98×10^{-3}	1.15×10^{-4}
6.98	254	0	4.57	8.17×10^{-3}	1.63×10^{-4}
6.98	318	0	4.69	1.24×10^{-2}	3.91×10^{-4}
7.67	127	0	4.90	6.88×10^{-4}	1.42×10^{-5}
7.67	191	0	4.97	1.22×10^{-3}	3.09×10^{-5}
7.67	254	0	4.88	1.89×10^{-3}	3.53×10^{-5}
7.67	318	0	4.90	2.66×10^{-3}	1.98×10^{-5}
7.67	382	0	4.92	3.46×10^{-3}	1.29×10^{-4}
6.96	85	2.99	4.89	2.43×10^{-3}	5.38×10^{-5}
6.96	127	2.99	4.90	4.24×10^{-3}	1.12×10^{-4}
6.96	191	2.99	4.87	7.36×10^{-3}	2.32×10^{-4}
6.96	254	2.99	4.92	1.15×10^{-2}	2.39×10^{-4}
6.96	318	2.99	5.06	1.62×10^{-2}	6.03×10^{-4}

[a] Uncertainties in k_{obs} denote 95% confidence intervals.

Table C-4. Experimental Rate Constants from Variable pH Experiments Without Added Chloride for α-Ionone

pH	$[FAC]_o$ (μM)	$[Cl^-]_{added}$ (mM)	Extrapolated $[ionone]_o$ (μM)	k_{obs} (s^{-1})	Uncertainty in k_{obs} (s^{-1}) [a]
5.68	129	0	6.47	1.45×10^{-2}	1.97×10^{-3}
5.80	129	0	6.47	1.38×10^{-2}	1.34×10^{-3}
6.04	129	0	5.12	1.05×10^{-2}	7.61×10^{-4}
6.17	129	0	5.31	1.06×10^{-2}	5.54×10^{-4}
6.39	129	0	5.03	8.88×10^{-3}	1.41×10^{-4}
6.61	129	0	4.77	7.54×10^{-3}	9.83×10^{-5}
6.78	129	0	4.70	6.42×10^{-3}	1.81×10^{-4}
6.91	129	0	4.70	5.63×10^{-3}	6.37×10^{-5}
7.10	129	0	4.70	4.38×10^{-3}	6.70×10^{-5}
7.22	129	0	4.84	3.72×10^{-3}	9.72×10^{-5}
7.28	129	0	4.71	3.19×10^{-3}	3.32×10^{-5}
7.37	129	0	4.66	2.78×10^{-3}	4.24×10^{-5}
7.50	129	0	4.81	2.28×10^{-3}	9.60×10^{-5}
7.59	129	0	4.90	1.94×10^{-3}	5.63×10^{-5}
7.71	129	0	4.74	1.42×10^{-3}	4.60×10^{-5}
7.92	129	0	4.82	9.01×10^{-4}	1.66×10^{-5}
8.17	129	0	4.79	5.12×10^{-4}	4.31×10^{-6}
8.41	129	0	5.17	3.23×10^{-4}	1.90×10^{-5}
8.59 [b]	129	0	N/A	1.87×10^{-4}	3.75×10^{-5}
8.76 [b]	129	0	N/A	1.13×10^{-4}	1.59×10^{-5}
9.00 [b]	129	0	N/A	6.73×10^{-5}	2.84×10^{-6}
9.22 [b]	129	0	N/A	4.72×10^{-5}	8.98×10^{-6}

[a] Uncertainties in k_{obs} denote 95% confidence intervals.

[b] Value of k_{obs} at $[carbonate]_{tot} = 0$ extrapolated from k_{obs} versus $[carbonate]_{tot}$ data at each pH. Uncertainty denotes 95% confidence intervals of the slope of linear regression.

Table C-5. Experimental Rate Constants from Variable pH Experiments with Added Chloride for α-Ionone

pH	$[FAC]_o$ (μM)	$[Cl^-]_{added}$ (mM)	Extrapolated $[ionone]_o$ (μM)	k_{obs} (s^{-1})	Uncertainty in k_{obs} (s^{-1}) [a]
5.95	129	2.96	10.14	6.02×10^{-2}	2.45×10^{-2}
6.20	129	2.96	7.08	4.01×10^{-2}	5.42×10^{-3}
6.40	129	2.96	6.26	2.93×10^{-2}	2.02×10^{-3}
6.59	129	2.96	5.70	2.05×10^{-2}	1.01×10^{-3}
6.74	129	2.96	5.50	1.61×10^{-2}	4.39×10^{-4}
6.92	129	2.96	5.35	1.21×10^{-2}	4.75×10^{-4}
7.08	129	2.96	5.07	7.99×10^{-3}	1.82×10^{-4}
7.29	129	2.96	4.83	5.38×10^{-3}	2.41×10^{-4}
7.59	129	2.96	5.00	2.71×10^{-3}	3.31×10^{-5}
5.99	129	1.00	6.26	2.45×10^{-2}	3.00×10^{-3}
6.22	129	1.00	5.44	1.81×10^{-2}	1.37×10^{-3}
6.42	129	1.00	5.51	1.52×10^{-2}	9.69×10^{-4}
6.61	129	1.00	5.15	1.19×10^{-2}	3.74×10^{-4}
6.81	129	0.99	5.18	9.29×10^{-3}	4.73×10^{-4}
6.99	129	1.00	4.95	6.83×10^{-3}	1.52×10^{-4}
7.31	129	0.99	5.05	3.94×10^{-3}	7.25×10^{-5}

[a] Uncertainties in k_{obs} denote 95% confidence intervals.

Table C-6. Experimental Rate Constants from Variable [FAC] Experiments for α-Ionone

pH	$[FAC]_o$ (μM)	$[Cl^-]_{added}$ (mM)	Extrapolated $[ionone]_o$ (μM)	k_{obs} (s^{-1})	Uncertainty in k_{obs} (s^{-1}) [a]
7.28	97	0	4.79	2.08×10^{-3}	1.98×10^{-5}
7.28	129	0	4.71	3.19×10^{-3}	3.32×10^{-5}
7.28	193	0	4.77	5.93×10^{-3}	1.41×10^{-4}
7.28	257	0	4.72	9.05×10^{-3}	1.75×10^{-4}
7.28	322	0	4.87	1.31×10^{-2}	6.71×10^{-4}
7.59	129	0	4.90	1.94×10^{-3}	5.63×10^{-5}
7.59	193	0	4.98	3.44×10^{-3}	3.93×10^{-5}
7.59	257	0	4.95	5.25×10^{-3}	6.40×10^{-5}
7.59	322	0	5.03	7.39×10^{-3}	2.94×10^{-4}
7.59	386	0	5.10	9.89×10^{-3}	2.42×10^{-4}

[a] Uncertainties in k_{obs} denote 95% confidence intervals.

Table C-7. Experimental Rate Constants from Variable $[Carbonate]_{tot}$ Experiments Without Added Chloride for α-Ionone [a]

pH	$[carbonate]_{tot}$ (mM)	$[FAC]_o$ (μM)	Extrapolated $[ionone]_o$ (μM)	k_{obs} (s^{-1})	Uncertainty in k_{obs} (s^{-1}) [b]
8.60	5.0	129	4.95	2.04×10^{-4}	6.14×10^{-6}
8.56	10.0	129	4.96	2.57×10^{-4}	1.34×10^{-5}
8.59	15.0	129	4.74	2.75×10^{-4}	7.56×10^{-6}
8.61	20.0	129	4.80	2.93×10^{-4}	1.58×10^{-5}
8.61	25.0	129	4.64	3.27×10^{-4}	2.43×10^{-5}
8.76	5.0	129	4.93	1.36×10^{-4}	2.75×10^{-6}
8.75	10.0	129	4.73	1.59×10^{-4}	5.11×10^{-6}
8.76	15.1	129	4.63	1.71×10^{-4}	5.93×10^{-6}
8.77	20.1	129	4.76	1.98×10^{-4}	8.29×10^{-6}
8.76	25.1	129	4.63	2.24×10^{-4}	3.26×10^{-6}
9.00	5.0	129	5.02	7.80×10^{-5}	3.78×10^{-6}
9.00	15.1	129	4.73	1.01×10^{-4}	6.79×10^{-6}
9.01	20.1	129	4.77	1.11×10^{-4}	8.99×10^{-6}
8.99	25.1	129	4.61	1.22×10^{-4}	7.75×10^{-6}
9.21	5.0	129	4.75	5.47×10^{-5}	6.40×10^{-6}
9.22	10.0	129	4.77	6.20×10^{-5}	4.95×10^{-6}
9.21	15.0	129	4.76	7.25×10^{-5}	2.36×10^{-6}
9.22	20.0	129	4.57	7.71×10^{-5}	1.69×10^{-5}

[a] At each pH, k_{obs} was extrapolated to $[carbonate]_{tot} = 0$. The extrapolated k_{obs} values are the ones shown in **Figure 4-4b** (Chapter 4) and **Table C-4**.

[b] Uncertainties in k_{obs} denote 95% confidence intervals.

Table C-8. Experimental Rate Constants from Variable pH Experiments Without Added Chloride for Dehydro-β-ionone

pH	$[FAC]_o$ (μM)	$[Cl^-]_{added}$ (mM)	Extrapolated $[ionone]_o$ (μM)	k_{obs} (s^{-1})	Uncertainty in k_{obs} (s^{-1}) [a]
5.64	126	0	5.89	3.21×10^{-2}	3.02×10^{-3}
5.76	126	0	5.26	2.94×10^{-2}	2.20×10^{-3}
5.97	126	0	5.27	2.81×10^{-2}	7.82×10^{-4}
6.18	126	0	5.05	2.65×10^{-2}	1.23×10^{-3}
6.39	126	0	4.69	2.35×10^{-2}	9.95×10^{-4}
6.58	126	0	4.91	2.20×10^{-2}	4.32×10^{-4}
6.83	126	0	4.60	1.81×10^{-2}	3.69×10^{-4}
7.00	126	0	4.61	1.62×10^{-2}	2.18×10^{-4}
7.05	126	0	4.48	1.53×10^{-2}	2.35×10^{-4}
7.22	126	0	4.56	1.31×10^{-2}	3.77×10^{-4}
7.35	126	0	4.38	1.06×10^{-2}	1.75×10^{-4}
7.42	126	0	4.56	9.92×10^{-3}	1.16×10^{-4}
7.50	126	0	4.39	8.96×10^{-3}	2.18×10^{-4}
7.75	126	0	4.27	5.74×10^{-3}	2.53×10^{-4}
7.98	126	0	4.46	3.79×10^{-3}	1.23×10^{-4}
8.13	126	0	4.13	3.05×10^{-3}	1.40×10^{-4}
8.18	126	0	4.39	2.57×10^{-3}	7.95×10^{-5}
8.24	126	0	4.59	2.27×10^{-3}	7.31×10^{-5}
8.32	126	0	4.40	1.97×10^{-3}	9.10×10^{-5}
8.35	126	0	4.66	1.76×10^{-3}	3.70×10^{-5}
8.56	126	0	4.73	1.14×10^{-3}	2.89×10^{-5}
8.79	126	0	4.76	7.19×10^{-4}	2.54×10^{-5}
9.04	126	0	4.77	3.96×10^{-4}	1.53×10^{-5}
9.19	126	0	4.75	2.95×10^{-4}	1.46×10^{-5}

[a] Uncertainties in k_{obs} denote 95% confidence intervals.

Table C-9. Experimental Rate Constants from Variable pH Experiments with Added Chloride for Dehydro-β-ionone

pH	$[FAC]_o$ (μM)	$[Cl^-]_{added}$ (mM)	Extrapolated $[ionone]_o$ (μM)	k_{obs} (s^{-1})	Uncertainty in k_{obs} (s^{-1}) [a]
6.59	126	2.96	5.59	4.08×10^{-2}	1.69×10^{-3}
6.74	126	2.96	5.08	3.18×10^{-2}	1.44×10^{-3}
6.91	126	2.96	4.89	2.53×10^{-2}	4.10×10^{-4}
7.16	126	2.96	4.73	1.76×10^{-2}	5.61×10^{-4}
7.37	126	2.96	4.32	1.24×10^{-2}	2.56×10^{-4}
7.64	126	2.99	4.20	7.89×10^{-3}	1.11×10^{-4}
7.81	126	2.99	4.12	6.19×10^{-3}	2.40×10^{-4}
6.78	126	9.69	6.24	5.76×10^{-2}	5.41×10^{-3}
7.01	126	9.69	4.88	3.12×10^{-2}	6.25×10^{-4}
7.18	126	9.69	4.97	2.47×10^{-2}	6.12×10^{-4}
7.43	126	9.69	4.37	1.46×10^{-2}	4.79×10^{-4}
7.52	126	9.69	4.09	1.24×10^{-2}	4.38×10^{-4}
7.58	126	9.69	4.33	1.08×10^{-2}	9.25×10^{-5}
7.69	126	9.69	4.27	8.58×10^{-3}	2.41×10^{-4}

[a] Uncertainties in k_{obs} denote 95% confidence intervals.

Table C-10. Experimental Rate Constants from Variable [FAC] Experiments for Dehydro-β-ionone

pH	$[FAC]_o$ (μM)	$[Cl^-]_{added}$ (mM)	Extrapolated $[ionone]_o$ (μM)	k_{obs} (s^{-1})	Uncertainty in k_{obs} (s^{-1}) [a]
7.55	94	0	4.25	5.69×10^{-3}	2.14×10^{-4}
7.55	126	0	4.45	7.89×10^{-3}	2.30×10^{-4}
7.55	189	0	4.29	1.22×10^{-2}	6.55×10^{-4}
7.55	252	0	4.59	1.68×10^{-2}	2.52×10^{-4}
7.55	314	0	4.55	2.16×10^{-2}	6.08×10^{-4}

[a] Uncertainties in k_{obs} denote 95% confidence intervals.

C. 7. References

1. Liu, W.; Zhou, J.; Geng, G.; Lin, R.; Wu, J. H. Synthesis and in vitro characterization of ionone-based compounds as dual inhibitors of the androgen receptor and NF-κB. *Investigational New Drugs* **2014,** *32*, 227-234.

2. Lau, S. S.; Abraham, S. M.; Roberts, A. L. Chlorination revisited: Does Cl^- serve as a catalyst in the chlorination of phenols? *Environ. Sci. Technol.* **2016,** *50*, 13291-13298.

Vita

Stephanie Sin-Ying Lau was born on May 5, 1989 in Hong Kong. She moved to Connecticut in 2001 and graduated from Shelton High School in Shelton, Connecticut in 2007. After earning a Bachelor of Arts degree in Chemistry from Wellesley College (Wellesley, Massachusetts) in 2011, she began her graduate studies at the Johns Hopkins University (Baltimore, Maryland). She was awarded a Master of Science degree from the Department of Geography and Environmental Engineering (DoGEE) in 2013. Her doctoral research at Johns Hopkins focused on the roles of previously overlooked chlorine species in the aqueous chlorination on organic compounds. She also conducted research that led to the development of a novel quenching and quantification method for free halogens. Upon completion of her doctoral research in October 2017, she accepted a post-doctoral research position in the Department of Civil and Environmental Engineering at Stanford University (Stanford, California).